

# Expert Guide

## Part 2 Responsive Building Elements



### IEA ECBCS Annex 44 Integrating Environmentally Responsive Elements in Buildings

Expert Guide – Part 2 Responsive Building Elements

Editors: Øyvind Aschehoug, NTNU, Norway  
Marco Perino, Politecnico di Torino, Italy

November 2009  
[www.civil.aau.dk/Annex44](http://www.civil.aau.dk/Annex44)



International Energy Agency  
Energy Conservation in  
Buildings and Community  
Systems Programme

# 1. FOREWORD

This report resumes and presents the research activity done in Subtask A of IEA-ECBCS Annex 44 “Integrating Environmentally Responsive Elements in Buildings”. It is mainly focused on the results obtained as far as the following five Responsive Building Elements are concerned:

- Advanced Integrated Façade (AIF),
- Thermal Mass Activation (TMA),
- Earth Coupling (EC),
- Phase Change Materials (PCM),
- Dynamic Insulation (DI).

It is based on the contributions from the participating countries.

This publication is one of the Annex products. It focuses on innovative building elements that dynamically respond to changes in climate and user demands.

The report describes and analyses the outcomes of the research done within Subtask A of the Annex44. In particular an overview of materials, components and systems that have been studied and tested in laboratories is given. For each responsive element the available and/or purposely developed design methods and tools are described and guidance and recommendation are illustrated. Example of applications are used to highlight strength, weakness, advantages and potential barriers for their widespread implementation in the building sector.

This report is aimed at researchers and specialist in the field and gives an overview of how these elements work together, what methods/procedures can be used to analyze (theoretically and experimentally) their performance and what are the available performance data.

It is hoped, that this report will be helpful for designers and researchers in their continuous search for new solutions to the problem of designing and constructing sustainable buildings.

Øyvind Aschehoug  
Marco Perino

Editors



## 2. ACKNOWLEDGMENTS

The contents of this publication have been developed and collected within an Annex of the IEA Implementing Agreement Energy Conservation in Buildings and Community Systems: Annex 44 “Integrating Environmentally Responsive Elements in Buildings”.

The report is the result of an international joint effort conducted in 14 countries. All those who have contributed to the project are gratefully acknowledged.

The editors are grateful to Mandy Reynolds/Buro Happold for having supplied the Lowry picture.

In particular the following researchers actively contributed in collecting information, drafting, reviewing and editing the Expert Guide – part 2:

### Authors

#### Chapter 1, 2 and 3

##### **Marco Perino**

Politecnico di Torino – DENER

C.so Duca degli Abruzzi, 24

10129 TORINO

Italy

Phone: + 39 011 564 4423

Fax: +39 011 564 4499

[www.polito.it/tebe](http://www.polito.it/tebe)

E-mail: [marco.perino@polito.it](mailto:marco.perino@polito.it)

#### Chapter 4

##### **Fernando Marques da Silva**

LNEC, National Laboratory for Civil Engineering

Av. do. Brasil, 101

1700-066 Lisbon

Portugal

Phone: + 351 218 443 862; Fax: + 351 218 443 025;

E-mail: [fms@lnec.pt](mailto:fms@lnec.pt)

##### **Fabio Zanghirella**

Politecnico di Torino – DENER

C.so Duca degli Abruzzi, 24

10129 TORINO

Italy

Phone: + 39 011 5644 400

Fax: +39 011 564 4499

[www.polito.it/tebe](http://www.polito.it/tebe)

E-mail: [fabio.zanghirella@polito.it](mailto:fabio.zanghirella@polito.it)

## **Chapter 5**

### **Jakub Kolarik**

Int. Centre for Indoor Environment and Energy  
DTU  
Nils Koppels Alle, Building 402  
2800 Kgs. Lyngby  
Denmark  
Tel.: +45 4525 4045  
Fax: +45 4593 2166  
Email: [jakol@byg.dtu.dk](mailto:jakol@byg.dtu.dk)

### **Lina Yang**

The University of Hong Kong  
Department of Mechanical Engineering  
Hong Kong  
China  
Phone: + 86 852 96076926; Fax: + 86 852 28585415  
E-mail: [lnyang@hkusua.hku.hk](mailto:lnyang@hkusua.hku.hk)

## **Chapter 6**

### **Paolo Principi**

Dipartimento di Energetica  
Università Politecnica delle Marche  
Via Brece Bianche  
60015 Ancona  
Italy  
Phone: +39 (71) 2204773, E-mail: [p.principi@univpm.it](mailto:p.principi@univpm.it)

### **Roberto Fioretti**

Dipartimento di Energetica  
Università Politecnica delle Marche  
Via Brece Bianche  
60015 Ancona  
Italy  
Phone: + 39 071 2204880; Fax: + 39 071 2204770; E-Mail: [r.fioretti@univpm.it](mailto:r.fioretti@univpm.it)

## **Chapter 7**

### **Fariborz Haghighat**

Concordia University  
Dept. of Building, Civil and Environmental Engineering  
1455 de Maisonneuve Blvd. West  
Montreal, Quebec, H3G 1M8  
Canada  
Phone: + 1 514 848 2424; Fax: + 1 514 848 7965; E-mail: [haghi@bcee.concordia.ca](mailto:haghi@bcee.concordia.ca)

**Jian Zhang**

Concordia University  
Dept. of Building, Civil and Environmental Engineering  
1455 de Maisonneuve Blvd. West  
Montreal, Quebec, H3G 1M8  
Canada  
E-mail: zhangjian\_1977@yahoo.com

**Chapter 8****Fariborz Haghghat**

Concordia University  
Dept. of Building, Civil and Environmental Engineering  
1455 de Maisonneuve Blvd. West  
Montreal, Quebec, H3G 1M8  
Canada  
Phone: + 1 514 848 2424; Fax: + 1 514 848 7965; E-mail: [haghi@bcee.concordia.ca](mailto:haghi@bcee.concordia.ca)

**Kai Qiu**

Concordia University  
Dept. of Building, Civil and Environmental Engineering  
1455 de Maisonneuve Blvd. West  
Montreal, Quebec, H3G 1M8  
Canada  
E-mail: qiu\_kai71@hotmail.com

**Contributors****Chapter 4**

Marco Perino, Fabio Zanghirella, Mathias Haase, Armando Pinto, António Santos, Jorge Patrício, M. Glória Gomes, A. Moret Rodrigues, Jennifer Gosselin, Isamu Ohta, Faribors Haghghat, Alli Fallahi.

**Chapter 5**

Nikolai Artmann, Jan Babiak, Jakub Kolarik, Yuguo Li, Bjarne Olesen, Åsa Wahlström, Lina Yang, Pengcheng Xu, Zhi Zhuang

**Chapter 6**

Paolo Principi, Roberto Fioretti, Marco Perino

**Chapter 7**

Fariborz Haghghat, Jian Zhang, Gerard Guerracino, Tor Elge Dokka

**Chapter 8**

Fariborz Haghghat, Mohammed Salah-Eldin Imbabi, Kai Qiu

## Internal Reviewers

### **Mats Sandberg**

Centre for Built Environment

University of Gävle

SE-801 76 Gävle

Sweden

Phone: + 46 26 64 81 39; Fax: +4626648181; E-mail: [Mats.Sandberg@HiG.se](mailto:Mats.Sandberg@HiG.se)

### **Hans Cauberg**

Technical University Delft

PO Box 5043

2600 GA Delft

The Netherlands

Phone: + 31 650297169; Fax: + 31 433476347; E-mail: [h.cauberg@chri.nl](mailto:h.cauberg@chri.nl)

### **David Warwick**

Buro Happold

2 Brewery Place, Brewery Wharf

Leeds, WFJ 3BE

United Kingdom

Phone: + 44 0113 204 2200; Fax: -; E-mail: [david.warwick@burohappold.com](mailto:david.warwick@burohappold.com)

## International Energy Agency

The International Energy Agency (IEA) was established in 1974 within the framework of the Organization for Economic Co-operation and Development (OECD) to implement an international energy program. A basic aim of the IEA is to foster co-operation among the twenty-four IEA participating countries and to increase energy security through energy conservation, development of alternative energy sources and energy research, development and demonstration (RD&D).

## Energy Conservation in Buildings and Community Systems

The IEA sponsors research and development in a number of areas related to energy. The mission of one of those areas, the ECBCS - Energy Conservation for Building and Community Systems Program, is to facilitate and accelerate the introduction of energy conservation, and environmentally sustainable technologies into healthy buildings and community systems, through innovation and research in decision-making, building assemblies and systems, and commercialization. The objectives of collaborative work within the ECBCS R&D program are directly derived from the ongoing energy and environmental challenges facing IEA countries in the area of construction, energy market and research. ECBCS addresses major challenges and takes advantage of opportunities in the following areas:

- exploitation of innovation and information technology;
- impact of energy measures on indoor health and usability;
- integration of building energy measures and tools to changes in lifestyles, work environment alternatives, and business environment.

## The Executive Committee

Overall control of the program is maintained by an Executive Committee, which not only monitors existing projects but also identifies new areas where collaborative effort may be beneficial. To date the following projects have been initiated by the executive committee on Energy Conservation in Buildings and Community Systems (completed projects are identified by (\*) ):

- Annex 1: Load Energy Determination of Buildings (\*)
- Annex 2: Ekistics and Advanced Community Energy Systems (\*)
- Annex 3: Energy Conservation in Residential Buildings (\*)
- Annex 4: Glasgow Commercial Building Monitoring (\*)
- Annex 5: Air Infiltration and Ventilation Centre
- Annex 6: Energy Systems and Design of Communities (\*)
- Annex 7: Local Government Energy Planning (\*)
- Annex 8: Inhabitants Behaviour with Regard to Ventilation (\*)
- Annex 9: Minimum Ventilation Rates (\*)
- Annex 10: Building HVAC System Simulation (\*)
- Annex 11: Energy Auditing (\*)
- Annex 12: Windows and Fenestration (\*)
- Annex 13: Energy Management in Hospitals (\*)
- Annex 14: Condensation and Energy (\*)
- Annex 15: Energy Efficiency in Schools (\*)
- Annex 16: BEMS 1- User Interfaces and System Integration (\*)
- Annex 17: BEMS 2- Evaluation and Emulation Techniques (\*)
- Annex 18: Demand Controlled Ventilation Systems (\*)
- Annex 19: Low Slope Roof Systems (\*)

- Annex 20: Air Flow Patterns within Buildings (\*)
- Annex 21: Thermal Modelling (\*)
- Annex 22: Energy Efficient Communities (\*)
- Annex 23: Multi Zone Air Flow Modelling (COMIS) (\*)
- Annex 24: Heat, Air and Moisture Transfer in Envelopes (\*)
- Annex 25: Real time HEVAC Simulation (\*)
- Annex 26: Energy Efficient Ventilation of Large Enclosures (\*)
- Annex 27: Evaluation and Demonstration of Domestic Ventilation Systems (\*)
- Annex 28: Low Energy Cooling Systems (\*)
- Annex 29: Daylight in Buildings (\*)
- Annex 30: Bringing Simulation to Application (\*)
- Annex 31: Energy-Related Environmental Impact of Buildings (\*)
- Annex 32: Integral Building Envelope Performance Assessment (\*)
- Annex 33: Advanced Local Energy Planning (\*)
- Annex 34: Computer-Aided Evaluation of HVAC System Performance (\*)
- Annex 35: Design of Energy Efficient Hybrid Ventilation (HYBVENT) (\*)
- Annex 36: Retrofitting of Educational Buildings (\*)
- Annex 37: Low-exergy Systems for Heating and Cooling of Buildings (LowEx) (\*)
- Annex 38: Solar Sustainable Housing (\*)
- Annex 39: High Performance Insulation Systems (\*)
- Annex 40: Building Commissioning to Improve Energy Performance (\*)
- Annex 41: Whole Building Heat, Air and Moisture Response (MOIST-ENG) (\*)
- Annex 42: The Simulation of Building-Integrated Fuel Cell and Other Cogeneration Systems (FC+COGEN-SIM) (\*)
- Annex 43: Testing and Validation of Building Energy Simulation Tools (\*)
- Annex 44: Integrating Environmentally Responsive Elements in Buildings
- Annex 45: Energy Efficient Electric Lighting for Buildings
- Annex 46: Holistic Assessment Tool-kit on Energy Efficient Retrofit Measures for Government Buildings (EnERGo)
- Annex 47: Cost-Effective Commissioning for Existing and Low Energy Buildings
- Annex 48: Heat Pumping and Reversible Air Conditioning
- Annex 49: Low Exergy Systems for High Performance Built Environments and Communities
- Annex 50: Prefabricated Systems for Low Energy / High Comfort Building Renewal
- Annex 51: Energy Efficient Communities
- Annex 52: Towards Net Zero Energy Solar Buildings (NZEBS)
- Annex 53: Total Energy Use in Buildings: Analysis & Evaluation Methods

Working Group - Energy Efficiency in Educational Buildings (\*)

Working Group - Indicators of Energy Efficiency in Cold Climate Buildings (\*)

Working Group - Annex 36 Extension: The Energy Concept Adviser (\*)

(\*) - Completed

## Participants

### Austria

**Karl Hoefler**

*AEE INTEC*

Phone: + 43 3112 5886 25

E-mail: [k.hoefler@aee.at](mailto:k.hoefler@aee.at)

**Ernst Bluemel**

*University of Applied Science Burgenland GmbH.*

Phone: + 43 3357 45370 1130

E-mail: [ernst.bluemel@fh-burgenland.at](mailto:ernst.bluemel@fh-burgenland.at)

### Canada

**Fariborz Haghghat**

*Department of Building, Civil and Environmental Engineering*

*Concordia University*

Phone: + 1 514 848 2424 (ext. 3192)

E-mail: [haghi@bcee.concordia.ca](mailto:haghi@bcee.concordia.ca)

### China

**Yuguo Li**

*The University of Hong Kong, Dep. of Mech. Eng.*

Phone: + 852 2859 2625

E-mail: [liy@hku.hk](mailto:liy@hku.hk)

### Denmark, Operating Agent

**Per Heiselberg**

*Aalborg University*

Phone: + 45 9635 8541

E-mail: [ph@civil.aau.dk](mailto:ph@civil.aau.dk)

**Bjarne W. Olesen**

*Technical University of Denmark*

Phone: + 45 45 25 41 17

E-mail: [bwo@byg.dtu.dk](mailto:bwo@byg.dtu.dk)

**Jakub Kolarik**

*Silesian University of Technology*

E-mail: [kolarikjk@gmail.com](mailto:kolarikjk@gmail.com)

### France

**Etienne Wurtz**

*INES - Savoie Technolac*

Phone: +33 479 44 4554

E-mail: [etienne.wurtz@univ-savoie.fr](mailto:etienne.wurtz@univ-savoie.fr)

**Faure Xavier**

*CSTB*

Phone: + 33 0476762574

E-mail: [xavier.faure@cstb.fr](mailto:xavier.faure@cstb.fr)

## **Italy, Leader of subtask A**

**Marco Perino**

*Politecnico di Torino – DENER*

Phone: + 39 011 5644423

E-mail: [marco.perino@polito.it](mailto:marco.perino@polito.it)

**Paolo Principi**

*Dipartimento di Energetica - Università Politecnica delle Marche*

Phone: +39 (71) 2204773,

E-mail: [p.principi@univpm.it](mailto:p.principi@univpm.it)

## **Japan**

**Takao Sawachi**

*National Institute for Land and Infrastructure Management*

Phone: + 81 298 64 4356

E-mail: [tsawachi@kenken.go.jp](mailto:tsawachi@kenken.go.jp)

**Ryuichiro Yoshie**

*Tokyo Polytechnic University*

Phone: + 81 (0) 46-242-9556

E-mail: [yoshie@arch.t-kougei.ac.jp](mailto:yoshie@arch.t-kougei.ac.jp)

**Shinsuke Kato**

*University of Tokyo*

Phone: + 81 3 5452 6431

E-mail: [kato@iis.u-tokyo.ac.jp](mailto:kato@iis.u-tokyo.ac.jp)

**Yuji Hori**

*Building Research Institute*

Phone: +81 (29) 864 6679

E-mail: [horii@kenken.go.jp](mailto:horii@kenken.go.jp)

**Tomoyuki Chikamoto**

*Ritsumeikan University*

Phone: + 81 77 561 3029

E-mail: [tomoyuki@se.ritsumei.ac.jp](mailto:tomoyuki@se.ritsumei.ac.jp)

**Yuichiro Kodama**

*Kobe Design University*

Phone: +81 78 796 2571

E-mail: [y-kodama@kobe-du.ac.jp](mailto:y-kodama@kobe-du.ac.jp)

**Tatsuya Hayashi**

*Nikken Sekkei Ltd*

Phone: + 81-3-5226-3030

E-mail: [hayashit@nikken.co.jp](mailto:hayashit@nikken.co.jp)

**Isamu Ohta**

*Misawa Homes Institute of Research and Development Co., Ltd.*

Phone:

E-mail: [Isamu\\_Ohta@home.misawa.co.jp](mailto:Isamu_Ohta@home.misawa.co.jp)

**Yasuo Takahashi**

*Tateyama Aluminum Industry Co.,Ltd.*

E-mail: [y\\_takahashi@sthdg.co.jp](mailto:y_takahashi@sthdg.co.jp)

**Akinori Hosoi**  
*FUJITA Corporation*  
Phone: +8146 250 7095  
E-mail: [ahosoi@fujita.co.jp](mailto:ahosoi@fujita.co.jp)

**Norway, Leader of subtask B (until January 2007)**

**Inger Andresen**  
*Skanska Norway*  
Phone: + 47 92851625  
E-mail: [inger.andresen@skanska.no](mailto:inger.andresen@skanska.no)

**Øyvind Aschehoug**  
*Norwegian University of Science and Technology, NTNU*  
Phone: +47 73 59 50 46  
E-mail: [Oyvind.Aschehoug@ntnu.no](mailto:Oyvind.Aschehoug@ntnu.no)

**Portugal**

**Fernando Marques da Silva**  
*LNEC, National Laboratory for Civil Engineering*  
Phone: + 351 218 443 862  
E-mail: [fms@lnec.pt](mailto:fms@lnec.pt)

**Antonio Moret Rodrigues**  
*IST-DeCivil, Technical University of Lisbon*  
Phone: + 351 218 418 360  
E-mail: [ahr@civil.ist.utl.pt](mailto:ahr@civil.ist.utl.pt)

**Sweden**

**Eva-Lotta W. Kurkinen**  
*SP Technical Research Institute of Sweden*  
Phone: +46(0)10 516 50 00, (direkt) +46(0)10 516 51 77  
E-mail: [eva-lotta.kurkinen@sp.se](mailto:eva-lotta.kurkinen@sp.se)

**Mats Sandberg**  
*Centre for Built Environment*  
*University of Gävle*  
Phone: + 46 26 64 81 39  
E-mail: [Mats.Sandberg@HiG.se](mailto:Mats.Sandberg@HiG.se)

**The Netherlands, Leader of subtask C**

**Ad van der Aa**  
*Cauberg-Huygen Consulting Engineers*  
Phone: + 31 10 4257444  
E-mail: [a.vanderaa@chri.nl](mailto:a.vanderaa@chri.nl)

**Hans Cauberg**  
*Technical University Delft*  
Phone: + 31 152283174  
E-mail: [J.J.M.Cauberg@citg.tudelft.nl](mailto:J.J.M.Cauberg@citg.tudelft.nl)

## **United Kingdom**

**Mohammed Salah-Eldin Imbabi**

*The University of Aberdeen*

Phone: + 44 (0) 1224 272506

E-mail: [m.s.imbabi@abdn.ac.uk](mailto:m.s.imbabi@abdn.ac.uk)

**Maria Kolokotroni**

*Brunel University*

Phone: + 44 1895 266688

E-mail: [maria.kolokotroni@brunel.ac.uk](mailto:maria.kolokotroni@brunel.ac.uk)

**David Warwick**

*Buro Happold*

Phone: + 44 0113 204 2200

E-mail: [david.warwick@burohappold.com](mailto:david.warwick@burohappold.com)

## **USA**

**Qingyan Chen**

*Purdue University*

Phone: +1 765 494 2138

E-mail: [yanchen@purdue.edu](mailto:yanchen@purdue.edu)

# CONTENTS

<b>1. FOREWORD</b> .....	2
<b>2 ACKNOWLEDGMENTS</b> .....	3
<b>3. INTRODUCTION</b> .....	19
<b>3.1 Scope and focus</b> .....	19
<b>3.2 Responsive Building Elements - Preface</b> .....	19
<b>3.3. Definitions</b> .....	20
<b>3.4 Principles</b> .....	20
<b>3.5 Classification</b> .....	21
<b>4. ADVANCED INTEGRATED FACADES</b> .....	24
<b>4.1 Description of principles &amp; technologies</b> .....	24
<u>4.1.1 Transparent ventilated façades</u> .....	24
<u>4.1.2 Advanced Fenestration Systems</u> .....	25
<u>4.1.3 Opaque ventilated facades</u> .....	25
<b>4.2 Classification facades</b> .....	26
<u>4.2.1 Type of ventilation facades</u> .....	26
<u>4.2.2 Flow path facades</u> .....	26
<u>4.2.3 Façade configuration facades</u> .....	26
<u>4.2.4 Energy production facades</u> .....	27
<u>4.2.5 Integration with other RBEs facades</u> .....	27
<b>4.3 Design tools &amp; Analysis methods</b> .....	28
<u>4.3.1 Component simulation tools</u> .....	29
<u>4.3.2 Building simulation tools</u> .....	30
<u>4.3.3 Numerical Analysis Methodologies</u> .....	31
<u>4.3.3.1 Dynamic Airflow Model for Buildings</u> .....	31
<u>4.3.3.2 The Concordia University model</u> .....	32
<u>4.3.3.3 Mechanically ventilated AIF model (PoliTo)</u> .....	33
<u>4.3.3.4 DSF Numerical Model (IST – Portugal)</u> .....	36
<u>4.3.4 Experimental Analysis: test rig, performance parameters</u> .....	38
and measurement procedures	
<u>4.3.4.1 Politecnico di Torino test facility - TWINS</u> .....	38
<u>4.3.4.2 Experimental AIF module – LNEC</u> .....	39
<u>4.3.4.3 Performance parameters definition for transparent AIF</u> .....	41
<b>4.4 Guidance and recommendation</b> .....	44
<b>4.5 Examples for illustration</b> .....	48
<u>4.5.1 The Dragonair/CNAC Building</u> .....	49

4.5.2 Atrium Saldanha .....	49
4.5.3 Peking Road .....	50
4.5.4 ARAG 2000 .....	50
4.5.5 Technical University of Delft Library .....	51
4.5.6 Moravian Library .....	51
4.5.7 Environment Park .....	52
4.5.7.1 <i>General Information</i> .....	52
4.5.7.2 <i>Component description and working principles.</i> .....	53
4.5.7.3 <i>Measurements for performance assessment</i> .....	53
4.5.8 SOMEC Building .....	55
4.5.8.1 <i>General Information</i> .....	55
4.5.8.2 <i>Component description and working principles</i> .....	55
4.5.8.3 <i>Measurements for performance assessment</i> .....	57
4.5.9 Solar XXI .....	58
4.5.10 Buildings with AIF in Lisbon (Portugal) .....	59
<b>4.6 Barriers to overcome</b> .....	61
4.6.1 Costs .....	62
4.6.2 Fire standards and regulations .....	62
4.6.3 Other construction regulations and laws .....	63
4.6.4 Lack of knowledge and lack of design tools .....	64
<b>4.7 References</b> .....	64
<b>5. THERMAL MASS ACTIVATION (TMA)</b> .....	74
<b>5.1 Description of principles &amp; technologies</b> .....	74
<b>5.2 Classification of the thermal mass activation concepts</b> .....	75
<b>and technologies</b>	
5.2.1 <u>Airborne systems</u> .....	78
5.2.2 <u>Water based systems</u> .....	79
5.2.3 <u>Other types of core activation components</u> .....	81
<b>5.3 Design/analysis method and tools</b> .....	81
5.3.1 <u>Design method for passive cooling of</u> .....	81
<u>building construction by night-time ventilations</u>	
5.3.1.1 <i>Climatic Cooling Potential</i> .....	82
5.3.1.2 <i>Dynamic Heat Storage Capacity</i> .....	82
5.3.1.3 <i>Night-time Air change Rate</i> .....	83
5.3.2 <u>Design method for surface thermal mass activation</u> .....	85
5.3.2.1 <i>Virtual sphere concept and</i> .....	85
<i>three design parameters</i>	
5.3.2.2 <i>Dynamic thermal networks</i> .....	86
5.3.3 <u>Design method for core thermal mass</u> .....	87
<u>activation - capacity evaluation</u>	
5.3.4 <u>Available design tools – core thermal mass activation</u> .....	88
5.3.4.1 <i>Summary of principal input parameters</i> .....	88
<i>to be considered for capacity calculation/simulation</i>	

<u>5.3.4.2 Results from the calculation</u> .....	89
<u>5.3.5 Design method for core thermal mass activation –</u> .....	89
<u>performance assessment</u>	
<u>5.3.5.1 Simulated performance</u> .....	89
<u>5.3.5.2 Measured performance of the core thermal</u> .....	91
<u>mass activation components/systems</u>	
<b>5.4 Guidance and recommendation</b> .....	92
<u>5.4.1 Climate context</u> .....	93
<u>5.4.2 Coupling with a night-time ventilation</u> .....	93
<u>5.4.2.1 Ventilation of the buildings equipped with</u> .....	94
<u>core thermal mass activation</u>	
<u>5.4.3 Thermal mass properties</u> .....	94
<u>5.4.4 Heat transfer between room and thermo active component</u> .....	96
<u>5.4.5 Location/positioning of the surface thermal mass activation</u> .....	98
<u>5.4.5.1 Internal thermal mass</u> .....	98
<u>5.4.5.2 External thermal mass</u> .....	98
<u>5.4.5.3 Thermal mass and insulation</u> .....	99
<u>5.4.6 Operation strategies for the core thermal</u> .....	99
<u>mass activation</u>	
<u>5.4.6.1 Thermal behaviour of the core thermo-active components</u> .....	101
<u>5.4.6.2 CA performance controls</u> .....	102
<u>5.4.6.2.1 Water (heat carrier) temperature control</u> .....	102
<u>5.4.6.2.2 Water (heat carrier) flow rate control</u> .....	102
<u>5.4.6.2.3 Control with respect to a weather forecast</u> .....	103
<u>5.4.7 International standards dealing with core thermal</u> .....	104
<u>mass activation components</u>	
<u>5.4.8 Suitability of the thermal mass activation components</u> .....	105
<u>to be used with other building elements</u>	
<b>5.5 Examples for illustration</b> .....	106
<u>5.5.1 Air conditioning system utilizing building</u> .....	106
<u>thermal storage (ACSuBTS)</u>	
<u>5.5.1.1 Working principles</u> .....	106
<u>5.5.1.2 Measurements and simulations for</u> .....	106
<u>performance assessment</u>	
<u>5.5.1.3 The “claimed” benefits and limitations of</u> .....	111
<u>the presented concept:</u>	
<u>5.5.2 Chinese kang</u> .....	111
<u>5.5.2.1 Working principle</u> .....	111
<u>5.5.2.2 Theoretical study and field survey</u> .....	113
<u>5.5.3 The Centre for Sustainable Building (ZUB)</u> .....	114
<u>5.5.4 Office building of Bertelsmann C. Verlag GmbH</u> .....	115
<u>5.5.5 Berliner Bogen</u> .....	116
<b>5.6 Potential barriers and limitations</b> .....	117
<u>5.6.1 General barriers and limitations to the application</u> .....	117
<u>of surface thermal mass activation (SA)</u>	

5.6.2 Barriers to the application of core thermal mass activation (CA) .....	117
<b>5.7 List of Symbols</b> .....	117
<b>5.8 References</b> .....	118
<b>6. EARTH COUPLING</b> .....	123
<b>6.1 Description of Principles and Technologies</b> .....	123
6.1.1 Heat flows in the Earth .....	124
6.1.2 Ground temperature distribution .....	124
6.1.3 Heat and mass transfer processes in ETAHE .....	126
6.1.4 Energy cost for fan .....	128
<b>6.2 Classification</b> .....	128
<b>6.3 Design/Analysis method and tools</b> .....	129
<b>6.4 Guidance and recommendations</b> .....	130
<b>6.5 Examples for illustration</b> .....	131
6.5.1 <u>Schwerzenbacherhof building, Zurich, Switzerland</u> .....	132
6.5.1.1 <i>General information</i> .....	132
6.5.1.2 <i>Component description</i> .....	132
6.5.1.3 <i>Control strategy</i> .....	132
6.5.2 <u>Mediå School, Grong, Norway</u> .....	133
6.5.2.1 <i>General information</i> .....	133
6.5.2.2 <i>Component description</i> .....	133
6.5.2.3 <i>Control strategy</i> .....	136
6.5.3 <u>Jaer School, Oslo, Norway</u> .....	136
6.5.3.1 <i>General information</i> .....	136
6.5.3.2 <i>Component description</i> .....	137
6.5.3.3 <i>Control strategy</i> .....	138
<b>6.6 Potential barriers</b> .....	138
<b>6.7 References</b> .....	139
<b>7. PHASE CHANGE MATERIALS (PCM)</b> .....	141
<b>7.1 Description of principles &amp; technologies</b> .....	141
<b>7.2 Classification</b> .....	145
7.2.1 <u>Wall application</u> .....	145
7.2.1.1 <i>Opaque envelope component</i> .....	145
7.2.1.2 <i>Solar wall</i> .....	147
7.2.2 <u>Underfloor application</u> .....	149
7.2.3 <u>Ceiling air exchanger</u> .....	150
7.2.4 <u>Thermal Storage unit and air exchanger applications</u> .....	151
<b>7.3 Design/analysis method and tools</b> .....	151
7.3.1 <u>FEM approach</u> .....	153
7.3.2 <u>The thermal network approach (zone model)</u> .....	153
7.3.3 <u>Simplified tools</u> .....	154

<b>7.4 Guidance and recommendation</b>	154
<b>7.5 Examples for illustration</b>	155
<u>7.5.1 The “3-Litre” House (DE)</u>	155
<u>7.5.2 The “Domat EMS“ building (CH)</u>	157
<u>7.5.3 Building of Stevenage Borough Council (UK)</u>	158
<b>7.6 References &amp; selected bibliography</b>	159
<b>8. DYNAMIC INSULATION</b>	166
<b>8.1 Description of technologies and classifications</b>	166
<b>8.2 Design/analysis method and tools</b>	168
<u>8.2.1 Thermal performance</u>	168
<u>8.2.2 Air quality</u>	170
<b>8.3 Guidance and recommendation</b>	170
<b>8.4 Examples for illustration</b>	171
<u>8.4.1 Example of DI wall Technologies</u>	171
<u>8.4.2 Product development and practical application</u>	172
<b>8.5 Market introduction</b>	175
<b>8.6 Barriers to overcome</b>	175
<b>8.7 References</b>	175

## LIST OF APPENDIX

### APPENDIX 4A

4A.1 AIF Politecnico di Torino model (PoliTo)

### APPENDIX 4B

4B.1 AIF IST model (Portugal)

### APPENDIX 4C

4C.1 Details of the experimental analysis of transparent ventilated façades with the TWINS facility (Polito)

4C.2 The experimental campaigns

4C.2.1 Winter conditions

4C.2.2 Summer conditions

4C.2.3 Resume of main results (Hybvent module)

### APPENDIX 4D

4D.1 Experimental analysis of transparent ventilated façades with the LNEC facility

4D.2 The experimental campaigns

## **APPENDIX 4E**

4E.1 Daylighting

## **APPENDIX 4F**

4F.1 – Acoustics

## **APPENDIX 4G**

4G.1 - Wind Action

## **APPENDIX 4H**

4H.1 Sustainability

## **APPENDIX 4I**

4I.1 Assessment of the convective heat transfer coeff.,  $h_c$

## **APPENDIX 4J**

4J.1 Measured data – Field monitoring of real Buildings in Lisbon (Portugal)

## **APPENDIX 4K**

4K.1 Coupling AIF with TMA

## **APPENDIX 7A**

7A.1 Design/analysis methods and tools

7A.1.1 Detailed analysis of the element with FEM method

7A.1.2 Building simulation software (network approach)

## **APPENDIX 8A**

8A.1 Design/analysis methods and tools



# 3. INTRODUCTION

## 3.1 Scope and focus

This report is complementary to the short summary report presented in the “Basic Design Guide” and gives a more comprehensive information about the Responsive Building Elements (RBE) and a review of the results of the research activity performed within SubTask A of the Annex 44.

The report is targeted to researchers and specialists (engineers, consultants and component manufacturers) working in the field of sustainable building technologies.

The RBEs covered in this report are mainly associated with the building envelope and other major construction elements: foundations, exterior walls, interior walls, floors, roof, windows etc.

These RBEs are designed to work in close interaction with the building mechanical and electrical systems, such as heating, cooling, ventilation, lighting, electricity supply, and control systems, in order to reduce the demand for energy (as thoroughly illustrated in the “Expert Guide – part 1”).

After a brief description of working principles and a general classification of different RBE types and technologies, attention is focused on five specific responsive building elements, whose perspective of improvement and widespread implementation in the building sector seems to be much more promising, that is:

- Advanced Integrated Facades (AIF – as for example ventilated transparent facades),
- Thermal Mass Activation (TMA – building elements used for energy storage),
- Earth Coupling (EC – as for example foundation elements and buried ducts and culverts used to pre-cool or pre-heat the ventilation air),
- Dynamic Insulation (DI – as for example breathing walls and roofs to pre-heat the ventilation air),
- Phase Change Materials (PCM – materials and systems integrated in building elements/installations to enhance their ability to store energy).

This report covers different applications of the RBEs, illustrates available design tools, gives general guidelines and recommendations, supplies data for design and performance analysis, and, finally, discusses barriers to application and needs for more research.

## 3.2 Responsive Building Elements - Preface

Research and technological innovation, over the last decade, have determined a significant improvement of performances of specific building elements like the building envelope - including walls, roofs and fenestration components - and building equipments - such as heating, ventilation, cooling equipment and lighting.

Whilst most building elements still offer some opportunities for efficiency improvements, the greatest future potential seems to lie with technologies that promote the integration of “dynamic” and “adaptive” building elements with building services.

This means that functions, features and thermophysical properties of such building components may change over the time and adapt to different requirements.

Within Annex 44 such components have been defined as ***Responsive Building Elements (RBE)***.

The general accepted meaning of the word *responsive* is: “a system or organism readily reacting to a stimulus or people or events”; that is a system/element **showing a positive response**: reacting quickly, strongly, and favourably to something.

The development, application and implementation of responsive building elements are considered to be a necessary step towards further energy efficiency improvements in the built environment.

### 3.3. Definitions

*Responsive Building Elements* are defined as building construction elements which are actively used for transfer and storage of heat, light, water and air.

In the design philosophy of the integrated building concepts<sup>1</sup>, RBEs are logically and rationally combined and integrated with building service functions such as heating, cooling, ventilation and lighting.

RBEs are, thus, building components that assist to maintain an appropriate balance between optimum interior conditions and energy performance by reacting in a controlled and holistic manner to outdoor and indoor environment changes and to occupants requirements.

### 3.4 Principles

The key principles on which a Responsive Building Element relies on are:

- dynamic behaviour,
- adaptability,
- capability to perform different functions,
- intelligent control.

The “dynamic” and “adaptable” concepts translate into the fact that functions, features and/or thermophysical properties of these elements may change over the time and suitably fit to different building/occupants requirements/needs (heating/cooling, higher/lower ventilation, ...) and to different boundary conditions (meteorological, internal heat/pollution loads, ...).

The coherence between the energy & comfort requirements and the RBE behaviour/properties is guaranteed by the “intelligence” of the control.

This last concept, moreover, is the one that allows the correct integration of the operational principle of a single RBE with the rest of the building and the installations.

In other words, the proper functionality of one (or more) RBEs – at the component level – is fitted and tuned by the intelligent control to proactively contribute - at the system and concept level – to the overall Integrated Building Concept.

Only by integrating the RBEs under the supervision of an intelligent control, driven by a suitable strategy, it is possible to effectively exploit their potentialities.

The range of application of the RBEs, and their conceptual working principles, are extremely wide. They switch from building envelope components with “adjustable” U-value and/or with variable air permeability, to building structures or components able to store thermal energy, to glazed systems with variable optical properties, to elements exploiting evaporative cooling,...

From a practical point of view, examples of existing RBE include, among the others:

- *façades systems* (ventilated facades, double skin facades, adaptable facades, dynamic insulation, PV façades...),
- *foundations and other underground systems* (earth coupling systems, embedded ducts, ...),
- *energy storages* (active use of thermal mass, material - concrete, massive wood - core activation for cooling and heating, phase change materials, ...),
- *roof systems* (green roof systems, dynamic insulation,...),

---

<sup>1</sup> See “Expert Guide – Part 1”.

- *passive solar systems, daylighting technologies, evaporative cooling elements* (roof ponds, water walls, spray ponds, ...).

As it is possible to observe from these non exhaustive examples, some RBEs elements are well known and used since long time (green roof and basic technologies for thermal energy storage have been used since ancient age. Ventilated façades are largely applied since the eighties/nineties). However, their adoption traditionally lacked of integration and control. It was just one dynamic element used in an “unplugged” way. For this reason their actual performance in the field frequently revealed to be poorer than expected. Furthermore, in many cases the available design and analysis methods are still not enough reliable and/or easy-to-use, so there is a lack of tools to support the designers.

Other Responsive Building Elements are relatively new, like Dynamic Insulation, or, in further cases, they are advanced technologies tested in the laboratory and seldom adopted in existing buildings.

### 3.5 Classification

From a general point of view RBEs can be classified on the basis of:

- building technological system (envelope, structure, ...) and element (façade, wall, roof, ...) where the RBE can be integrated,
- action performed (heating, cooling, ventilation, daylighting, energy storage,...),
- connection with HVAC systems and type of fluid used for thermal purposes.

Table 3.1 gives a non-exhaustive overview of Responsive Building Elements, highlighting their performed functions and the type of integration with the building & installations (this table is not intended to be a tool to select RBE suitable for a certain application, but it just gives a general idea of the RBEs features and actions).

It has to be highlighted that for some typologies of RBEs, various configurations may be conceived. This is the case, for example, of Advanced Integrated Facades and Thermal Mass Activation.

Advanced Integrated Façades (AIF) is a family of elements that gathers a number of different technological solutions. Among the most well known and widespread types it is possible to mention:

- |   |             |
|---|-------------|
| - Transparent ventilated façade               | (AIF – TVF) |
| - Opaque ventilated façade                    | (AIF – OVF) |
| - Integrated photovoltaic, transparent façade | (AIF – PVT) |
| - Integrated photovoltaic, opaque façade      | (AIF – PVO) |
| - Integrated solar (air/water) collector      | (AIF – SC)  |
| - With transparent insulated materials        | (AIF – TIM) |

Some façades may also result from a combination of the above listed configurations.

Moreover, it has to be considered that fenestrations play an important role as façade components, and can behave like a RBE (this is the case of intelligent fenestration systems like, for example, the SWindow described in section 4).

Analogously to AIF, different configurations for Thermal Mass Activation exist, that can be grouped into two main categories:

- Thermal Mass Activation – Surface Activation (TMA – SA),
- Thermal Mass Activation – Core Activation (TMA – CA).

As far as the first category is concerned, the typical use is to exploit the thermal inertia of usual, non modified, building elements (like building structures, floors, ceilings, ...), furniture and internal

structures (suitably selected for their large heat capacity) by means of a proper integration with the building and the ventilation system (a typical example is represented by the so-called “night cooling”). In such kind of configurations the heat exchange typically takes place at the surface of the building component.

In case of TMA - CA, instead, the exploitation of the thermal inertia is obtained by means of a fluid (usually air or water) that is flown through a proper network of ducts or channels integrated inside the inner structure of the element itself (in some special cases the fluid is constituted by flue combustion gases, like in the Chinese “Kang”).

In such kind of systems the heat exchange takes place not only at the surface of the components, but it mainly involves the inner part (core) of the elements.

In the research activity of the IEA - Annex 44, attention has been focused only on five specific responsive building elements, whose perspective of improvement and widespread implementation in the building sector seems to be more promising.

These are:

- Advanced Integrated Facades (AIF),
- Thermal Mass Activation (TMA),
- Earth Coupling (EC),
- Phase Change Materials (PCM),
- Dynamic Insulation (DI).

These RBEs will be analysed in sections 4, 5, 6, 7 and 8 respectively.



#### List of symbols used in table 3.1:

AIF – TVF:	Transparent Ventilated Façade	DI:	Dynamic Insulation
AIF – OVF:	Opaque Ventilated Façade	PCM:	Phase Change Materials
AIF – PVT:	Integrated Photovoltaic, Transparent façade	TVR:	Transparent Ventilated Roof
AIF – PVO:	Integrated Photovoltaic, Opaque façade	OVR:	Opaque Ventilated Roof
AIF – SC:	Integrated solar air/water Collector	PVTR:	Integrated Photovoltaic, Transparent Roof
AIF – TIM:	With Transparent Insulation Materials	PVOR:	Integrated Photovoltaic, Opaque Roof
TMA – SA:	Thermal Mass Activation – Surface Activation	SCR:	Integrated Solar air/water Collector - Roof
TMA – CA:	Thermal Mass Activation – Core Activation	TIMR:	Transparent Insulated Materials - Roof

**Table 3.1 – Actions and possible integration of Responsive Building Elements in buildings.**

Building System	Element	Intervention		Actions								Type of RBE	Connection of the element with the fluid network of the HVAC system is needed			When integrated with HVAC systems the thermal fluid is:		
		Surface	Internal	Reduction of heating loads	Reduction of cooling loads	Heating	Cooling	Electric energy production	Thermal energy storage	Ventilation	Daylighting		Yes	No	Not necessarily	air	water	
Envelope	Walls	✓		✓	✓	✓				✓	✓	AIF - TVF			✓	✓		
		✓	✓	✓	✓	✓				✓	✓	AIF - OVf			✓	✓		
		✓			✓			✓				✓	AIF - PVT		✓			
		✓			✓			✓					AIF - PVO		✓			
		✓			✓		✓						AIF - SC	✓			✓	✓
		✓			✓		✓					✓	AIF - TIM		✓			
		✓			✓		✓						TMA - SA			✓	✓	
			✓		✓		✓	✓					TMA - CA	✓				✓
	Roof	✓	✓	✓	✓						✓		DI	✓			✓	
		✓		✓	✓								PCM		✓			
		✓	✓	✓	✓	✓					✓	✓	TVR			✓	✓	
		✓	✓	✓	✓	✓					✓	✓	OVR			✓	✓	
		✓		✓	✓			✓				✓	PVTR		✓			
		✓		✓	✓			✓					PVOR		✓			
		✓		✓	✓		✓						SCR	✓			✓	✓
		✓		✓	✓							✓	TIMR		✓			
			✓		✓								TMA - SA			✓	✓	
			✓		✓								TMA - CA	✓				✓
			✓		✓							✓	DI	✓			✓	
		Floors	✓		✓	✓								PCM		✓		
			✓	✓	✓								TMA - SA		✓			
			✓	✓	✓		✓	✓					TMA - CA	✓			✓	✓
			✓	✓	✓								PCM			✓	✓	✓
	Ceilings	✓		✓	✓								TMA - SA		✓			
		✓	✓	✓		✓	✓					TMA - CA	✓			✓	✓	
		✓	✓	✓								PCM			✓	✓	✓	
Fenestration	✓									✓	✓	AIF - Swindow	✓			✓		
Superstructure	Column/Beam	✓										TMA - SA		✓				
			✓									TMA - CA	✓			✓		
			✓										PCM		✓			
	Load bearing wall	✓										TMA - SA		✓				
			✓									TMA - CA	✓				✓	
			✓										PCM		✓			
Load Bearing Floors	✓											TMA - SA		✓				
		✓										TMA - CA	✓				✓	
		✓										PCM		✓				
Substructures	Piles		✓									TMA - CA	✓				✓	
	Foundation beams		✓									EC			✓	✓		
Underground system	Earth to Air Heat Exchangers		✓								✓	EC	✓			✓		
	Underground spaces		✓								✓	EC	✓			✓		
	Cellar	✓									✓	TMA - SA			✓	✓		
	Garages	✓									✓	TMA - SA			✓	✓		
Renders & Finishes	Partition wall		✓									PCM		✓				
	Floor	✓										TMA - SA		✓				
	Ceiling		✓									PCM		✓				
Other spaces	Sun space, courtyards & atria	✓	✓							✓	✓			✓				
	Staircase & Corridors	✓	✓								✓			✓				
	Roof gardens & Winter gardens									✓	✓			✓				

# 4. ADVANCED INTEGRATED FACADES

## 4.1 Description of principles & technologies

An *Advanced Integrated Façade* (AIF) is the outer, weather-protecting layer of a building that can contribute to heating, cooling, ventilation and lighting requirements and can promote interior comfort through efficient, energy-saving measures. It exhibits adaptive characteristics that are in tune with both the physical/ climatic conditions of a particular location and the indoor environment requirements. AIF are the actual development of what started with passive architecture principles and evolved, originally, into Double Skin Façades (DSF) and, recently, into the intelligent skins concepts. An intelligent skin may be defined as “*a composition of construction elements confined to the outer, weather-protecting zone of a building, which performs functions that can be individually or cumulatively adjusted to respond predictably to environment variations, to maintain comfort with the least use of energy*” [Wigginton, M., Harris, J. (2002)].

An AIF should therefore result from an “intelligent design” rather than just an assembly of “intelligent components”. The concept of “intelligence” associated with DSF represents *a change from a static envelope to a dynamic and responsive envelope*.

Thermophysical properties and performance of advanced integrated façades are application dependent and are a function of the operative conditions. They may be obtained through simulations and experimental tests.

Providing general guidelines for designing and using Advanced Integrated Façades is not an easy task due to the great number of different configurations, their dynamic behaviour and the strong connection with the building energy system.

### 4.1.1 Transparent ventilated façades

The working principle of a transparent ventilated façade is to use the air gap between the two glazed panes to reduce the thermal impact of the outdoor environment on the indoor climate conditions. The air gap may use natural, mechanical or hybrid ventilation schemes, or simply act as a still air buffer. Figure 4.1 sketches the façade physics, showing the complexity and impact of solar radiation, conduction, convection and airflow through the double-skin gap.

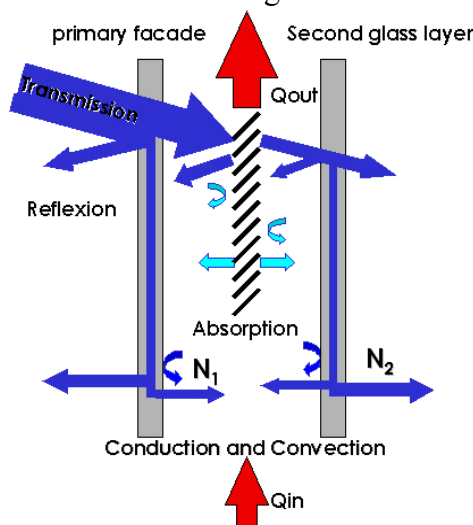


**Figure 4.1 - DSF/AIF working principles.**

The main functions that should be provided by a transparent ventilated façade are:

- to recover heat during cold season and/or to preheat the ventilation air,

- to improve the thermal insulation of the glazed system during both hot and cold seasons,
- to reduce solar loads and enhance natural lighting control without the drawback of increasing the heat gains,
- to extend the use of natural ventilation systems, particularly in the case of high rise buildings.

#### **4.1.2 Advanced Fenestration Systems**

Advanced fenestration systems may consist of windows capable of providing self-adjusting opening areas and/or of windows acting like a small-scale transparent ventilated façade (i.e. ventilated windows).

An example of window with a self-adjusting opening angle (analysed during the Annex 44 activity) is represented by the so-called *Swindow*.

There are two types of Swindows: air supply and exhaust. The Swindow is in the open position at 45° from vertical when the wind is calm. It then starts to move when the wind blows. The Swindows located on the windward side, automatically reacts to the wind speed, decreasing the opening angle, whilst the Swindows located on the leeward side, due to the negative pressure, tends to increase the opening angle (figure 4.2). The Swindow operates even in weak winds and provides unidirectional air flow in the supply or exhaust direction, while limiting the surplus air flow rate.

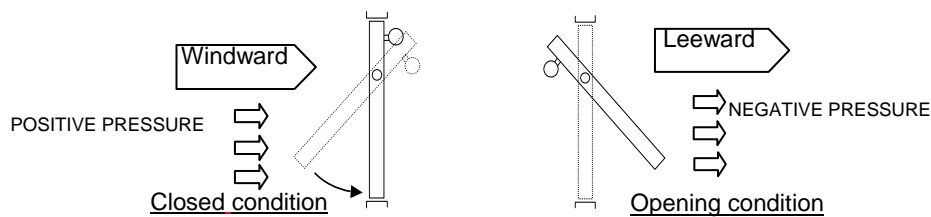


**Figure 4.2 - SWINDOW working principle.**

#### **4.1.3 Opaque ventilated façades**

Opaque ventilated façades (OVF), or Opaque Double Skin Façades (ODSF), refer, essentially, to two different configurations: two opaque layers separated by a ventilated air gap or a transparent layer and an opaque layer (usually massive) separated by a ventilated air gap.

The first structure is quite similar to a fully transparent ventilated façade and the working principle is the same, with the only significant difference that there are no short wave heat gains through the façade.

The second configuration, instead, is typically called *Trombe wall* and acts, during winter time, as a large air solar collector. In modern Trombe walls, there are air vents on the top and bottom of the air gap, between the glazing and the opaque layer (that has a relevant thermal mass. See also section 7.2.1.2).

During the heating season the system is configured so as to direct the heated air into the building. In this way thermal losses are reduced and the overall free gains are improved. The vents have one-way louvers that prevent convection at night, thereby making heat flow strongly directional.

During the cooling season, instead, the vents are configured so as to remove part of the solar gain from the façade (i.e. the vents facing to the interior are closed and the heated air flowing in the air gap is rejected toward the outdoor environment).

## 4.2 Classification

AIF classification is not a straightforward task due to the number of different features and operative strategies to be considered. Most common classifications consider the type of ventilation, the flow path and the system configuration as major items.

### 4.2.1 Type of ventilation

The driving force of the air flow within the cavity defines the type of ventilation. Types to be considered are: natural ventilation (NV), mechanical ventilation (MV), and hybrid ventilation (HV). Hybrid ventilation utilizes both natural and mechanical ventilation as driving forces.

### 4.2.2 Flow path

The air flow path is a very important issue that is strongly associated with the AIF integration and the building energy and control systems. Possible arrangements, shown in Fig. 4.3, are: exhaust air (EA), supply air (SA), reversible air flow (RAF), outdoor air curtain (OAC) and indoor air curtain (IAC).

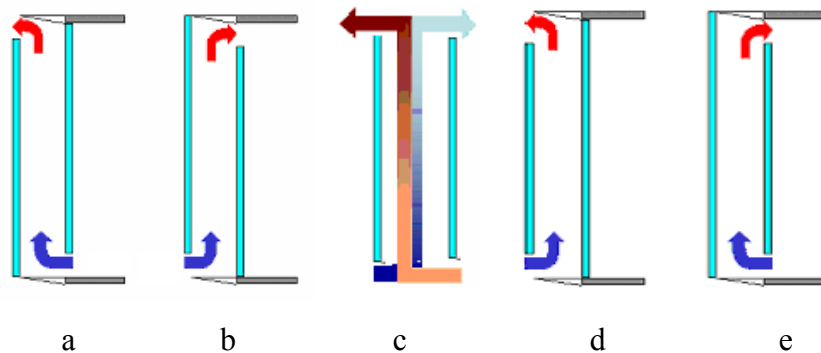
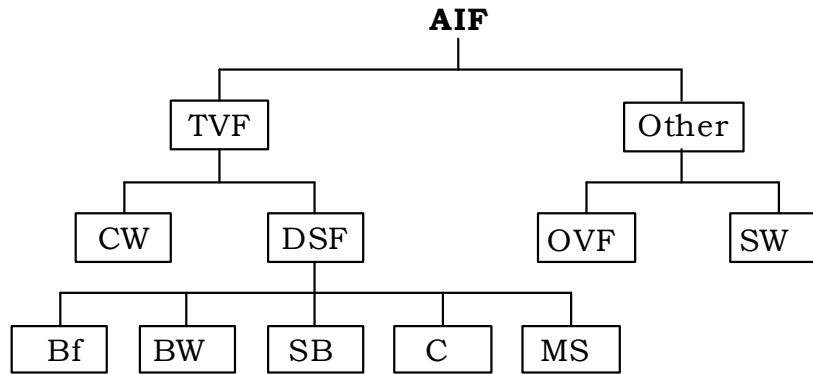


Figure 4.3 - AIF flow path: a) EA; b) SA; c) RAF; d) OAC; e) IAC [State-of-the-Art Report Annex 44 (2005)].

### 4.2.3 Façade configuration

Façade configuration is based on the well-known Belgium Building Research Institute's (BBRI) classification for double skin façades. Modifications were proposed to this classification, by the Annex 44 research group, in order to take into account the main specific characteristics of an AIF. This proposed classification, represented schematically in Fig. 4.4, divides AIFs into transparent vertical façades (TVF) and other concepts including opaque vertical façades (OVF) and the Swindow (SW). These classes are then characterized by a number of different technologies:

- **Climate wall (CW):** merges the climate façade/climate window concepts, the difference between them being the existence or lack of a window division. A CW is characterized by an external double glazed pane, an internal single glazed pane or curtain, a MV connection to the building ventilation system, and a small gap (~10 mm) under the interior pane that allows air to flow into the cavity. This arrangement is similar to a box-window.
- **Double Skin Façade (DSF):**
  - Buffer (Bf):** the still air within the cavity acts as a thermal buffer. The cavity is connected to the outdoor air for pressure balance purposes.
  - Box-window (BW):** The façade is divided both vertically and horizontally, forming a box.
  - Shaft-box (SB):** The SB has a similar configuration to the BW, except that the shaft box discharges exhaust air to a lateral building-height cavity.



**Figure 4.4 - Proposed simplified classification of AIF.**

**Corridor (C):** the Façade is horizontally divided, forming a storey level corridor. Inlet and outlet openings are placed in such a way that the mixing of exhaust air and supply air to the above storey is avoided.

**Multi-storey (MS):** A MS system is a DSF with no cavity partitions. Louvered façades are a particular case of MS, in which the external skin is composed of louvers that can be moved from a closed to an open position. In the open position, they no longer act as a second skin.

- **Swindow (SW):** This is an automatically operable window, developed for natural ventilation purposes with the capability of being integrated with the HVAC systems. The basic configuration consists of a horizontally pivoted window that is hinged just above mid-height. When opened, the weight of the window is balanced with a counterweight located at the top of the window. Different constructions with the same working principle are used for exhaust and supply modes.

#### **4.2.4 Energy production**

Any type of AIF is compatible with the integration of photovoltaic modules producing electrical energy. Furthermore, during the heating season, some AIF typologies can be used as a sort of an air solar collector to pre-heat the ventilation air.

#### **4.2.5 Integration with other RBEs**

Integration of AIF with other Responsive Building Elements can effectively contribute to overall energy efficiency of the system both in winter and summer conditions.

A promising experimental configuration that has been investigated within Annex 44 is represented by the integration of AIF with thermal mass activated elements (SA concept) [Fallahi, A. (2009)].

The outcomes of a detailed study devoted to analyse the integration between thermal mass and AIF are resumed in Appendix 4K.

A positive effect of thermal mass coupled to AIF could be achieved both in summer and winter. In summer the thermal energy due to high solar gains is absorbed and released with some delay to air channel between panes. As a result of the heat absorbed by the thermal mass a lower temperature of the air in the air gap is reached. This leads to a reduction of the cooling loads in the room located behind the AIF. Overheating and discomfort condition during high solar radiation periods of summer day are, therefore, limited or avoided.

Moreover, the stored heat is released gradually and the attached-room air temperature variations are reduced. In winter, such behaviour allows to reduce the heating loads.

### 4.3 Design tools & Analysis methods

The ability to accurately estimate the energy performance and the indoor comfort implications of an AIF during the design process is essential. This may be achieved through the use of simulation tools that are able to model the façade, properly evaluate its behaviour and compare different solutions. On the basis of such results is then possible to make educated design decisions.

Together with simulation tools, the behaviour of AIF technologies can also be investigated by means of experimental techniques. The assessment of recognized and reliable performance indices is a typical and fundamental step for the certification of usual building envelope components (e.g. the U value of walls and/or fenestrations) and, therefore, it should even more enforced in case of innovative elements like AIF. The measurement techniques to perform such task are, however, not trivial and there are, so far, no standardized approaches

Furthermore, due to the complex behaviour of DSF, the usually adopted parameters (like the U-value) are no longer applicable and/or useful.

Within Annex 44 AIF modelling was developed either by using available tools or proposing new ones. The ideal simulation tool should accurately model the outdoor climate (temperature, humidity, wind and radiation), the DSF/AIF configuration (glazed panes, shading devices, ventilation strategy, thermal properties), the building (physics, occupancy schedule, air conditioning system), the control system and the interaction of all these variables simultaneously. Such a tool does not yet exist in a form that is ready for designers.

Each part of such a tool is required to perform specific tasks, as is briefly described below:

#### Outdoor climate

- Both wind speed and direction are important for ventilation purposes and should be accurately predicted and/or taken into account, especially for the case of naturally or hybrid ventilated façades. Ground reflected radiation should be known in order to completely determine incident solar radiation and its transmittance through glazing near the ground.

#### Façades

- The shading device is particularly difficult to model due to the complex interaction with solar radiation and airflow, but its thermal simulation is fundamental.
- In naturally ventilated façades, the combination of the stack and wind effects has to be considered, because they can act cumulatively or in opposition and directly influence airflow rate.
- In order to operate an AIF, a dynamic control system is needed. Modelling of such a control system is difficult since an accurate tool for simulation purposes is not readily available.
- Materials that transmit or reflect light via a nonlinear manner (light-redirecting daylight, prisms, metallic shades, angular selective coatings) needs to be accurately simulated through complex mathematical models [Lee, et al (2002)].

From the literature review it emerges that many analytical and numerical models have been used so far to study the performance and optimize DSF [State-of-the-Art Report Annex 44 (2005)]. These models have several levels of complexity, ranging from simple to more complex ones such as CFD. The simple methods include the lumped, non-dimensional, network and control volume approaches [Tanimoto and Kimura (1997); Saelens (2002); Faggembauu, et al (2003a); Faggembauu, et al (2003b); Balocco (2004); Park et al. (2004b); Jiru and Haghghat (2005)].

The more sophisticated approaches are able to simulate DSF/AIF with different levels of complexity and, typically, were developed by different research groups using commercial CFD based software such as [Kautsch, et al (2002); Manz (2003)]: FLUENT(<http://www.fluent.com>); FloVent (<http://www.flomerics.com>), Star-CD, or CFX.

However the use of CFD codes requires specific expertise; its features are, frequently, too sophisticated and unnecessary for the draft or preliminary design stage. It follows that they are usually not suitable for designers, but more appropriate for the research activity.

A more simple modelling procedure uses zonal airflow network models. However it is limited to modelling simple airflow and nearly uniform temperature distributions. These limitations can only be overcome by coupling the model with CFD [Kalyanova, et al (2005)].

In general, analysing the approaches so far adopted, two categories for simulation tools can be identified:

- component – for the thermal, energetic and lighting simulation of the element behaviour;
- building – for the thermal simulation of the whole building, including the façades [see e.g. BBRI (2002)].

As far as the experimental investigation techniques are concerned, instead, the activity developed within Annex 44 has been mainly focused on the design and development of suitable test cells, on which the AIF components can be tested and analyzed. Two different facilities were constructed (one at LNEC- Lisbon and the other at Politecnico di Torino). These test cells were used to study different types of AIF and to verify the applicability of specifically defined performance indexes for the certification of AIF elements.

#### **4.3.1 Component simulation tools**

To date there is a poor availability of design tools specifically created for the analysis of advanced integrated façades. Available tools for the design and analysis of DSF that are tailored for designers and consultants are listed below:

- WIS (<http://www.windat.org>)  
WIS is a European software tool for the calculation of thermal and solar properties of commercial and innovative window systems on the basis of thermal and solar/optical interactions between the components. With WIS it is possible to describe the façade structure in combination with glazing and shading devices. Each “solid” layer (glass or solar shading device) must be separated from the adjacent layers by an air cavity. The air cavity can be closed, naturally ventilated or mechanically ventilated.  
Information about each component is stored in a database. This data includes, for instance, spectral optical properties of the available commercial glazing and shading devices as well as the thermal properties of edge spacers and of numerous window frame profiles existing on the market.  
Through WIS it is possible to simulate a complete window system. WIS models the one-dimensional window system by assuming uniform and steady state conditions over the glass pane. It provides, as a result, the temperature distribution and heat fluxes across the various layers (glass, solar shading, air). Other outputs of WIS software are: the overall thermal and solar properties of the window system, the thermal and solar properties of each component, and the surface and centre (average) temperature of each layer, according to the different incident angles of solar radiation. It should be noted that the thermal analysis may only be performed for steady-state conditions.  
Vertical gradients (along the air flow path) of the variables of influence are not taken into account [Perino, M. (2005)].
- BISCO/TRISCO/VOLTRA (<http://www.physibel.be>) [Flamant, G, et al (2004)]  
Developed by the Physybel company (<http://www.physibel.be>), this tool has the potential to calculate both temperature distribution and heat loss in the façade. The interaction between the glass, the shading layers and the thermal bridging effect of the subcomponents around the DSF (supporting mullions and transoms, connections between inlet and outlet openings, etc.) can be modelled.

- OPTIC5 :(<http://eetd.lbl.gov/btp/software.html>) [Lee, et al (2002)]  
OPTIC5 can be used to determine the optical and radiative properties of glazing materials. It has not the ability to simulate the entire DSF behaviour.
- FRAME (<http://www.frameplus.net>)  
This modelling tool can be used to determine glazing U-value, SHGC, light transmission and glazing temperatures under any set of conditions that may be used for ventilated windows.
- BESTFACADE (<http://www.bestfacade.com>)  
Developed within the BESTFACADE (2007) EU project, it has a simple and user friendly model for DSF, estimating the energy use contribution and daylight distribution on the room behind the façade.

All the above listed tools are either shareware or commercially available software.

### **4.3.2 Building simulation tools**

Building simulation tools may be used to analyze AIF as an integral building component. In fact, they not only simulate the thermal behaviour of the façade, but also allow to “pass” these results to the overall mass and energy balance of the building. In this way it is possible to assess the effect of the AIF on the overall energy demand and to analyse the implication of different integration and control strategies.

These tools, however, are typically suited for a “whole building approach”, and so the AIF simulation is usually quite simplified and not sufficiently detailed. They, consequently, do not appear to be effective for the study and design of the façade as “stand-alone” component.

Building energy consumption can be assessed by simulating the building with software packages. At the moment there are more than 240 simulation software packages available that have been in existence for more than 20 years and evaluated by comparison with the monitored data for the performance of existing buildings [Clarke (2001)].

A good list can be found on the US Government’s Department of Energy website at: [http://www.eere.energy.gov/buildings/tools\\_directory](http://www.eere.energy.gov/buildings/tools_directory).

A short list of the most representative building simulation tools is presented below:

- CAPSOL (<http://www.physibel.be/>) [Flamant, G, et al (2004)]  
This tool calculates multi-zone transient heat transfer as a function of heat fluxes (solar radiation and internal gains) and controls (heating, cooling, mechanical ventilation and shading).
- TRNSYS (<http://sel.me.wisc.edu/TRNSYS/> or <http://www.transsolar.com>) [Flamant, G, et al (2004); Crawley, D, et al (2005)]  
This tool has been in use for more than 25 years to simulate the dynamic thermal behaviour of the building and systems. The modular approach includes a graphical interface, a simulation engine and an extensive library of components. This software can be coupled with COMIS (<http://epbl.lbl.gov/COMIS/>), thus allowing for multizone airflow analysis. Special “Types” (i.e. routines) have been developed worldwide by different research institutions for the AIF simulation (see e.g. section 4.3.3.1).
- ESP-r (<http://www.esru.strath.ac.uk>) [Flamant, G., et al (2004) ; Crawley, D, et al (2005)]  
ESP-r is an open source program developed by the University of Strathclyde, Glasgow, Scotland. Its a transient energy simulation program capable of modelling the energy and fluid flows within combined building plant systems when constrained by control actions and subjected to dynamically varying conditions.
- TAS (<http://ourworld.compuserve.com/homepages/edsl>) [Flamant, G., et al (2004)]  
TAS is a suite of software products that simulate the dynamic thermal performance of buildings and their systems, accessing environmental performance, conducting a natural ventilation analysis, etc. The main module (A-TAS, building designer) performs a dynamic simulation with integrated natural and forced flow. The module may also be coupled with

HVAC systems and a controls module (TAS Systems). A third module (Tas Ambiens – 2D CFD) produces a cross section of micro climate in a space.

- ENERGYPLUS (<http://www.eere.energy.gov/buildings/energyplus/>) [Crawley, D., et al (2005)]

EnergyPlus is a new-generation building energy simulation tool based on DOE-2 and BLAST, with numerous added capabilities, including the possibility of third party module and interface development. It is a modular system that is integrated with a heat balance based zone simulation that models multi-zone airflow (through fully integrated COMIS), radiant heating and cooling and PV simulation. There are limitations to modelling DSF with this software. Particularly, it is difficult to model cavity placed shading devices.

- ECOTECH ([www.ecotec.com](http://www.ecotec.com)) [Crawley, D., et al (2005)]

ECOTECH is a highly visual and interactive whole building design and analysis tool that links a comprehensive 3D modeller with a wide range of performance analysis functions. Thermal energy, lighting, shading, acoustics, resource use and cost aspects can be simulated and analyzed. Since this program is able to handle geometries of any size and complexity, it is tailored for holistic approaches to the building design process.

### **4.3.3 Numerical Analysis Methodologies**

This category of tools gathers purposely developed simulation models aimed at the detailed simulation of the thermo fluid dynamic phenomena that takes place in the normal operation of an AIF. They typically consist of sophisticated numerical models specifically developed by research groups and, so far, they are not commercially available. Their use requires a quite high level of expertise and they have not yet been implemented into an easy-to-use design tool with a friendly interface. In the following sections a brief overview of some numerical analysis methodologies developed, tested and applied during the Annex 44 research activities will be presented.

More details of these simulation models are resumed in Appendix 4A and 4B. For a full description and validation of these models, the reader can refer to the literature listed in the references.

#### **4.3.3.1 Dynamic Airflow Model for Buildings**

In order to simulate the thermal behaviour of DSF, a purposely developed “type” (i.e. a specific additional routine) has been written and linked in TRNSYS. This resulted in a combined thermal and airflow simulation model, TRNSYS and TRNFLOW (coupled with COMIS), that was used to analyse the influence of DSF on the overall building energy balance. The analysis method was validated against measurements made at a real scale building [Haas, M. (2008); Haas, M. *et al*, (2008), (<http://dx.doi.org/10.1016/j.enbuild.2008.11.008>)]. Figures 4.5 schematically sketch the vertical section of the modelled façade and building (figure 4.5 left: scheme of the experimental apparatus used to monitor the real façade performance, figure 4.5 right: scheme of the nodes of the calculation network).

Figure 4.6 shows, as an example, a comparison between measured (symbols: *\_m*) and simulated (symbols: *\_sim*) results.

This tool revealed to be effective in conducting an overall assessment (i.e. coupled AIF and building simulation) of the energy and thermal (comfort issues) performance of the system.

The level of details in the AIF simulation is high enough to provide reliable estimate of the indoor climate conditions and of the energy fluxes through the façade. However, it is not enough to perform simulations aimed at the design and optimization of the façade and façade components.

The model is not, so far, commercially available.

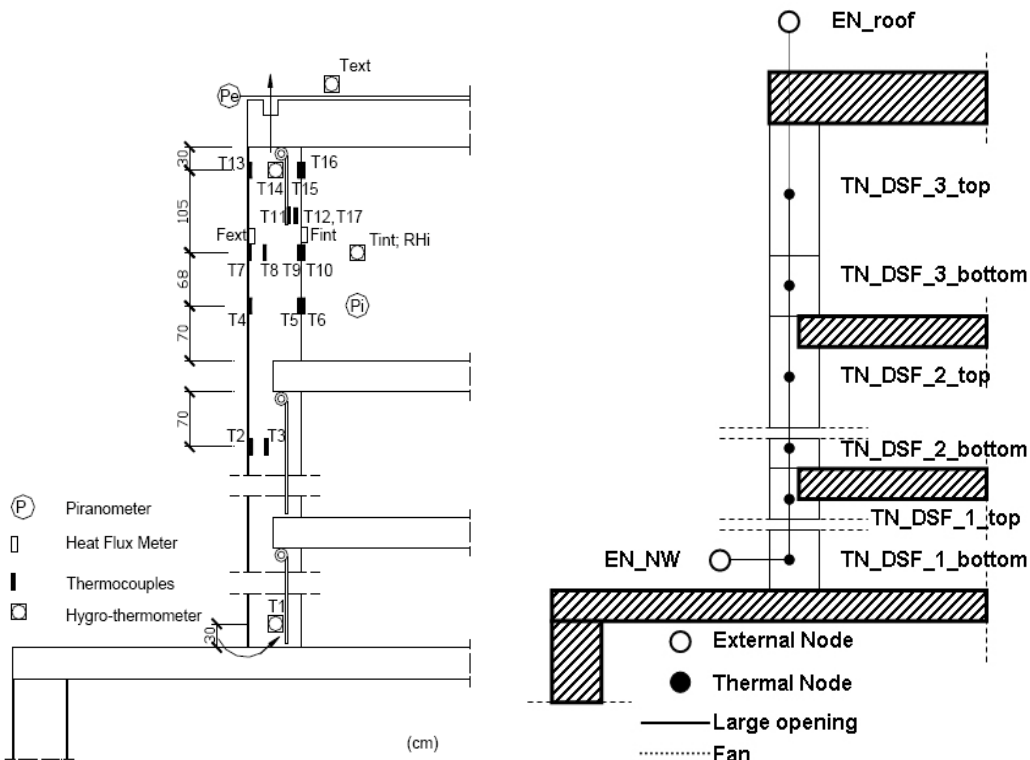


Figure 4.5 – Sketch of the measured façade and numerical model.

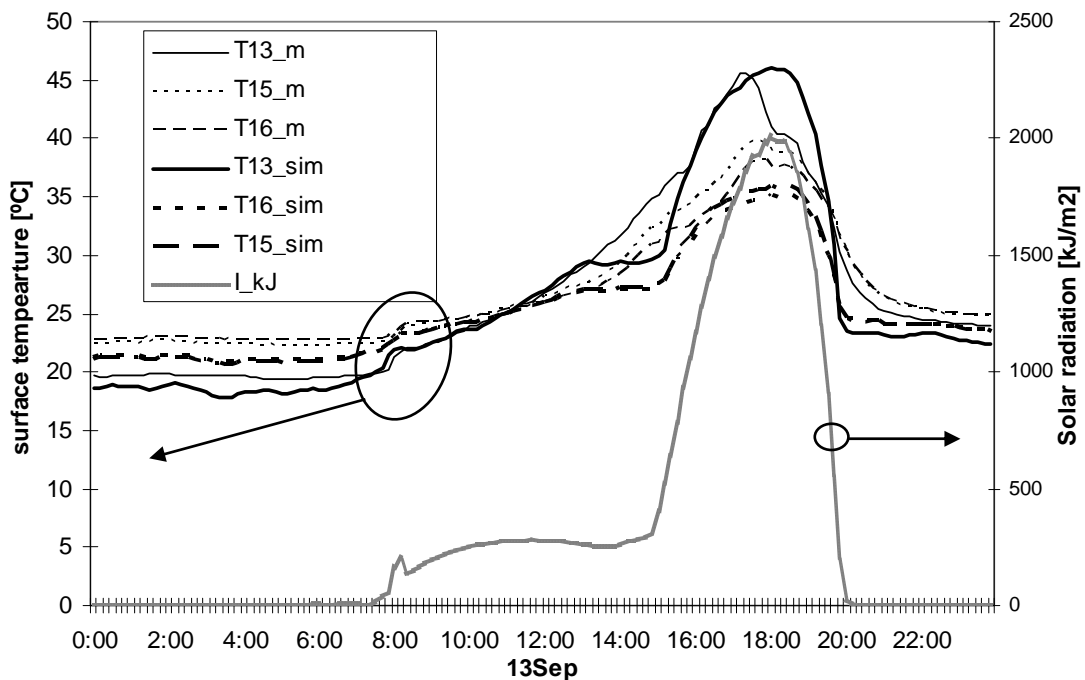


Figure 4.6 – Measured and simulated results.

#### 4.3.3.2 The Concordia University model

Another analysis method has been developed at Concordia University – Canada. It was developed, in particular, to analyse the combined use of AIF and TMA elements. Two models were developed: one for mechanically and the other for naturally ventilated AIF. These tools are composed of a thermal and an airflow model (only for naturally ventilated base-case). They are able to predict

temperature distribution, heat fluxes and energy needs of attached-room to AIF to keep room temperature at set point. The model for naturally ventilated AIF is capable of predicting airflow rate of AIF, as well. These models have been implemented into a whole building energy simulation tools, TRNSYS, combined with CONTAM [Teshome, E. J. (2006)].

The two models were verified with two test-cell facilities: mechanically-ventilated model was verified with TWINS test facility located in Politecnico di Torino (see section 4.3.4.1) and naturally-ventilated with a test-cell facility in Technical university of Munich. Generally, there is a good agreement between measurements and simulation results in winter and summer. At daytime, results show less agreement due to uncertainties of angular properties of AIF transparent components, solar distribution, convection coefficient and the amount of long-wave heat transfer rate between AIF and attached-room (due to lack of room surface temperature measured data). Between winter nighttimes and summer nighttimes, winter shows more deviation due to steeper temperature gradient with outdoor air. Uncertainties of airflow modelling parameters are higher for the naturally-ventilated base-case than the mechanical counterpart. However, the maximum deviation was always below  $|2.6|$  K.

Furthermore, in order to identify what source of uncertainty weights more on the simulation result a sensitivity analysis was also performed (details of this study can be found in Teshome, E. J., 2006). The model is not, so far, commercially available.

#### 4.3.3.3 Mechanically ventilated AIF model (PoliTo)

A further numerical analysis methodology was developed at the Department of Energetics - Politecnico di Torino. It is an approach based on zonal-modelling and it is aimed at the detailed simulation of the thermal behaviour of mechanically ventilated AIF. The model was implemented adopting the block algebra approach in the Simulink/Matlab® environment [Zanghirella F., (2008)]. The model is intended to be used as a design tool. It is particularly suitable for sensitivity analysis.

The system is simulated through an equivalent network, in which each node condenses the properties of macroscopic part of the system (figure 4.7a)

The centre vertical section of the façade is considered, neglecting the effects due to the frame. The façade is discretized in several horizontal zones (one over the other) connected by means of the air flowing in the ventilated gap (figure 4.7b). Along the horizontal direction the heat flux is assumed to be one-dimensional and orthogonal to the façade (2D model).

Each horizontal zone consists of solid vertical layers, either transparent (glasses) and /or semitransparent (shading device), separated by closed (as in the case of a double glass) or mechanically ventilated cavities. Heat and energy conservation equations are written and solved for each horizontal zone.

For each solid layer the absorbed solar radiation is assessed and convective and the infrared fluxes exchanged with the adjacent elements are calculated. In figure 4.8 a scheme of the heat fluxes calculated for each horizontal zone is shown.

Each glass pane is discretized adopting three layers (figure 4.9). The absorbed, reflected and transmitted solar radiation (direct and diffuse) is calculated by means of the “net radiation method” (Edwards, 1977), and the absorption, transmission and reflection coefficient of each material have to be known. In transparent layers, the diffuse radiation is considered as beam radiation with an equivalent angle of  $60^\circ$  [Duffie and Beckman, (1991)]. The façade is considered as a grey body surrounded by black bodies, the sky temperature is calculated by means of the Swinbank model [Ong (2003)]. The convection with the outdoor environment is calculated as natural convection in case of absence of wind, and it turns to a mechanically driven convection when the wind velocity increases. The convection with the indoor environment is assessed by means of the Alamdari and Hammond model [Alamdari and Hammond, (1983)] in case no heating device is present, or with the Khalifa and Marshall model [Khalifa and Marshall, (1990)] if a heating or cooling device are present in the indoor environment.

The shading device is considered as a semitransparent layer with no thermal resistance.

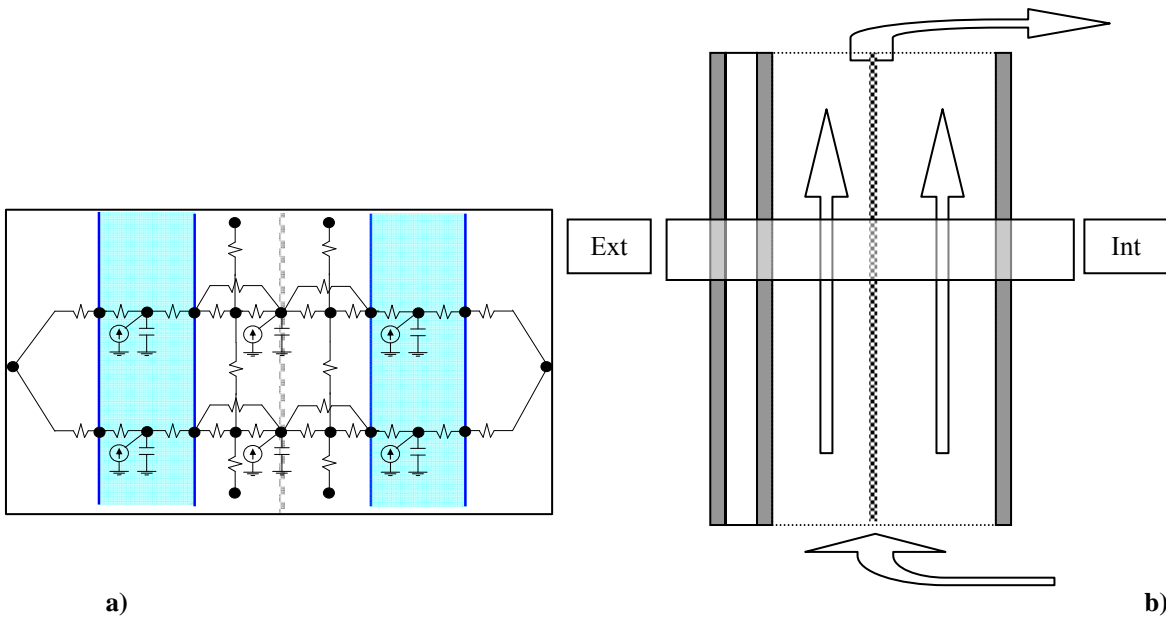


**Fig. 4.7 - Façade discretization and nodes network.**

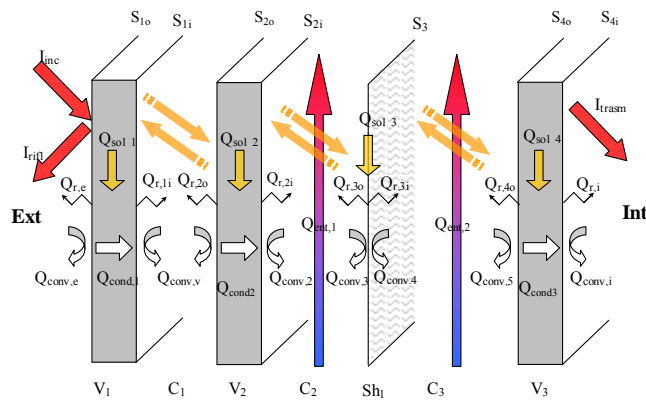


**Fig. 4.8 – Heat fluxes for each horizontal zone.**

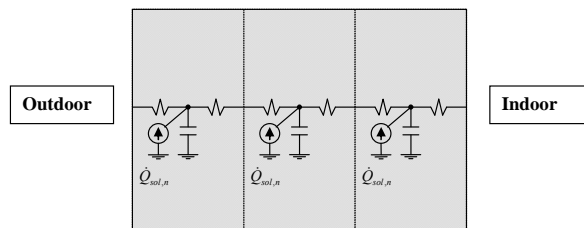


**Fig. 4.9 – Glass pane discretization.**

The input parameters required by the model are:

- time profiles of:
  - o outdoor air temperature,
  - o indoor air temperature,
  - o irradiance (diffuse and direct),
  - o direct solar radiation incident angle,
  - o wind speed,
- airflow rate into the air cavity
- façade geometry,

- thermophysical and optical properties of materials.

The model provides as outputs: the temperature of each node and the heat fluxes through the various layers and cavities.

The model was validated using the experimental data obtained in the measurement campaign of the climate façade carried out using the TWINS test facility at the Politecnico di Torino (see section 4.3.4.1 and Appendix 4C). The comparison between simulated and measured data showed a good accuracy as far as the glass and air temperatures are concerned (figures 4.13 and 4.14, the percentage root mean square error, PRMSE – see Appendix 4A – for all the tested cases was always between 2.6% and 12.2%). The heat fluxes were, instead, overestimated (the root mean square error, RMSE – see Appendix 4A – resulted to be:  $10.3 \text{ W/m}^2 < \text{RMSE} < 13.6 \text{ W/m}^2$ ).

Figures 4.10 and 4.11 show, as an example, the measured and predicted time profile of glass/air temperatures and specific heat fluxes for some of the tested configurations.

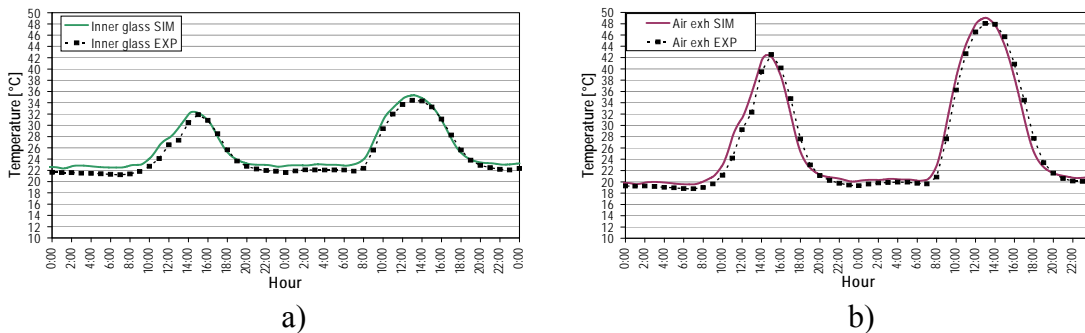


**Figure 4.10 – Simulated (continuous lines) and measured (symbols) glass (a) and air (b) temperatures, roller screen configuration.**

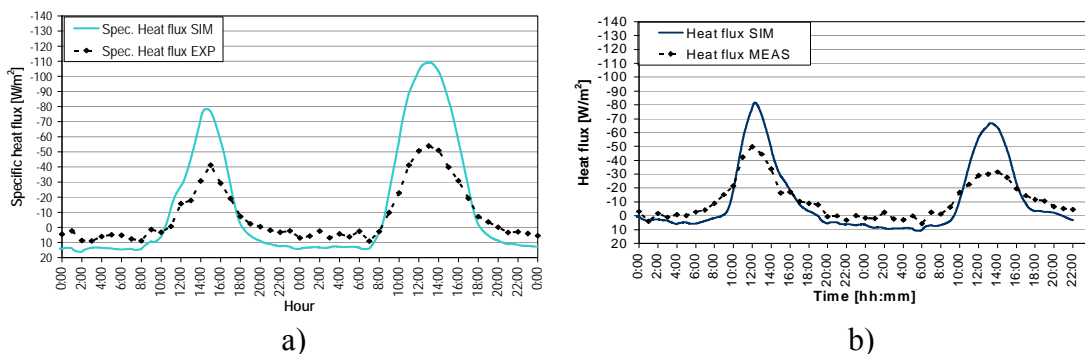


**Figure 4.11 – Simulated and measured heat fluxes, roller screen (a) and venetian blind (b) configuration.**

More details about this numerical model and its validation can be found in Appendix 4A and in [Zanghirella F., (2008)].

This numerical analysis model has been applied for different configurations of AIF (both mechanically and hybrid ventilated) and proved to be effective for the detailed analysis of the component. It has been used to develop new concept of AIF and to do their detailed thermal design and optimization.

The model is, so far, not commercially available (information can be found/requested at [www.polito.it/TEBE](http://www.polito.it/TEBE)).

A set of experimental data, collected by means of the TWINS experimental test rig was prepared within the Annex 44 activity in order to provide a database for the simulation tools validation.

This set of data is available at the Annex 44 web site.

#### 4.3.3.4 DSF Numerical Model (IST – Portugal)

Another network numerical model for modelling both airflow and temperatures in double skin façade was developed at IST – Portugal [Gomes, M.G. and Moret Rodrigues, A., (2006)]. It is intended to be used, besides by researchers, also by designers – architects, engineers - and façade manufacturers, there was an attempt to make the interface as much user-friendly as possible.

It is a two-dimensional model where the section of the double skin façade is divided into “n” vertical layers (including a shading layer as an additional one). Each layer is, in turn, divided into “m” horizontal slices, as schematically illustrated in Fig. 4.12. The model is intended to predict both the thermal and the ventilation performance of different configurations of double skin facades and, as a consequence, uses two coupled iteration cycles: the temperature and the airflow cycles.

The first one determines the temperature distribution depending on the net infrared radiation, convective and conductive heat transfer and the absorbed solar radiation. The second calculates the airflow rate for the temperature distribution assessed in the previous cycle, using the Newton-Raphson method. Heat balance equations are written for each node of the DSF.

A proper model for the radiant analysis of the venetian blind is also implemented. It is based on the net radiation method, considering a fictive cavity between two adjacent slats. The model allows the assessment of the radiative properties of a venetian blind as a function of the boundary conditions and of the slats position [Gomes, M.G. and Moret Rodrigues, A., (2006)]. Some numerical results obtained from the model were compared with experimental measurements carried out in an outdoor test cell [Gomes, M.G., Santos, A. and Moret Rodrigues, A., (2008)] (see also section 4.3.4.2 and Appendix 4D). As an example, figure 4.13 shows the predicted and measured solar irradiance in different positions, within the thickness of the façade, for a 45° tilt angle of the venetian blind slats (simulation performed under clear sky conditions - CSC). The predicted and measured overall solar transmittance is shown in figure 4.14.

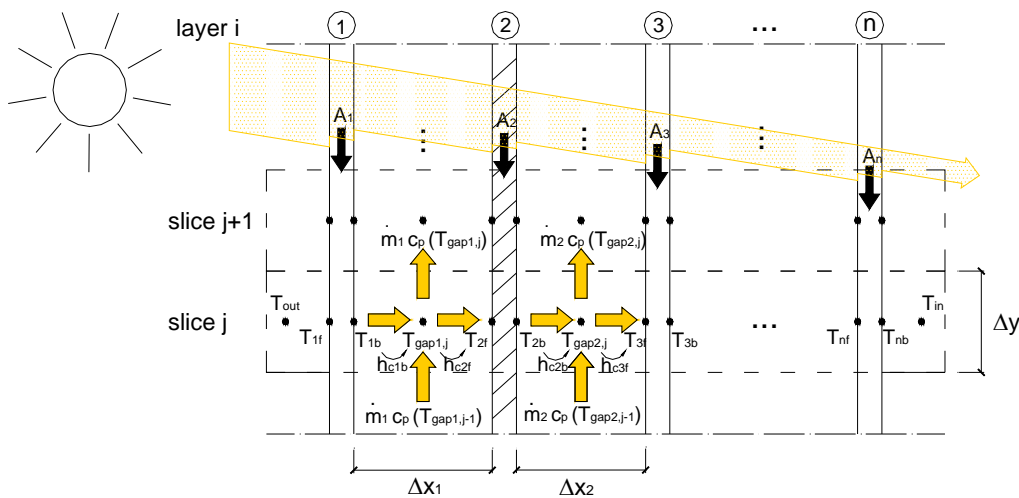


Figure 4.12 – Scheme of the network model.

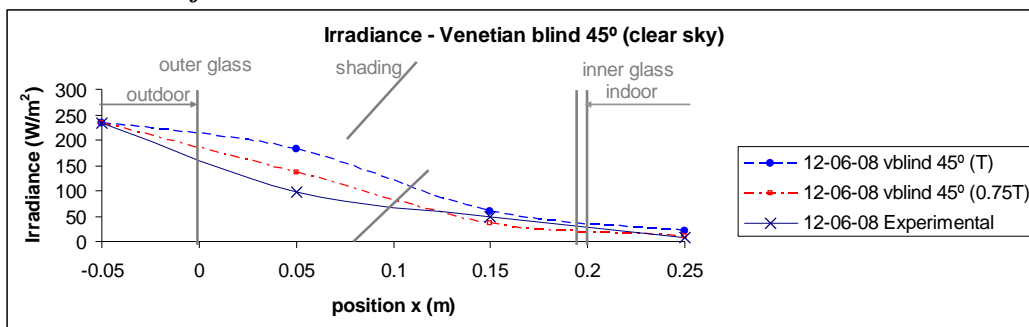


Figure 4.13 - Irradiance for different slat angles under Clear Sky Conditions. Experimental and numerical data (numerical results obtained for  $T$ , the glass manufacturer transmittance, and  $0.75T$ ).

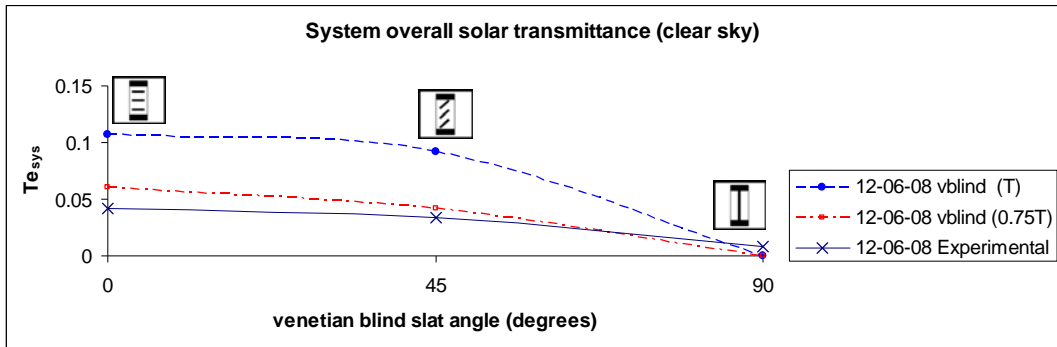


Figure 4.14 - System overall solar transmittance for different slat angles under CSC.

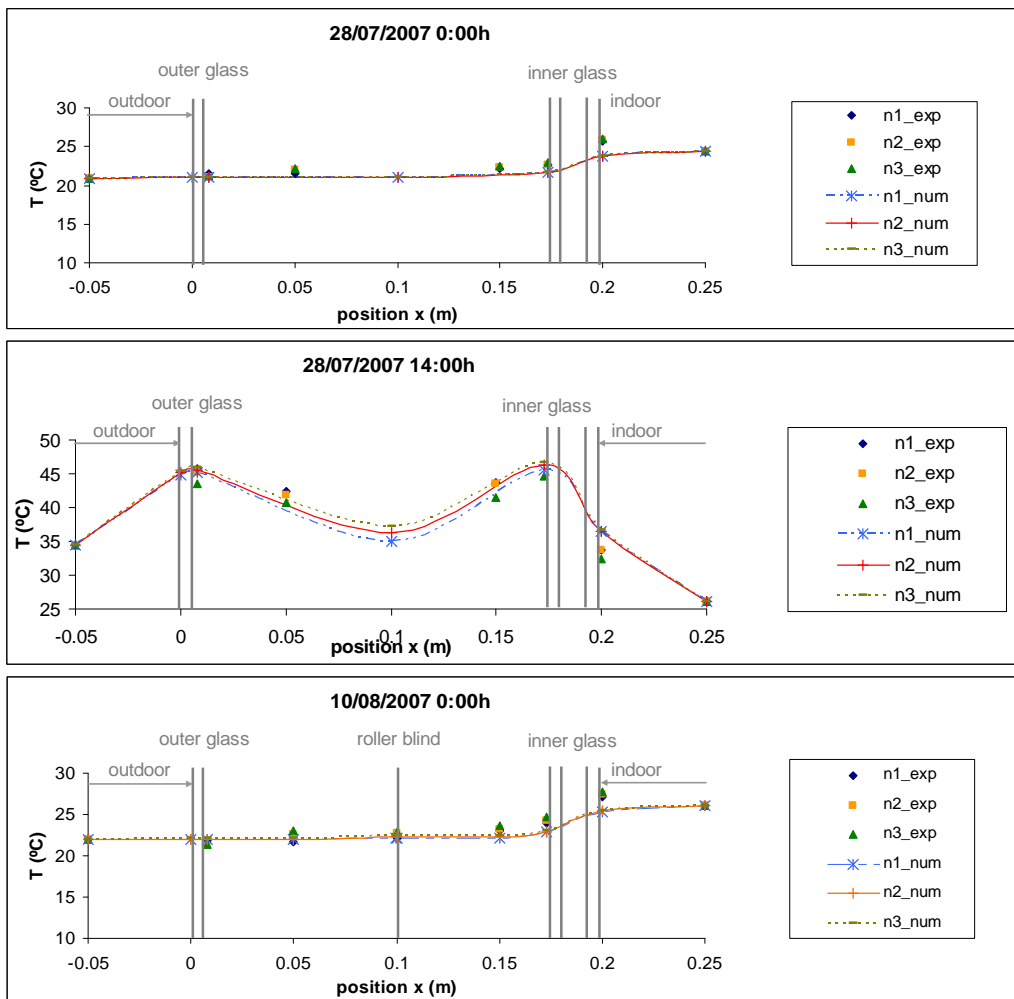


Figure 4.15 - Comparison between experimental (LNEC test cell – section 4.3.4.2) and numerical results.

Finally, the validation of the simulation model, as far as the temperature field prediction is concerned, is still underway. The preliminary results, nevertheless, show promising achievements, as shown in figure 4.15, where measured and simulated temperature profiles across the façade are plotted.

More details about this model and its validation can be found in Appendix 4B. The model has been applied for different configurations of AIF.

The model is, so far, not commercially available.

#### **4.3.4 Experimental Analysis: test rig, performance parameters and measurement procedures**

The experimental analysis of an AIF requires specific techniques and facilities to be performed. Moreover, the typical performance parameters, used to evaluate and analyse traditional, non responsive, building envelope components (like e.g the U-value) do not apply for the majority of AIF configurations.

Furthermore, it has been demonstrated [Corgnati et al., (2007)] that adopting field measurements it is extremely difficult to perform sensitivity analyses and, hence, the use of such procedures for a product development and optimization results almost impossible.

These issues pose major challenges and need to introduce innovative methods and indices to correctly address the thermo physical behaviour of AIFs.

For these reasons, during the Annex 44 activity, some test rigs were purposely designed, developed and optimized. Measurement procedures and data analysis methods were conceived and tested.

The aim was to set-up and select experimental techniques suitable for the analysis of AIF.

##### **4.3.4.1 Politecnico di Torino test facility - TWINS**

In order to make sensitivity analyses possible in an easy and reliable way, a suitable laboratory facility has been designed and built at the Politecnico di Torino [Zanghirella, (2008), Serra et al. (2009a, 2009b)].

The experimental test rig, called TWINS, consists of two identical test cells, one used as a reference (test cell A) and left unchanged during the monitoring campaign, the other adopting different solutions of active façades (test cell B). The use of a reference test cell allows comparisons between various configurations and gives the possibility to analyse the influence of some façade components (such as shading devices, width of the air gap, internal or external glazing, and air flow rate), even with different boundary conditions.

Test cells A and B are fully exposed to the solar radiation, as the façades are facing south. The indoor air temperature of both cells is controlled by means of a full air system and is kept at a set-point of about 20°C in winter, 26°C in summer and 23°C during mid season.

Quantities that can be measured are: air, glass and frame temperatures, incident and transmitted irradiance, heat fluxes, ventilation air flow rate, pressure difference.

The reference façade is typically monitored by means of 18 sensors connected to a datalogger. The measurement apparatus for the tested AIF may consists of over 50 different sensors and probes.

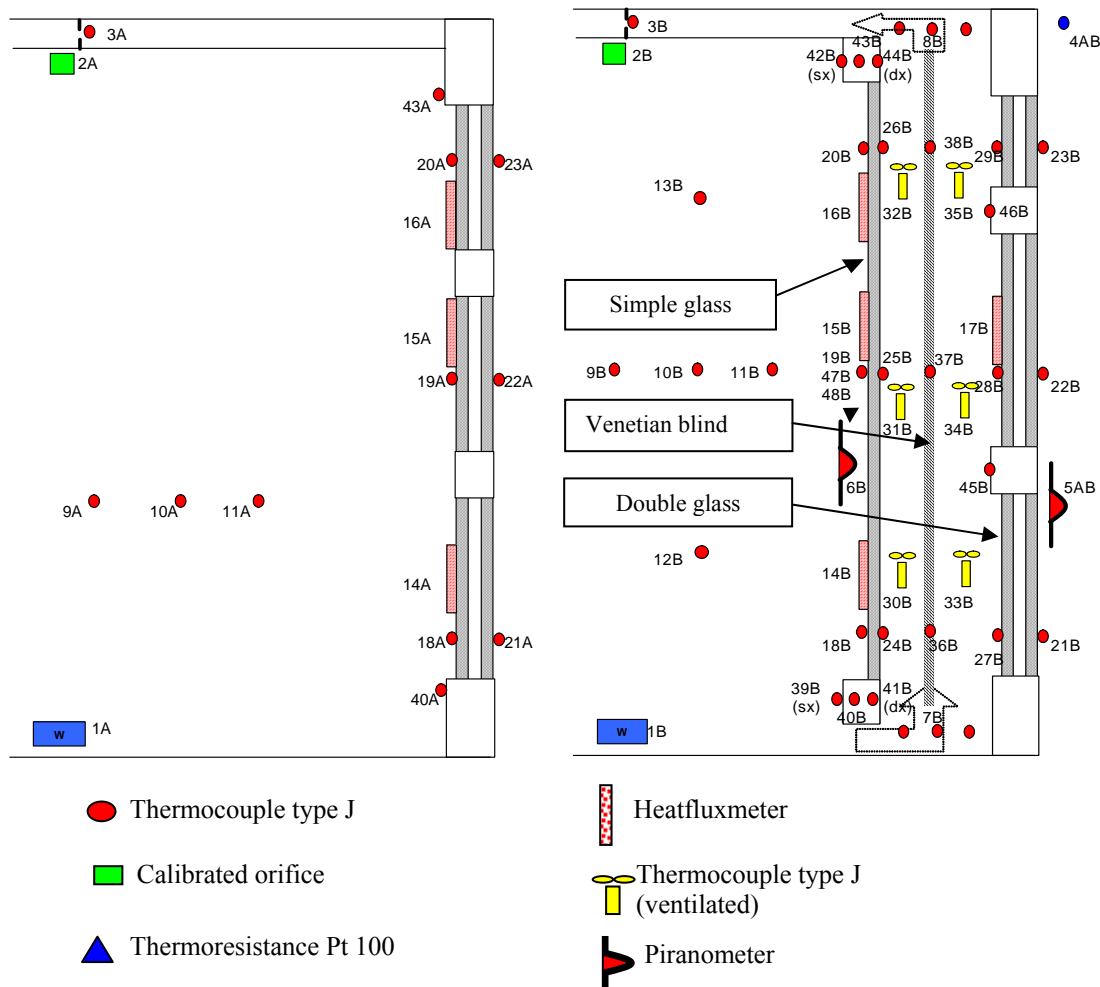
In figure 4.17 a scheme of the sensors set up for the reference and the tested façade is shown.

Figure 4.16 shows a picture of the TWINS apparatus.



**Figure 4.16 – pictures of: a) Façade under test (in this case a hybrid ventilated façade), b) Reference façade.**

Two different AIF were investigated during the Annex 44 research activity: a mechanically ventilated climate façade and a hybrid ventilated DSF with an outdoor air curtain ventilation scheme (with microfans powered by PV modules). A résumé of these results is presented in Appendix 4C. A more detailed description of the TWINS apparatus and of the measurement campaigns can be found in [Micono et al (2006)], [Perino et al. (2007)], [Zanghirella, (2008)].



**Figure 4.17 – Scheme of the sensors for the reference and the test façade (for this test cell, the set-up may vary, depending on the type of component under test).**

#### 4.3.4.2 Experimental AIF module – LNEC

In order to evaluate the thermal behaviour of transparent double skin façades, LNEC (39° N) assembled a nearly south facing (160°) test facility allowing changing among some of the possible configurations.

This experimental test rig is conceptually similar to the TWINS facility; it makes use of test cells and is suitable for making comparative studies between different technologies (figure 4.18).

The test cells can operate as a ventilated double skin façade with reversible air flow (type c, section 4.2.2, figure 4.3). In this way it is possible to test configurations such as: Outdoor Air Curtain (OAC), Indoor Air Curtain (IAC), Exhaust Air (EA), or Supply Air (SA). It is also possible to use any kind of ventilation type, the layout being established as a box window (BW) or, as a limit, as a Buffer (Bf) configuration.

**Table 4.1 – Test cells - materials main characteristics.**

Material	$\rho$ [kg/m <sup>3</sup> ]	K [W/mK]	$c_p$ [kJ/kg K]
Concrete	2300	1,75	0,880
AAC	650	0,20	1,000
Mortar	1950	1,15	0,653



**Figure 4.18 – The AIF at LNEC and louver detail.**

The glazed façade under test may have a size of 2.5 m height and 3.5m length, the gap depth being of 0.20 m. Different configurations can be built.

For the analyses performed during the Annex 44 activity the following features were adopted for the façade: the outer glass pane has a simple annealed 5 mm glass ( $U=5,7$  W/m<sup>2</sup>/K;  $T_v=87\%$ ;  $T_e=75\%$ ;  $A_e=18\%$ ;  $g=0,80$ ) and the inner one is a double glass (6-16-5), with a low emissive coating facing the gap ( $U=1,4$  W/m<sup>2</sup>/K;  $T_v=69\%$ ;  $T_e=36\%$ ,  $A_e=34\%+3\%$ ;  $g=0,41$ )<sup>1</sup>. The shading device is a grey roller blind.

The gap has eight sets of louvers, 0.225 m high and 1.63 m long each, four in the outer pane and four in the inner one. The solar shading device blades have an adjustable position. They can be set between fully closed and fully open (blades perpendicular to the façade plane).

The test cells are bounded by surfaces whose main features are listed in table 4.1.

A major difference from the TWINS facility lies on the fact that the LNEC is a free running indoor temperature system. Furthermore, the ventilation scheme at LNEC is fully natural (this implies the need to continuously monitor the air flow rate through the façade).

The main idea of the tests to be performed at LNEC's facility is to evaluate the thermal performance of a set of different DSF configurations.

Figure 4.19 shows the scheme of the AIF arrangements tested during the Annex 44 measurement campaign and sketches the test rig configuration and the sensors set up.

In the LNEC test facility the following parameters can be measured: temperature differences, like the one between the bulk air gap and outdoor or indoor air; the total energy entering the inner space,  $q_i$  = heat flux + radiation, the dynamic insulation,  $\epsilon$ , as defined in equation (2).

The ventilation air flow rate in the air gap is estimated through the measurements of the pressure difference between the inlet and outlet opening (details about this measurement procedure are available in Appendix 4D and in [Marques da Silva, (2004)]).

During the experimental campaign performed in the frame of the Annex 44 activities, a value of about 900 m<sup>3</sup>/h with no shading (assumed  $C_d=0.55$ ) was measured for a sunny day. This datum was confirmed by independent measurements done by means of a tracer gas equipment.

Finally, the environmental parameters can also be measured: outdoor and indoor temperature (with Gemini stand alone loggers); wind velocity and direction (NRG with Ammonit logger); and solar

<sup>1</sup> “T” and “A” standing for the transmissivity and absorptivity, “v” refers to the visible part of the spectrum and “e” refers to energy.

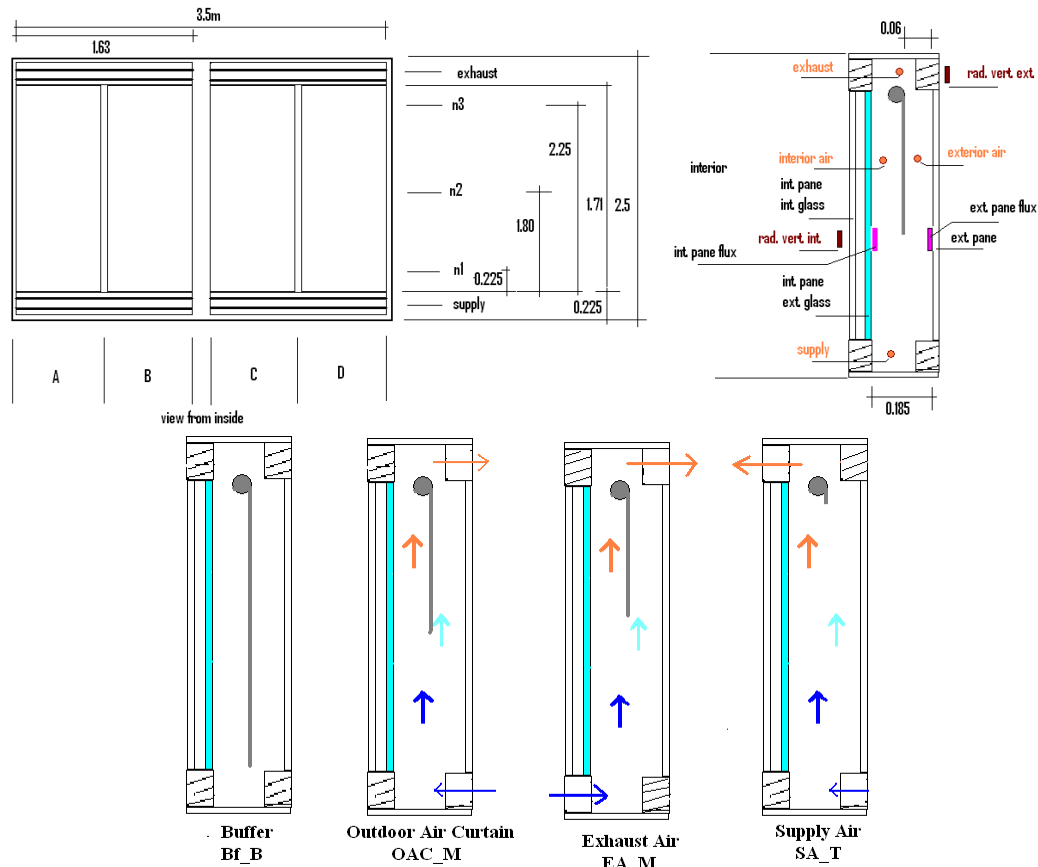


**Figure 4.19 – Scheme for measuring levels and test facility sensors and the tested configurations.**

radiation on horizontal and vertical (indoor and outdoor) planes (with pyranometer). Measurements can be recorded every 10 minutes like averages from 30 seconds readings.

A monitoring campaign was carried out by means of this experimental facility between July 2007 and January 2008. Different double skin façade configurations and two positions of the shading device (midway between glazed panes and closer to the inner pane) were tested.

A résumé of these measurement results is presented in Appendix 4D.

#### 4.3.4.3 Performance parameters definition for transparent AIF

As previously mentioned, the performance of a transparent AIF in terms of energy savings and comfort conditions can't be simply assessed adopting traditional parameters, such as the U-value.

During the experimental campaigns performed within the Annex 44 activities, the following performance parameters revealed to be useful for analysing the AIF behaviour:

- a) Pre-heating efficiency,
- b) Dynamic insulation efficiency,
- c) Average "long-wave" heat flux through the façade,
- d) Thermal total flux through the façade,
- e) Total daily energy crossing the façade,
- f) "Long-wave" daily energy crossing the façade,
- g) Normalized heat flux,
- h) Normalized transmitted thermal energy,
- i) Normalized surface temperature of inner glass,
- j) PMV and percentage of the floor area in comfort conditions.

These parameters can be easily determined either through numerical simulations or by means of measured quantities. To measure all the listed indices a laboratory test rig based on a reference cell and a test cell is required, however, some of them (indices a through f) can also be assessed by

means of field measurements. The quantitative definition of the proposed evaluation parameters is given in the following part of this section.

The proposed indices were assessed and tested on the basis of the measurements done in the TWINS facility (section 4.3.4.1). Furthermore, they were also verified by means of the results collected with the LNEC facility (section 4.3.4.2). In Appendix 4C.2 and 4D.2, a resume of the results obtained during the experimental campaigns are presented and discussed.

*a) Pre-heating efficiency,  $\eta$*

The capacity of the façade to pre-heat the ventilation air (flowing inside the air gap) is evaluated by calculating the pre-heating efficiency, defined as [DiMaio and Van Paassen, (2001)]:

$$\eta = \frac{T_{\text{exh}} - T_{\text{amb}}}{T_{\text{amb}} - T_o} \quad (1)$$

Where:

$T_{\text{exh}}$  is the temperature of the air extracted from the façade

$T_{\text{amb}}$  is the temperature of the air inside the test cell

$T_o$  is the temperature of the outdoor air

The pre-heating efficiency is a parameter representative of the performances of the façade in winter and mid season conditions, when the external temperature is lower than the indoor temperature.  $\eta$  represents the ratio between the enthalpy flux related to the air that flows in the gap and the enthalpy flux required in order to heat the ventilation air. By analysing the value that  $\eta$  assumes it could be assessed if the façade isn't doing any energy recovery ( $\eta < 0$ ), if the façade is preheating the extracted air ( $0 < \eta < 1$ ), or if the façade can completely compensate the losses for ventilation and, eventually, some heat losses through the envelope ( $\eta \geq 1$ ).

*b) Dynamic insulation efficiency,  $\varepsilon$*

In order to evaluate the performance of the façade in terms of the reduction of the entering heat gains, the dynamic insulation efficiency,  $\varepsilon$ , may be adopted.

$\varepsilon$  was introduced in [Corgnati et al., (2007)] and is defined as:

$$\varepsilon = \frac{\dot{Q}_R}{\dot{Q}_{IN}} \quad (2)$$

Where:

$\dot{Q}_R$  is the heat flux removed by the air that flows in the gap of the façade;

$\dot{Q}_{IN}$  is the total heat flux entering the façade through the exterior surface.

From a phenomenological point of view the dynamic insulation efficiency represents the amount of total thermal load on the façade that is removed by the ventilation of the air gap.

The dynamic insulation efficiency is a parameter representative of the performance of the façade for summer and mid season (cooling mode).

*c) Average "long-wave" heat flux through the façade*

The average "long-wave" heat flux  $\dot{q}_{lw,i}$  is the mean specific heat flux that cross the façade and enters into the indoor environment (that is, the specific heat flux exchanged at the inner surface of the façade). The term "long-wave" is conventionally used here to mean the sum of the convective and of the radiative (infrared – long wave) contribution. This "long-wave" heat flux can be measured by means of heat flux meters placed on the façade surface facing the indoor environment.

d) *Thermal total flux through the façade*

The thermal total flux  $\dot{q}_{t,i}$  is the sum of the radiative short-wave specific heat flux,  $\dot{q}_{s,i}$ , measured by al pyranometer located in front of the inner glass pane, and the “long-wave” specific heat flux  $\dot{q}_{lw,i}$  (measured by means of heat flux meters).

e) *Total daily energy crossing the façade*

The total daily energy is the integral of the thermal total flux over the time interval from 8:00 am to 8:00 pm (considered representative of the typical office occupation time):

$$E_{t,i,d} = \int_{8am}^{8pm} \dot{q}_{t,i}(\tau) d\tau \quad (3)$$

f) *“Long-wave” daily energy crossing the façade*

The “long-wave” daily energy is the integral of the “long-wave” heat flux from 8:00 am to 8:00 pm:

$$E_{lw,i,d} = \int_{8am}^{8pm} \dot{q}_{lw,i}(\tau) d\tau \quad (4)$$

g) & h) *Normalized heat flux and transmitted thermal energy*

The influence of the airflow rate and of the use of different solar shading devices on the thermal fluxes entering the indoor environment can be performed using the so-called normalized heat fluxes and normalised thermal energies, that is:

$$\varphi_X = \frac{\dot{q}_{X,B} - \dot{q}_{X,A}}{\dot{q}_{X,A}} \quad (5)$$

$$\Sigma_X = \frac{E_{X,B} - E_{X,A}}{E_{X,A}} \quad (6)$$

Where the subscript  $X$  must be replaced with “lw” when considering “long-wave” heat fluxes and “long-wave” thermal energies, and must be replaced with “t” when considering total heat fluxes and total thermal energies. The subscript “A” refers to quantities measured on the façade under test (test Cell A), and the subscript “B” refers quantities measured on the reference façade (test Cell B). The assessment of these two parameters requires, necessarily, the use of a “reference and test cells” experimental facility.

i) *Normalized surface temperature of inner glass*

In order to compare the thermal comfort performance achievable with an AIF façade with those provided by a traditional glazed façade, the normalized surface temperature of the inner glass,  $\theta_{gi}$ , can be used. This index is defined as:

$$\mathcal{G}_{gi} = \frac{t_{gi,B} - t_{gi,A}}{t_{gi,A}} \quad (7)$$

Where the subscript A refers to the façade under test (test Cell A), and the subscript B refers to the reference façade (test Cell B).

$\mathcal{G}_{gi}$  represents the percentage of increase (or decrease) in the internal surface temperature of the AIF with respect to the internal surface temperature of a reference façade.

The AIF shows a better performance, in terms of thermal comfort, if  $\theta_{gi} > 0$  during winter and midseason and if  $\theta_{gi} < 0$  during summer.

The assessment of this parameters requires, necessarily, the use of a “reference and test cells” experimental facility.

*j) PMV and percentage of the floor area in comfort conditions*

It is defined as the percentage of the floor area in comfort conditions.

Comfort conditions are assessed by means of the Predicted Mean Vote (PMV). Accordingly to international standard ISO 7730/2006, three different comfort classes can be adopted, depending on the acceptable interval for the PMV value:

- 0.2 < PMV < + 0.2, corresponding to a “class A” building;
- 0.5 < PMV < + 0.5, corresponding to a “class B” building;
- 0.7 < PMV < + 0.7, corresponding to a “class C” building.

Moreover, considering that comfort conditions in the presence of a fully glazed building envelope, are not only related to temperature values of the boundary surfaces of the indoor environment, but they also depend on the irradiance entering through the glazed façade, a modified PMV can also be used. In particular, the Windows and Daylighting Group at LBLN, Berkeley [Sullivan, (1986)], suggest to adopt the PMV\* index, defined as:

$$PMV^* = PMV + \Delta PMV \quad (8)$$

where:

$$\Delta PMV = I_{in} * 0,0024 \quad (9)$$

Being  $I_{in}$  the irradiance entering the indoor environment through the transparent façade.

## 4.4 Guidance and recommendation

In general, among the several stake holders of the construction field, there is a positive opinion concerning AIF. Nevertheless sometimes excessive optimistic views (due to the lack of full knowledge) lead to less careful design and to poor performance. Furthermore, it frequently happens that architects focus primarily on concept decision and façade appearance and do not take into a proper account the influence of different design choices on the energy and comfort performance.

Within AIF, fully glazed facades are the ones demanding exceptional care in the design, because the margin for error shrinks as the glass area increases.

AIF performance depends on climate, façade orientation and type of façade, requiring a holistic approach since the preliminary design phase, as the façade is an element of the global building system. Sometimes, integration with HVAC and BEMS (building energy management system) may lead to compromise situations due to incompatible optimal solutions as, for example, maximize comfort and minimize energy consumption or ventilation (IAQ) and sound insulation (vents opening).

Special care should be paid to double skin facades as their core behaviour lies in the gap formed between inner and outer panes of the façade. Decisions about the material to use, configuration of the solar shading device and type of arrangement (that is, flow path and ventilation) are then of high importance. In fact, it has been highlighted that the critical problem of DSF is typically due to overheating phenomena. This drawback is not exclusive of warmer climates, since many of such problems have also been reported in northern Europe. Key point in the design of the façade are then represented by the gap ventilation (strategy and flow rate) and thermophysical properties of glass panes and solar shading devices. Furthermore, during night periods, in the heating season and when the facade receives low amounts of solar radiation, the gap should not be ventilated.

The proper gap depth – from 10 cm to 2 m for known cases – depends on the type of ventilation. For example, natural ventilation in narrow gaps, especially with enclosed shading devices, proves to be difficult, thus increasing the overheating risk.

The inner and outer panes features depends on the use of the air within the gap. For outdoor air curtains the inner pane should provide a thermal barrier and, hence, it should be a double glazed, eventually coated, while the outer pane may have a single glass. For indoor air curtains, usually, the panes layout is reversed, preventing the indoor air to loose heat. Optimal flow path choice depends, among other parameters, on the climate environment. For example in warmer climates, were cooling is the main requirement; outdoor air curtains performs better than exhaust air configuration. Similar conclusions have been found within BESTFACADE project. On the other hand for colder environments the overall performance is similar, but outdoor air curtain configurations, if not properly managed, may increase the energy demand in the heating season [BESTFACADE- WP5 (2007)].

If the façade is used to pre-heat the ventilation air during the winter seasons, an increase of the air flow rate leads to a progressive reduction of the pre-heating efficiency. It is, furthermore, important to control the temperature of the air exhausted by the façade, in order to eventually use it in a heat exchanger.

For many analysed configurations it came out that the pre-heating efficiency is negative for at least 50% of the operative time (i.e the façade cools the air flowing in the gap instead of heating it). This means that the use of the façade as an exhaust of the ventilation system often leads to a reduction of the heat that could be recovered using a traditional heat recovery system located at the exhaust of the HVAC system.

In summer conditions the ability of the façade in reducing thermal loads increases with an airflow rate increase.

Shading devices are enclosed into the gap for protective reasons (against the action of outdoor environment). When lowered they collect a large part of the incident solar radiation and become, thus, the warmer element in the façade, exchanging heat with all the other façade elements, and so lowering both energy and comfort performances. In such conditions the façade interior should be well ventilated in order to remove the heat in excess.

Attention should also be paid to the thermophysical properties of the solar shading device. A solar shading device with high solar absorptance, for instance an aluminium venetian blind, will reach higher temperature values than a shading device with a reflective coating, i.e. a PVC reflecting roller screen. Higher temperatures of the shading device have positive effects in winter time, increasing the pre-heating efficiency of the façade, but lower its capacity to remove part of the solar load (decrease of the dynamic insulation efficiency) during summer time.

From the thermal comfort and energy conservation point of view, an external shading (outside the outer pane) is the best possible solution to prevent excessive solar gains, during the cooling seasons. However, such configuration (if the system is not adjustable) decrease the performance of the façade during the heating season. Furthermore, when the solar shading device is located outdoor the protective action of the outer glass pane is lost and maintenance may become a concern.

Comparing the performance of a climate façade (mechanically ventilated AIF) and of a traditional reflective double glazing façade, in winter conditions the climate façade presents higher temperature values of the inner glass with respect to the traditional one. The climate façade presents a lower risk of local discomfort due to the presence of a cool surface. The effect of the ventilation rate is to lower the temperature difference between the two façades. In winter conditions an increase of the ventilation rate always leads to a lower performance of the façade, both considering energy efficiency and thermal comfort performance issues. In winter, in the presence of high irradiance the climate façade represents an additional radiant surface rather than a source of local discomfort.

In summer conditions the climate façade presents overheating risks in the air gap, reaching inner glass temperatures which may lead to local discomfort problems. The analysis of the normalized surface temperature in summer conditions shows that a lower temperature of the inner glass can be

achieved increasing the air flow rate. In summer, a higher air flow rate, thus, improves both the energy efficiency and the thermal comfort performance of the active façade. Nevertheless, it has to be outlined that, if a climate façade is chosen, the maximum adoptable air flow rate value is strictly related to the flow rate needed for IAQ issues (so higher values can't be justifiable from an energy point of view).

The adoption of a low-e inner glass pane leads to improvements in both the energy and the thermal comfort performance.

A mechanically ventilated façade with a clear single glazing has shown to be able, in summer conditions, to keep a inner glass temperature 11% lower than a traditional (non ventilated) glazed façade with a reflective glass.

For similar boundary conditions, in case of a hybrid ventilated façade with a low-e double glazing (in the inner skin) the maximum temperature reduction is of about 70% and this improvement is mainly related to the adoption of a low-e double glazing and to an increase of the air flow rate in the air gap (in this case, being the air flow path an outdoor air curtain, there are no restrictions or drawbacks in the increase of the air flow rate).

One of the universally recognized advantages attainable with double skin façades is the possibility to effectively manage the wind action for naturally ventilated buildings (specially in case of high rise buildings). In fact, the wind-building interaction determines the building envelope pressure distribution, which has a significant effect on ventilation flows in case of natural ventilation.

A positive effect of the double skin is that turbulent fluctuations are “dumped” due to the combined effect of openings in the inner and outer panes in conjunction with the cavity, which acts as a buffer. This is of particular importance in high-rise buildings where gust loads may induce high peak pressure values [Oesterle, et al (2001)].

A major factor that influences pressure distribution is the building shape. DSF configuration can dramatically change cavity pressures when compared to an “unsheltered” envelope. Figures 4.20 shows, as an example, the distributions of the  $C_p$  values obtained on wind tunnel tests over a 10 storey building, scaled model under an urban boundary layer wind velocity profile, for a normal and double skin façade respectively. Potential difficulties in manoeuvring doors or windows to the cavity may also be affected by such pressure values.

For naturally ventilated facades, stack effect is the main flow driver as the wind plays, usually a negligible role. As a matter of fact for most of the AIF layouts the façade local pressure coefficients are quite similar for the inlet and outlet openings, reducing the driving pressure difference close to zero. The exceptions are multi-storey layouts and facades with ventilation openings (serving the same gap area) on different sides of the building. Another possible influence rises from moderate winds facing a façade causing enough pressure to block exhaust air.

In the end, from the structural point of view, wind constitutes the strongest load on AIF and the present codes are not suited for the analysis of double skin façades [Marques da Silva, et al, (2008), BESTFACADE-WP5 (2007)] (More details about wind interaction are resumed in Appendix 4G).

If from the point of view of thermal comfort the major concern, as previously underlined, is typically due to risk of overheating and high radiant temperatures (and possibly radiant asymmetries), it has to be considered that also the visual comfort and acoustic performance are influenced by the AIF.

In particular, connected to the thermal issues is the daylighting performance, since both these elements are influence by the solar shading device features and use.

In general, from daylighting point of view double skin façades are not significantly different from single skin glazed facades, granting good daylight conditions in areas not far from the façade. However, under sunny sky the shading devices are fully lowered in order to prevent glare and/or overheating of the indoor environment. This frequently leads to the need of artificial light use and has an impact on comfort and energy demand (see for example figure 4.21).

In order to avoid daylighting problems a couple of strategies may be used as (for example): double horizontal blade slope (see e.g. figure 4.22), or adequate control of the shading, accounting not only

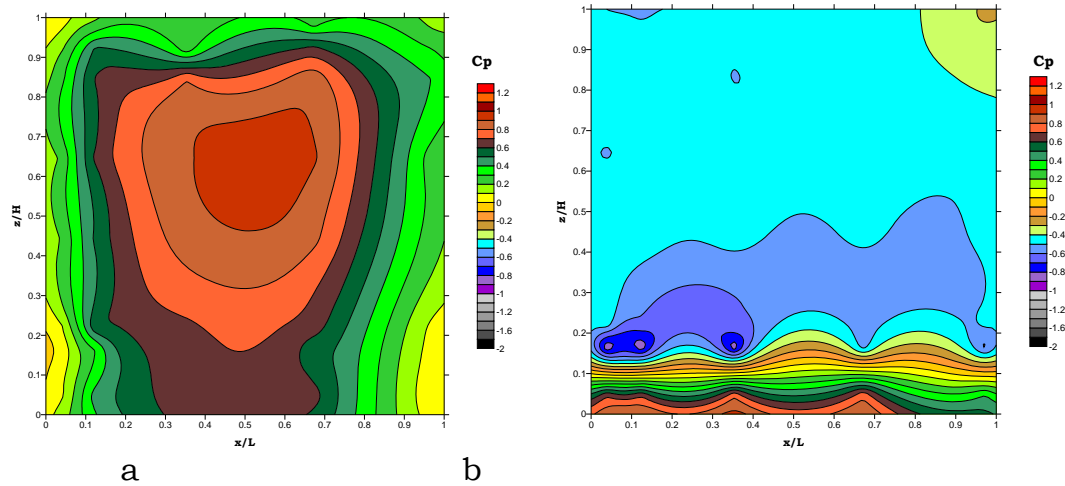


**Figure 4.20 -  $C_p$  distribution over an “unsheltered” envelope a), and a MS-DSF b), for a  $0^\circ$  (perpendicular) wind incidence (The DSF has a multi-storey configuration, open at the bottom and top and closed on the sides. The bottom edge of the DSF is 3 m above ground level, and the cavity has a depth of 0.8 m [Marques da Silva, F. and MG. Gomes (2005)].**

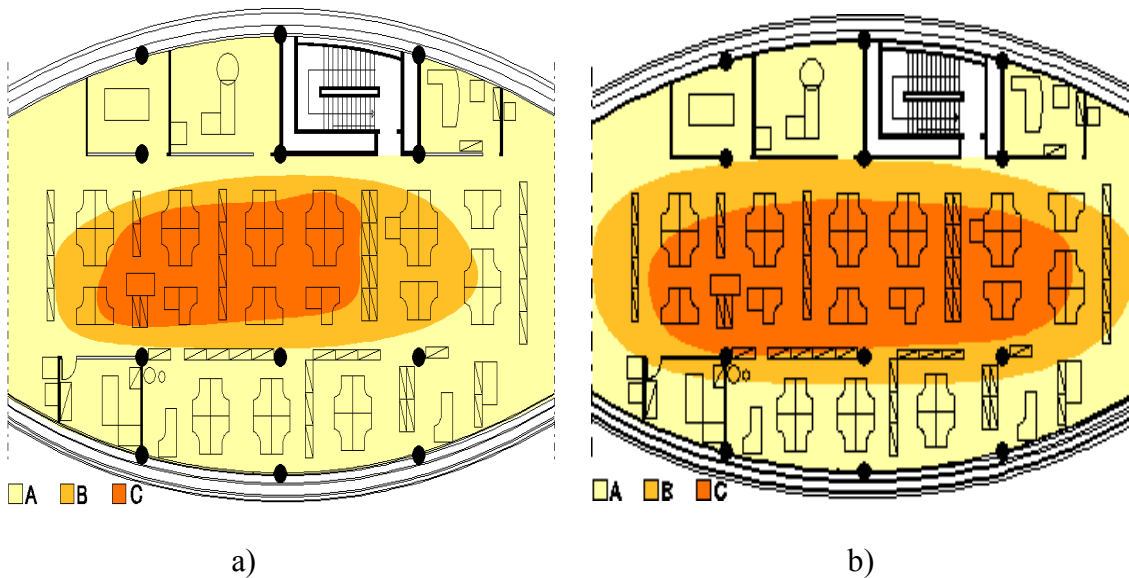


**Figure 4.21 – Daylight distribution in a building with double skin façade: A – Good to reasonable; B – intermediate to insufficient; C- inadequate and shading different positions – a) cloudy day with shading fully open and, b) sunny day with shading fully closed in the Southern façade (figure bottom) and partially closed in the Northern façade.**

for daylight distribution but also for the presence of users and for the personal control (More details about daylighting are resumed in Appendix 4E).

As far as the acoustic performance are concerned, it has to be considered that noise insulation improvement is one of the advantages of DSF and, in many cases, it could be the main reason to adopt it. The insulation level depends on the façade construction and used materials as shown in figure 4.23, where the measured acoustic insulation,  $D_{n,w}$ , in two different DSF buildings is shown (evaluation is done accordingly to standard EN ISO 140-4, 2000).

Building A façade has two single tempered clear glazed panes (12 - 705 - 10 mm) and a very low mechanical ventilation air flow rate. Building B façade has an outer single clear glazed pane and a double glazing, also clear glass inner pane (12 - 980 - 3- 12 - 6 mm) and a variable mechanical ventilation flow. Another relevant issue concerning DSF acoustics properties is the airborne noise

transmission through the air gap. For some type of AIF (e.g. corridor façade) acoustic bridges from room to room may be a concern (see also Appendix 4F).



Figure 4.22 – Reflective double blade Venetian blinds.

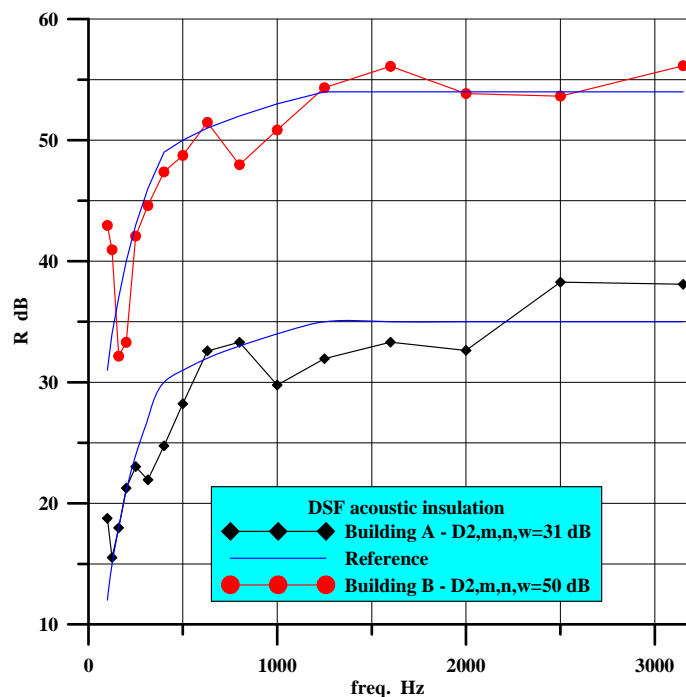


Figure 4.23 – Example of measured acoustic insulation,  $D_{n,w}$ , in two different buildings with double skin façades.

Finally, during the Annex 44 activity, a preliminary study on the environmental impact of double skin façades in buildings has been done. It resulted that in northern climates the major environmental load during the expected life of buildings is related to the operational energy consumption (almost 90%) and the environmental load of material could be less than 10%. In warm climates (Southern Europe) well designed and managed buildings could have very low energy consumption for (HVAC, lighting) and in such cases the environmental load of material could be the key factor for sustainable constructions (almost 90% of the environmental impact of buildings) More details on this analysis are available in [Pinto, (2008)] and a résumé can be found in Appendix 4H.

## 4.5 Examples for illustration

Buildings using AIF may be found worldwide, although the highest number of cases is present in central Europe. Concerning the working philosophy the most common are naturally ventilated (NV) multi-storeyed (MS) buildings with outdoor air curtain (OAC). In the following sections a selected collection of cases will be shown, trying to cover the various arrangements and to show some typical features/performance.

### 4.5.1 The Dragonair/CNAC Building

The Dragonair/CNAC Building at Chek Lap Kok International Airport in Hong Kong, China, is an example of a naturally ventilated, outdoor air curtain, corridor DSF (C-NV-OAC). It was built by Wong Tung & Partners and completed in 2002. Meinhardt Facade Technology (HK) Ltd. carried out the facade engineering. The problem of aircraft noise was addressed by the adoption of a double-skin cavity wall system which provides 60 dBA of sound attenuation. An 800 mm cavity separates the 19 mm thick external layer of fully-tempered glass and the inner layer, which is an insulated low-E coated unit.

The cavity wall system not only fulfils the engineers' requirements, but also avoids condensation problems through its use of acoustic baffles to ventilate the system. The cavity also facilitates maintenance and improves the building's thermal performance.

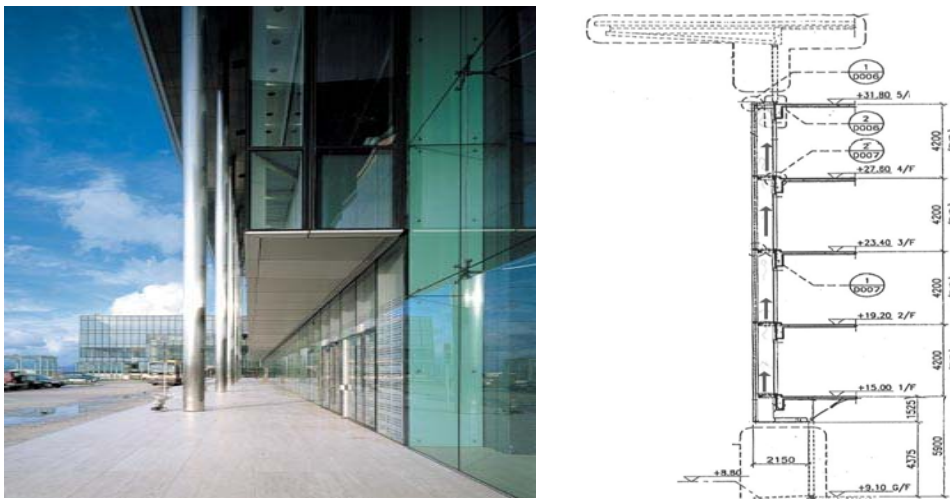


*Figure 4.24 - The Dragonair/CNAC Building at Chek Lap Kok International Airport in Hong Kong.*

### 4.5.2 Atrium Saldanha

Atrium Saldanha is an office and mall building in Lisbon, Portugal, completed in 1997, using a



*Figure 4.25 - The Atrium Saldanha in Lisbon, Portugal.*

multi-storey DSF in each two storey (three for the top ones), mechanically ventilated under an outdoor air curtain flow path (MS-MV-OAC). Both fully glazed panes have regular transparent glass separated by a 0.7 m width gap. Shading is provided by manually operated roller blinds within the gap, their colour being white in N and NE facades and black for NW and SW facades. Occupied spaces facing SW experience problems due to both gap air overheat and daylighting. A poor ventilation mass flow is insufficient to remove heat accumulated in the black roller blinds (an architectural decision adding ~10K on gap air temperature) being also responsible for low lighting levels when pulled down.

### **4.5.3 Peking Road**

Peking Road, in Kowloon, Hong Kong, design strongly emphasizes the green building approach and includes roof integrated BIPV.

The facade layout recognizes the different orientations of the building and there was a special interest in exploiting the use of natural daylight in the offices.

The tower features a triple-glazed active wall system, combining three layers of low emissive (low-e) clear glass with a ventilated cavity that results in high light transmission yet a low overall thermal transfer value. The cavity of the DSF (BW-MV-IAC) is mechanically ventilated with a controlled airflow that transports heat gain to the HVAC-unit. Venetian blinds are housed in a 200 mm air gap in the glazing system and are operated by a computerized system based on sunlight sensors.

The south elevation features innovative arrangements to reduce solar gain yet allow increased light transmission at the same time. Outside the windows, aluminium sun shading fins serve as reflectors bouncing light up onto the angled ceiling to transmit more natural light inside while at the same time limiting the entry of direct sun.



*Figure 4.26 - The Peking Road building, in Kowloon, Hong Kong.*

### **4.5.4 ARAG 2000**

The ARARG 2000 tower is sited in Düsseldorf, Germany, is a high rise building with a naturally ventilated shaft box DSF arranged in eight storey high sections (SB-NV). The flow path depends on the opening of the inner pane allowing fresh air. In each storey a box window arrangement allows fresh air to be admitted into the space at floor level, via an operable flap, or drawn directly to the shaft. The warm air from the space is exhausted to the shaft at ceiling level. The shaft air is drawn out at the top of each eight storey section. All flow passage areas can be closed providing a buffer configuration (Bf).

Venetian blinds in the 70 mm depth gap, close to the outer pane (12 mm laminated glass), provide solar control and the low-e inner pane is provided with open able windows.



*Figure 4.27 - ARAG 2000 tower in Düsseldorf, Germany.*

### **4.5.5 Technical University of Delft Library**

The three facades of this Dutch building are an example of the climate window (CW) configuration. The outer pane is made of low-e double glass units (8-15-6 mm) separated from the 8 mm inner pane by a 14 cm gap. Indoor air flows mechanically driven through the gap to the ventilation system where heat is removed. Shading is provided by automatically operated Venetian blinds within the gap.



*Figure 4.28 - Technical University of Delft Library, The Netherlands.*

### **4.5.6 Moravian Library**

The Moravian Library is sited in Brno, Czech Republic, show a façade with open able louvers on the outer pane allowing a multi-storey DSF, in the heating season, to be transformed into a single skin façade for the cooling season. When closed the DSF admits air from the bottom into the 550 mm depth gap and releases the heated air flow to the ventilation system at the top.

Shading is provided by means of adjustable shutters close to the inner pane and porous horizontal pathways (in the gap and outside), also used for maintenance, at each storey level.





**Figure 4.29 - The Moravian Library in Brno, Czech Republic.**

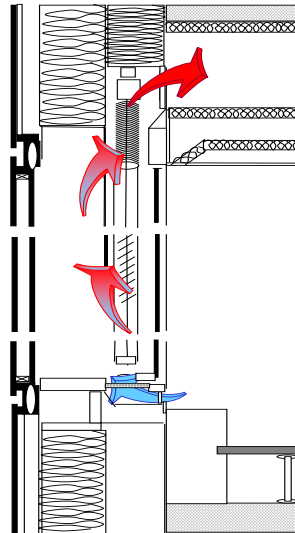
## **4.5.7 Environment Park**

### **4.5.7.1 General information**

Environment Park, in Turin, is a scientific and technological hub hosting firms, consultancy and research groups dealing with environment issues. The hub is characterised by the adoption of energy and environment conscious solutions as high performance building envelope, high performance heating and cooling system (heating and cooling beams), low emission wood chip furnace, lighting/daylighting control systems. Most of the South facing façades of the hub buildings are climate façades (Figure 4.30a).



**(a)**



**(b)**

**Figure 4.30 – (a) The monitored climate façade at the Environment Park, in Turin, Italy –( b) Scheme of the working principle of the façade at the Environment Park, in Turin, Italy.**

### **4.5.7.2 Component description and working principles**

The climate façades are one story ventilated façade modules integrated with the HVAC system. The outer pane is made of a fixed clear double glazing (8/16/6 mm); the inner pane is a clear single glazing (8 mm), that can be opened for cleaning and inspection purposes; the air gap (140 mm) presents venetian blinds on the inside, that are both manually and electrically controlled.

The air gap between the external and the internal glazing is used as a duct to extract the exhaust air from the room (Exhaust Air - EA – type). The air from the room flows through an opening (filter equipped) located in the lower part of the façade, and it is then extracted in the upper part through a duct located above the ceiling (Figure 4.30b). The exhaust air leaves the façade, passes through a controlled air lock and then flows along a duct up to the Air Handling Unit.

The operating strategies of the façade and its integration with the HVAC system are outlined in Fig. 4.31. In the HVAC system, the air can be handled in two different ways, depending on the season and/or on the thermodynamic properties of the air (cases 2a and 2b).

During the winter period the ventilated façade can act either as a sort of solar collector or as a building envelope component with improved thermal insulation.

In the former case, when solar radiation is high, the temperature of the air that leaves the façade is higher than the indoor air temperature, and this energy flux can be used, through a heat recovery unit (Fig. 4.31a), to pre-heat the outdoor ventilation air flow rate. When both solar radiation and the outdoor air temperature are low, the temperature of the air that leaves the façade is usually lower than the indoor air temperature. Depending on the air temperature at the façade exhaust, the extracted air can either be driven through the AHU heat recovery system or, in the worst conditions, it can be diverted directly towards the outdoor environment.

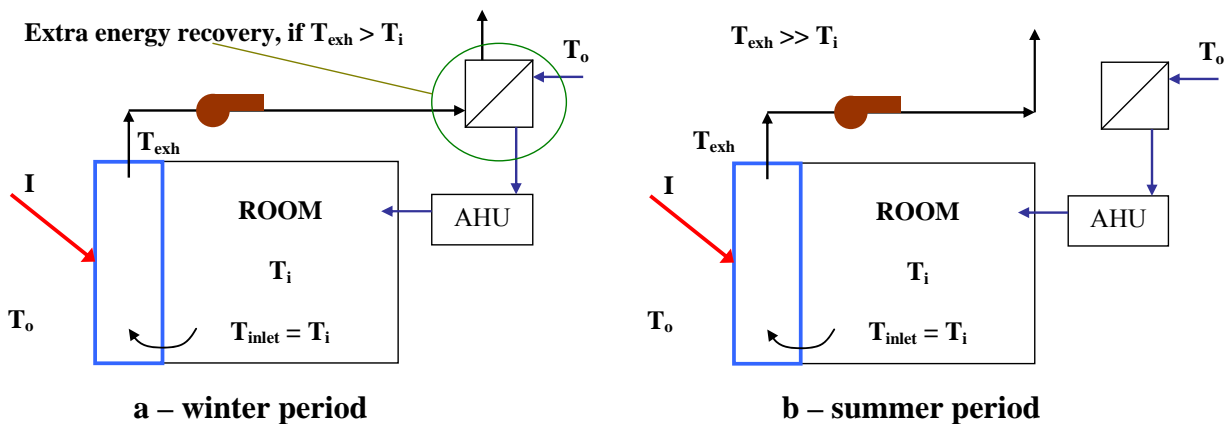


**Figure 4.31 – Operating strategies of the ventilated façade and integration with the HVAC system.**

During the summer period, the exhaust air flowing inside the air gap removes part of the heat loads through the façade, thus reducing the heat gains in the indoor environment. In these conditions, the temperature of the air flow at the exhaust of the façade is, usually, much higher than the indoor air temperature and the exhaust air by-passes the heat recovery system and is discharged directly into the outdoor environment (Fig. 4.31b).

#### 4.5.7.3 Measurements for performance assessment

The façade has been investigated by means of a long term monitoring campaign which lasted 2 years and was coupled with a post-occupancy evaluation of the office building. The measurement apparatus set-up on the ventilated façade consisted of 34 sensors connected to a datalogger with a scan rate of 15 min. The results were divided into three main categories:

1. heat fluxes;
2. energy efficiencies (that are related to the achievable energy savings);
3. surface temperatures of the indoor facing glass pane (that influence the thermal comfort in the indoor environment).

As far as the winter season is concerned (Figure 4.32), when the solar radiation is high, the heat fluxes are always positive independently of the ventilation strategy.

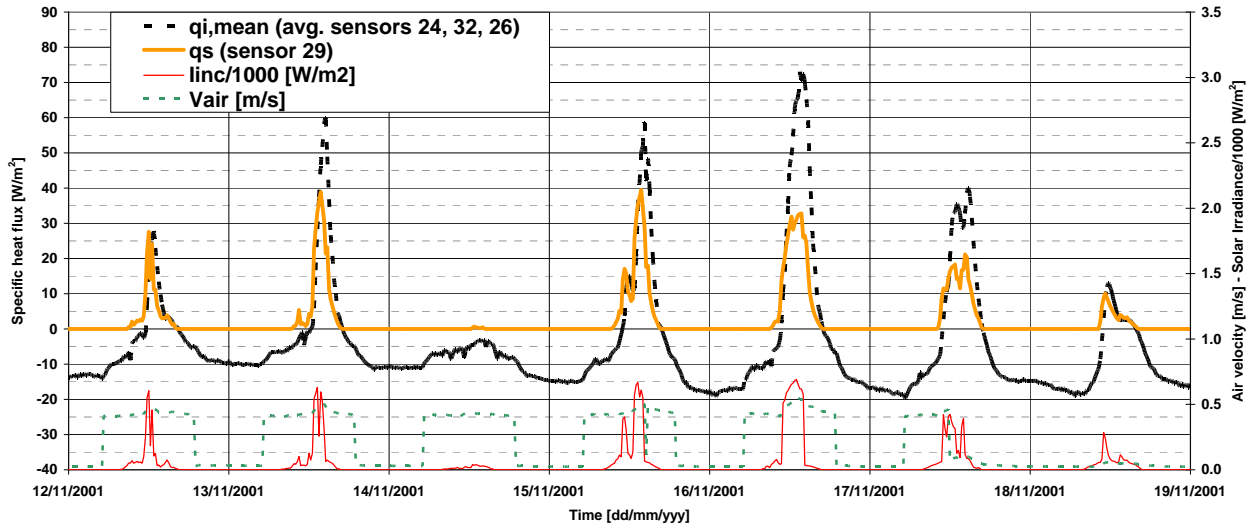


**Figure 4.32 – Heat fluxes – time profiles during the winter season.**

When solar radiation is very small the heat fluxes are negative. The presence of the mechanical ventilation improves the performances of the system. The transmission losses through the façade are lower due to a dynamic insulation effect which is higher than the one obtained with natural ventilation.

During the summer season, as shown in Figure 4.33, when the HVAC system is off, the heat flux tends to increase significantly and can reach values as high as 90 W/m<sup>2</sup>. This is due to the overheating of the air inside the gap and of the venetian blinds. The performance improves with mechanical ventilation. However, the influence of the air flow rate on the façade behaviour is far from linear and it can be deduced that the shading device features are a key factor in influencing the thermal behaviour of the façade. The only way of significantly reducing the overheating of the solar shading device in summer season is through: the shading device optimisation (low-e, double reflective screen, etc.), the correct choice of the glass type and the creation of a proper air flow rate inside the air gap.

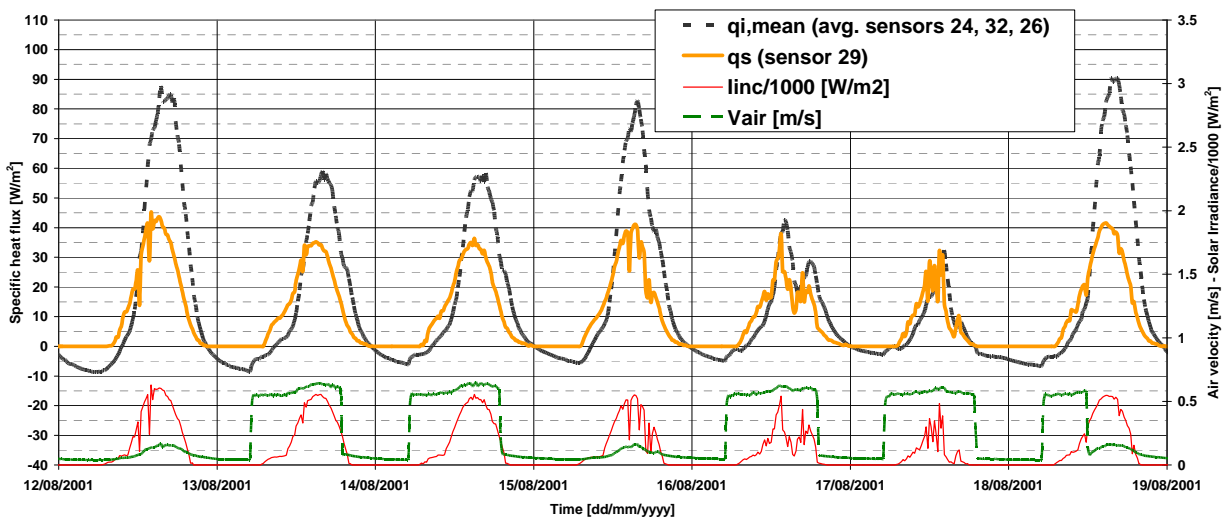


**Figure 4.33 – Heat fluxes – time profiles during the summer season.**

In relation to the thermal comfort conditions (internal glass surface temperatures) the performance of the monitored façade are, in general, satisfactory and the temperature differences between the indoor air and the internal glass pane are quite low for most of the operating time ( $\Delta T$  lies between -2 °C and +5 °C for about 70% of the time).

As far as the energy performances of the façade are concerned, it has been shown that the pre-heating efficiency is quite low for most of the operational time of the HVAC system both during the winter and during those periods of the mid seasons for which the building needs to be heated.

In short it can be stated that the analysed ventilated façade:

- provides good performances throughout the year compared to more traditional transparent façades,
- it is still not competitive with windowed opaque façades, because of problems of overheating, which worsen both the energy and thermal comfort performances.

## **4.5.8 SOMEK Building**

### *4.5.8.1 General information*

The SOMEK headquarter is sited in Zoppè di San Vendemiano, Italy. The office building presents a two storeys climate façade, facing south.



**Figure 4.34 - The SOMEK headquarter in Zoppè di San Vendemiano, Italy.**

### *4.5.8.2 Component description and working principles*

A scheme of the façade is shown in figure 4.36. The outer pane is a fixed 12 mm clear single glazing. The inner pane is a fixed extra clear low-e double glazing (5+5/15/8 mm) with a pvb layer for acoustic insulation. The ventilated cavity is 714 mm wide and hosts a reflective roller blind on the inside, located at 112 mm from the outer pane. The shading device is automatically controlled by a system equipped with a luxmeter placed on the roof of the building. Additional roller shadings, operable by the occupants, are placed in the indoor environment, close to the inner pane.

The exhaust air from all the offices of the two storeys building is collected by the HVAC system, sent to a heat exchanger (air-air) to pre-heat (in winter) or to pre-cool (in summer) the ventilation air. In winter conditions (Figure 4.35a) the air is then sent to the channel placed in the lower part of the façade. The air flows along the façade, is extracted in the upper part of the cavity and is exhausted to the outdoor. In summer conditions (Figure 4.35b), a second heat exchanger (air-water) is activated and the air is pre-cooled before entering the ventilated cavity of the façade. To pre-cool the air, the water of a well, at 14°C, is used. This heat exchanger (i.e. the cooling of the ventilation air of the facade by means of the well water) is activated when the temperature of the air at the exhaust of the façade exceeds a value of 25°C.

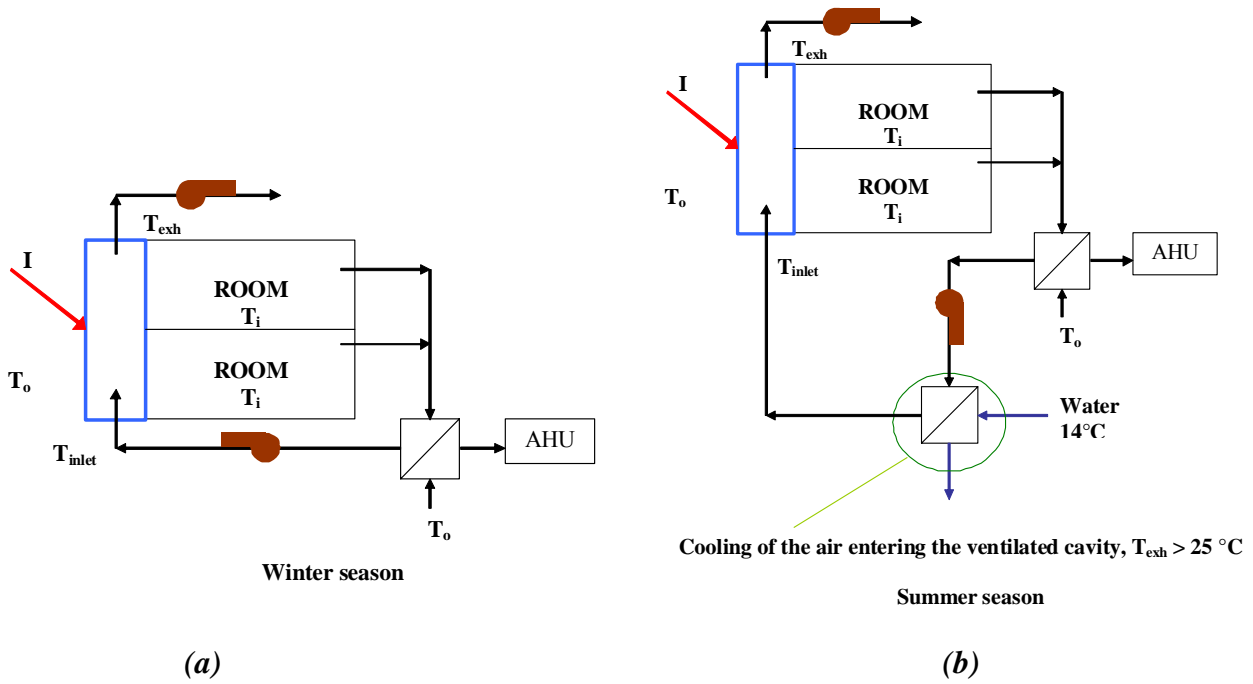


Figure 4.35 – Operating strategy of the ventilated façade, (a) winter season, (b) summer season.

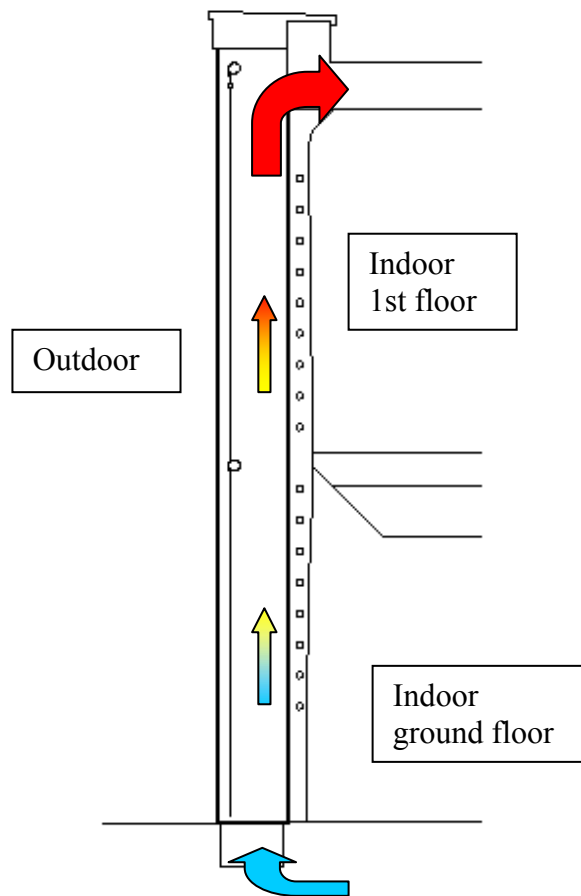


Figure 4.36 – Scheme of the ventilated façade at the SOMEK Building.

### 4.5.8.3 Measurements for performance assessment

The façade is still under investigation. A long term monitoring campaign started in April 2008 and that will last until March 2010.

The measurement apparatus consists of 39 sensors connected to a datalogger. The sensors set-up allows to measure: temperature of the air (outdoor, indoor, in the ventilated cavity), temperature of the surfaces (of the glazing, of the shading device), heat fluxes through the external and the internal skin, incident and transmitted solar irradiance, incident and transmitted illuminance, the influence of the shading device placed in the indoor environment.

The results were divided into two main categories:

1. heat fluxes and energies through the façade;
2. surface temperatures of the indoor facing glass pane, PMV and percentage of the floor area in comfort conditions.

As far as the heating season is concerned, the dynamic insulation provided by the façade is effective in limiting the heat losses. If compared with a more traditional glazed façade (a solar control double glazing,  $U=1.1 \text{ W/m}^2\text{K}$ ,  $g\text{-value}=0.32$ ), the ventilated façade provides a better performance both considering the energy savings and the thermal comfort. In Figure 4.37 the energy demand for the winter season 2008-2009, normalized according to the actual degree days, for the two façades are shown. In summer and in midseason the influence of the pre-cooling effect due to the interaction with the well water have been investigated. The comparison between summer 2008 (without the pre-cooling effect) and summer 2009 (with the pre-cooling effect) shows that pre-cooling the air lowers the temperature of the air flowing in the gap of about  $5^\circ\text{C}$ , and this lowers the

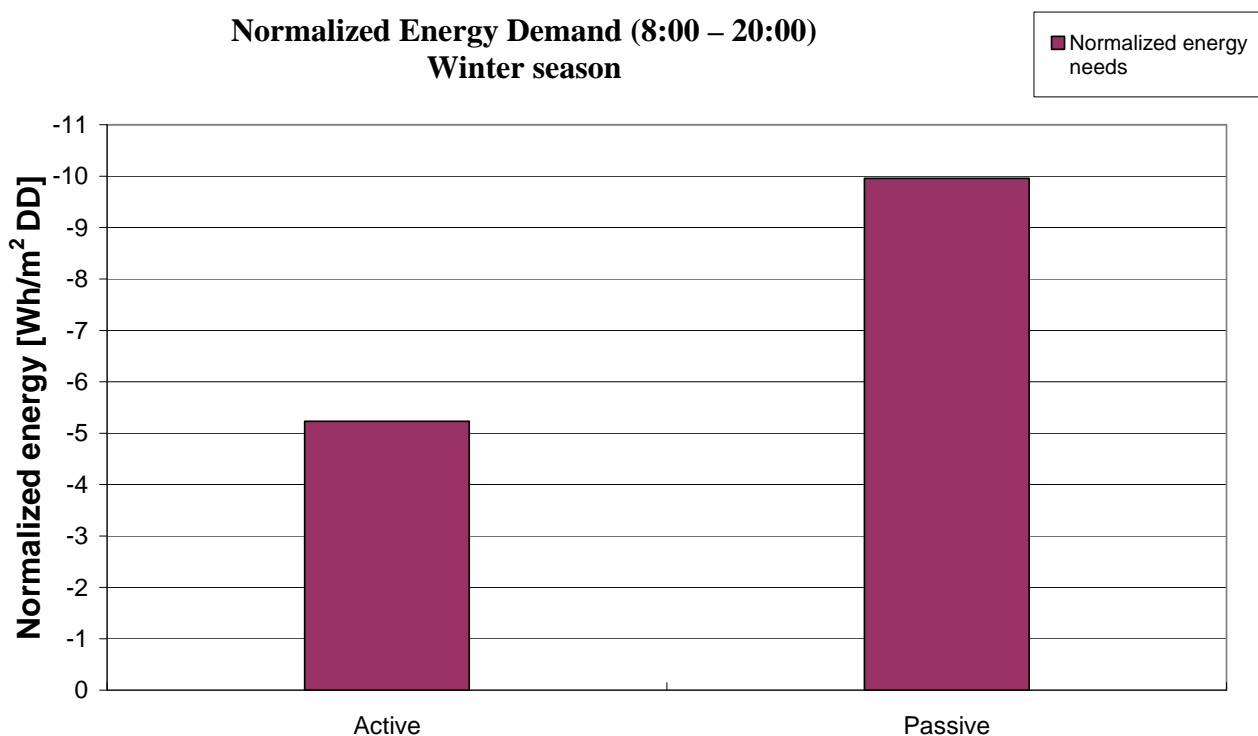


**Figure 4.37 – Normalized energy demand for the ventilated and for the traditional façade.**

cooling loads entering the indoor environment of about 6%.

As far as the midseason is concerned, in Figure 4.38 the heat fluxes between the façade and the indoor environment with three different operating conditions for the pre-cooling effect, are shown. The pre-cooling effect is useful to lower the entering cooling loads in the afternoon, however, its activation during the morning hours may increase the heat losses. A correct choice of the value for the control temperature is therefore essential to switch on and off the well water heat exchanger.

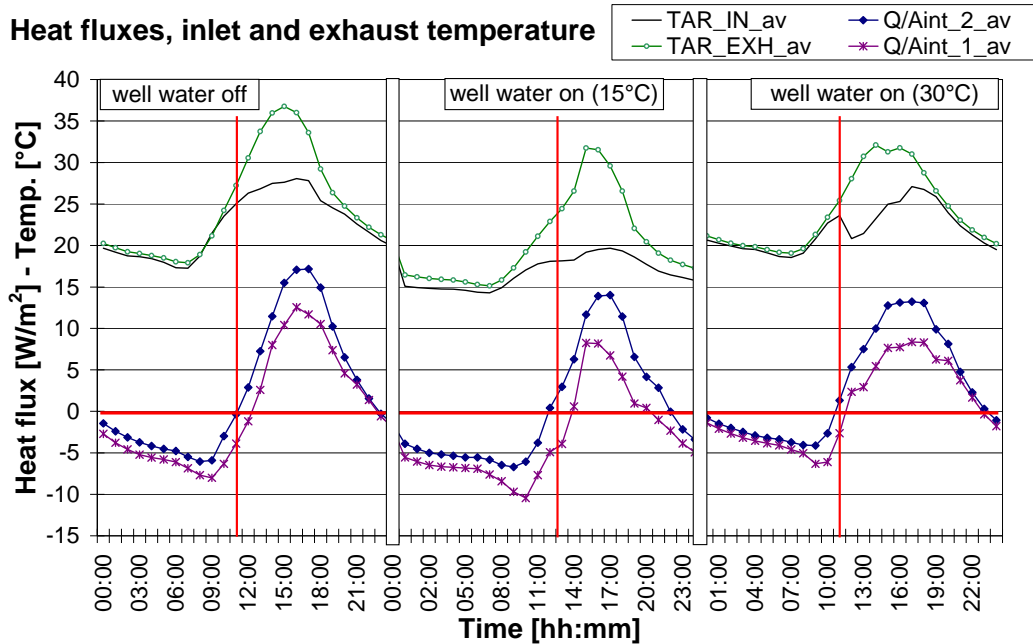


Figure 4.38 – Heat fluxes for different control strategies for the activation of the pre-cooling.

#### 4.5.9 Solar XXI

The building is located in Lisbon, Portugal, has a total area of 1500 m<sup>2</sup>, and was designed as an example of integration of renewable energies in a services building through the use of active and passive solar energy, natural ventilation and daylighting, together with responsive technologies, with a final cost of €1.3M. It also aims to be an example of a low energy efficient building.

The majority of the glazed surfaces are placed on the south façade to allow a maximum solar caption in the heating season. For long periods with no solar radiation the building uses a set of hot water convectors supplied by a boiler supported by a set of CPC type solar collectors, and hot water tank, sited on the roof.

The building (in the South façade and between the windows) is also equipped with a set of vertical PV panels (100 m<sup>2</sup>; 12 MWh/yr corresponding to 30-50% of power consumption) forming a translucent double skin façade between the panels and the opaque part of the external wall (BW-NV-RAF). Within this gap the heat is used, in the heating season, to introduce hot air to the rooms via two openings top and bottom placed. An additional set of PV panels (95 m<sup>2</sup>; 6 12 kWh<sub>p</sub>) is used as a car park cover. The two PV systems cover for 74% of the building's electric energy use (2007 yearly data).



Figure 4.39 – Solar XXI in Lisbon, Portugal.

For cooling purposes, besides the DSF contribution in removing heated indoor air using the stack effect, an earth coupling system was used. It is composed of a set of buried ventilation pipes 15 m long and 4.6 m deep, that connects a supply well to each office. Ventilation may be natural or mechanically assisted.

In summer the air was supplied to the rooms at 21°C-22°C, being responsible for a 2°C-3°C decay in room temperature.

For six month of summer period (2006/07) the average temperatures of exterior and interior air was  $T_{ex}= 22.5^{\circ}\text{C}$  and  $T_{in}= 24.6^{\circ}\text{C}$ , and for nine winter month (2006-08), was  $T_{ex}= 11.9^{\circ}\text{C}$  and  $T_{in}= 20.0^{\circ}\text{C}$ .



**Figure 4.40 – Solar XXI details.**

Globally the energy needs, estimated according to the Portuguese regulations, are 6.6 kWh/m<sup>2</sup> and 25 kWh/m<sup>2</sup>, for heating and cooling respectively, compared to the allowed maximums of 51.5 kWh/m<sup>2</sup> and 35 kWh/m<sup>2</sup>. Occupants were asked to evaluate the acceptance on issues like overall and thermal environment, air quality, acoustic and lighting. Minimum acceptance levels of 73% were found for thermal environment in summer and air quality in winter.

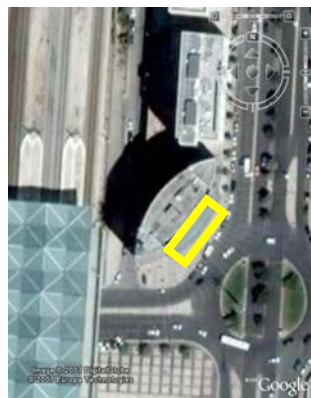
#### **4.5.10 Buildings with AIF in Lisbon (portugal)**

Monitoring AIF was one of the tasks within the Annex 44; so three different types of DSF (figure 4.42) belonging to real buildings under typical use were selected, all sited in Lisbon (figure 4.41). Measured parameters were: gap and outdoor air temperature, vertical plane (façade) solar radiation, horizontal temperature profiles across the façade, and heat fluxes on both DSF panes (assumed positive when leaving the building).

An example of some monitored temperature profiles across the AIF (related to days with the highest gap temperature records) is shown in figures 4.43 (summer season) and 4.44 (winter season).



Building 1



Building 2

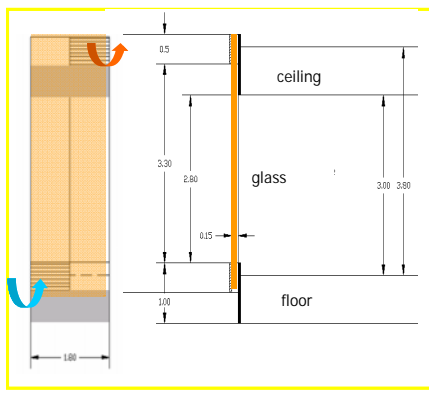


Building 3

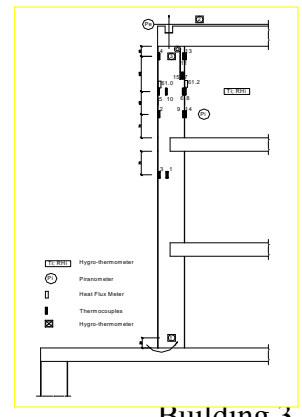
**Figure 4.41 - Three monitored buildings.**



Building 1



Building 2



Building 3

Figure 4.42 - Three DSF layouts.

Table 4.2 – Brief DSF description and monitoring periods.

	Building 1	Building 2	Building 3
Type	MS-OAC-MV	C-OAC-MV	BW-OAC-NV
Gap	0.71 m	0.98 m	0.15 m
Glazing	12(e) + 10(i)	12(e)+[8-12-6](i)	10 (e) + [8 +16+33](i)
Shading	Black roller blind	White ven. blind	White ven. blind
Summer	05/09/08-21 NW 06/06/27-07/21-NW+NE	06/08/03-31	06/06/1/20-30
Winter	05/12/15-21 NW	06/02/03-28	06/01/18-27

All clear glazing except \*: parsol gris

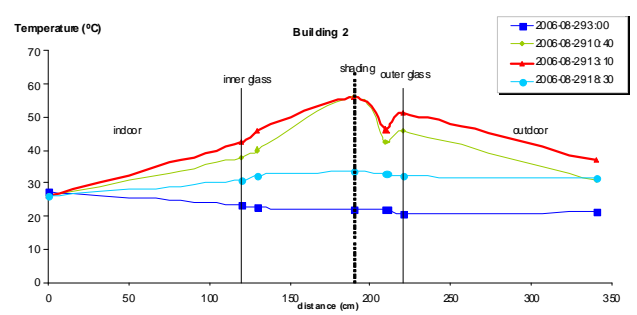
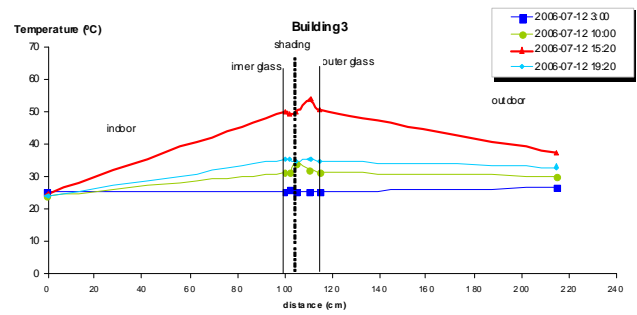
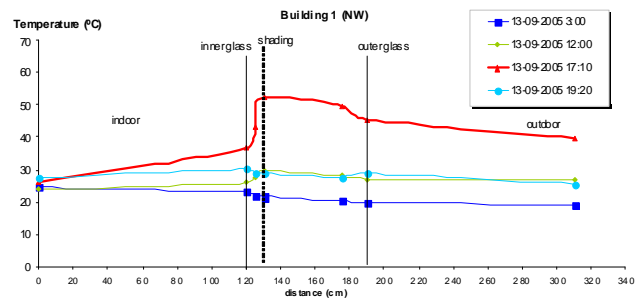
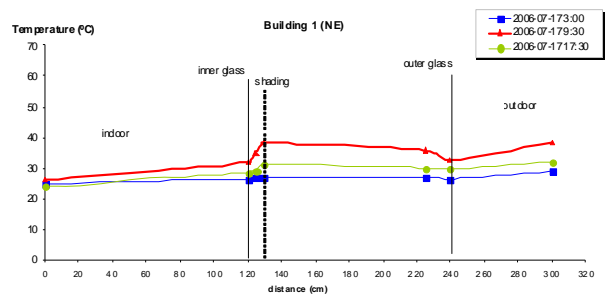
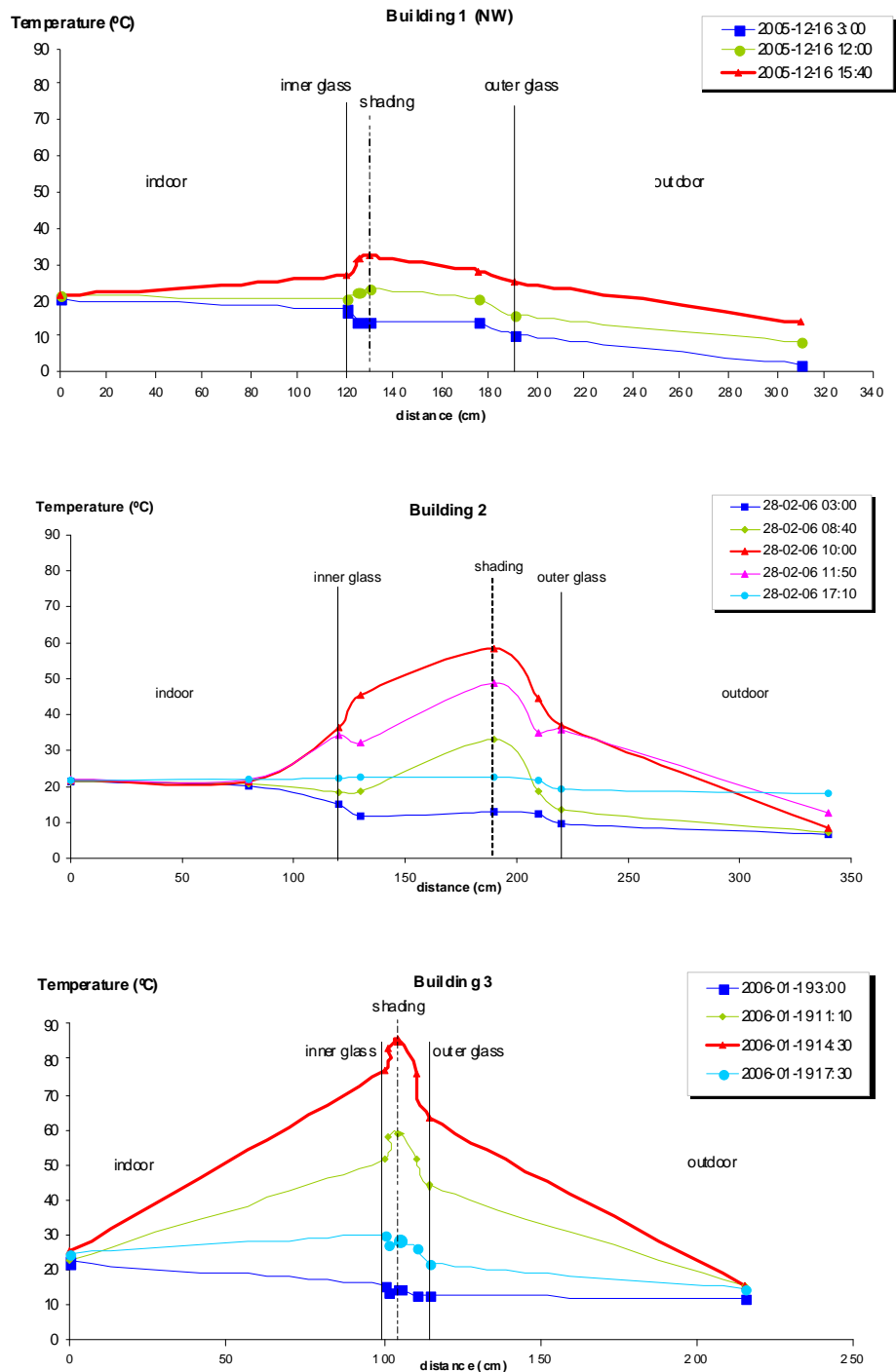


Figure 4.43 – Example of DSF Summer monitoring results.



**Figure 4.43 – Example of DSF Winter monitoring results.**

A poor ventilation rate, due to a very small depth of the air gap (partially obstructed by the shading venetian blind), is responsible for the high temperatures registered on the south faced façade of building 3, mainly in winter when the sun is in a lower position (figure 4.43).

In building 2, also a south facing façade, is clear the effect of turning on the mechanical ventilation on lowering the temperature, again in winter, under sunshine (figure 4.43 - comparison between red and pink curves related to – respectively – 10.00 am and 11.50 am).

The analysis of the heat fluxes (appendix 4J) has highlighted that the air gap overheating is the cause of the problems on sunny days (the exception being building 2 after the mechanical ventilation is turned on). Some more details about heat fluxes across the AIF are resumed in Appendix 4J.

## 4.6 Barriers to overcome

Barriers to AIF implementation arise from several factors, either technological or non-technological.

Inquiries to the construction community (investors, designers, and owners) allow identifying a set of barriers such as:

- cost,
- risk,
- lack of guidelines and tools,
- poor cooperation among the designing team,
- lack of experience and specific regulations,
- poor availability of certified and reliable performance data (concerning both energy and comfort issues).

### 4.6.1 Costs

Cost analysis of AIF is not a simple task as different elements have to be considered, whose impact is not so straightforward to predict. The most appropriate way of economical evaluation of an AIF is a Life Cycle Cost (LCC) analysis or, in an extended way, the Total Economic Value (TEV) that accounts also for people productivity.

Such analysis should take into account at least investment, maintenance and energy performance and needs to consider all relevant aspects. The best approach is to develop a comparative study with other façade solutions (comprehending also traditional solutions).

Construction investments in Europe may be summarized as [Poizaris (2004)]:

- Standard façade – 300 to 500 €/m<sup>2</sup>
- AIF façade (fixed components) – 600 to 800 €/m<sup>2</sup>
- AIF façade (adjustable in and outlets) – 700 to 1000 €/m<sup>2</sup>
- AIF façade (external louvers) – 800 to 1300 €/m<sup>2</sup>

Fire protection (sprinklers) within the DSF cavity represents 2-3% of its investment costs.

Overhead and maintenance costs show values as:

- Standard façade – 2.5 to 3.5 €/m<sup>2</sup> + cleaning
- AIF façade – 4.0 to 7.5 €/m<sup>2</sup> + cleaning

Maintenance costs to be considered belong not only to the AIF itself, but also to the influence it has on related building systems such as lighting and HVAC [Magali and Gratia (2002)].

The presented figures make clear that a reliable energy performance evaluation is crucial for the economical analysis, since without this information it is hardly possible to have a consistent figure for the pay back period of the investment.

For a TEV analysis it is also difficult to quantify the increase in indoor thermal comfort or to find the monetary equivalent for the increase in productivity of the occupants and/or the increase of the floor area that can be occupied as a result of better thermal comfort.

Cost-benefit evaluation depends both on financially measurable aspects (construction, energy cost, ...) - which are dependent on objective criteria - and non economically quantifiable aspects. These last can either be based on objective criteria, like noise reduction, or on subjective criteria, like aesthetics. The solution of this problem needs decision support methods to be evaluated and compared with each other in an *a priori* incomparable process [Flamant, et al (2004)].

### 4.6.2 Fire standards and regulations

Fire regulation may be a further concern due to the fact that no specific standards or regulations usually exist for AIF. This leads to interpretation and application problems, but in most cases the general fire regulations may be a threat, depending on specific appreciation from the fire safety departments.

Such regulations, may forbid the use of building envelope technologies that put into direct connection more than two/three stories. Sometimes, it is possible to overrule such prescriptions after a suitable analysis proving that an equivalent safety degree is obtained by alternative strategies [Loncour, et al (2003); Martin and Loncour (2004)].

Fire propagation is referenced in EU standard EN 13830 (2003). There a mention is done that precautions should be taken to prevent the transmission of fire and smoke through voids in the curtain wall construction. Fire and smoke stops shall be incorporated at all (or at certain) stories with structural floor slabs. However no standard, test methods or alternatives are given to avoid transmission of fire and smoke through the cavity. The same standard (curtain wall – product standard) refers three guidelines concerning fire prevention:

- EN 13501-1:2002 for fire reaction classification of construction products. A specific fire scenario is being developed for testing façades.
- prEN 13501-2:2002 for fire resistance classification of construction products and building elements, from fire resistance tests. Curtain walls shall be tested according to EN 1364-Part3 and parts of curtain walls shall be tested according to EN 1364-Part4.

In Belgium a newly proposed regulation for fire safety on DSF buildings [(Martin and Loncour (2004)] introduces some interesting concepts and gives remarkable advices:

- Experience shows that an automatic sprinkler-like system is more efficient than fire dampers on every storey in preventing or retarding fire propagation. Multi-storey DSF with such systems and smoke exhaustion in the cavity do not need fire dampers.
- Inner pane glass should be tempered. An alternative consists on automatically opening the external pane, thus avoiding the stack effect. In this case, the inner pane should follow single glaze façade (SGF) safety rules. If this is not possible, the inner pane should have a fire resistance class of (“E” meaning to keep the element integrity, “I” refers to insulation and the figure for the number of minutes it should withstand): a) E60 full length; b) EI30 full length, or; c) EI60 every two stories. Partitioned cavities are acceptable if the partitions are of E60 class.

Furthermore, the Swiss Cantonal Association of Fire Insurances (<http://ppionline.vkf.ch>) underlines that there is no test expertise allowing one to know how a fire develops in a DSF building, being certain that they can constitute a problem both from protection and fire fight points of view. For people protection, a safety level equal to the single glazed façade (SGF) should be mandatory. The minimum complementary measures for DSF (adapted from the Swiss Fire-fighters Federation agreement) are:

- No combustible materials for the inner pane, except for window frames where it may be allowed, and for external panes except for sealants and bonds. This should be applied to refurbishment involving the addition of a double-skin over an existing façade,
- Full interdiction of combustible materials for shading devices,
- EI60 class protection between the cavity and ventilation plenum above ceiling (if present),
- Escape ways should not use the cavity. If the cavity is usable (corridor type), access to the interior should be carefully considered. In other words, doors with the same fire resistance of the inner pane should be used.

### **4.6.3 Other construction regulations and laws**

The improvement of the energy efficiency in building has become a worldwide goal. This should constitute a major issue for a wider use of AIF.

However, as previously underlined, in many cases it is quite difficult to reliably assess the actual energy saving achievable by using AIFs

In the EU, for example, the so called (EPBD) Directive (Energy Performance of Buildings Directive, 2002) asks for a verification that involves a method in which the annual energy building consumption is compared with a reference value (variable within the EU countries). Problems may

arise if no validated models are used to simulate AIF behaviour and its integration into the building system.

Thermal insulation is also specified as a mean to achieve the global goal of energy consumption, via U-values. Although this may be viewed as an opportunity and not as a barrier to AIF, ventilated facades has no unique U-value and in most of the cases it is really hard to reach a meaningful value. Local and country regulations concerning taxes and building permissions may also have an influence on application. For example, in some countries, the space comprised between the two skins is considered to be a "built environment". This means that the use of a DSF determines an increase in the gross volume of the building and implies problems with the "urban indices" and results in an increase in the due taxes.

#### **4.6.4 Lack of knowledge and lack of design tools**

AIF technologies, as well as its integration into the building services, are well known specially in research institutions. Purposely developed simulation tools are available among researchers. Their use is, however, limited to the research activity and the level of development, at the present, still does not allow their use as widespread design tools.

Among designers, architects and engineers, there is good general knowledge of AIF technologies, but capacity of quantitative analysis on energy and comfort performance is generally relegated to few experts working in major companies.

Confidence on simulation results will become more and more essential as contractors demand that cost effectiveness and claimed comfort conditions would be evaluated in post occupancy and be included in "warranty". The lack of specific models for AIF behaviour, and its validation, may therefore slow the use of those kinds of solutions.

### **4.7 References**

- AEAI (VKF) (2001). "Note explicative de protection incendie 1004. Mesures de protection incendie pour façades double-peau." Association des établissements cantonaux d'assurance incendie, Berne, Suisse. (<http://ppionline.vkf.ch>).
- Alamdari F, Hammond, GP (1983). "Improved data correlations for buoyancy-driven convection in rooms" *Building Services Engineering Research & Technology*, 4(3): 106-112.
- Altan, H., Ward, I., Mohelnikova, J. and Vajkay, F., (2008), "An internal assessment of thermal comfort and daylighting conditions of a naturally ventilated building with an active glazed façade in a temperate climate", *Energy and Buildings*, 40:36-50.
- Amato, A (1996). "A Comparative Environmental Appraisal of Alternative Framing Systems for Offices." Oxford Brookes University UK, Oxford.
- Andersen, KT (2003). "Theory for natural ventilation by thermal buoyancy in one zone with uniform temperature." *Building and Environment*, 38(11):1281-1289.
- Annex 44. Integrating Environmentally Responsive Elements in Buildings (2007). State of the art Review. IEA, ECBCS. <http://annex44.civil.aau.dk>
- Aschehoug, Ø, et al (2000). "BP Amoco Solar Skin – A Double Façade With PV." *Proceedings of EuroSun 2000*, Copenhagen.
- Aschehoug, Ø and D Bell (2003). "BP Solar Skin – A facade concept for a sustainable future." SINTEF Report, Trondheim.
- Aschehoug, Ø and A Wyckmans (2003). "BP Solar Skin – Occupant surveys before and after the construction of prototype." SINTEF Report STF50 A05079, Trondheim.
- Aschehoug, et al (2005). "Double facades at high latitudes – some user experiences." Paper at the International Conference *Glass in Buildings*, April 7-8, Bath, UK.

- Baker, JA and R Henry (1997). "Determination of size-specific U-factors and solar heat gain coefficients from rated values at established sizes - A simplified approach." *ASHRAE Transactions*, 103 (1):1021-1025.
- Baker, PH and ME McEvoy (2000). "Test cell analysis of the use of a supply air window as a passive solar component." *Solar Energy*, 69(2):113-130.
- Baker, P, et al (2003). "Improving air quality in homes with supply air windows." Draft BRE Information Paper for a DTI Partners in Innovation Project: Guidelines for implementation of an innovation whole-house ventilation system and its comparison with established approaches to house ventilation.
- Ballestini, G., Di Carli, M., Masiero, N. and Tombola, G. (2005). "Possibilities and limitations of natural ventilation in restored industrial archaeological buildings with a double-skin façade in Mediterranean climates." *Building and Environment*, 40: 983-995.
- Balocco, C (2002). "A simple model to study ventilated facades energy performance." *Energy and Buildings*, 34(5):469-475.
- Balocco, C (2004). "A non-dimensional analysis of a ventilated double façade energy performance." *Energy and Buildings*, 36:35-40.
- Balocco, C. and Colombari, M. (2006). "Thermal behaviour of interactive mechanically ventilated double glazed façades: Non-dimensional analysis." *Energy and Buildings*, 38: 1-7.
- Barakat, SA (1987). "Thermal performance of a supply-air window." Proceedings of the 12<sup>th</sup> Annual Passive Solar Conference, 12:152-158.
- Belgian Building Research Institute (BBRI) (2002). "Source book for a better understanding of conceptual and operational aspects of active facades." Department of Building Physics, Indoor Climate and Building Services, BBRI, Belgium. (<http://www.bbri.be/activefacades/>)
- Belgian Building Research Institute (BBRI) (2004). "Ventilated double facades. List of buildings equipped with ventilated double facades." Department of Building Physics, Indoor Climate and Building Services, BBRI, Belgium. (<http://www.bbri.be/activefacades/>)
- BESTFACADE - <http://www.bestfacade.com/>
- Biwole, P. H., Woloszyn, M. and Pompeo, C, (2008) "Heat transfers in a double skin roof ventilated by natural convection in summer time", *Energy and Buildings*, 40: 1487-1497
- Bodart, M a DH, A (2002). "Global energy savings in offices by the use of daylight." *Energy and Buildings*, 34(5):421-429.
- Boonyatikarn, S (1987). "Performance of an air-flow envelope." Proc. 12<sup>th</sup> Passive Solar Conference.
- Brandle, K and RF Boehm (1982). "Airflow windows: performance and applications." ASHRAE/DOE Conference, Proceedings of Thermal Performance of the Exterior Envelopes of Buildings II. Las Vegas, NV.
- Chiu, Y and L Shao (2001). "A parametric study of solar double skin façade on energy saving effect." *Proceedings of the 7<sup>th</sup> Clima 2000 World Congress*, Napoli, Italy.
- Chow, W. K. and Hung, W. Y. (2006). "Effect of cavity depth on smoke spreading of double-skin façade." *Building and Environment*, 41: 970-979.
- Ciampi, M, Leccese, F and G Tuoni (2003). "Ventilated facades energy performance in summer cooling of buildings." *Solar Energy*, 75:491-502.
- Clements-Croome, D (1997). *Naturally ventilated buildings*, E&FN. Spon, UK.

- Compagno, A (2002). "Intelligente Glasfassaden: Material, Anwendung, Gestaltung = Intelligent glass facades: material, practice, design." *Intelligent glass facades*, Basel; Boston:183.
- Corgnati, SP, Perino, M and V Serra (2003). "Energy performance evaluation of an innovative active envelope: results from a year round field monitoring." Proceedings of the 2<sup>nd</sup> International Conference on Building Physics, September 14-18: 487–496.
- Corgnati, SP, et al (2004). "Performance of a transparent active façade in terms of thermal comfort: experimental assessments." Climamed – Congresso Mediterraneo de Climatização, Atti del Congresso su CD-ROM, 16 e 17 Abril de 2004, Lisboa.
- Coussirat, M., Guardo, A., Jou, E., Egusquiza, E., Cuerva, E. and Alavedra, P., (2008), "Performance and influence of numerical sub-models on the CFD simulation of free and forced convection in double-glazed ventilated facades", *Energy and Buildings*, 40:1781-1789.
- Crawley, DB, et al (2005). "Contrasting the capabilities of building energy performance simulation programs." Joint report by US Dept of Energy, Un of Strathclyde (Scotland, UK) and Un of Wisconsin (USA). ([www.energytoolsdirectory.gov](http://www.energytoolsdirectory.gov))
- Deneyer, A and N Moenssens (2004). "Les doubles façades ventilées. Analyse quantitativ coûts-bénéfices de l'utilisation de doubles façades ventilées. Comportement à la lumière naturelle des doubles façades ventilées à lamelles. Illustration sur base de mesures réalisées dans le bâtiment Berlaymont." CSTB. (<http://www.bbri.be/activefacades/>)
- Dickson, A (2004). "Modelling Double-Skin Facades" MsC Thesis, Dep. Mechanical Engineering, Un. Strathclyde, Glasgow, Scotland, UK
- van Dijk, D and H Oversloot (2003). "WIS, the European tool to calculate thermal and solar properties of windows and window components." 8<sup>th</sup> Int IBPSA Conf, Eindhoven, Netherlands.
- Ding, W., Hasemi, Y. and Yamada, T. (2005). "Natural ventilation performance of a double skin façade with a solar chimney: Non-dimensional analysis." *Energy and Buildings*, 33: 411-417.
- van Dijk D (2003). "*WIS version 2.0.1 User Guide*." (<http://www.windat.org>)
- van Dijk D and J Goulding (editors) (1996). Reference Manual WIS, Advanced Windows Information System. Univ of Dublin, Ireland. ([http://windat.ucd.ie/wis/html/wis201/docs/WIS\\_ref\\_manual\\_10.pdf](http://windat.ucd.ie/wis/html/wis201/docs/WIS_ref_manual_10.pdf))
- DiMaio, F., van Passen, A. H. C. (2001). "Modelling the air infiltrations in the second skin façade", Proc. IAQVEQ Conf., Changsha, China, pp 873-880.
- Energy Performance of Buildings Directive 2002/91/EC of the European Parliament and of the Council of 16 December 2002 on the energy performance of buildings, <http://eur-lex.europa.eu/LexUriServ/LexUriServ.do?uri=CELEX:32002L0091:EN:HTML>
- Duarte, R, et al (2005). "Glazing-related problems due to high temperatures in double skin façades." CISBAT 2005, Lausanne, Switzerland.
- Duffie, J.A. and Beckman, W.A. (1991). Solar engineering of thermal processes, 2 ed., New York, John Wiley & Sons.
- Eicker, U., Fux, V., Bauer, U., Mei, L. and Infield, D., (2008), "Facades and summer performance of buildings", *Energy and Buildings*, 40:600-611.
- EN 13830 (2003) - Curtain walling. Product standard
- EN ISO 140-4 (2000) - Acoustics. Measurement of sound insulation in buildings and of building elements. Part 4: Field measurements of airborne sound insulation between rooms.

- Etzion, Y and E Erell (2003). "Controlling the transmission of radiant energy through windows: a novel ventilated reversible glazing system." *Building and Environment*, 35(5):433-444.
- Erell E, et al (2004). "'SOLVENT': Development of a reversible solar-screen glazing system." *Energy and Buildings*, 36(5):467-480.
- Ferguson, JE and JL Wright (1984). "VISION: A computer program to evaluate the thermal performance of super windows." NRC Canada, Report No. Passive-10.
- Fallahi A (2009)., "Thermal Performance of Double-skin Façade with Thermal Mass", Ph.D. Thesis, Department of Building, Civil and environmental Engineering, Concordia University, Canada.
- Faggembauu, D, et al (2003a). "Numerical analysis of the thermal behaviour of glazed ventilated facades in Mediterranean climates. Part II: applications and analysis of results." *Solar Energy*, 75:229-239.
- Faggembauu, D, et al (2003b). "Numerical analysis of the thermal behaviour of ventilated glazed facades in Mediterranean climates. Part I: development and validation of a numerical model." *Solar Energy*, 75:217-228.
- Flamant, G, Heijmans, N, and E Guiot (2004). "Determination of the energy performances of ventilated double facades by the use of simulation integrating the control aspects - modelling aspects and assessment of the applicability of several simulation software. Final Report." Belgian Building Research Institute (BBRI), Department of Building Physics, Indoor Climate and Building Services. (<http://www.bbri.be/activefacades/index2.htm>)
- Flamant, G, et al (2004). "Real-scale testing of ventilated double façades. Performance assessment in a PASLINK test cell." Belgian Building Research Institute (BBRI), Dept of Building Physics, Indoor Climate and Building Services. (<http://www.bbri.be/activefacades/index2.htm>)
- Gan, G (1998). "A parametric study of Trombe walls for passive cooling of buildings." *Energy and Buildings*.
- Gan, G., (2006), "Simulation of buoyancy-induced flow in open cavities for natural ventilation", *Energy and Buildings*, 38:410-420.
- Garcia-Hansen, V, Esteves, A, and A Pattini (2002). "Passive solar systems for heating, daylighting and ventilation for rooms without an equator-facing facade." *Renewable Energy*, 26(1):91-111.
- Garde-Bentaleb, F, et al (2002). "Bringing scientific knowledge from research to the professional fields: the case of the thermal and airflow design of buildings in tropical climates." *Energy and Buildings*, 34(5):511-521.
- Gomes, M.G. and Moret Rodrigues, A., (2006). "Numerical modelling of venetian blinds radiative properties". *Proceedings of Healthy Buildings 2006*. Lisbon, Portugal, Jun 4-8.
- Gomes, M.G., Santos, A. and Moret Rodrigues, A., (2008). "Experimental and Numerical Determination of Radiative Properties of Fenestration Systems". *PLEA 2008*. Dublin, Ireland, October 22-24, abs n° 313, pp. 240.
- Gosselin, JR (2005). IEA-ECBCS Annex 44, Subtask A contribution to the state of the art report.
- Gosselin, J. and Chem, Q., (2008), "A computational method for calculating heat transfer and airflow through a dual-airflow window", *Energy and Buildings*, 40:452-458.
- von Grabe, J (2002). "A prediction tool for the temperature field of double facades." *Energy and Buildings*, 34(9):891-899.

- Gratia, E and A de Herde (2004a). "Natural cooling strategies efficiency in an office building with a double-skin facade." *Energy and Buildings*, 36(11):1139-1152.
- Gratia, E and A de Herde (2004b). "Natural ventilation in a double-skin facade." *Energy and Buildings*, 36(2):137-146.
- Gratia, E and A de Herde (2004c). "Optimal operation of a south double-skin facade." *Energy and Buildings*, 36(1):41-60.
- Gratia, E., A. De Herde, (2004d) Is day natural ventilation still possible in office buildings with a double-skin facade?, *Building and Environment* 39 (4) 399-409.
- Gratia, E., A. De Herde, (2007), "The most efficient position of shading devices in double skin facades", *Energy and Buildings*, 39:364-373.
- Gratia, E., A. De Herde, (2007a), "Are energy consumptions decreased with the addition of a double skin?", *Energy and Buildings*, 39:605-619.
- Gratia, E., A. De Herde, (2007b), "Green-house effect in double skin facade", *Energy and Buildings*, 39:199-211.
- Grimme, FW a L, M (1999). "Energy Efficiency in Tropical Office Buildings. Latest Developments in Daylight Guidance Systems. Modern Glazings - Efficient for Cooling and Daylighting. Development of Energy Efficiency Policy for Buildings and Research Activities after 1970 in the field of Low Energy." *Conferencia Internacional de Energía Renovable y Educación Energética*, Havana, Cuba.
- Haase, M, Wong, F and A Amato (2004). "Double-skin facades for Hong Kong." *International Conference on Building Envelope Systems & Technology*. Sydney, Australia.
- Haase, M, and A Amato (2005a). "Double-skin facades in Hong Kong." *5th International Postgraduate Research Conference*, Salford, U.K.
- Haase, M, and A Amato (2005b). "Fundamentals for climate responsive envelopes". *Glass in Buildings 2*, Bath, UK.
- Haase, M (2005c). IEA-ECBCS Annex 44, Subtask A contribution to the state of the art report.
- Haase, M., Amato, A., (2005c), Development of a double skin façade system that combines airflow windows with solar chimneys, Sustainable Building 2005, Tokyo, Japan,.
- Haase, M., Amato, A., (2005d), Double-skin facades in Hong Kong, 5th International Postgraduate Research Conference, University of Salford, Salford, U.K.
- Haase, M., Marques da Silva, F. Amato, A., (2007), "Model validation of double-skin façade simulation", Sustainable Building conference 2007 (SB07), Hong Kong SAR
- Haase, M., (2008), Double-skin facades for Hong Kong, PhD Thesis, University of Hong Kong, Dep. of Architecture.
- Haase, M., Marques da Silva, F. Amato, A., (2008), "Energy Implications of Control Strategies in ventilated facades", 29<sup>th</sup> International AIVC Conference, Kyoto, Japan, October 2008, vol.2, pp 123-139
- Haddad, Kamel H and AH Elmahdy (1998). "Comparison of the monthly thermal performance of a conventional window and a supply-air window." *ASHRAE Transactions: Symposia*. SF-98-13-3.
- Haddad, KH and AH Elmahdy (1998). "Comparison of the thermal performance of an exhaust-air window and a supply-air window." *ASHRAE Transactions*. Vol. 105, Part 2. SE-99-12-4.
- Hamza, N., (2008), "Double versus single skin facades in hot arid areas ", *Energy and Buildings*, 40:240-248.

- Hensen, J, Bartak, M, and F Drkal (2002). "Modelling and simulation of a double-skin facade system / Discussion." *ASHRAE Transactions*. 108:1251.
- Hensen, Bartak, M., Drkal, F. (2002), Modelling and simulation of a double-skin facade system / Discussion, *ASHRAE Transactions* 108 1251
- Holmes, MJ (1994). "Optimization of the thermal performance of mechanically and naturally ventilated glazed facades". *Renewable Energy*. 5:1091-1098.
- Hoseggen, R., Wachenfeldt, B. J. and Hanssen, S. O., (2008), "Building simulation as an assisting tool in decision making. Case study: with or without double skin façade?", *Energy and Buildings*, 40:821-827.
- IEA, EAH (2002). "HybVent - Hybrid ventilation."  
<http://hybvent.civil.auc.dk/>
- IEA-ECBCS Annex 44, (2004), 2<sup>nd</sup> Annex preparation workshop, Trondheim.
- Inger, A (2005). IEA-ECBCS Annex 44, Subtask A contribution to the state of the art report.
- Inoue, T, et al (1985). "Study on the thermal performance of ventilation window." *International Symposium on Thermal Application of Solar Energy*. 221-226.
- Jiru, TE and F Haghghat (2005) "Airflow and thermal modeling of DSF." IEA-ECBCS Annex 44, Subtask A contribution to the state of the art report.
- Jiru, TE and F Haghghat, (2008), "Modeling ventilated double skin façade. A zonal approach ", *Energy and Buildings*, 40:1567-1576.
- ISO Standard 7730, (2006), Moderate thermal environments – determination of the PMV and PPD indices and specification of the conditions for thermal comfort.
- ISO 14040: (2006) - Environmental management — Life cycle assessment - Principles and framework.
- ISO 14044: (2006) - Environmental management — Life cycle assessment - Requirements and guidelines.
- Jones, J, Messadi, T and L Shang-Shiou (1999). "Experimental study of the cooling season performance of ventilated double-glass envelope cavities." *Int Building Physics Conference*.
- Kalyanova, O, Poizaris, H and P Heiselberg (2005). IEA-ECBCS Annex 44, Subtask A contribution to the state of the art report.
- Kalyanova, O and P Heiselberg (2008)., Empirical Validation of Building Simulation Software: Modelling of Double Facades, IEA-ECBCS Annex 43, Subtask E Technical Report.
- Karsai, P (1997). "Façade procurement - the role of the façade consultant." *International Conference on Building Envelope Systems and Technology*. Ottawa, Canada, 167-172.
- Kleiven, T and Aschehough (2005). "Double facades at high latitudes. User experiences from Hamar Town hall." SINTEF report STF50 A05030, Trondheim, Norway.
- Kopstad, S and O-J Engelstad (2001). "Double facades in Norway – use and future potential." Student project at the Norwegian University of Science and Technology, Department of Civil and Transport Engineering, Trondheim, Norway.
- Lam, JC and DHW Li (1998). "Daylighting and energy analysis for air-conditioned office buildings." *Energy*, 23(2):79-89.
- Lam, JC and DHW Li (1999). "An analysis of daylighting and solar heat for cooling-dominated office buildings." *Solar Energy*, 65(4):251-262.

- Leal, V, et al (2003). "Modeling a reversible ventilated window for simulation within ESP-R – the SOLVENT case." Proceedings from Building Simulation 2003.
- Leal, V, et al (2004). "An analytical model for the airflow in a ventilated window with known surface temperatures." Proceedings from Roomvent 2004.
- Lee, E, et al (2002). "High-performance commercial building façades." Lawrence Berkeley National Laboratory, Un of California, Berkeley. LBNL-50502. (<http://gaia.lbl.gov/hpbf/main.html>)
- Loncour, X, et al (2003). "Ventilated double facades. Evaluation of the existing standards/requirements applying on buildings equipped with ventilated double facades-overview of the existing documents and potential problems."
- Loncour, X, Flamant, G and P Wouters (2004a). "Les doubles façades ventilées."
- Loncour, X, et al (2004b). "Ventilated double facades.", <http://www.bbri.be/activefacades/new/download/Ventilated%20Doubles%20Facades%20-%20Classification%20&%20illustrations.dvf2%20-%20final.pdf>
- Magali, B and E Gratia (2002). "Ventilated double facades Project. Maintenance and durability of ventilated double facades." Un Catholique de Louvain (UCL).
- Manz, H (2003). "Numerical simulation of heat transfer by natural convection in cavities of facade elements." *Energy and Buildings*, 35(3):305-311.
- Manz, H., Schaelin, A. and Simmler, H.. (2004). "Airflow patterns and thermal behaviour of mechanically ventilated glass double façades." *Energy and Buildings*, 39: 1023-1033.
- Manz, H., Frank, Th.. (2005). "Thermal simulation of buildings with double skin façades." *Energy and Buildings*, 37: 1114-1121.
- Marques da Silva, F., (2004) "Building Natural Ventilation. Atmospheric Turbulence", PhD Thesis, LNEC TPI 33, ISBN 972-49-2020-8 (in portuguese).
- Marques da Silva, F and MG Gomes (2005). "Effects of different multi-storey double skin façade configurations on surface pressures." CISBAT 2005, Lausanne, Switzerland.
- Marques da Silva, F., Duarte, R., Cardoso e Cunha, L., (2006a) Monitoring of a Double Skin Façade Building: Methodology and Office Thermal and Energy Performance, Healthy Buildings 2006, Lisbon,.
- Marques da Silva, F and MG Gomes, (2006b) Double-Skin Façade Thermal Monitoring, Healthy Buildings 2006, Lisbon.
- Marques da Silva, F.; Gomes, M. Glória; Pereira, I.; Pinto, A.; Moret Rodrigues, A. – "Evaluation of a double skin façade performance: Results from summer and winter monitoring", *Proceedings of ROOMVENT 2007*, Helsinki, Finland, 13-15 Jun. 2007, session C06 - abs n° 1100, pp. 240
- Marques da Silva, F and MG Gomes, (2008) Gap inner pressure in multy-storey double skin facades, *Energy and Buildings*, 40 (08) 1553-1559.
- Marques da Silva, F and MG Gomes, Pinto A., I. Pereira, Moret Rodrigues, (2008), "Performance Evaluation of a Reversible Flow Double Skin Facade", 29<sup>th</sup> International AIVC Conference, Kyoto, Japan, October 2008, vol.2, pp 117-123.
- Martin, Y and X Loncour (2004). "Les doubles façades ventilées. Exigences en matière de securité incendie." CSTB. (<http://www.bbri.be/activefacades/>)
- McEvoy, ME and SG Southall (2000). "Validation of a computational fluid dynamics simulation of a supply air 'ventilated' window." CISBE Conference, Dublin, Ireland.

- McEvoy, ME, et al (2003). "Test cell evaluation of supply air windows to characterize their optimum performance and its verification by these modeling techniques." *Energy and Buildings*, 35(2003):1009-1020.
- Mei, L, Infield, D., Eicker, U. and Fux, V. (2003). "Thermal modelling of a building with an integrated ventilated PV façade." *Energy and Buildings*, 35:605-617.
- Micono, C., Perino, M., Serra, V., Zanghirella, F. and Filippi, M. (2006). Performance assessment of innovative transparent active envelopes through measurements in test cells. Research in Building Physics and Building Engineering - Proceedings of the 3rd International Building Physics Conference, Concordia University, Montreal, Canada, 27-31 August 2006, pp. 293-300, London, UK, Taylor & Francis.
- Müller, H (1983). "Exhaust-air ventilated windows in office buildings." Proceedings of the 18<sup>th</sup> Intersociety Energy Conversion Conference, 5:2015-2018.
- Oesterle, E, et al (2001). Double-skin facades: integrated planning : building physics, construction, aerophysics, air-conditioning, economic viability. Prestel, Munich.
- Ong, K.S. (2003). "A mathematical model of a solar chimney", *Renewable Energy*, 28: 1047-1060.
- Onur, N, et al. "An experimental study on air window collector having a vertical blind for active solar heating." *Solar Energy*, 57(5):375-380.
- Pappas, A. and Zhai, Z., (2008), "Numerical investigation on thermal performance and correlations of double skin façade with buoyancy driven flow", *Energy and Buildings*, 40:466-475.
- Park, C-S (2003). "Occupant-Responsive optimal control of smart facade systems." PhD thesis, Georgia Institute of Technology, Georgia.
- Park, C-S, et al (2004a). "Real-time optimization of a double-skin façade based on lumped modelling and occupant preference." *Building and Environment*, 39:939-948.
- Park, C-S, et al (2004b). "Calibration of a lumped simulation for double-skin façade systems." *Building and Environment*, 36:1117-1130.
- Parkin, S (2003). "Development of a contemporary classification for ventilated double-skin façades." PLEA-20th Conference on Passive and Low Energy Architecture, Santiago, Chile.
- Parkin, S (2004). "A description of a ventilated double-skin façade classification." International Conference on Building Envelope Systems & Technology, Sydney, Australia.
- Parmentier, B (2002). "Les doubles façades ventilées. Aspects relatifs à la stabilité et à la sécurité." CSTB. (<http://www.bbri.be/activefacades/>)
- Pasquay, T (2004). "Natural ventilation in high-rise buildings with double facades, saving or waste of energy." *Energy and Buildings*, 36(4):381-389.
- van Paassen AHC and W Stec (2001). "Controlled double facades and HVAC." Proceedings of the 7<sup>th</sup> Clima 2000 World Congress, Napoli, Italy.
- van Paassen AHC and M van der Voorden (2000). "Development of simplified tools for evaluation energy performance of double façades." Proceedings of the International Building Physics Conference, Eindhoven, Netherlands.
- Patrício, J., Santos, A. and Matias, L., (2006). "Double-Skin Facades:Acoustic, Visual and Thermal Comfort Indoors". Proceedings of *Healthy Buildings* . Lisbon, Portugal, Jun 4-8
- Patrício, J. (2006), "As fachadas de dupla pele e o ambiente acústico interior", V Congresso Ibero-Americano de Acústica, Santiago, Chile (*in portuguese*)
- Perino, M (2005). IEA-ECBCS Annex 44, Subtask A contribution to the state of the art report.

- Perino M., Serra V., Zanghirella F., Issoglio R. (2007). "Energy Efficiency Assessment of Active Transparent Façades by Measurements in Test Cells", Proceedings of CLIMAMED 2007 Conference, 5-7 September 2007, pp. 273-289, Genova, Italy.
- Perino M., Serra V., Zanghirella F., Issoglio R., Marques da Silva, F, MG Gomes, I. Pereira and Pinto A., (2008), " Performance Evaluation of Advanced Integrated Façades in Laboratory Facilities", 29<sup>th</sup> International AIVC Conference, Kyoto, Japan, October 2008, vol.2, pp 41-47.
- Pinto, A. (2008), "Building environmental and energetic analysis" (in Portuguese), PhD. Lisbon, IST,.
- Poirazis, H (2004). "Double-skin facades for office buildings. Literature Review" EBD-R-04/3, Division of Energy and Building Design, Dept of Construction and Architecture, Lund Inst of Tech, Lund Univ, Lund.
- Poirazis, H (2008). "Single and Double-skin Glazed Office Buildings. Analyses of Energy Use and Indoor Climate" EBD-T-08/8, Division of Energy and Building Design, Dept of Construction and Architecture, Lund Inst of Tech, Lund Univ, Lund.
- Reichrath, S, and TW Davies (2002). "Using CFD to model the internal climate of greenhouses: past, present and future." *Agronomie*, 22(1):3-19.
- D. Saelens, (2002) Energy performance assessment of single storey multiple-skin facades, PhD, Department of Civil Engineering, KATHOLIEKE UNIVERSITEIT LEUVEN.
- Saelens, D, Carmeliet, J and H Hens (2003). "Energy performance assessment of multiple skin facades." *Intl Journal of HVAC&Research*, 9(2):167-186.
- Saelens, D, Roels, S and H Hens (2008). "Strategies to improve the energy performance of multiple skin facades." *Building and Environment*, 43:638-650.
- Shang-Shiou, L (2001). "A protocol to determine the performance of South facing double glass façade system." MSc Thesis in Architecture, Virginia Polytechnic Institute, Blacksburg, VA, USA. (<http://scholar.lib.vt.edu/theses/available/etd-04212001-152253/unresctrtd/>)
- Simapro [www.simapro.nl](http://www.simapro.nl)
- V. Serra, F. Zanghirella, M. Perino (2009a), *Experimental energy efficiency assessment of a hybrid ventilated transparent façade*, Proceedings of the 4th International Building Physics Conference - "Energy Efficiency and new approaches", pg 247 – 254, Istanbul Technical University, Istanbul, Turkey, 15 – 18 June 2009, edited by N.T. Bayazit, G. Manioglu, G.K. Oral, Z. Yilmaz, ISBN 978-975-561-350-5.
- Serra V., Zanghirella F., Perino M., (2009b)*Experimental Evaluation of a Climate Façade: Energy Efficiency and Thermal Comfort Performance*, Energy Buildings (2009), doi:10.1016/j.enbuild.2009.07.010.
- Sodergren, D and T Bostrom (1971). "Ventilating with the exhaust-air window." ASHRAE Journal, April, 51-57.
- Southall, RG and M McEvoy (2000). "Results from a validated CFD simulation of a supply air 'ventilated' window." Proceedings from Roomvent 2000.
- Stec, W and AHC van Paassen (2001). "Controlled double facades and HVAC." 7th Clima 2000 World Congress, Napoli (I).
- Stec, W and AHC van Paassen (2002). "Validation of the simulation models of double skin facade." ABT2002, Hog Kong.

- Stec W and AHC van Paassen (2003). "Defining the performance of the double skin façade with the use of the simulation model." Proceedings of the 8<sup>th</sup> International IBPSA Conference Building Simulation 2003, Eindhoven, The Netherlands.  
([http://www.ocp.tudelft.nl/et/Research/EnergyInBuiltEnvironment/SecondSkinFacade/DSF/publications/p492final\\_v2.pdf](http://www.ocp.tudelft.nl/et/Research/EnergyInBuiltEnvironment/SecondSkinFacade/DSF/publications/p492final_v2.pdf))
- Stec, WJ, AHC Paassen and Mariarz, A. (2005), "Modeling the double skin façade with plants", *Energy and Buildings*, 37:419-427.
- Sullivan, R (1986) Thermal comfort issues in the LRI study Internal Memorandum/Report, Windows and Daylighting Group, LBLN, Berkeley.
- Takahashi, Y (2005). IEA-ECBCS Annex 44, Subtask A contribution to the state of the art report.
- Takemasa, Y, et al (2004). "Performance of hybrid ventilation system using DSF and vertical airshaft." ([http://kajima.co.jp/tech/katri/technical/annualj/vol\\_52/pdf/52-33.pdf](http://kajima.co.jp/tech/katri/technical/annualj/vol_52/pdf/52-33.pdf))
- Tanimoto, J and K Kimura (1997). "Simulation study on an airflow window system with an integrated roll screen." *Energy and Buildings*, 26:317-325.
- Tomory, T (1983). "Extract-air window." Proceedings of 9<sup>th</sup> CIB Congress, Stockholm, Sweden.
- Teshome, E. J., (2006) "A New Generation of Zonal Models: Development, Verification and Application" Ph.D. Thesis (Building), Department of Building, Civil and Environmental Engineering, Concordia University
- Welleershoff, F and M Hortmanns (1999). "Wind loads on double façade systems with gaps greater than 15 cm." 10<sup>th</sup> ICWE, Copenhagen, Denmark.
- Wigginton, M and J Harris (2002). *Intelligent Skins*. Butterworth-Heinemann, Oxford.
- Wright, JL (1986). "Effective U-values and shading coefficients of preheat/supply air glazing systems." Proceedings of Renewable Energy Conference '86, Solar Energy Society of Canada, Ottawa, Canada.
- Wong, C., Prasad, D. and Behnia, M., (2008), "A new type of double skin façade configuration for the hot and humid climate", *Energy and Buildings*, 40:1941-1945.
- Xu, L. and Ojima, T (2007). "Field experiments on natural energy utilization in a residential house with a double-skin façade system." *Building and Environment*, 42: 2014-2023
- Xu, X. and Yang, Z., (2008), "Natural ventilation in double skin façade with Venetian blind ", *Energy and Buildings*, 40:1498-1504.
- Zanghirella, F (2008). "Numerical and experimental analysis of active transparent façades", PhD Thesis, Department of Energetics, Politecnico di Torino, Torino, Italy (in Italian).



# 5. THERMAL MASS ACTIVATION (TMA)

## 5.1 Description of principles & technologies

Thermal mass is defined as the mass of the building that has the ability to store thermal energy (heat or cooling energy). Thermal capacity of building mass is defined as the amount of heat essential for increase the temperature of a given mass by one Kelvin [ASHRAE, (1999)]. Utilization of the building's thermal mass helps to reduce wide fluctuations of the outdoor temperature and keep the indoor temperature within a comfortable range [Asan and Sancakta, (1998)]. Therefore, the thermal mass offers the engineers and architects powerful opportunity to manage the building's energy consumption efficiently.

The thermal mass plays important role in the thermal performance of buildings, helps to satisfy occupant comfort and as well as brings substantial energy savings. In winter, the solar gain stored by the thermal mass can be released back into the room at nighttime, which can cover significant part of the heat losses of the building. In specially designed buildings, so called "passive houses", no additional heating system is necessary [Badescu and Sicre, (2003)]. In summer, the thermal mass can store large part of the indoor heat gains as well as delay the heat transfer from outside to inside, thus it can reduce the peak cooling loads in the building. The night ventilation (natural, mechanical or hybrid) can be utilized to remove the excess heat and cool down the thermal mass. It is very important to maximize the storage capacity of the thermal mass during daytime. In transition (middle) seasons, the thermal mass can have same positive effects on indoor conditions. It can absorb excess heat at daytime and release it in later afternoon and evening.

There are many successful techniques/concepts that help to passively – i.e. without a need for a consumption of additional mechanical work – utilize the thermal mass of the buildings. These applications include passive cooling systems, such as night flush cooling and earth cooling [Lechner, (2001)], thermal storage heating system or passive solar heating system.

Besides the passive utilization of the thermal mass, where the heat transfer processes in the thermal mass are left to follow only natural processes, there are also building components where the process of heat storage/release can be intensified and, to some extent, controlled.

Such elements allow to exploit a concept often commonly called "***thermal mass activation***".

There exists many examples of thermally activated elements; some refer to quite innovative and new components and concepts, others, like the Chinese "Kang" are simple, but effective, technologies used since ancient times.

The "Chinese Kang" represents a simple example of the thermal mass activation, which has been used for many years. Chinese kang (Figure 5.1) consists of three main components: stove, heated bed and chimney. The kang is often a rectangular platform made of bricks. Its interior cavity, leading to a flue channel that exhausts fume from a wood or coal stove. The stove fume heats up the kang's body, used as thermal mass, which stores the heat, and releases it to the bedroom later, keeping the room warm during non-cooking periods. Up to date, Chinese kangs play a very important role in the rural energy management and the rapid urbanization development, since more than 170 million rural people in northern China use it for heating. Similar traditional heating systems also existed in other countries, such as ondol in Korea [Yeo et al, (2003)] and hypocaust in the ancient Rome [Bansal, (1998)], but only Chinese Kangs are still widely used today in more than 40 million homes.



**Figure 5.1 - Some photos of traditional kangs from field survey [Li et al.( 2007)].**

Since the utilization of hypocaust in ancient Rome, thermal mass activation was newly recognized in Europe in 1937 when the system called “Crittall” was installed in Switzerland representing water based thermal mass activation system. The embedded steel welded pipes in a concrete slab provided radiant heating and cooling [Deecke et al. (2003)]. Most of the early cooling ceiling systems developed in the 1930s failed, because the condensation often occurred during operation in cooling mode. Subsequent studies showed that this problem could be avoided if the radiant system was used in conjunction with a small ventilation system designed to lower the dew point of the indoor air (by means of extracting the moisture internal load). This combination proved to be successful in a department store built in 1936-1937 in Zurich [Giesecke (1946)] and in a multi-story building built in the early 1950s in Canada [Manley (1954)]. The water-based thermal mass activation components had their comeback in the beginning of nineties again in Switzerland [Meierhans (1993 and 1996)]. Since then, newly built systems utilize thermal storage capacity of the concrete slabs between each storey of multi-storey building. The TermoDeck® system was developed in Scandinavia by two Swedish engineers Mr. Loa Anderson and Dr. Engelbrekt Isfält in the 1970s. Since 1970s over 360 buildings have been constructed incorporating TermoDeck, mainly in Scandinavia, Northern Europe, UK, the Middle East and North America. In the early days TermoDeck concentrated on office type buildings, but nowadays the applications are spread to school buildings, hotels theatres, hospitals and public buildings.

## **5.2 Classification of the thermal mass activation concepts and technologies**

According to its location, there are two basic types of thermal mass in the building [Li and Xu (2006)], i.e. external and internal thermal mass.

- The external thermal mass such as walls and roofs is directly exposed to ambient temperature variation.
- The internal thermal mass such as furniture and purpose-built internal concrete partitions is exposed to indoor air temperature.

Various combinations of internal and external thermal mass utilization are possible in a building as shown in Figure 5.2 [Li and Xu (2006)]. A typical interior wall installation, as shown in Figure 5.2B, is effectively an internal thermal mass problem if the exterior insulation is perfect. Depending on the relative location of the insulation layer, a concrete wall can act either as internal thermal mass (Figure 5.2B, 5.2D and 5.2F) or external thermal mass (Figure 5.2C, 5.2E).

According to its thermal storage capability, there are two primary thermal mass in buildings, i.e. butterfly-type (lightweight) and elephant-like (heavyweight) thermal mass [Randall et al. (1999)]. Butterfly-type buildings will have highly responsive skins with a great deal of glass and will react quickly to respond to the environment, such as changes in solar radiation, light and temperature by altering their properties. Elephant-like buildings have much more thermal mass and lack quick response, which will change temperature with environment slowly - after a period of time.

Generally, adobe brick, earth, natural rocks, stones, concrete and other forms of masonry, as well as the water are commonly used materials for thermal mass elements. Some heat-storage materials used in buildings are compared as shown in Table 5.1 [Lechner (2001)].

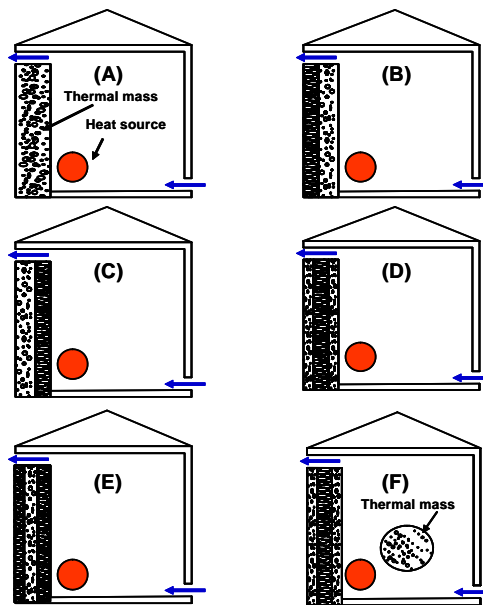


**Figure 5.2 - Illustration of six simple building models with different relative location of the thermal mass to the insulation and the existence of internal thermal mass [Li and Xu (2006)].**

**Table 5.1 - Comparison of various heat-storage materials [Lechner (2001)].**

Material	Advantages	Disadvantages
Water	Quite compact Free	A water storage tank is required, which means additional costs Leakage is possible
Concrete (stone)	Very stable Can also serve as wall, floor, etc	Expensive to buy and install because of weight
Phase-change material (PCM)	Most compact Can fit into ordinary wood-frame construction	Most expensive Long-term reliability is not yet proven

Basically the thermal mass activation components can be divided into two main categories, accordingly to the “activation principles”: *1) Surface Thermal Mass Activation – SA* and *2) Core Thermal Mass Activation – CA*; these basic principles are illustrated in Figure 5.3.

Core thermal mass activation (“CA”)<sup>1</sup> systems are such heating/cooling systems that are integrated (or thermally coupled) with a building construction having high thermal capacity (floor/ceiling slab, walls etc.). The thermal mass is “equipped” with ducts for circulation of air or embedded pipes (mostly made from cross linked polyethylene; PE-X) for circulation of a heat carrier (usually water). Building components with embedded water pipes are mostly used today (Figure 5.4a). Besides the water-based systems, also airborne systems like TermoDeck in Sweden [Smith and Raw (1999), Karlström (2005)] were developed. Ventilation air is led through ducts in a concrete slab placed in the ceiling, which is used as thermal mass and then supplied into the room (Figure 5.4b).

<sup>1</sup> The International standard EN 15377 (2008) uses term “Thermo Active Building System” (TABS). The systems are also called “Thermally activated Building System” in some literature. Moreover, the new REHVA Guidebook by Babiak et al. (2007a) uses term “Thermally-Active Building System”.

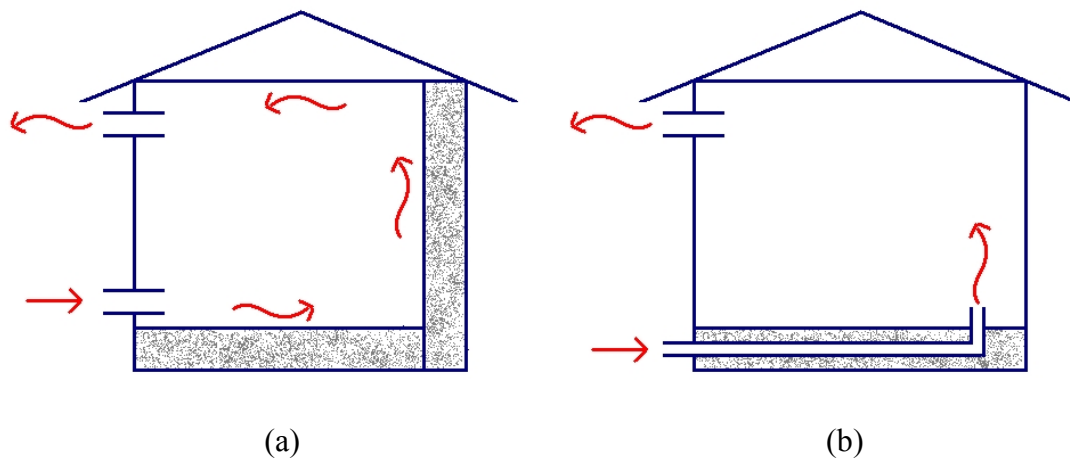


**Figure 5.3 - Thermal mass activation working principles: a) SA: activation involves only the surface of the element; b) CA: activation involves whole structure (core) of the element.**

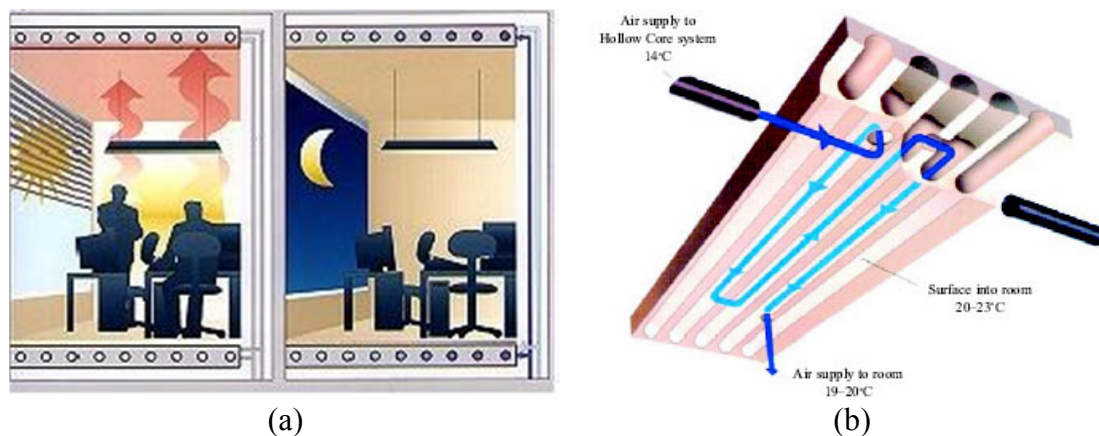


**Figure 5.4 - Examples of TMA – CA systems. a) Principle of the Thermo Active Building System - TABS ([www.velta.de/](http://www.velta.de/) October 2006); b) Principle of the ThermoDeck® system.**

ThermoDeck has primarily been used in office type buildings but also in school buildings, hotels theatres, hospitals and public buildings.

In comparison to other radiant heating/cooling systems, the operation of a boiler/chiller can lack behind the building thermal loads. Circulation of the heat carrier (air or water) has not only a direct heating/cooling effect, but also reduces the peak load (transfers a part of the load outside the period of occupancy).

The daily heat loads are accumulated in the thermal mass and consequently extracted during the night. This shift of the loads into the night time allows chillers to be operated using cheaper night-tariff electricity prices. Moreover, the temperatures of the heat carrier are usually close to room the temperature. This increases efficiency of mechanical cooling equipment - chiller or a heat pump. Moreover, it also gives an opportunity to utilize renewable energy sources like ground heat exchangers etc.

Figure 5.5 illustrates the three basic types of the core thermal mass activation elements. They can be divided according to the heat transfer media, which is used for the activation. It can be either air (airborne systems) or water (water based systems; in some applications water with anti-freezing additives can be used).

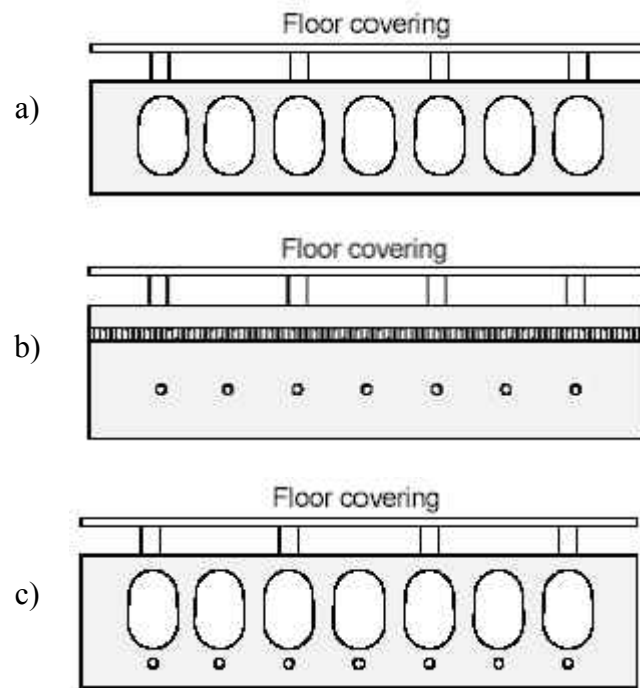


**Figure 5.5 - Basic types of currently used thermo active building components (Wietzmann 2002): a) hollow deck with cavities for air circulation; b) on-site constructed floor (with insulation); c) hollow deck with integrated pipes (hollow can be also filled up with polystyrene or other light materials).**

### **5.2.1 Airborne systems**

The cavities are used to circulate air through the concrete slabs, Figure 5.5a. In this way the concrete mass is heated or cooled. The circulated air can be also supplied to the premises. The decks are constructed to ensure large heat exchange surface between the air stream and the concrete. The cavities also allow the air to get through the whole floor construction. The TermoDeck® system is an example of such airborne system. It consists of prefabricated hollow core concrete elements of width 1.2 m. The maximum span of the element is 18 meters. The thickness of the elements varies with the span.

The standard system can be operated both for cooling and heating. Figure 5.6 shows how the slabs are incorporated into the building. The elements are supplied with ventilation air from a main supply duct, which runs along a central corridor. Normally it is located behind a suspended ceiling. Air is supplied to the rooms through supply diffusers located in the ceiling and the air is extracted from the room through extract grills located at ceiling level.

The construction time for a pre-fabricated building can be reduced by up to 30% compared to a conventional concrete building. There is also a reduction in capital cost due to a reduction in fans, chillers, ducts and radiators (in hot climates 40-50%). Furthermore, there is no need for suspended ceilings. There is no need for a ceiling void and therefore the storey heights may be reduced by 15-25% per floor.

System also enables reduction of peak power demand. TermoDeck projects in Europe showed that the system could have up to 40% lower energy consumption for heating compared to equally sized conventional buildings (installations in Middle East have resulted 15.30 % lower bills for electricity).

The fact that the system enables ventilation of the occupied space with air that passed through the hollow core slab raises a question of eventual pollution coming from the concrete ducts. The suitability of using concrete ducts for building ventilation has been an issue discussed over many years.

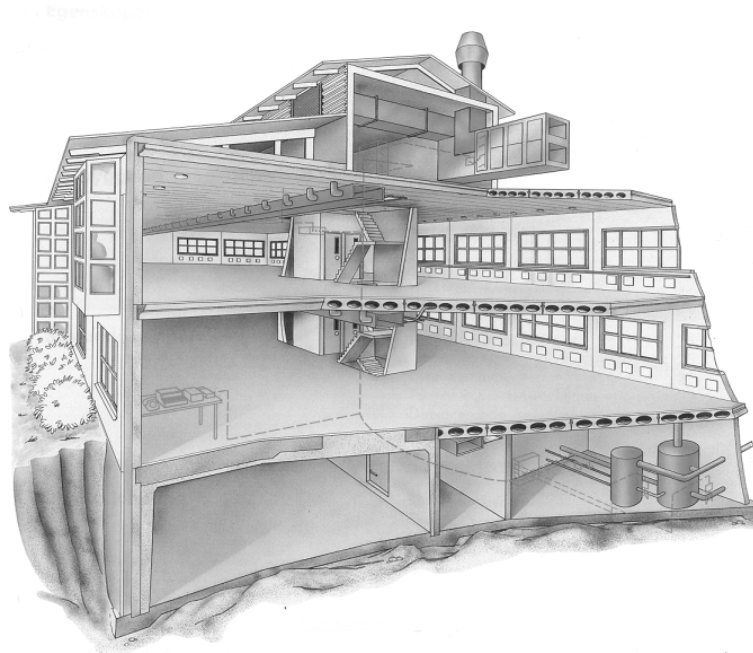


**Figure 5.6 - Typical built up of the ventilated hollow concrete core slab system - TermoDeck® .**

The questions have been following:

- Do concrete ducts emit particles to the ventilation air?
- Do concrete ducts cause a smell of cement in the ventilated room?
- Is it possible to clean concrete ducts?

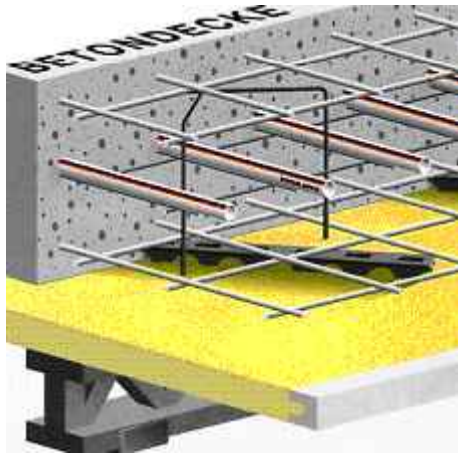
Regarding the first question a number of studies were carried out in the 1980's. In all studies the result was the same. Compared to standard ductwork made from metal sheets, concrete ducts did not increase the risk of fungal growth or other hygienic related problems. Smell of cement hasn't occurred unless the concrete was newly made or if there was a water leakage into the duct.

Regarding the cleaning issue, number of systems has been developed. They mostly use a combination of compressed air and vacuum technology. Compressed air is blown into the duct with a nozzle whose direction can be changed 360°. At the same time air is sucked with a vacuum pump connected to the slab with a hose.

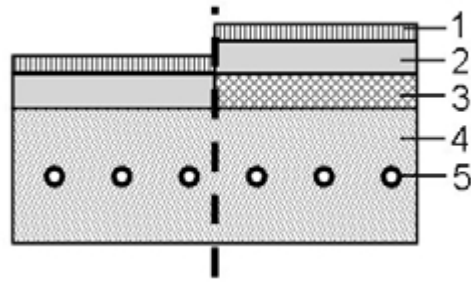
## **5.2.2 Water based systems**

Water based thermo active components are typically used in buildings in central Europe (Figure 5.5b). Pipes are commonly installed in the centre of concrete slab among reinforcements. Usual diameter of the pipes varies between 17 and 20 mm. The distance between pipes is within the range 150 - 300 mm. Figure 5.7a shows a cross-section of commercially available system.

If the system is constructed on site, the pipes are supplied in modules, which include a pipe coil attached on a metal grid and equipped with fittings (see Figure 5.8). A layer of insulation to direct the heat flows downwards and prevent noise transmission can be installed between the concrete slab and the floor surface (Figure 5.7b). Other option is to construct the floor as a raised one with option of leading the channels, pipes and wires in the space gap of double floor. If no prefabricated modules are used or building shape is more complicated, pipes can be manually attached to the reinforcement. The reinforcement grid with the pipes is then covered by a concrete mass (Figure 5.9).



a)



b)

**Figure 5.7 - a) Cross-section of the on-site constructed system ([www.uponor.de/](http://www.uponor.de/) August 2008); b) TABS with and without acoustic insulation, 1=floor surface covering, 2=screed, 3=acoustic insulation, 4=building structure and 5= plastic pipes [Babiak et al.( 2007a)].**



**Figure 5.8 - The pipe coil module supplied to be embedded in a concrete slab on-site ([www.rehau.de/](http://www.rehau.de/) October 2006).**



**Figure 5.9 - Concrete lying on the reinforcement grid with attached pipes [Hauser et al.( 2005)].**

### **5.2.3 Other types of core activation components**

Besides the systems with pipes embedded in various depths in the reinforced ceiling slab or/and wall (eventually in the hollow core slab), there are also systems using capillary micro pipes embedded in a layer at the inner ceiling surface or placed in additional plaster or gypsum layer (see Figure 5.10).

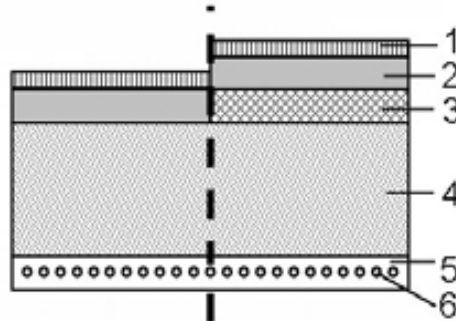


**Figure 5.10 - Example of TMA – CA system: TABS with capillary micro-pipes embedded in a layer at the inner ceiling surface with and without acoustic insulation, 1=floor surface covering, 2=screed, 3=acoustic insulation, 4=building structure, 5=plastic micro-pipes and 6=plaster or gypsum [Babiak et al. (2007a)].**

According to [Babiak et al. (2007a)] micro-pipe cooling grids can be situated on the floor, attached to the wall or mounted on the ceiling panels such as acoustic ceiling elements. The system is especially suitable for retrofit applications with a low thickness of a construction. Advanced system for the refurbishment and light-structure buildings with the capillary grids embedded in a gypsum board with micro encapsulated Phase Change Material (PCM) was developed by [Koschenz and Lehmann (2004)]. The application of PCM increases thermal capacity of the construction and promotes active energy accumulation and discharge (see also sections 7.2.1 and 7.2.2). According to [Koschenz and Lehmann (2004)], the PCM can store up to 300 Wh/(m<sup>2</sup>·day) of latent heat during the phase change. A thermally activated PCM panel system of 50-70 mm thickness has a heat storage capability comparable to 300 mm thick concrete slab.

## **5.3 Design/analysis method and tools**

### **5.3.1 Design method for passive cooling of building construction by night-time ventilations**

This paragraph describes a design method for the early design stage estimation of the potential of passive cooling of the building construction by night-time ventilation. Detailed information about the method is available in the following publications, [Artmann et al (2007), (2008), (2008a)].

The climatic conditions can be characterised by the climatic cooling potential,  $CCP$  (Kh), the thermal mass of the building can be estimated by the dynamic heat storage capacity,  $c_{dyn}$  (kJ/m<sup>2</sup>K), and the air flow pattern including the resulting heat transfer can be described by the temperature efficiency of the ventilation,  $\eta$ .

In order to assure thermal comfort two criteria need to be satisfied:

1. The thermal capacity of the building needs to be sufficient to accumulate the daily heat gains within an acceptable temperature variation.
2. The climatic cooling potential and the effective air flow rate need to be sufficient to discharge the stored heat during the night.

If both criteria are satisfied for each day of the year, the building temperature will stay within the comfort range. As the heat gains and the climatic cooling potential are highly variable, it might not be possible to satisfy both criteria for every day of the year. In this case a certain extent of overheating will occur especially during hot periods, when high heat gains coincide with a low cooling potential. Assessing the extent of overheating during hot spells requires a dynamic model considering all parameters jointly. However, for a first estimation during the concept design phase, the two criteria can be considered separately. Furthermore each day/night cycle is considered separately, and therefore dynamic effects with time periods longer than 24 hours are not taken into account.

### 5.3.1.1 Climatic Cooling Potential

Degree-days or degree-hours methods are often used to characterise a climate's impact on the thermal behaviour of a building. The daily climatic cooling potential,  $CCP_d$ , was defined as degree-hours for the difference between building temperature,  $T_b$  and external air temperature,  $T_e$  (Figure 5.11):

$$CCP_d = \sum_{t=t_i}^{t_f} m_{d,t} (T_{b(d,t)} - T_{e(d,t)}) \begin{cases} m = 1 \text{ h} & \text{if } T_b - T_e \geq \Delta T_{crit} \\ m = 0 & \text{if } T_b - T_e < \Delta T_{crit} \end{cases} \quad (1)$$

where  $t$  stands for the time of day, with  $t \in \{0, \dots, 24 \text{ h}\}$ ;  $t_i$  and  $t_f$  denote the initial and the final time of night-time ventilation, and  $\Delta T_{crit}$  is the threshold value of the temperature difference, when night-time ventilation is applied. In the numerical analysis, it was assumed that night-time ventilation starts at  $t_i = 19 \text{ h}$  and ends at  $t_f = 7 \text{ h}$ . As a certain temperature difference is needed for effective convection, night ventilation is only applied if the difference between building temperature and external temperature is greater than 3 K.

As heat gains and night-time ventilation are not simultaneous, energy storage is an integral part of the concept. In the case of sensible energy storage, this is associated with a variable temperature of the building structure. This aspect is included in the model by defining the building temperature as a harmonic oscillation around 24.5°C with an amplitude of 2.5 K:

$$T_{b(t)} = 24.5 + 2.5 \cos\left(2\pi \frac{t - t_i}{24}\right) \quad (2)$$

The maximum building temperature occurs at the starting time of night ventilation, and given a ventilation time of 12 hours, the minimum building temperature occurs at the end time (Figure 5.11). The temperature range  $T_b = 24.5 \text{ °C} \pm 2.5 \text{ °C}$  corresponds to that recommended for thermal comfort in offices.

### 5.3.1.2 Dynamic Heat Storage Capacity

To assess the necessary amount of thermal mass, the daily heat gains,  $Q_d$  (Wh) need to be estimated and the maximum acceptable daily temperature variation,  $\Delta T$  (K) needs to be determined. For the internal heat gains, the heat from people, equipment and lighting need to be considered. The solar heat gains can be estimated from the solar irradiation, the glazed area and the total solar energy transmittance (g-value) of the facade. If the outdoor temperature is higher than the indoor temperature, additional heat gains arise from thermal transmission and ventilation during the day.

The total amount of dynamic heat storage capacity,  $C_{dyn}$  (J/K) can then be estimated as,

$$C_{dyn} = \sum_i c_{dyn,i} \cdot A_i > \frac{Q_d \cdot 3600 \text{ s/h}}{\Delta T} \quad (3)$$

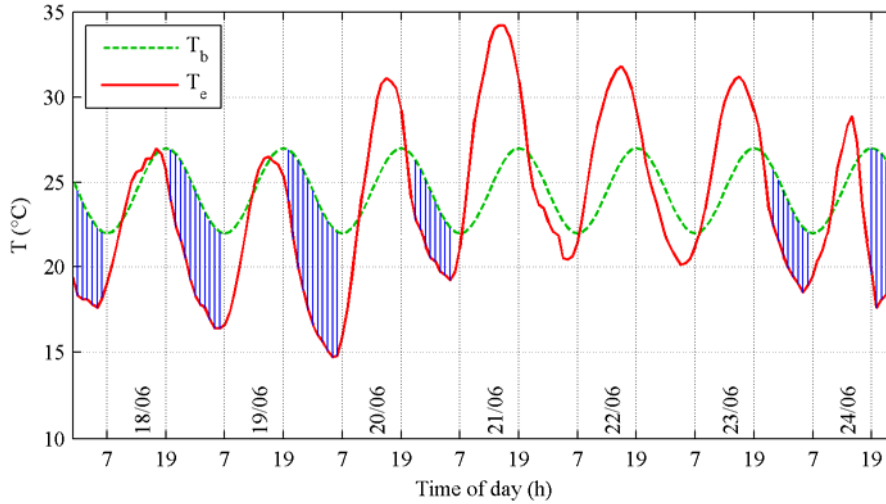


**Figure 5.11- Building temperature,  $T_b$  and external air temperature,  $T_e$  during one week in summer 2003 for Zurich SMA (ANETZ data). Shaded areas illustrate graphically the climatic cooling potential, CCP.**

In the calculation of the heat storage capacity,  $c_{dyn}$  of the building elements in the room, the surface heat transfer during the day needs to be considered. Figure 5.12 shows a example of the diurnal heat storage capacity,  $C_{dyn}$ , of a concrete slab.

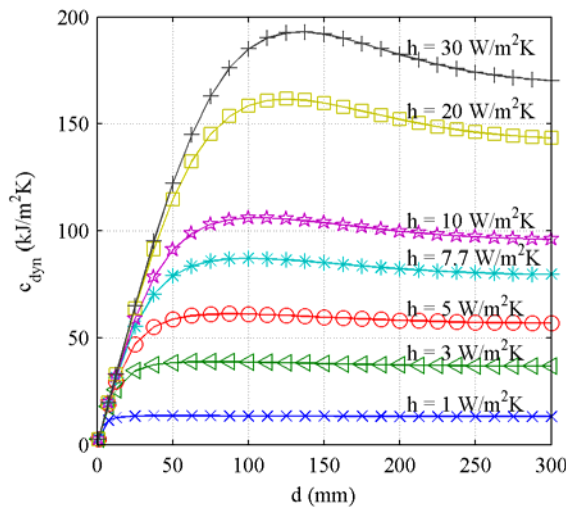


**Figure 5.12 - Diurnal heat storage capacity,  $c_{dyn}$  of a concrete slab depending on the thickness,  $d$  for different heat transfer coefficients,  $h$ .**

### 5.3.1.3 Night-time Air change Rate

The estimation of the air change rate and daily cooling potential,  $CCP_d$  necessary to discharge daily heat gains,  $Q_d$  is based on the conservation of energy during one daily cycle of charging and discharging the thermal mass:

$$Q_d = \eta \cdot A_{Floor} \cdot H \cdot \frac{ACR}{3600 \text{ s/h}} \cdot \rho_{Air} \cdot c_{p, Air} \cdot CCP_d \quad (4)$$

where  $\eta$  is the temperature efficiency of the ventilation,  $A_{Floor}$  the floor area,  $H$  the room height,  $\rho_{Air}$  the density of air and  $c_{p, Air}$  the heat capacity of air. The daily cooling potential,  $CCP_d$  available at a certain location can be determined from cumulative distributions as presented in Figure 5.13. Rearranging equation 4 yields the daily heat gains per unit floor area and  $CCP_d$  ( $Wh/m^2Kh$ ), which can be discharged at a given air change rate ( $ACH = \text{Air change per hour}$ ) depending on the temperature efficiency,  $\eta$ :

$$\frac{Q_d}{A_{Floor} \cdot CCP_d} = \eta \cdot H \cdot \frac{ACH}{3600 \text{ s/h}} \cdot \rho_{Air} \cdot c_{p, Air} \quad (5)$$

For the temperature efficiency found in the experiments with mixing and displacement ventilation [Artmann (2008a)], this correlation is shown in Figure 5.14. This diagram provides a descriptive illustration of night-time ventilation performance.

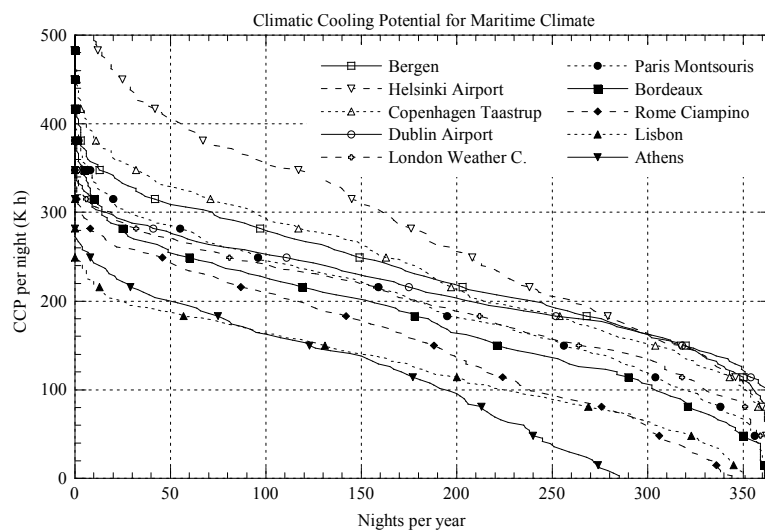


Figure 5.13 - Cumulative frequency distribution of CCP for different locations.

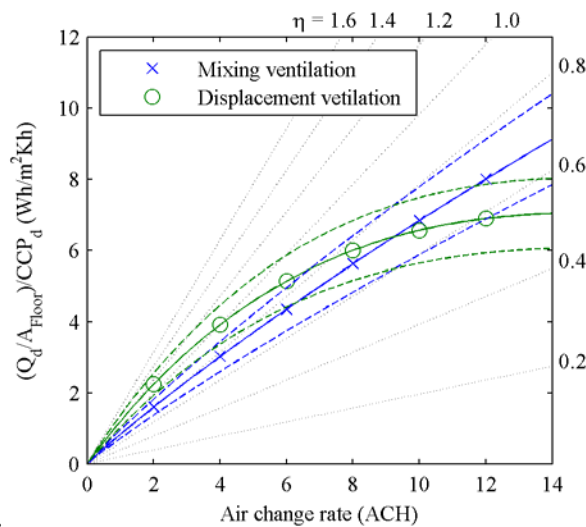


Figure 5.14 - Heat discharged during night-time ventilation per unit floor area and daily CCP depending on the air change rate; based on experimental results for mixing and displacement ventilation (including range of uncertainty) and lines of constant efficiency  $\eta$ ; room height  $H = 2.93 \text{ m}$ .

Additionally, such a diagram can be used as design chart to estimate the air flow rate, necessary to discharge daily heat gains at a given CCPd. However, in order to make this method more generally applicable, further work is needed to determine the temperature efficiency for various room geometries, constructions (amount and location of thermal mass) and air distribution principles (location of inlet and outlet openings). A catalogue of design charts for various cases will be of immediate use for estimating the performance of night-time ventilation during the concept design phase.

### **5.3.2 Design method for surface thermal mass activation**

A large number of the previous studies and computational methods on thermal mass were reviewed by [Balaras (1996)]. Sixteen different parameters were found for describing thermal mass effects, such as the total thermal time constant [Givoni, (1976)], the admittance factor [Burberry, (1983)], diurnal heat capacity [Balcomb, (1983)], the thermal effectiveness parameter [Ruud et al., (1990)], and the effective thermal storage [Mathews et al., (1991)]; [Antonopoulos and Koronaki, (1998)]. There were also many studies on different factors affecting the thermal mass performance, such as the surface area of thermal storage [Sodha et al., (1992)], the wall properties [Asan and Sancakta, (1998)], and the thickness of the wall [Antonopoulos and Koronaki, (2000)]. [Yang and Li (2008)] provide a quantitative understanding of the relationship between the thermal mass and cooling load in office-building model, which can be useful for designing thermal mass together with night ventilation.

CIBSE Guide Volume A (1988) derived some factors for analyzing the transient behavior of a building structure. These factors, including the admittance, decrement factor and surface factor, are the functions of the thickness, thermal conductivity, density and specific heat capacity, as well as locations of the materials. However, the CIBSE method may not be used directly for thermal design. Two recently developed design/analysis tools are listed below. The first one is a simple design method, using virtual sphere concept and three design parameters, and the second one is the dynamic thermal networks.

There are also several more complex tools - advanced programs. They often require a great amount of input information, but provide highly accurate results. Some of them are well-known software packages available on the market, for example ESP [Clarke (1985)] and [TRNSYS (Klein 1988)]. They are more likely to be used by people with advanced knowledge.

#### **5.3.2.1 Virtual sphere concept and three design parameters**

The concept of the virtual sphere method, originally proposed by [Gao and Reid (1997)], is to use a virtual sphere to represent the work piece of any geometry. The idea of virtual sphere originates from the similarity of the Heisler charts for the center temperature of infinite plate, long cylinder and solid sphere. If the same characteristic length is used, the three Heisler charts were found to be nearly identical, although not exactly identical. The idea is to lump up the mass elements into a virtual solid sphere with the radius determined from some significant dimensions of the thermal mass (e.g. volume and surface area) [Li and Yam (2004)], [Li and Xu (2006)]. This approach saves a calculation time as it allows to substitute the detailed thermal analysis of each individual mass element with a single large-scale heat transfer calculation (the various elements are conceptually “packed” together and represented by a virtual sphere). The method could not give accurate results, but yet provide some basic guideline for the building thermal mass design.

The characteristic length or radius of the virtual sphere is determined by the following formula:

$$R = \frac{3V}{A} \quad (6)$$

where  $V$  is the volume and  $A$  is the effective surface area.

A list of equivalent radius for some typical geometries of solid mass is reproduced from work by [Gao et al. (2000)] in Table 5.2.

**Table 5.2 - The radius of the virtual sphere for some typical geometry.**

<b>Geometry</b>	<b>Radius of the virtual sphere</b>
Sphere (radius $R$ )	$R$
Short cylinder (radius $R$ and height $H$ )	$3R(2R/H+2)^{-1}$
Long cylinder (radius $R$ and infinite height)	$1.5R$
Rectangular prism (width $W$ ; height $H$ ; length $L$ )	$3(WHL)/[2(HL+HW+WL)]$
Cube (length $L$ )	$0.5L$
Long square (cross section $L \times L$ ; infinite height)	$3L/4$
Long rectangle (cross section $L \times 2L$ ; infinite height)	$L$
Infinite plate (thickness $L$ )	$3L/2$

When the ventilation flow rate is constant, the following three parameters are found [Yam et al. (2003)], [Li and Yam (2004)] to be able to characterize the thermal mass performance, i.e. the time constant,  $\tau$ , the convective heat transfer number,  $\lambda$ , and the Fourier time constant,  $\eta$ . The Fourier time constant was derived using the concept of virtual sphere.

The three parameters are defined as follows:

$$\tau = \frac{MC_M}{\rho c_p q} \quad (7)$$

$$\lambda = \frac{h_M A_M}{\rho c_p q} \quad (8)$$

$$\eta = R^2 / \kappa \quad (9)$$

The criteria for classifying the buildings in thermally heavy, medium and light, can be based on the mathematical approach just defined [Li and Xu (2006)]:

- thermally light building: time constant  $\tau = 0-4$  hours;
- thermally medium building: time constant  $\tau = 4-20$  hours;
- thermally heavy building: time constant  $\tau > 20$  hours.

Using the virtual sphere concept and three important design parameters characterizing the thermal properties of the elements, simple general design method was developed [Li and Xu (2006)].

The method consists of five consecutive steps:

**Step 1:** Identify the total heat capacity, the radius of the virtual sphere and the effect thermal diffusivity for all internal thermal mass elements.

**Step 2:** Estimate the total ventilation flow rate.

**Step 3:** Estimate the effective  $U$ -value of all external wall elements.

**Step 4:** Estimate the three thermal mass design-related parameters.

**Step 5:** Estimate the phase shift of the indoor air temperature and attenuation factor.

### 5.3.2.2 Dynamic thermal networks

Dynamic thermal network is a theory that aims to increase insight into the factors that influence dynamic heat losses in buildings which depends on the building's construction and materials. Today the theory has been programmed into a calculation tool mainly aimed for researchers. With the tool it is easy to compare thermal behaviour and thermal mass benefits for different building components and their materials and constructions. The intention is to further develop the methodology to make it a simple, illustrative and easy-to-use design tool for engineers.

A new methodology called *dynamic thermal networks* is being developed by [Claesson (2002), (2003)] at the Department of Building Physics at Chalmers University. The relations between boundary heat fluxes and boundary temperatures for any time-dependent heat conduction process in a solid material are represented in the same way as for an ordinary thermal network (for steady-state heat conduction). The thermal conductance between the boundary surfaces remained unchanged, but a new *absorptive* component has to be introduced at each node or surface. The memory effect is accounted for by the use of certain averages of preceding boundary temperatures.

The methodology has a conceptual simplicity that should make it easy to implement in energy balance modeling. The time-dependent or *dynamic* components for heat conduction in the solid parts are simply added to the ordinary network for ventilation, heating system etc. The problem of the very different time scales for different components may be addressed in a coherent way.

The method requires that the heat fluxes through the surfaces are calculated for a unit step change at one surface while keeping zero temperature at the other surfaces. The relations between surface temperatures and heat flows for any time-dependent process are obtained by superposition of the basic step responses. This means that step-response flows contain all information required for any particular case. The theory is discussed in more detail in [Claesson (2002 and 2003)].

The heat flow problems considered above have two boundary surfaces with different temperatures. The heat flow problem may in a more general case have  $N$  boundary surfaces with different temperatures. Then the dynamic thermal network has  $N$  nodes. Each node or boundary surface has an absorptive component. There are transmittable components between all pairs of nodes just as in the corresponding steady-state network (see [Claesson (2003)]). The theory may also be applied for a subsurface of the indoor area. An example is [Wentzel (2003)], where the heat loss dynamics of different parts of the floor is analyzed. Another application for composite walls is presented in [Wentzel and Claesson (2003)], where the analyses are extended to the annual heating cost for a variable energy price.

### **5.3.3 Design method for core thermal mass activation - capacity evaluation**

The part 1 of the standard [EN 15377 (2008)] includes methods for estimation of heating and cooling capacity of the thermo active building systems. The standard suggests using of the Thermal Resistance method for steady-state conditions. Thermal resistance method uses "linear" thermal resistances for calculating heat flow density. The total heat exchange between the element and the space consists of the sum of heat fluxes from the ceiling and floor. The influence of the pipe properties (diameter, thickness, material), pipe spacing, water flow rate and the resistance of the conductive layer is integrated in the virtual resistance term. Because of the component's slow thermal dynamics it is recommended to support the calculations by the dynamic simulation; see part 3 of the [EN 15377 (2008)]. Based on the input of boundary conditions (thermal properties of building, proportions of the rooms, occupants' behavior, transient internal/external heat loads) the simulations allow to determine the development of operative temperature (to evaluate human thermal comfort conditions) in the different zones of the building as well as parameters of the system itself together with hourly development of the energy use.

Figure 5.15 shows the example of the temperature distribution in an active concrete ceiling slab, calculated using transient FEM software.

Summing up the possible methods for the TABS's capacity estimation [Babiak et al. (2007a)]:

- Thermal resistance method: steady state calculation in accordance with [EN 15377 (2008)]
- Finite Element Method (FEM) or Finite Difference Method (FDM), (dynamic state) or with other software design tools based on different methods like RC method calculation or heat transfer function [De Carli (2002)] (see the next section)
- Measurements by testing

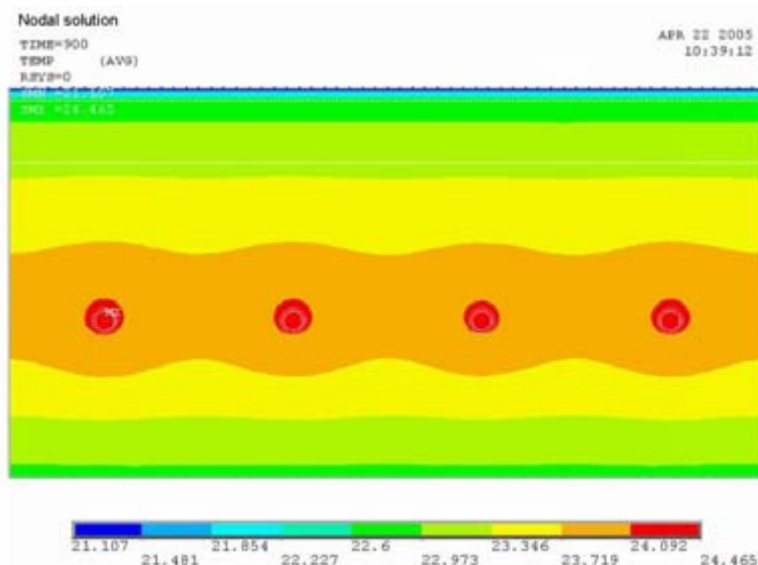


*Figure 5.15 - Temperature distribution calculated by FEM software [Babiak et al. (2007b)].*

### **5.3.4 Available design tools – core thermal mass activation**

Commercially available building simulation programs can be used to determine behaviour of the system when installed in a particular building. Available capacity of the system, distributions of indoor temperatures and thermal comfort indices can be also evaluated. For the dynamic simulation of the entire system with embedded pipes acting together with the building construction, a validated model for a floor heating system and concrete core conditioning - provided as a module of simulation program TRNSYS (TRNSYS 2004) - can be used [Schmidt et al. (2000)], [Fort (1999)]. Building simulation code IDA ICE (Indoor Climate and Energy 3.0) [Sahlin and Grozman (2003)], a whole-building simulator, offers the opportunity to simulate floor surface systems and TABS with pipes integrated to any depth under the surface. It also allows simultaneous performance assessments of all building issues such as fabric and construction, glazing, HVAC systems, controls, indoor air quality, human thermal comfort and energy consumption. The IDA ICE was also used by [Hauser (2004)] using an own TABS modelling module as an alternative to the one that is offered by the software provider.

There are many simulation tools available in the market that are capable of simulating TABS. BLAST, DOE 2.1E, CLIM2000, EnergyPlus, ESP-r and IES <VE> can be mentioned as examples. Moreover, dominative producers of the TABS solutions usually handle the design of the activated thermal mass components with their own design (selection) software tools, which are intended only for internal use.

#### **5.3.4.1 Summary of principal input parameters to be considered for capacity calculation/simulation**

- Operational mode (heating /cooling)
- Supply water temperature
- Temperature difference (supply-return, and thus the return water temperature)
- Upper and down room air temperature
- Relative air humidity (cooling)
- Horizontal position of pipes
- Distance between pipes
- Length of pipes
- Material and dimension of pipes

- Ceiling structure, floor structure, cover layer (physical parameters of layers)
- Combined heat transfer coefficient

#### 5.3.4.2 Results from the calculation

- Steady-state heating/cooling capacity through the floor and/or ceiling side
- Steady-state mean floor and/or ceiling surface temperature
- Heating/cooling water mass flow rate
- Pressure drop of the piping

### **5.3.5 Design method for core thermal mass activation - performance assessment**

An experimental testing is not typically done and necessary in case of TABS. For testing and predicting operational behaviour it is more efficient to use mathematical models (simulations) based on FEM/FDM. Software validation procedure is listed in the part 2 of [EN 15377 (2008)]

#### 5.3.5.1 Simulated performance

In the study by [Meierhans (1993, 1996)], system with embedded pipes in the slab constructions of office buildings for heating and cooling was introduced. Results in the form of simulations (compared to the measurements) were presented for an office building in Horgen, Switzerland. Three identical rooms, without cooling and natural ventilation, and two cases with TABS cooling and mechanical ventilation were tested. Case one and two with heat load of 52.5 W/m<sup>2</sup> and third with 17.5W/m<sup>2</sup>. Even during very hot outdoor air temperatures (up to 35°C) the results indicated that the indoor temperature was kept at an acceptable range (below the upper comfort temperature). Computer simulations of heating/cooling system with pipes embedded in the concrete slabs between the floors in a multi-storey building were conducted by [Hauser et al. (2000)]. The simulated system supplied or removed the heat from the space by heated/cooled water flowing in the pipes. The results showed a significant improvement of thermal comfort by reducing the annual maximum operative temperature by 10 K (39°C - 29°C) compared to no cooling.

[Brunello et al. (2001)] introduced a mathematical model for simulation of thermo-active systems with activated thermal mass. The model uses suitable transfer functions to treat conduction between the water flowing through the pipes and the surroundings. The model considers transient conditions and allows analysis of the influence of different parameters such as piping pattern, thermal storage capacity, water supply temperature etc. under different climatic conditions.

[Olesen and Dossi (2004)] performed dynamic simulation of a room in an office building using the program TRNSYS. The ceiling/floor consisted of concrete slabs with plastic pipes embedded in the middle. Heat was supplied or removed by the heated or cooled water flowing in the pipes. The multidimensional heat transfer processes in the slab were modelled. The simulation was done for two locations of the building – Wurzburg (Germany) and Venice (Italy). Different ventilation strategies, control algorithms for the water temperature (inlet- $\theta_{supply}$  or mean slab- $\theta_{mean}$ ) and circulation pump operation times were examined. Figure 5.16 shows energy transfer through the activated thermal slab and pump running hours for summer conditions with simple ventilation strategy. On the horizontal axis, the results for different control strategies (marked A ~ D) for inlet water temperature are depicted. As can be seen from Figure 5.17, during most of the working hours the operative temperature was within the range 22 – 25°C. The ranges of operative temperatures were sufficient to meet the thermal comfort requirements of the current standards. Regarding the water circulation pump, researchers concluded that its operation only during the night time had almost the same effect as continuous operation. This can be explained by larger temperature difference between the water in the pipe and the concrete core, and therefore a larger heat transfer between core and water.

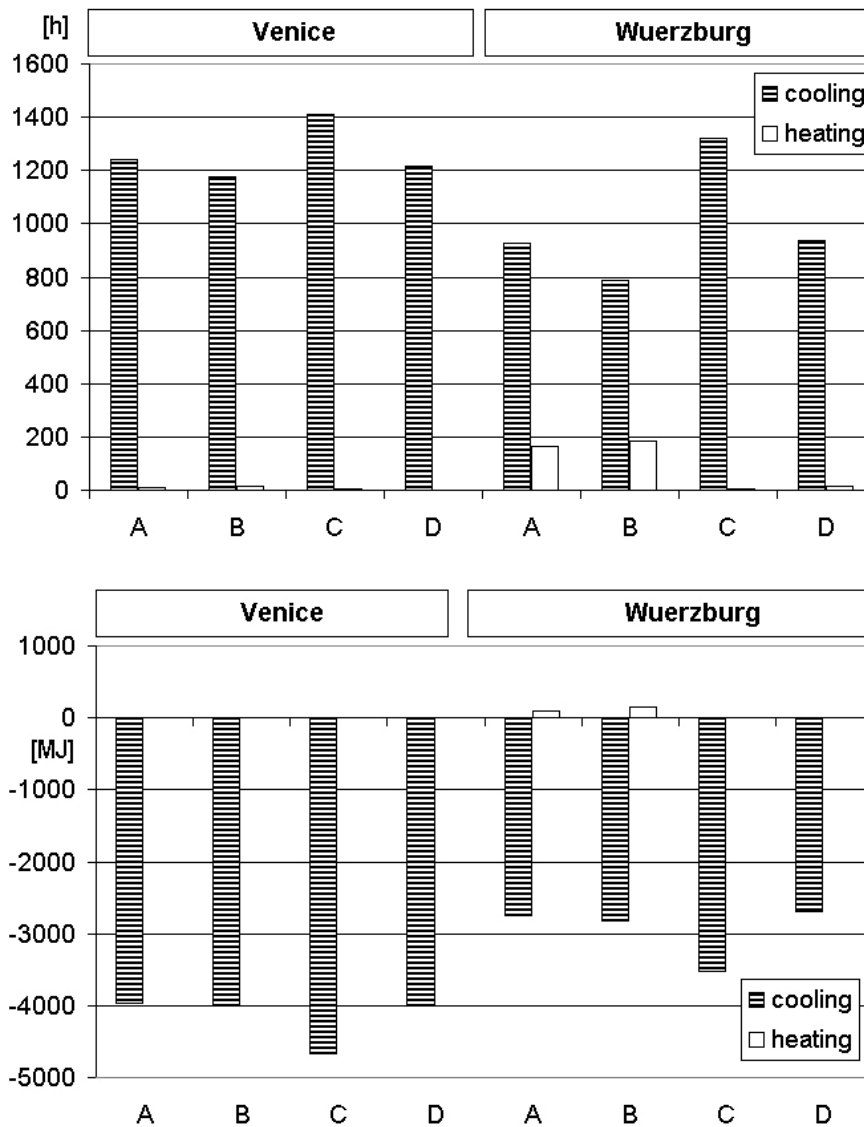


**Figure 5.16 - Energy transfer (top) and pump running time (bottom) for different water temperature control strategies (marked A ~ D). Circulation pump dead-band: 22 – 23°C. Ventilation rate: 4.7 l/s (0.3 ach) from 17:00 to 8:00, 22 l/s (1.5 ach) from 8:00 to 17:00, summer conditions: 1 May-30 September; Control strategies: A:  $\theta_{mean} \approx f(\theta_{outdoors}, \theta_i)$ , B:  $\theta_{supply} \approx f(\theta_{outdoors}, \theta_i)$ , C:  $\theta_{mean} \approx const$  (22°C in summer, 25°C in winter), D:  $\theta_{mean} \approx f(\theta_{outdoor})$ ; (figures based on the data from [Olesen and Dossi (2004)]).**

Evaluation of the energy consumption and thermal comfort in a building equipped with active thermal slabs system was done by [De Carli et al. (2003)]. The computer simulation showed that the office building examined could achieve good comfort conditions. Furthermore, the work by [Kolarik and Olesen (2007)] showed that the ability of the system to keep required thermal comfort conditions strongly depended on the control strategy applied with respect to the building construction, occupants' behaviour and climate conditions.

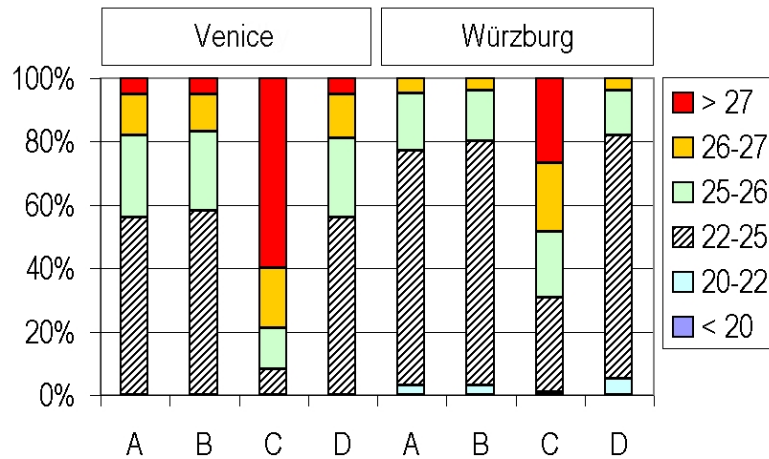


**Figure 5.17 - Simulated operative temperature distribution for different water temperature control strategies: A:  $\theta_{mean} \approx f(\theta_{outdoor}, \theta_i)$ , B:  $\theta_{supply} \approx f(\theta_{outdoor}, \theta_i)$ , C:  $\theta_{mean} \approx const$  (22°C in summer, 25°C in winter), D:  $\theta_{mean} \approx f(\theta_{outdoor})$  (figure based on the data from [Olesen and Dossi (2004)]).**

### 5.3.5.2 Measured performance of the core thermal mass activation components/systems

[De Carli and Olesen (2002)] measured thermal environment parameters in four buildings heated or cooled by hydronic radiant systems. Buildings with the following systems were examined: (a) wall-floor-ceiling heating-cooling system (light structure building), (b) floor heating-cooling system, and, (c) active thermal slab system with pipes embedded in the deck. Results of the measurements are summarized in Table 5.3. The table shows the most frequent ranges of operative temperatures measured in the examined buildings and the most frequently observed operative temperature drifts.

**Table 5.3 - Summary of the results from the field measurements by [De Carli and Olesen (2002)]; building 1 - wall-floor-ceiling heating-cooling system (light structure building), building 2 and 3 - floor heating-cooling system and building 4 - active thermal slab system.**

Building (location)	Operative temperature, $t_o$		Operative temperature drift	
	Most prevalent $t_o$ range [°C]	Prevalence of the $t_o$ range [% of time]	Most prevalent ramp [K/h]	Prevalence of the ramp [% of time]
building 1 (Bregenz, Austria)	21 – 22	26.9	0.2 – 0.3	38
	22 – 24	42.9	0.3 – 0.4	38
building 2 (Halle, Germany)	21 – 22	15.5	0.2 – 0.3	26
	22 – 24	46.5	0.3 – 0.4	22.5
building 3 (Stuttgart, Germany)	21 – 22	19	<0.1	98.7
	22 – 24	20	0.1 – 0.2	1.3
building 4 (Milan, Italy)	21 – 22	12.7	0.1 – 0.2	52
	22 – 24	53.3	0.2 – 0.4	36.6

As can be seen from the table, the operative temperature in the occupied spaces varied between 21°C and 24°C during most of the working hours. This resulted in a temperature drift from 0.2 to 0.4 K/h.

Figure 5.18 presents operative temperatures measured during the heating and cooling period by [De Carli (2002)] in an office building situated in Stuttgart, Germany. The building was equipped with an active thermal mass heating/cooling system.

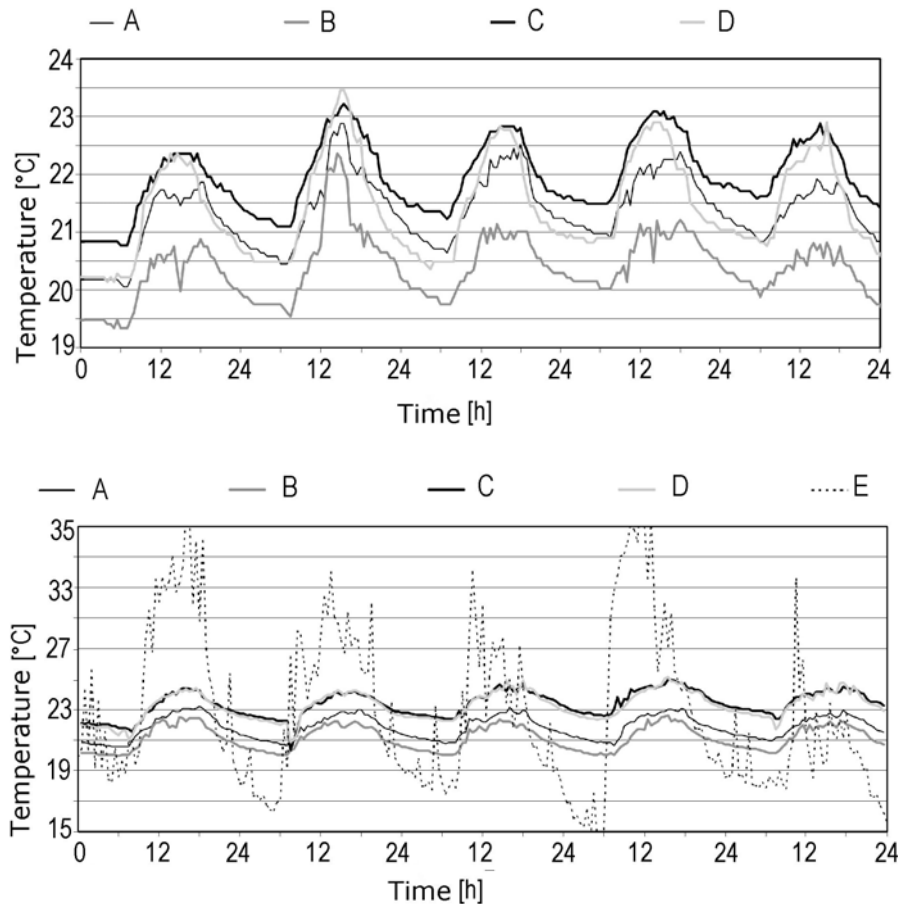


**Figure 5.18 - Sample of operative temperatures measured during a working week in the heating season (top) and the summer season (bottom) in an office building equipped with active thermal mass heating/cooling system; A - 4th floor east, B - 4th floor south, C - 5th floor east, D - 5th floor west, E - outside temperature (bottom figure only) [De Carli (2002)].**

## 5.4 Guidance and recommendation

Optimization of thermal mass size, positioning and activation principle depends on the climatic conditions, properties of the used building-materials, orientation of the building, thermal insulation, ventilation strategy and occupancy patterns [Santamouris and Asimakopoulos, (1996)]. Activation of the thermal mass has two main effects on whole building operation and indoor environment. The first one is direct cooling/heating effect and the second effect is a peak load reduction, due to the absorption of the heat by massive construction. Part of the load can, therefore, be shifted outside the period of occupancy. Whether it is a heating or cooling mode, the system (activated element – heat transfer fluid) is operating with temperatures close to the room temperature. This gives better opportunities to use renewable energy sources (heat pumps, ground heat exchangers etc.). With systems involving thermal mass activation also a high level of “self control” can be obtained – small change in the temperature difference between cooled or heated surface and the space will significantly influence the actual heat transfer.

### 5.4.1 Climate context

In general the application of thermal mass activation has been found to be particularly suitable for climates with a big diurnal temperature variation.

Regarding the core thermal mass activation (“CA”) the majority of the applications can be observed in moderate climatic zones. Installations in cold climatic zones are limited mainly by heating capacity of the system. Using the systems in tropics is limited by the fact that the temperature of the activated slab must be higher than the dew point of the air in the space to avoid condensation. This means that in the climatic zones where high relative humidity occurs, TMA system must be combined with mechanical ventilation equipped with dehumidification devices. The air dehumidification will significantly increase cooling capacity and indoor air quality in the room.

### 5.4.2 Coupling with a night-time ventilation

Cooling of the thermal mass by the night-time ventilation is one of the most efficient applications. It can be used if night temperatures outdoors are low enough to be able to remove heat from the building’s thermal mass. There are generally two systems [CIBSE (2001)]:

- Direct interaction system – the thermal mass directly exposed to the indoor air. Both convection and radiation play roles in heat transfer (see Figure 5.19a). With natural ventilation, the air flow in the building may be weak. Exposed ceilings, external walls and partitions may be used to add thermal mass. Carpets and/or a false floor can limit the exposed surface area of a floor. For exposed plane surfaces typical heat transfer coefficients are  $5 \text{ W/m}^2\text{K}$  for radiation and  $2\text{-}3 \text{ W/m}^2\text{K}$  for natural convection. High surface emissivity is generally preferred to enhance thermal radiation. Obviously, the air flow design should enhance convective heat transfer between the thermal mass and ambient air. Exposed surface areas can be increased by forming coffers or profiling the surface. If a suspended ceiling is needed, partial thermal exposure of a ceiling slab surface can be achieved by using open cell or perforated ceiling tiles. A conductive ceiling may also make the heat transfer between the thermal mass and room air possible.
- Indirect interaction system – the ambient air passes through floor/ceilings voids, cores and air paths and there is no direct interaction between the room air and the heat mass surfaces. Convective heat transfer is the main heat transfer mode. Mechanical fans may be used to drive the air flow and increase the heat transfer rate, however, design is needed to ensure the fan energy demand does not exceed the mechanical cooling energy saved (see Figure 5.19b). A higher forced convective heat transfer coefficient above  $10\text{-}15 \text{ W/m}^2\text{K}$  is possible. It is reported that in the UK, night-cooled solutions can provide up to  $50\text{-}60 \text{ W/m}^2$  cooling [CIBSE (2001)].

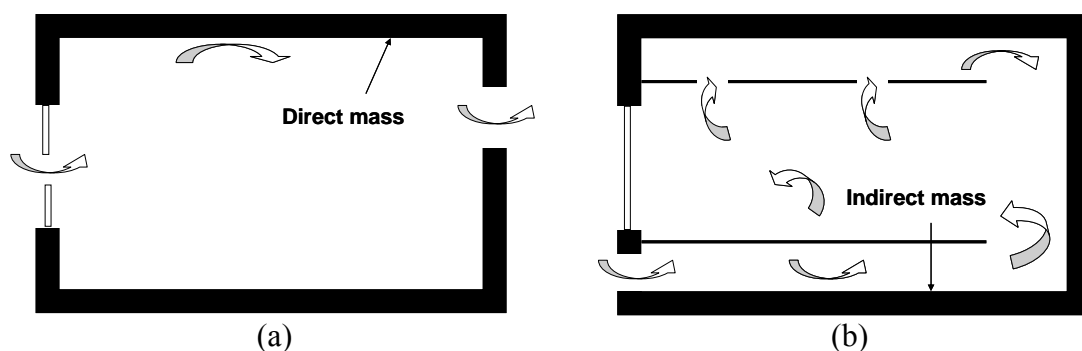


Figure 5.19 - Direct and indirect interaction thermal mass [CIBSE (2001)].

[Givoni (1990)] recommends the application of nocturnal convective cooling mainly in arid and desert regions, which have a large diurnal temperature range (above about 15 K) and where the night minimum temperature in summer is below about 20°C. Axley and Emmerich analysed a climate suitability for night-time natural ventilation of commercial buildings in different climatic zones of the United States. Cooling by natural ventilation was found to be feasible and effective in the cooler locations for moderate to high specific internal gains, but not for hot and humid climates, as for example in Miami, Florida, where relatively high night-time ventilation rates would be needed to offset moderate specific internal gains [Axley and Emmerich, (2002)].

In Europe a climatic potential for passive cooling of buildings by night-time ventilation has been analyzed by [Artmann et al. (2006a, 2006b, 2007b)] using a degree-hours method. In these studies, the climatic potential for ventilated cooling is defined as the number of night-time hours during which the outdoor temperature is below the building temperature, weighted by the outdoor-indoor temperature difference (see section 5.3.1). The detailed definition can be found in the reference [Artmann et al., (2007b)]. It was shown that in the whole of Northern Europe (including the British Isles) there is very significant potential for cooling by night-time ventilation and this method, therefore, seems to be applicable in most cases. In Central, Eastern and even in some regions of Southern Europe, the climatic cooling potential is still significant, but due to the inherent stochastic properties of weather patterns, series of warmer nights can occur at some locations, where passive cooling by night-time ventilation might not be sufficient to guarantee thermal comfort. If lower thermal comfort levels are not accepted during short time periods, additional cooling systems are required. In regions such as southern Spain, Italy and Greece climatic cooling potential is limited. Nevertheless, passive cooling of buildings by night-time ventilation might be promising for hybrid systems [Artmann et al. (2007b)]. [Artmann et al. (2008)] carried out the parametric study on performance of building cooling by night-time ventilation. A typical office room was modeled by using a building energy simulation program HELIOS [HELIOS (2007)], and the effect of different parameters such as building construction, heat gains, air change rates, heat transfer coefficients and climatic conditions, including annual variations on the number of overheating degree hours (operative room temperature >26°C), was evaluated. Climatic conditions and air flow rate during night-time ventilation were found to have the largest effect. But thermal mass and internal heat gains also had a significant effect on cooling performance and the achievable level of thermal comfort.

#### **5.4.2.1 Ventilation of the buildings equipped with core thermal mass activation**

Utilization of the thermally activated components effectively reduces the size of the ventilation system, which can be designed no more on the base of the heat loads to be extracted (cooling mode) or supplied (heating mode) from/to the building, but can be sized just to supply the amount of fresh air needed for the IAQ and for the occupants. This means that much lower air change rates can be used. If slightly cooled supply air can also be provided, some additional cooling potential can be achieved (this can be beneficial for covering peak loads during extremely hot days, and for installation of the system in warmer climatic zones).

#### **5.4.3 Thermal mass properties**

For storing heat in the thermal mass of buildings, two important thermal properties of the materials should be considered, i.e. the heat capacity by volume and the heat-absorption rate.

The first property determines the ability of the materials to store thermal energy, and the second property determines the ability of the element to readily accumulate/liberate the thermal energy. The time delay between external maximum and minimum temperature, and the internal maximum or minimum temperature is known as the *time lag*. Higher thermal mass can significantly reduce the daily fluctuations. Comparison of time lag for a 0.3 m thick wall made of different representative building materials is shown in Table 5.4. On the basis of the properties of common building materials by [Asan and Sancaktar (1998)], the rank of common building materials in terms of heat

storage capacity by volume and rank in terms of heat-absorption rate can be listed in Table 5.5 and Table 5.6.

**Table 5.4 - Time lag for 0.3 m wall of common building materials [Lechner, (2001)].**

Material	Time lag (hours)
Adobe	10
Brick (common)	10
Brick (face)	6
Concrete (heavyweight)	8
Wood	20*

\*) Wood has such a long time lag because of its moisture content

**Table 5.5 - Ranking of common building materials in terms of heat storage capacity by volume, water and air are added for comparison.**

Building materials	$\rho_M$ (kg/m <sup>3</sup> )	$C_M$ (J/kg K)	Heat capacity by volume $\rho_M C_M$ (kJ/ m <sup>3</sup> K)
Steel slab	7800	502	3916
Asphalt sheet	2300	1700	3910
Asbestos sheet	2500	1050	2625
Granite (red) block	2650	900	2385
Aluminum slab	2700	880	2376
Marble (white) block	2500	880	2200
Wood block	800	2093	1674
Clay sheet	1900	837	1590
Sandstone block	2200	712	1566
Brick block	1800	840	1512
Concrete block	1400	1000	1400
P.V.C. board	1379	1004	1385
Gypsum plastering	1200	837	1004
Plastic board	1050	837	879
Cement sheet	700	1050	735
Thermalite board	753	837	630
Siporex board	550	1004	552
Cork board	160	1888	302
Fibre board	300	1000	300
Formaldehyde board	30	1674	50
Polyurethane board	30	837	25
Water	998.2	4180	4172
Air	1.2	1005	1

**Table 5.6 - Ranking of common building materials in terms of heat-absorption rate (diffusivity), water and air are added for comparison.**

Building materials	$\rho_M$ (kg/m <sup>3</sup> )	$C_M$ (J/kg K)	$k$ (W/m K)	$\kappa \times 10^7$ (m <sup>2</sup> /s)
Aluminum slab	2700	880	210	883.84
Steel slab	7800	502	50	127.69
Granite (red) block	2650	900	2.9	12.16
Polyurethane board	30	837	0.03	11.95
Sandstone block	2200	712	1.83	11.68
Marble (white) block	2500	880	2	9.09
Formaldehyde board	30	1674	0.03	5.97
Plastic board	1050	837	0.5	5.69
Clay sheet	1900	837	0.85	5.34
Cement sheet	700	1050	0.36	4.90
Gypsum plastering	1200	837	0.42	4.18
Brick block	1800	840	0.62	4.10
Concrete block	1400	1000	0.51	3.64
Asphalt sheet	2300	1700	1.2	3.07
Thermalite board	753	837	0.19	3.01
Siporex board	550	1004	0.12	2.17
Fibre board	300	1000	0.06	2.00
Cork board	160	1888	0.04	1.32
P.V.C. board	1379	1004	0.16	1.16
Wood block	800	2093	0.16	0.96
Asbestos sheet	2500	1050	0.16	0.61
Air	1.2	1005	0.027	223.88
Water	998.2	4180	0.602	1.44

#### 5.4.4 Heat transfer between room and thermo active component

Three physical mechanisms of heat transfer take place in the space heated/cooled by activated thermal slab system (see also Figure 5.20) conduction, convection and radiation.

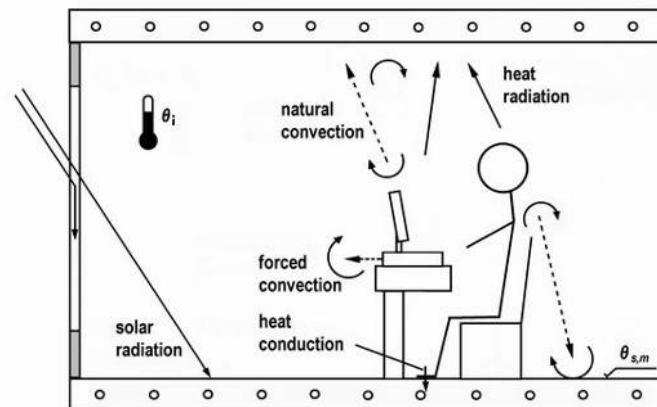


**Figure 5.20 - Thermal balance model of a room equipped with radiant heating/cooling [Koschenz and Lehmann (2000)].**

Thermo active components have a large radiant part in the heat transfer between heated/cooled surface and room, which can be seen by comparing the radiant and convective transfer coefficients. The coefficients depend on the position of surface (wall, ceiling, floor), the operation mode (heating/cooling) and on the temperature difference between heated/cooled surface and space. For radiation, the value of heat transfer coefficient is approximately 5.5 W/m<sup>2</sup>K in rooms under “normal” cooling conditions, while the convective coefficient is between 3 and 5.5 W/m<sup>2</sup>K. Influence of both convection and radiation can be expressed by means of total heat transfer coefficient. The approach to calculate the total heat transfer coefficient is included the part 2 of the [EN 15377 (2008)] standard. Table 5.7 shows: total heat transfer coefficients (sum of the convective and radiant heat transfer coefficients), acceptable surface temperatures and maximum heating/cooling capacities for different types of radiant heating/cooling systems.

**Table 5.7 - Total heat exchange coefficient between surface and space for heating and cooling, acceptable surface temperatures and capacity by 20°C room temperature for heating and 26°C room temperature for cooling [Olesen et. al.( 2000)].**

		Total heat exchange coefficient		Acceptable surface temperature		Maximum capacity	
		[W/m <sup>2</sup> K]		[°C]		[W/m <sup>2</sup> ]	
		Heating	Cooling	Max. Heating	Min. Cooling	Heating	Cooling
Floor	Perimeter	11	7	35	20	165	42
	Occupied Zone	11	7	29	20	99	42
Wall		8	8	~40	17	160	72
Ceiling		6	11	~27	17	42	99

It should be pointed out, that ceiling heating/cooling mentioned in the table does not refer to use of activated thermal slab of the ceiling, but to common radiant system with pipes close to the ceiling surface, so the heating/cooling capacities listed in Table 5.7 are higher than those which can be expected in case of using thermal mass activation.

The larger part of the heat transfer from the rooms above and below the concrete deck to its core will, for cooling, be through the ceiling surface. The distribution is found to be 2/3 through the ceiling and 1/3 through the floor [Koschrenz and Lehmann (2000)]. The actual distribution depends greatly on the actual configuration of the slab construction with respect to floor covering/structure and i.e. acoustic ceilings.

In case of micro pipes embedded in plaster or gypsum (Figure 5.10), the cooling grid is coupled to the concrete slab. In this way the building structure is “secondarily” activated, the system is faster in response when compared to pipes embedded directly in concrete core of the slab. Adding a layer of insulation below the floor reduces the cooling power transferred to the floor of the upper room.

The impact of different parameters on the heat storage capacity of building elements have been investigated by [Artmann et al. (2007a)]. In his study, an analytical solution to the heat transfer problem in a slab with convective boundary condition and sinusoidal variations of the air temperature were used. The following effects have been found:

- The heat storage capacity of thick thermally heavy elements significantly increases with an increasing of the heat transfer coefficient up to 30 W/m<sup>2</sup>K.
- The heat storage capacity of thin thermally light elements is almost constant for heat transfer coefficients higher than 3 W/m<sup>2</sup>K.

- The optimum thickness of an element depends on the heat transfer coefficient; the optimum half-thickness of a concrete slab increases from about 90 mm to 140 mm if the heat transfer coefficient increases from 5 W/m<sup>2</sup>K to 30 W/m<sup>2</sup>K.
- In most cases the thermal conductivity of concrete ( $\lambda = 1.8$  W/mK) is sufficient; only at a high heat transfer coefficient ( $h = 20$  W/m<sup>2</sup>K) does the storage capacity of a very thick slab ( $d = 200$  mm) increase with conductivities up to 50 W/mK.
- The integration of phase change materials can significantly increase the heat storage capacity of building elements. A 15 mm gypsum plaster board with 40 % PCM content shows similar performance to a 100 mm thick concrete slab.

## **5.4.5 Location/positioning of the surface thermal mass activation**

### **5.4.5.1 Internal thermal mass**

Typical internal thermal mass positioning with corresponding basic heat transfer processes is depicted in Figure 5.21. With the surface thermal mass activation (SA), the outdoor air enters the building by either mechanical or natural forces (i.e. mechanical ventilation, natural ventilation or infiltration), the thermal mass in the building absorbs or releases the heat through its surface and interior body. There is a convective heat transfer process at the surface of the heat mass and a radiant heat transfer between them and other surfaces. The conduction heat transfer takes place in the interior body. The surface heat transfer rate, determined by the convective heat transfer coefficient and surface area, can have an significant influence on the thermal storage and release process. With larger surface heat transfer rates more energy can stored or released. The convective heat transfer coefficient depends on the temperature difference between the thermal mass surface and the surrounding air and the air flow speed around the thermal mass. Generally, in buildings it is difficult to enhance the convective heat transfer rate significantly without using a mechanical fan. Thus, the surface area of the thermal mass is a crucial design parameter. The heat penetration through the thermal mass body is by the heat conduction, and the penetration depth is limited by the diffusivity of the material during one cycle [Li and Xu, (2006)].

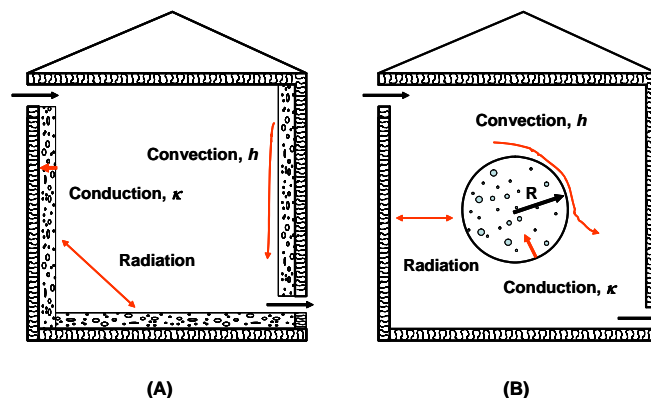


**Figure 5.21 - (A) Illustration of use of interior thermal mass in the walls, floor; and (B) Illustration of the heat transfer process of a thermal mass sphere in a room. [Li and Xu (2006)].**

### **5.4.5.2 External thermal mass**

For external thermal mass design, it is important to set the different time lags for different walls as each orientation experiences different amount of the solar heat gains. The south and west walls, which in most cases get highest solar heat gain, should have enough mass to sufficiently accumulate that loads. Also sufficient time lag is needed to transfer the accumulated heat to the night time of the day. If the wall does not have enough mass to yield long time lag, the heat stored in the morning will be liberated into the building in the afternoon, which will consequently increase the cooling load. North walls have generally a little need for the long time lag as they experience less solar heat

gains. The east wall has a high morning load and it should be delayed to the evening, but not to the afternoon, which can make the matter worse. Thus, either a very long time lag (more than 14 hours) or better insulation is needed. The roof of the building also experiences some heat gains from the morning, depending on its pitch angle [Lechner, (2001)]; [Santamouris and Asimakopoulos, (1996)].

### 5.4.5.3 Thermal mass and insulation

The insulation is usually adopted to reduce the heat loss through building envelope. The different location between thermal mass and insulation can have significant effect on the building performance. Figure 5.22 shows the placement of the thermal mass relative to the insulation.

In figure 5.22A mass on outside surface and interior insulation is represented. This configuration can extend the time lag for the heat penetration from exterior to the room. This solution is also good for fire and weather resistance of the wall as well as for its appearance. However, there is no guideline how to design such walls so far. The second placement (figure 5.22B), mass on inside surface, is good for night flushing cooling and for passive solar heating if proper utilizing with the night ventilation. Mass sandwich, that is mass in the middle (figure 5.22C), can have some of the benefits of both A and B in Figure 5.22 [Lechner, (2001)]. The location design should consider the climatic and environmental effect and may vary from region to region. Proper engineering design is needed to ensure that the thermal mass and insulation are correctly designed, but not wasted, or even play an adverse role.

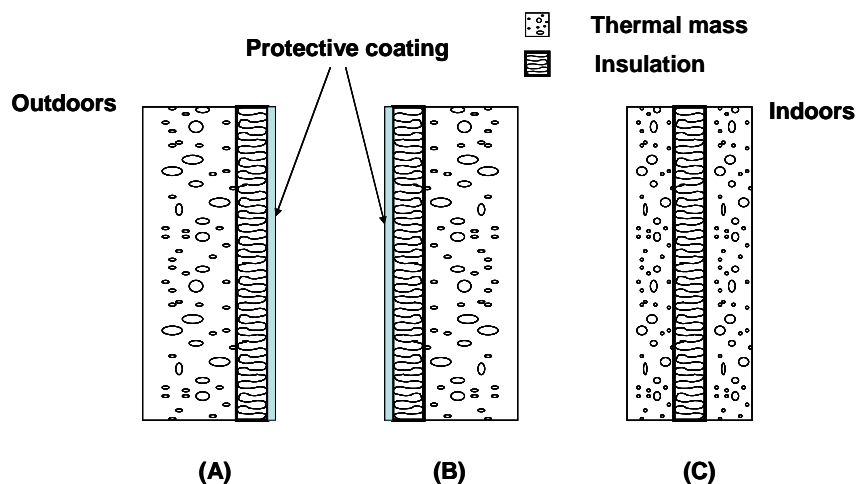


**Figure 5.22 - The placement of mass relative to the insulation can be critical in regard to time lag as well as have other implications. (A) Mass on outside – interior insulation (B) Mass on inside (C) Mass sandwich [Adapted and modified from Lechner, (2001)].**

### 5.4.6 Operation strategies for the core thermal mass activation

Technologically, the design of CA components is based on the same characteristics of typical radiant systems: distance, diameter of pipes, thickness of the concrete layer, position of the pipes inside the concrete, supply water temperature and water mass flow rate.

Besides the direct cooling and/or heating capacity, the CA components have also the thermal storage effect. The heat can be stored in the concrete slab. This effect has its dynamics, which is difficult to calculate using steady state assumptions and, hence, computer simulation is often required.

The effect of CA component's application is demonstrated in Figure 5.23. It shows the results from a simple simulation program [Meierhans and Olesen (1999)]. The Figure 5.23a shows the temperature variation over 24 hours for a space exposed to an internal load and without any cooling.

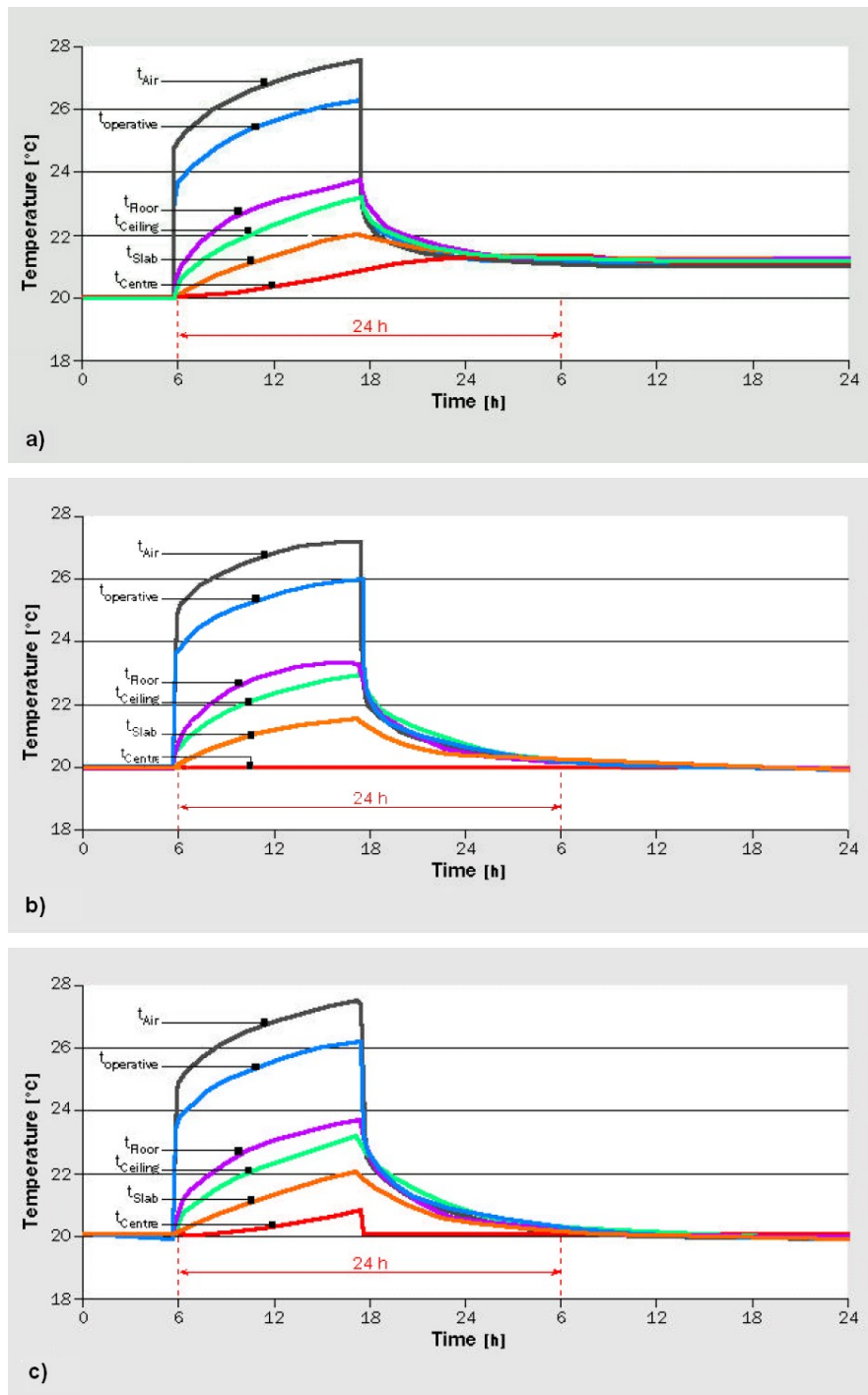


**Figure 5.23 - Core thermal mass activation: calculated air, operative, floor, ceiling, average slab and slab core temperatures for a space with a constant internal load of  $90 \text{ W/m}^2$  from persons, light, solar radiation etc. [Meierhans and Olesen (1999)].**

At the initial state 6:00 o'clock in the morning, all surface temperatures are  $20^\circ\text{C}$ . When the internal load is introduced, the room temperatures start to rise immediately. The operative temperature keeps increasing the whole day to approximately  $26^\circ\text{C}$  at 18:00 o'clock, when the internal load decline. During the night, (no internal loads) the space cools down and reaches by the next morning an operative and average slab temperature of  $21.3^\circ\text{C}$ , which is 1.3 K higher than the day before. Each day the temperatures will then increase progressively. If the core of the concrete slab is constantly kept at  $20^\circ\text{C}$  (Figure 5.23b), next morning, all the temperatures will decrease to the same level as the day before. During the day the average slab temperature increases to  $21.5^\circ\text{C}$ , but it is

decreased again during the night. The Figure 5.23c shows the temperatures in case that the core is only cooled to 20°C outside of the building occupation period (night). It can be seen from the figure that the results are almost the same as for the 24 hours cooling. The operative temperature is only slightly higher. During the period when the core is kept at 20°C, the temperature difference between core and average slab is higher and this causes an increased energy transport. Therefore, even if the shorter cooling time, the total cooling effect is about the same. This is one of the benefits of using core thermal mass components, the peak load during the day will be stored and removed by cooling during the night.

#### 5.4.6.1 Thermal behaviour of the core thermo-active components

The thermal capacity of the system depends on the thickness of the surface layer where the pipes are embedded. At the same time, it is the thickness of the concrete slab that has a significant influence on the time response of the system [Babiak et al. (2007b)]. The high thermal capacity results in slow response to the changes of the load on water side - in the concrete core. On the other hand, the system is quite fast in response on the room side because of the “self control” effect. It depends partly on the temperature difference between space and activated (ceiling/floor etc.) surface [Babiak (2007)], [EN 15377 (2008)] and partly on the temperature difference between space and the average temperature in the layer, where the pipes are embedded. Every change of the operative temperature in the room will immediately influence the total heat transfer coefficient representing heat exchange between the activated element and the room. Consequently, the heat exchange between the element and the room will be instantly affected – increase of the temperature difference will intensify the heat transfer and vice versa.

Response time of the system can be defined by a time constant ( $\tau$ ). The time constant indicates how fast the active layer (floor, slab) reacts to changes in boundary conditions – inputs (e.g. supply temperature). [Pfaffin (1980)] in his study showed that the heating and cooling responses of occupied spaces generally followed exponential curves (Figure 5.24).

The response for a unit step change in a first order system (linear system) is defined following equations for a passive (10) and active (11) trajectory respectively [Weitzmann (2002)]:

$$y(t) = e^{-\frac{t}{\tau}}, \quad (10)$$

$$y(t) = 1 - e^{-\frac{t}{\tau}}, \quad (11)$$

where  $y(t)$  is the generic variable (e.g. temperature). Substituting the time ( $t$ ) by the time constant ( $\tau$ ) in Equation (11) results in following:

$$y(\tau) = 1 - e^{-1} = 0.63, \quad (12)$$

Consequently, the time constant is the time required for a step (unit) temperature change of 63% of/from the total temperature change.

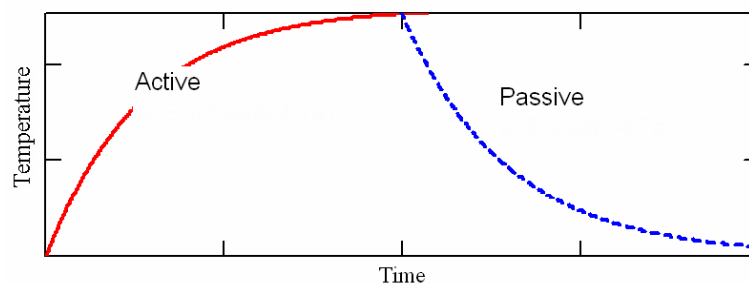


**Figure 5.24 - Heating and cooling trajectories from [Pfaffin (1980)].**

#### 5.4.6.2 CA performance controls

The response time of the system is rather long due to its high thermal mass. Therefore, an individual room control is not reasonable, but a zone control (south – north); where the supply water temperature, average water temperature or the flow rate may differ from zone to zone, is often the suitable solution [Deecke et al. (2003)]. The zoning considers the external and internal heat loads. Small difference between heated/cooled surfaces (supply water) and the ambient temperature results in a significant degree of self-control effect described above. In specific cases, (well-designed systems in buildings with low heat loads/loses) a concrete slab can be controlled at a constant core temperature all year round. If, for example, the core is kept at 22°C, the system will provide heating at room temperatures below 22°C and cooling at room temperatures above 22°C.

##### *5.4.6.2.1 Water (heat carrier) temperature control*

The following strategies are usually applied for control of the water temperature [Olesen and Dossi (2004)], [Olesen et al., Deecke et al. (2003)]:

- Mean water temperature as a function of outdoor temperature
- Supply water temperature as a function of outdoor temperature
- Mean water temperature kept constant
- Supply water temperature as a function of dew point temperature

Generally, it is preferable to control average temperature in the slab according to room operative and outdoor temperature. Controlling of average temperature includes the feedback from the room side. In order to get the right operative temperature signal from the room it is important that a heat transfer between temperature sensor and room environment follows the same pattern as if there is a person instead of the sensor [Simone et al. (2007)]. The colour, shape, size and position of the sensor in the room should reflect this fact. Detailed information on the investigation of the different sensor parameters is given in [Babiak (2007)].

In order to avoid condensation, the water temperature or the surface temperature and the absolute humidity should be controlled (surface temperature should be maintained above the room dew-point for all operational conditions). A control strategy to reduce the risk of damage due to condensation is that mean supply water temperature is controlled depending on the dew point temperature (absolute humidity). Another solution can be installation of dehumidification in a ventilation system. Then the humidity sensor is placed in the exhaust duct. If the dew-point is further reduced through dehumidification of the supply air, the temperature of the radiant surface can also be decreased, and higher sensible loads can be removed by radiation. However, increased performance of the system means also increase in its cost.

##### *5.4.6.2.2 Water (heat carrier) flow rate control*

The running time of a heat carrier circulation pump, and consequently the pump's electric power demand, can occasionally be significantly reduced. The fraction of time within a certain interval, when the water circulates in the floor pipes is called a duty cycle (d):  $0 < d < 1$  (0-100%). The limitation of the pump running time results in negligible decrease of heating/cooling capacity as  $d \geq 50\%$ . The study by [Deecke et al. (2003)] showed significant savings of electrical energy for pumps (up to 70 % by  $d = 25\%$ ) with the same system capacity on the room side. According to [Babiak (2007)] the intermittent operation with  $d > 50\%$  significantly increases (approximately by 60 %) the necessary maximum capacity of the chiller. This is caused by the fact that the slab return water temperature gets high when circulation is stopped. Consequently, just after starting the circulation again, high cooling capacity is needed to get the temperature back to operational level. Applicable control strategies for the heating/cooling water flow rate – circulation pump operation are described in [Babiak et al. (2007a)].

**Table 5.8 - Water flow rate control strategies for core thermal mass activation components.**

Control strategy	Pump operation	Description
Modulated, continuous heat supply	- 24 hour operation	For continuous heat carrier circulation, the heating power delivered to the room can be expressed as a linear function of the temperature difference between heat carrier and a room temperature ( $\theta_m - \theta_i$ ). The control of the air temperature in the room can be achieved by adjusting $T_w$ according to the instant power demand.
	- 12 hour night operation	
	- 8 hour night operation	
Discontinuous heat supply	- 15 min ON/ 45 min OFF (25% duty cycle)	The long response time justify the substitution of power control with energy control in terms of intermittent heat supply. The heat supply is then restricted to a characteristic time interval $\Delta\tau$ , which fulfils the requirement $\Delta\theta < 1$ K in order to avoid undesirable temperature fluctuations.
	- 1 h ON/ 1 h OFF (50% duty cycle)	
	- 0,5 h ON/ 0,5 h OFF (50% duty cycle)	

#### 5.4.6.2.3 Control with respect to a weather forecast

Traditional building control and regulation systems only take into consideration the current situation rather than the one that will occur in the near future. In practice, this means that in most buildings heating and cooling systems are regulated only according to instant outdoor (or indoor) temperatures (feedback control).

With weather forecast control the thermal mass of the building components can be actively used to reduce energy consumption at the same time as fluctuations in the indoor temperature are avoided. Weather forecast control considers several external factors (Figure 5.25), such as temperature, sunshine, wind strength and direction - and the control system receives this information in advance (feedforward control) [Uppström et al. (2004)].

Weather forecast control is based on utilizing the thermally activated mass in the building's components as walls, roofs, furniture etc. If one knows in advance that a cold night will be followed by a warm sunny day, the thermal mass in the building's components can become an advantage. Heating can be reduced several hours in advance without the indoor temperature having time to fall. And vice versa – when windy and overcast weather is on the way, heating can be increased in advance.

Thus one attains a balancing of the energy supply and a more stable indoor climate. This results in reduced energy consumption. Furthermore, the more stable indoor climate often is positively received by the occupants.

With weather forecast control the outdoor climate parameters (temperature, sunshine, wind), together with data on the building's characteristics are integrated into an algorithm that results in what is referred to as equivalent temperature (ET) (Figure 5.26). The value of ET replaces the outdoor temperature signal into the regulator.

An example of the commercially available weather forecast prognosis receiver for existing control systems in buildings can be the WeatherGain system developed by Honeywell in Sweden.

The forecast is delivered by the Swedish Meteorological and Hydrological Institute (SMHI). When the WeatherGain function is in use, new prognosis data for the equivalent temperature normally are

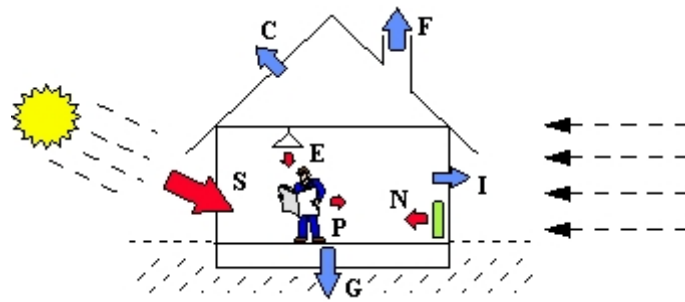


*Figure 5.25 - External factors in weather forecast control.*

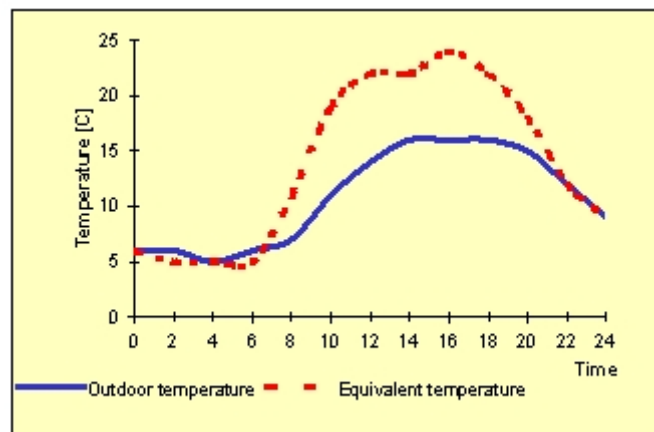


*Figure 5.26 - Comparison of outdoor or equivalent temperature during one day.*

sent via the Internet daily and each prognosis is for 5 days. This system has been used in several buildings in Sweden. However, like in a building equipped with a heating system controlled only on the basis of the outdoor temperature, also when weather forecast control is in use the indoor temperature sometimes can become too high in single office rooms. This is due to the fact that the internal heat loads, as well as the solar radiation, can differ from room to room. When a weather forecast control system is to be put into operation attention must be paid to unify the internal heat loads (lighting, people, office equipment etc.) in the whole building.

### **5.4.7 International standards dealing with core thermal mass activation components**

The new international standard [EN 15377 (2008)] part 1 to 3 addresses the design of embedded water based surface heating and cooling systems. It consists of the following parts: Part 1: Determination of heating and cooling capacity, Part 2: Design, dimensioning and installation and Part 3: Optimizing for use of renewable energy sources and dynamic considerations.

The standard includes design calculation methodology for systems thermally coupled with building structure, but also for other types of radiant heating/cooling systems. Three sizing methods for heat source/sink are also included: rough sizing method, simplified sizing method using diagrams and simplified model based on finite difference method (FDM).

The simplified calculation methods are specific for each type of system and include certain boundary conditions, which must be met before the given method could be applied. Standard [EN 12828 (2002)] defines the principles of control for water-based heating systems.

It is also worth to mention that the Technical Committee 205 of the International Organization for Standardization (ISO) started, under Working Group 8 (ISO/TC205/WG8), an activity on a brand new international standard on radiant heating and cooling systems. The work started in 2007 and the standard should be prepared in 2010. The standard will deal with system design, dimensioning, installation, testing methods, dynamic design tools, inspection, operation and IEQ aspects. Besides embedded systems the radiant panels will be also included.

#### **5.4.8 Suitability of the thermal mass activation components to be used with other building elements**

The suggestions regarding suitability of the thermal mass activation components to be used with other building elements are summarized in the table 5.9.

*Table 5.9 - Suitability for combined use of TMA components.*

<b>Building component</b>	<b>Suitability for combined use</b>	<b>Note</b>
Advanced facades	Yes	Very suitable combination, advanced façade systems provide solar shading to decrease solar gains in the summer and also sufficient thermal insulation during the winter, this helps keep heating/cooling demand on the low level and allows TMA components to work with the highest efficiency.
Natural ventilation	Yes	Natural ventilation provides clean air into the premises without additional energy consumption (fans etc.) and gives the occupants ability to adjust their thermal environment. Self-control behaviour of the TMA components is more pronounced.
Mechanical and hybrid ventilation	Yes (with limitations)	Certain limitation can be seen in the fact that using the whole surface of ceiling for TMA components does not give a space for duct installations. The ventilation system must be integrated into the walls, floor or leaded in corridors etc.
Lighting	Yes (with limitations)	Suspended ceiling cannot be used, lighting installations should be designed in different way.
Solar shading	Yes	It is important to passively decrease heat loads in the building – suitably controlled solar shading is one of the most effective solutions.
Earth coupling	Yes	TMA components are very suitable for utilization of low valued energy obtained from ground heat exchangers for cooling.
Phase-Change Materials	Yes	Research is still in process
Dynamic insulation systems	Not known	-
Raised floors	Yes	In the buildings where all ceiling surface is used for radiant heating/cooling usage of raised floor is sometimes only solution when a space for electrical and other installation is needed.
Suspended ceilings	No	Suspended ceilings cannot be used

## 5.5 Examples for illustration

### 5.5.1 Air conditioning system utilizing building thermal storage (ACSuBTS)

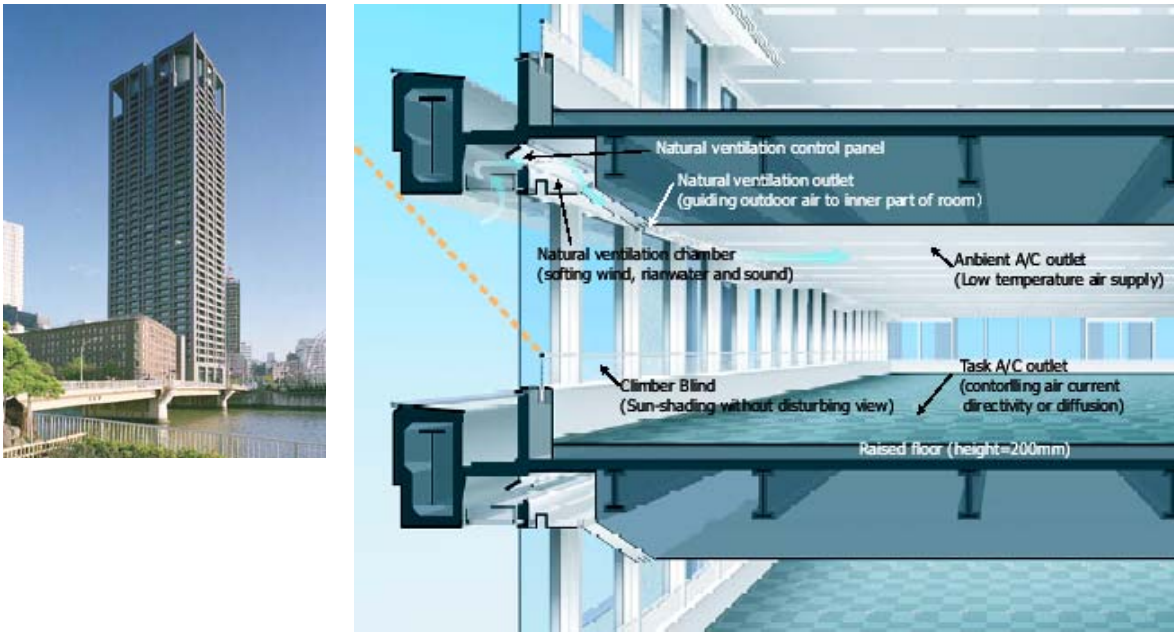


**Figure 5.27 - Existing application of ACSuBTS - KANDEN Building of Kansai Electric Power Company, Inc. (KEPCO) in Osaka.**

#### 5.5.1.1 Working principles

This configuration falls in the TMA – CA working principle. In Japan, an air conditioning system utilizing the building thermal storage capability (ACSuBTS) has been designed and adopted. The system is able to smooth the cooling load without increasing the initial costs, by using the large building thermal mass as a thermal storage medium (see Figure 5.27). In summer, by keeping the climate control system operating at night, the floor slabs, furniture and interior materials are cooled down. Then cold exergy (Shukuya and Hammache 2002, Shukuya 2004) stored in the building construction can be used to reduce electricity consumption of mechanical cooling during the daytime peak electricity usage period (see Figure 5.28).

Dampers are installed at supply air ducts in order to change over the air supply to the working space or to the plenum chamber. During the working hours, the conditioned air from the air conditioning unit is blown directly to the room through the supply duct, by opening the changeover dampers. The return air from the room through the opening in the ceiling panel is mixed with the air in the plenum and then flows into the air-conditioners. During night, the conditioned air is blown directly upon the floor slab by changing angle of the dampers and cools down the floor slab. Figure 5.29 shows the control of the dampers.

#### 5.5.1.2 Measurements and simulations for performance assessment

Measurement was carried out in the KANDEN building between 5th and 9th August. The temperatures of the slab were measured at five points, as shown in Figure 5.30 (marked from 1 to 5), while the room air temperatures were measured at two points (marked 6 and 7). Air conditioners had been installed in the perimeter (near point 1) and interior space (near point 3), and they could be operated independently. Figure 5.31 shows the measured values of the outdoor air temperature and the horizontal solar radiation. The working hours were from 8:00 to 19:00 (from 5th to 9th), while

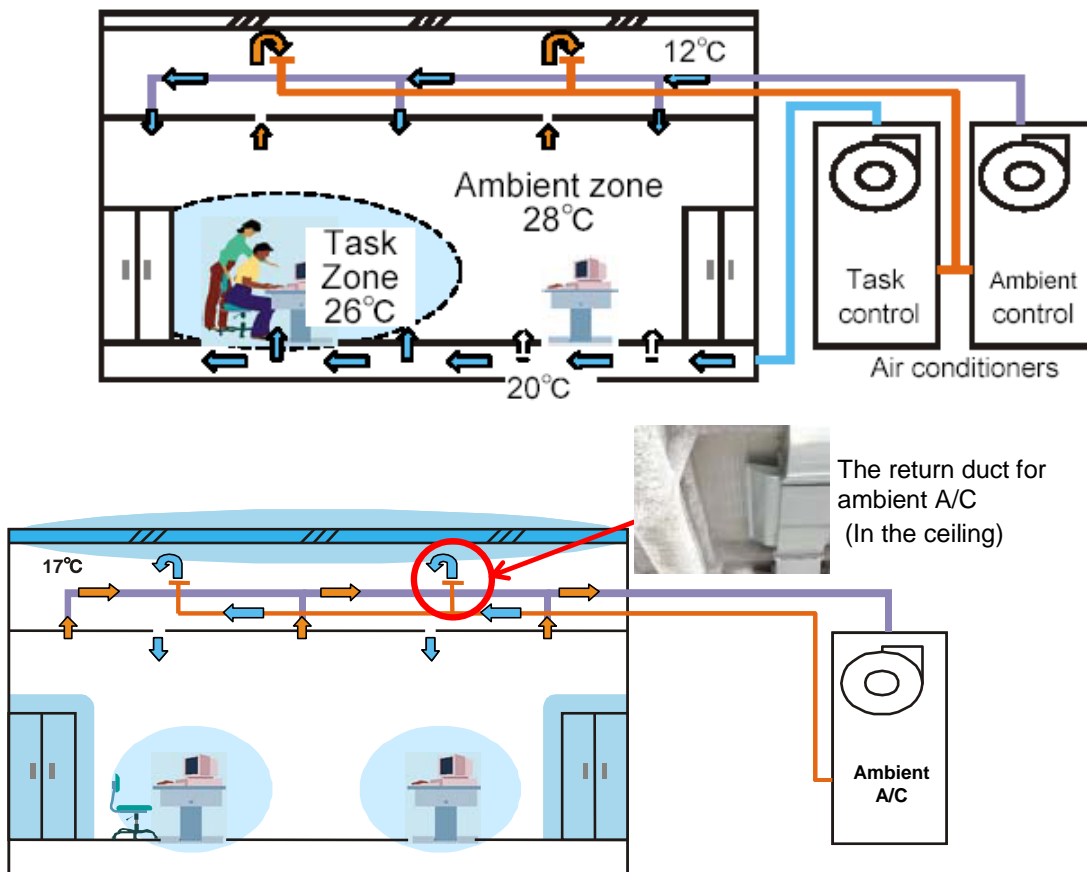


Figure 5.28 - Air conditioning system utilizing building thermal storage – operation principle.

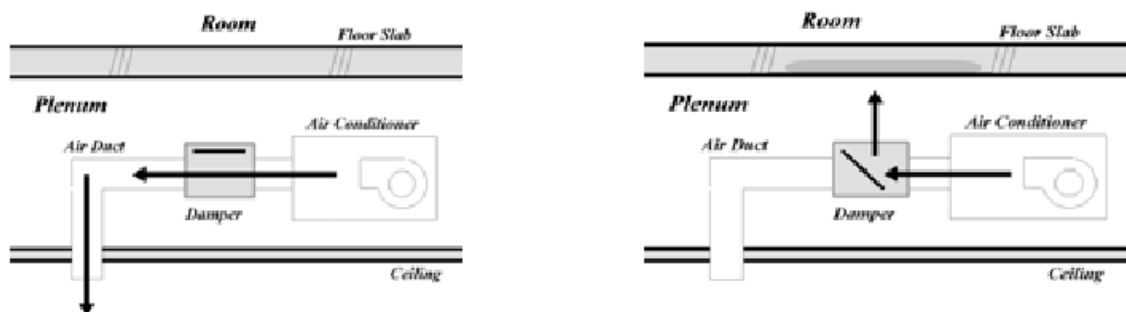


Figure 5.29 - Control of damper (left: working hours, right: thermal storage hours).

heat storage hours were from 22:00 to 8:00 on the following day (from 6th to 8th). Outlet air temperatures were measured at the upper part of the changeover damper.

The cooling load, determined based on the measurements of the airflow rate and the difference between the supply and return air temperatures, is shown in the Figure 5.32 (left). Comparison of the cooling load on 6th Aug. (without thermal storage) and that on 9th Aug. (with thermal storage) indicates a significant reduction of the peak cooling load (about 30 %). Figure 5.32 (right) shows the air temperatures at the measuring points number 6 and 7 in the room. The temperatures decrease due to the air leakage in the plenum during thermal storage hours.

Temperatures at several positions through the floor construction, that is, the surface of the carpet tile, the upper and lower surfaces of the concrete slab, at the measuring point 3 are shown in Figure 5.33 (left). At the point 3, which is located near the changeover damper, heat is released during the thermal storage hours, while absorbed during the working hours. Thus, heat is stored effectively to the floor slab at the point 3. During thermal storage hours, the temperature on the lower surface of the concrete slab (left figure) is almost equal to the air temperature blown through the upper opening of the changeover damper. It can be judged that the air impinges on the lower surface of

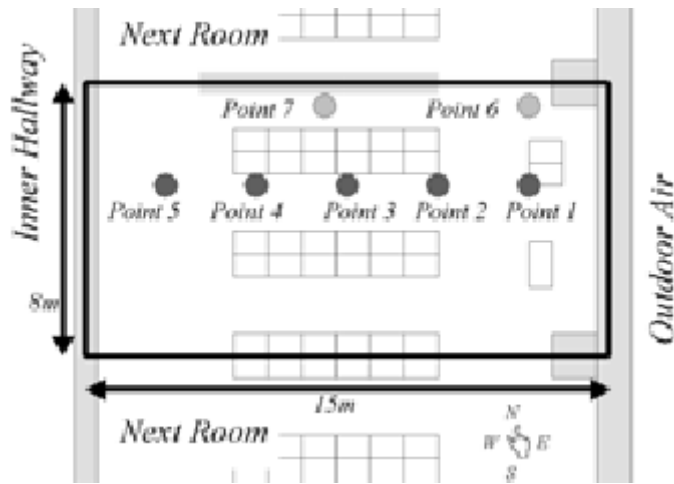


Figure 5.30 - Position of measuring points at the typical floor of the KANDEN building.

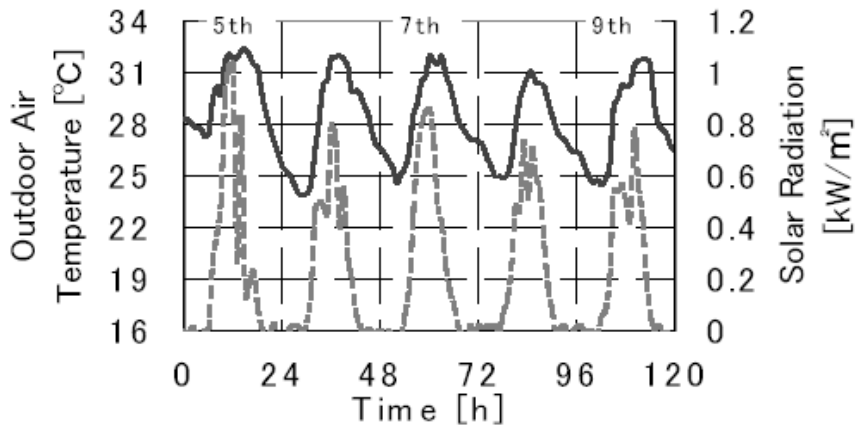


Figure 5.31 - Weather conditions.

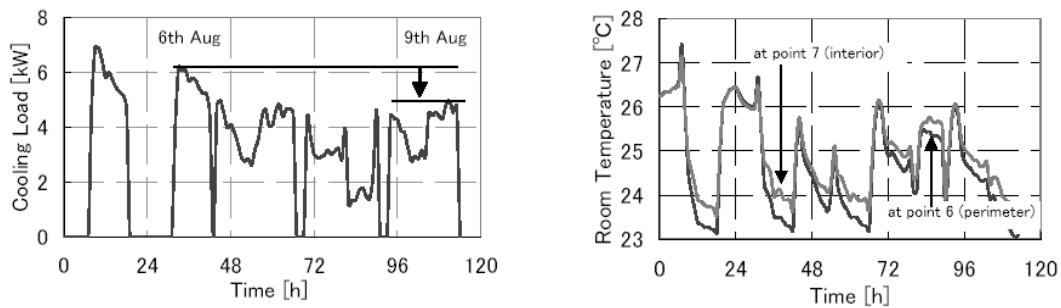
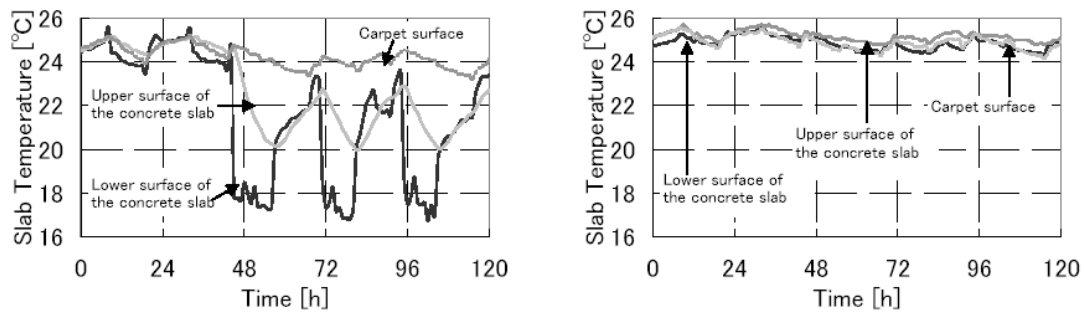


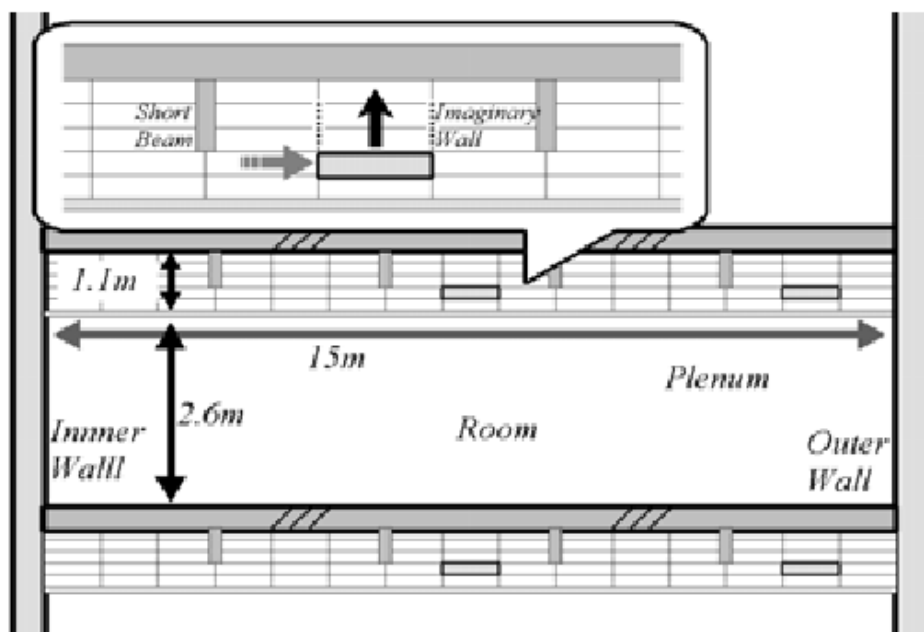
Figure 5.28 - Cooling load (left) and room air temperature (right) for measuring points number 6 and 7 of the examined room in KANDEN building.



**Figure 5.33 - Vertical distribution of floor slab temperature at measuring point number 3 (left) and number 4 (right).**

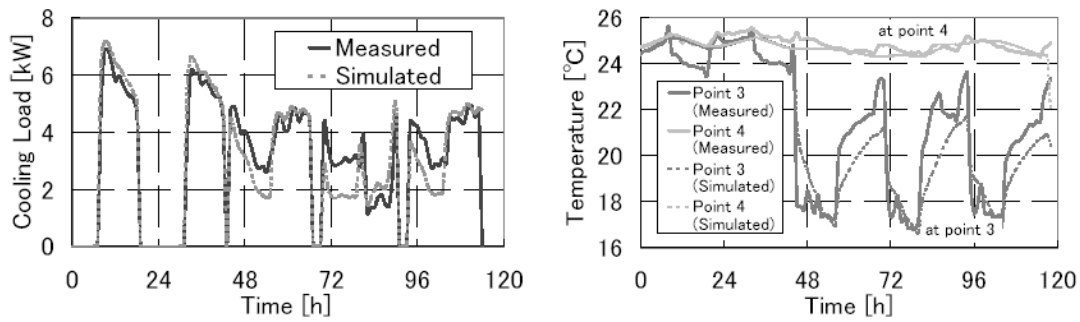
the concrete slab directly. At the measuring point 4, far from the changeover damper (Figure 5.33 - right), none of the floor temperatures show any appreciable change from 24 °C throughout the day. Thus, heat storage to the floor near the point 4 cannot be expected.

Figure 5.34 shows the simulation model for airflow in the plenum in KANDEN building. The room is divided into two zones that are the perimeter and interior zones. The plenum was divided into 75 rectangular cells. The airflow rate from the air-conditioners into the plenum was kept constant during working and accumulation period, respectively. During the accumulation period, imaginary walls indicated by broken lines were assumed in both sides of the upper cell to the changeover damper in order to give upward inertial force to the supply air. The block-model [Togari et al. (1991)] was used for an analysis of the airflow in the plenum. The cell pressure was calculated by Newton method, where an air density  $\rho$  was assumed uniform. The cell temperature was calculated by the heat flux due to airflow and heat transfer from the wall. Since the air temperature changes faster than the concrete slab temperature, the cell temperature was calculated assuming a steady state condition.



**Figure 5.34 - Cell division for plenum.**

The measured and simulated values of the lower surface temperatures and cooling load are compared in Figure 5.35. The simulated results agree fairly well with the measured.



**Figure 5.35 - Comparison of measured and simulated results (left: cooling load, right: lower surface temperatures of slab at points 3 and 4).**

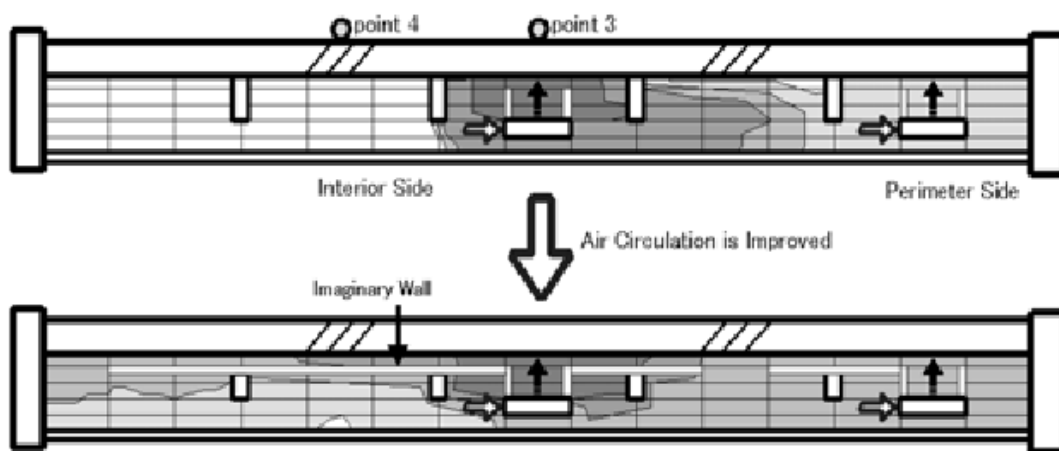


**Figure 5.36 - Temperature distribution in the plenum during heat storage hours (top: without improvement, bottom: with the improvement).**

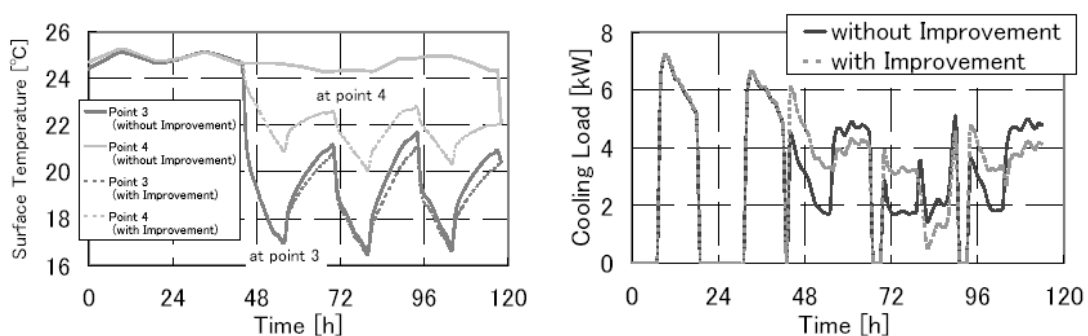


**Figure 5.37 - Calculated lower surface temperature of the slab (left) and cooling load (right) when air circulation is improved.**

Due to the non-uniform horizontal temperature distribution in the floor slab, the thermal storage potential of the floor slab can not be fully utilized for smoothing the peak loads. Therefore, the simulation model was used to predict the performance of the thermal storage after the improvement of the air circulation in the plenum. A hole was assumed to be in the short beams and extend the imaginary walls in order to improve the air circulation as depicted in the Figure 5.36 (bottom).

Because of this improvement, the non-uniformity in the temperature distribution in the plenum was significantly reduced. Owing to the improved uniform horizontal temperature distribution in the floor slab as shown in Figure 5.37 (left), the cooling load shifts to the storage hours can be seen in Figure 5.37 (right). To improve ACSuBTS performance, more effective system layout can be used when applying it to other buildings.

#### 5.5.1.3 The “claimed” benefits and limitations of the presented concept:

- The mechanism of the ACSuBTS is simple and easy to introduce into the practice.
- Initial cost of the ACSuBTS is lower than the conventional thermal storage systems because it does not have the thermal storage tank.
- ACSuBTS can use cheaper electricity at night.
- The thermal storage capacity of the ACSuBTS is not so large.
- The control of thermal storage and release is difficult.

The ability of the concrete slab to store thermal energy decreases significantly with the distance from the air supply opening.

## **5.5.2 Chinese kang**

### 5.5.2.1 Working principle

Chinese kang’s design varies quite a bit with different regions although the general principles are the same. Generally, there are three main components: stove, heated bed and chimney. The kang is often a rectangular platform (about 3 m length×1.8 m width×0.5 m height) made of bricks or other materials. The exhausted fumes from a wood or coal stove can flow through the flue channels inside the kang interior. The stove fume heats up the kang body, used as thermal mass, which stores the heat, and releases it to the bedroom later, keeping the room warm during non-cooking periods. Besides, kang uses the buoyancy force to exhaust the smoke and ventilate the room, diluting indoor air contaminants. But, a kang with smoke backflow can also pollute indoors with CO and particles. A good kang should be designed to satisfy occupant thermal comfort by keeping desired indoor air temperature constant. The stove, kang main body and chimney should be properly integrated, so that stove can easily start the fire, and the smoke can be easily exhausted through the chimney. The air-tightness of a kang is also important for buoyancy-induced force to circulate smoke. Good room air-tightness and a high level of envelope insulation are needed to maintain the desired indoor air temperature.

The commonly-used traditional kang in Northeastern China is directly built on ground in a bedroom. It consists of a solid earth or fired clay platform; upon which is an adobe flue, with an upward slope of 3% to draw air from the stove to the chimney. The flue consists of several channels, each of 150 - 250 mm high and 200 - 280 mm wide. It is paved with bricks, coated and leveled with plaster. The upper surface of a kang, i.e. the faceplate, must have a moderate temperature level and a uniform temperature distribution at all time, which is affected by layout of smoke flue layout, i.e. smoke passage. A kang may be also categorized by its flue layout. The heat storage capacity of kang is rather significant. It may take several hours of heating to reach its desired surface temperature, and a kang may keep warm through the night without the need of re-heating. A kang mainly uses thermal convection to heat up air, also use thermal radiation to heat up other surfaces. According to a field measurement in 1960s, the indoor air temperature could remain about 12°C in a very cold winter, and even reach 16°C sometimes for rooms with an ordinary level of air-tightness and envelope insulation [Yang (1963)]. However, a number of drawbacks have been identified in practice with the traditional kangs, such as high fuel consumption, smoke blocking up, smoke backflow, choking etc.

The new elevated kang emerged during the 80-90s. *Diao kang* is the Chinese name for the elevated kang. The major difference between a traditional kang and an elevated kang is that the latter is a suspended platform, while the former sits directly on the ground, as shown in Figure 5.38. In an

elevated kang, a reinforced concrete slab in one piece (soleplate) is built on several columns to a height of about 20cm, on which short pillars stand at regular intervals, rising to a total of up to 60 cm in height; a flat surface (faceplate), as a bed plate, is then made by laying brick plates on the top of the pillars. The stove used with a kang is often different from the stove being used alone, as the former is used for both food cooking and kang heating. The heating efficiency for a cooking stove with a traditional kang is usually not too high, about 25% - 35%. In order to regulate the thermal performance of an elevated kang, several control methods are applied. A fume stopper is built at the end of the heating chamber, which can be used to restrict the flow rate of hot smoke, increase the residence time of smoke, and increase turbulence to enhance heat transfer between smoke and plates. Generally, the dimension of a fume stopper is 420 mm length  $\times$  160 mm height  $\times$  50 mm width [Guo (2003)]. Besides, a stop plank at the smoke outlet of the kang body is used to moderate smoke circulation. Furthermore, an air damper is often installed to regulate heat transfer from the kang bottom to indoor air. In order to sustain good thermal conditions, the material for the plate should have both sufficient thermal storage and effective heat transfer, and obviously should be easy to find and also cheap in rural areas. The optional plate materials include slate, adobe or clay, and concrete has also been commonly used. Although slate is the best material as faceplate, it is hard to access, otherwise, brick is generally chosen.

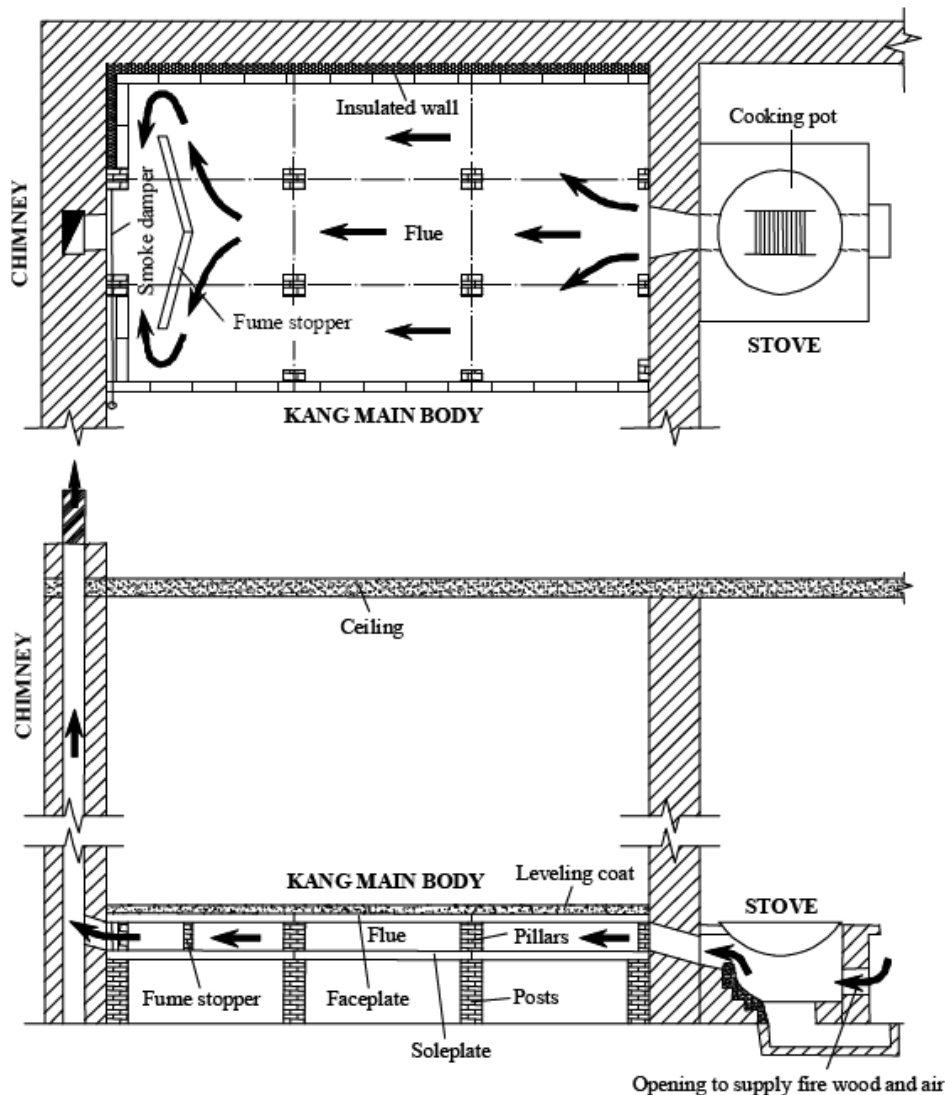


**Figure 5.38 - A complete illustration of elevated kang domestic heating system including the chimney, the kang and the stove.**

### 5.5.2.2 Theoretical study and field survey

Chinese kang is potentially an energy-saving heating system integrating with high thermal mass. However, the design of Chinese kang is mostly based on the experiments and lacks of the scientific support. Furthermore, such a widely used rural domestic heating system is rarely mentioned in the open research literature. Recently, several field survey and theoretical study has been carried out by [Li et al. (2007)]. The new stove may be used with the kang to improve the indoor air quality. The elevated kangs are estimated to be 30% more energy efficient than the traditional kangs. A rough estimate suggests that by using elevated kangs, the existing biomass resources would be sufficient to meet the energy use in rural Northern China.

In addition, a mathematical model for a House Integrated with an Elevated Chinese Kang (HIEK) heating system has been developed by [Li et al. (2007)] for building energy simulation. In this model, the heat transfer through the kang plates is treated as one-dimensional heat conduction process. The whole configuration of HIEK model is illustrated in Figure 5.39. Within this model, the MIX code [Li et al. (2000)] is implemented to analyze the ventilation for multi-zone building. This program can be used to predict the indoor air temperature for a multi-room house with the elevated kang heating system, and it also can be extended to investigate the thermal performance of kang system and its influence on indoor thermal environment and building energy consumption.

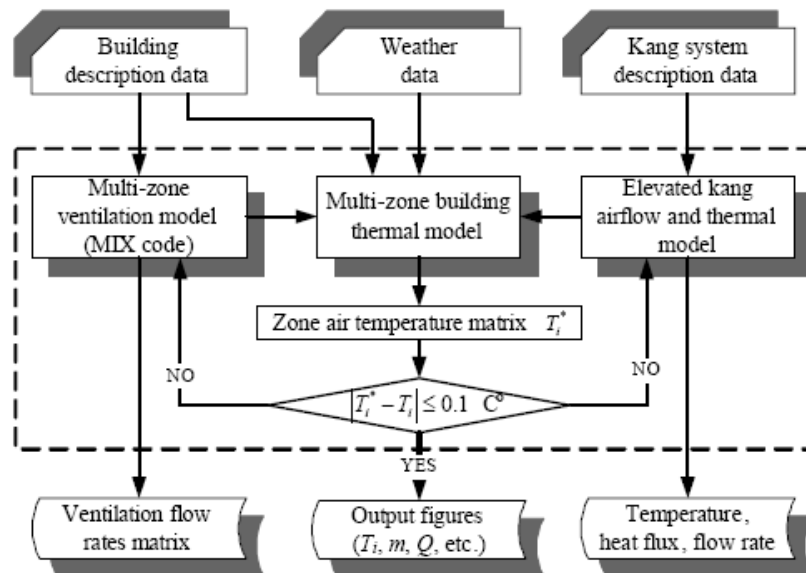


Figure 5.39 - The implementation procedure of the HIEK model [Li et al. (2007)].

The detailed descriptions of this model can be found in [Zhuang et al. (2007)]. Besides, this model has been preliminarily integrated into DeST software (Designer's Simulation Toolkit). DeST (Tsinghua University DeST group 2006) is a simulation tool for building thermal performance & HVAC developed by Tsinghua University during 1990s, and now widely used in the Chinese building industry. It will become more convenient to use this tool for HIEK design.

Chinese kang, serving as an energy-efficient heating system by utilizing the biomass heat, still has potential for improvements in energy saving and human thermal comfort. New advanced materials techniques such as PCM or modern light structure bed can be integrated into the kang system. Computational fluid dynamics and thermo-fluid dynamics tools can be applied to analyze the smoke distribution in the kang body for optimizing the flue design. The development of kang system is significant for developing sustainable building technologies in rural China.

### **5.5.3 The Centre for Sustainable Building (ZUB)**



***Figure 5.40 - The Centre for Sustainable Building (ZUB) in Kassel, Germany [De Carli et al. (2003)].***

The office building belongs to the Centre of Sustainable Building (ZUB), University of Kassel, Germany. The building is an example of new low temperature heating/cooling systems implementation. The ZUB office building consists mainly of three different parts: one part for exhibitions and events, one part for offices and an experimental part for different kinds of research in innovative building technologies and building services concepts. The load bearing skeleton, in reinforced concrete, consists of round pillars with a distance of 5.40 m and flat concrete slabs for the floor/ceiling construction.

A water-based conditioning system with embedded pipes is used for heating and cooling of the offices. In the case of heating operation mode, the system works with water inlet temperatures controlled according to the outdoor temperatures (approx. 24° C). In case of cooling needs, pipes embedded in the floor slab of the basement are used as a ground heat exchanger. Mechanical cooling is not required. Figure 5.41 shows the positions of the different cooling/heating systems installed in the building.

There are two layers of pipes in the floor constructions of the building. As shown in Figure 5.41, the pipes are embedded in the concrete slabs and in the upper floor construction (regular floor heating/cooling). This design was used to be able to test the properties of different systems and their advantages. Pipes are made in polyethylene with a diameter of 20 mm and a distance of 150 mm. In the basement, the pipes have a diameter of 25 mm. The distribution of the pipes in the slab has a coil shape. Each circuit of the floor radiant system and the active thermal slab system is supplied by approx. 600 kg/h water mass flow rate. The difference between supply and return water temperature is lower than 4 – 5 °C. Individual regulation of the thermal conditions in each room is possible because each room has its own heating/cooling circuit.

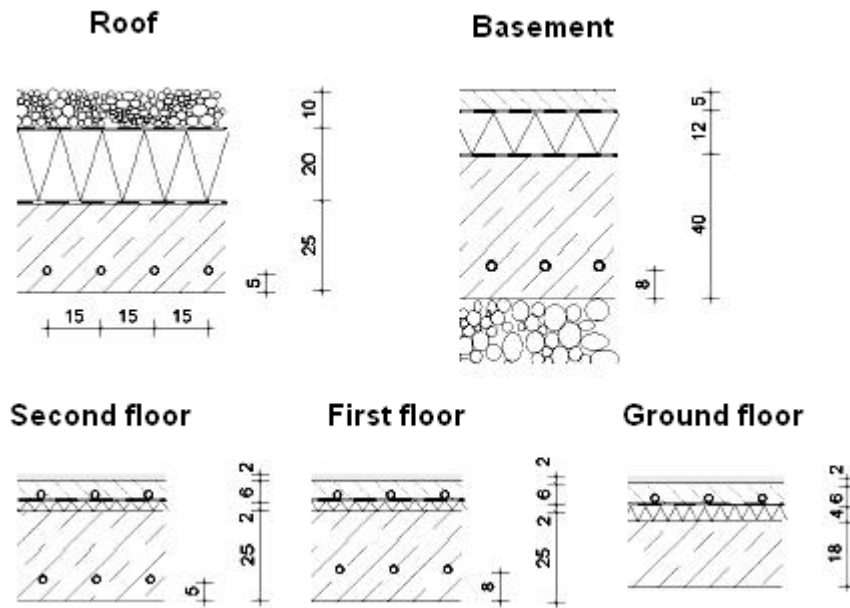


**Figure 5.41 - Different positions of pipes as used in the ZUB in building Kassel, Germany [De Carli et al. (2003)].**

#### **5.5.4 Office building of Bertelsmann C. Verlag GmbH**



**Figure 5.42 - Office building of Bertelsmann C. Verlag GmbH, Munich, Germany [www.uponor.de/ (August 2008)].**

The four-stories building consists of two main long parallel buildings, each with additional building wings. The building has offices facing all directions. A slab heating and cooling system is used. It is combined with a mechanical ventilation system and radiators as an additional heating system (Figure 5.43). Offices are also equipped with operable windows. In the spaces with higher internal loads (conference rooms), an additional cooling was installed. The building is divided in four zones with separate supply-return pipes and control, so they can be cooled or heated independently.

The design water temperatures were for cooling 16 °C supply/19 °C return and 24 °C supply/22 °C return for heating. The supply temperature is controlled separately for each zone according to an average zone temperature based on several room temperature sensors.

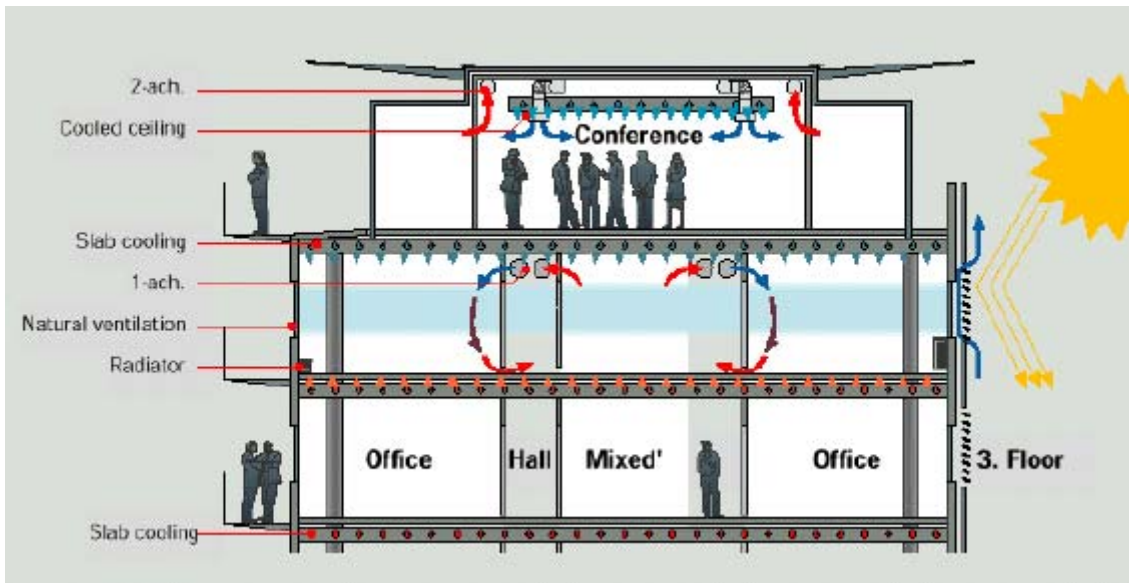


*Figure 5.43 - Office building in Munich, installation of activated thermal mass components [Olesen (2000)].*

### **5.5.5 Berliner Bogen**

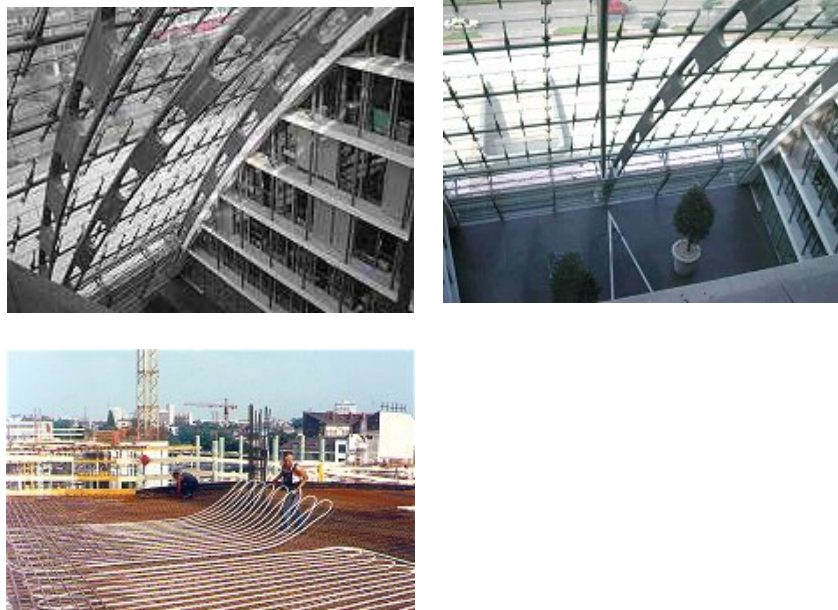


*Figure 5.44 - Berliner Bogen: example of the building construction – double skin facade and floor slabs, winter garden and installation of the pipe-work [www.uponor.de/ (August 2008)].*

The construction of a new office block in Hamburg was finished in December 2001. A modern concept with the glass facades in the outer shell is used. A heating/cooling system, made of 18,000 m<sup>2</sup> of activated concrete floor/ceiling slabs was used. The pipe-work system comprises the prefabricated pipe matrices (modules). Each module includes a coil of 20x2.3 mm pipe. Water supply temperature ranges between 16 and 20 °C during the cooling mode and between 22 and 28°C in heating mode.

## 5.6 Potential barriers and limitations

### 5.6.1 General barriers and limitations to the application of surface thermal mass activation (SA)

- The effect of the thermal mass activation is dependent on the climate context.
- The thermal properties of thermal mass elements should be carefully designed also in relation to the building type, room furnishing and occupation schedules
- For an effective thermal storage and release process, the surface heat transfer rate, governed by the convective heat transfer coefficient and by the surface area, needs to be sufficiently large. In case of surface thermal mass activation, it is generally difficult to enhance the convective heat transfer rate significantly without using a mechanical fan. Thus, the surface area of the thermal mass is a crucial design parameter.

### 5.6.2 Barriers to the application of core thermal mass activation (CA)

- Application of the core thermal mass activation is suitable for buildings with low heat/cooling loads (40 – 50 W/m<sup>2</sup>). High thermal insulation of the building envelope and proper solar shading is necessary.
- There should be the balance between heating losses and cooling loads, so that the system can work optimally all the year round (the same heat exchange surface is used for both cooling and heating).
- In office buildings, it is very common to use a raised floor for running cables. In the case of concrete slab cooling most of the heat transfer will then be over the ceiling side, which means suspended ceilings should not be used.
- Without the suspended ceiling, the acoustical requirements must be solved in other ways.
- Buildings with thermo active components cannot be expected to keep an indoor fixed temperature. The research is ongoing to evaluate occupant responses to the temperature drifts and the influence of these drifts on the performance of office work [Kolarik et al. (2007)].
- Individual control of the indoor thermal parameters is possible only when the core activation (CA) is applied in combination with additional air-conditioning/heating system.
- Individual room control is not possible. It is recommended to divide the building into zones.
- In climates with high air relative humidity, a dehumidification system is necessary.
- During the cooling period, the control according to relative humidity may limit the cooling capacity of the radiant system.
- High standard of building construction management is needed.
- Optimization of the system, based on the experience, measurements and simulations, is needed in the beginning of operation.
- During the heating period, there is the risk of cold downdraft at windows, which may be solved by the design of windows with glazing U-factors less than 1.2 W/(m<sup>2</sup>K), or with an additional heating in the perimeter area.

## 5.7 List of Symbols

$A$	effective heat surface area, m <sup>2</sup>	$h$	convective heat transfer coefficient, W/m <sup>2</sup> K
$C_M$	heat capacity of the thermal mass, J/kg K	$k$	thermal conductivity, W/m K
$C_p$	heat capacity of air, J/kg K	$L$	length, m
$E$	effective total heat power, W	$M$	mass of thermal mass, kg
$H$	height, m	$q$	ventilation flow rate, m <sup>3</sup> /s

$R$	radius, m	$\lambda$	convective heat transfer number
$t$	time, s	$\theta$	temperature, K
$T$	temperature, K	$\rho$	air density, kg/m <sup>3</sup>
$V$	mass volume, m <sup>3</sup>	$\rho_M$	density of the thermal mass, kg/m <sup>3</sup>
$W$	width, m	$\sigma$	flow rate transformation variable
<i>Greek symbols</i>		$\tau$	time constant, hr
$\beta$	phase shift, hr	$\omega$	frequency of outdoor temperature variation, hr <sup>-1</sup>
$\eta$	Fourier time constant, hr	$\xi$	stability criterion parameter
$\kappa$	thermal diffusivity, m <sup>2</sup> /s		

## 5.8 References

- Antonopoulos, K. A. and E. P. Koronaki. 1998. Apparent and effective thermal capacitance of buildings. *Energy* 23(3): 183-192
- Antonopoulos, K. A. and E. P. Koronaki. 2000. Thermal parameter components of building envelope. *Applied Thermal Engineering* 20(13): 1193-1211
- Artmann N, D. Gyalistras, H. Manz and P. Heiselberg. 2006b. Impact of climate warming on night-time passive cooling. (*Submitted to Building Research and Information*)
- Artmann N, Manz H and Heiselberg P. 2006a. Potential for passive cooling of buildings by night-time ventilation in present and future climates in Europe. In: *Proceedings of the 23rd Conference on Passive and Low Energy Architecture*, Geneva
- Artmann N, Manz H and Heiselberg P. 2007a. Parametric study on the dynamic heat storage capacity of building elements. In: *Proceedings of the 2nd PALENC and 28th AIVC Conference*
- Artmann N, Manz H. and Heiselberg P. 2007b. Climatic potential for passive cooling of buildings by night-time ventilation in Europe. *Applied Energy* 84:187-201
- Artmann N, Manz H, Heiselberg P. 2008. Parameter study on performance of building cooling by night-time ventilation. *Renewable Energy*, 33, pp. 2589-2598.
- Artmann N, Jensen R L, Manz H, Heiselberg P. 2008a. Experimental investigation of heat transfer during night-time ventilation. Submitted for publication in *Energy and Buildings*.
- Asan, H. and Y.S. Sancaktar. 1998. Effects of wall's thermophysical properties on time lag and decrement factor. *Energy and Buildings* 28(2):159-166
- ASHRAE. 1999. ASHRAE handbook – HVAC applications. Atlanta: American Society of Heating, Refrigerating and Air-Conditioning Engineers, Inc.
- Axley JW, Emmerich SJ. 2002. A method to assess the suitability of a climate for natural ventilation of commercial buildings. Proceedings: *Indoor Air 2002*, Monterey, CA
- Babiak J, Olesen B W, Petráš D. 2007a. REHVA Guidebook no. 7, Low temperature heating and high temperature cooling – Embedded water based surface systems, Forssan Kirjapaino Oy-Forssan, Finland, ISBN 2-9600468-6-2
- Babiak, J. 2007. Low temperature heating and high temperature cooling, Thermally activated building system. Doctoral Thesis, Department of Building Services, Faculty of Civil Engineering, Slovak University of Technology, Bratislava, Slovakia
- Babiak, J., Minárová, M., Olesen, B.W. 2007b What is the effective thickness of a thermally activated concrete slab, In proceedings of WellBeing Indoors – *Clima 2007 conference*, CD-ROM, Helsinki, Finland

- Badescu, V., Sicre, B. 2003. Renewable energy for passive house heating Part I. Building description. *Energy and Buildings* 35(11): 1077-1084
- Balaras, C. A. 1996. The role of thermal mass on the cooling load of buildings. An overview of computational methods. *Energy and Buildings* 24(1):1-10
- Balcomb, J. D. 1983. Heat storage and distribution inside passive solar buildings. In: Proceedings of the *2nd International PLEA Conference*: 547-561
- Bansal N.K. 1998. Characteristic parameters of a hypocaust construction. *Building and Environment* 34(3): 305-318
- Brunello, P., De Carli, M., Di Gennaro, G., Zecchin, R. 2001. Mathematical modelling of radiant heating and cooling with massive thermal slab, *Clima 2000 conference*, Naples, Italy
- Burberry, P. 1983. *Practical Thermal Design in Buildings*. London: Batsford Academic and Educational Ltd.
- CIBSE. 1988. *CIBSE Guide Volume A Design Data*. Chartered Institute of Building Services Engineers (CIBSE), London, UK
- CIBSE. 2001. *CIBSE Guide B2 – Ventilation and Air Conditioning*. Chartered Institute of Building Services Engineers (CIBSE), London, UK
- Claesson, J. 2002. *Dynamic Thermal Networks. Background studies I: Elements of a mathematical theory of thermal responses*. Report, Dept. of Building Physics, Chalmers Technical University, Gothenburg, Sweden
- Claesson, J. 2003. *Dynamic thermal networks: a methodology to account for time-dependent heat conduction*, Proceedings of the *2nd International Conference on Research in Building Physics*, Leuven, Belgium, p. 407-415. ISBN 90 5809 565 7
- Clarke, J. 1985. *Energy simulation in building design*. Adam Hilger Ltd, Bristol, UK
- De Carli, M. 2002. *New Technologies in Radiant Heating and Cooling*, Doctoral Thesis, University of Padova, Italy
- De Carli, M., Hauser, G., Schmidt, D., Zecchin, P., Zecchin, R. 2003. "An Innovative Building Based On Active Thermal Slab Systems", *58th ATI National Conference*, San Martino di Castrozza, Italy
- De Carli, M., Olesen, B.W. 2002. *Field Measurements of Operative Temperatures in Buildings Heated or Cooled by Embedded Water-Based Radiant Systems*. In: *ASHRAE Transactions*, Vol. 108 Part 2, pp. 714-725
- Deecke, H., Guenther, M., Olesen, B. W. 2003. *Betonkernaktivierung*, Velta Nordestedt, Germany
- EN 12828. 2002. *Heating systems in buildings - Design for water based heating systems*, CEN Brussels, Belgium, 2002
- EN 15377. 2008. *Design of embedded water based surface heating and cooling systems, Part1: Determination of the design heating and cooling capacity, Part2: Design, dimensioning and installation, Part 3: Optimizing for use of renewable energy sources*; CEN Brussels, Belgium, 2007
- EN 15251. *Indoor environmental parameters for assessment of energy performance of buildings, addressing indoor air quality, thermal environment, lighting and acoustics*. EN 15251. Brussels: Comité Européen de Normalisation, 2007. European Committee for Standardization (CEN), Brussels, 2007.
- Fort, K. 1999. *Type 160: Floor Heating and Hypocaust*, Transsolar Energietechnik GmbH, Stuttgart, Germany

- Gao, M. and C. N. Reid. 1997. A simple virtual sphere method for estimating equilibration times in heat treatment. *International Communications in Heat and Mass Transfer* 24 (1): 79-88
- Giesecke, F. E. 1946. Hot-water heating and radiant heating and radiant cooling, Technical Book Company, Austin, USA
- Givoni, B. 1976. *Man, Climate and Architecture*. 2nd ed. London: Applied Science.
- Givoni, B. 1990. Performance and applicability of passive and low-energy cooling systems. *Energy and Buildings*, 17 (1991) 177-199
- Givoni, B. 1998. Effectiveness of mass and night ventilation in lowering the indoor daytime temperatures. Part I: 1993 experimental periods. *Energy and Buildings* 28(1):25-32
- Guo, J. 2003. Energy-saving stove and kang. *China Agriculture Press*. (In Chinese)
- Hauser, G. Kaiser, J., Schmidt, D. 2005. Energy Optimised in Theory and Practice – The Centre for Sustainable Building. Submitted and accepted: Proceedings to the *Sustainable Building Conference* 2005, September 27-29, 2005, Tokyo, Japan
- Hauser, G., Kaiser, J., Rösler, M., Schmidt, D. 2004. Energetische Optimierung, Vermessung und Dokumentation für das Demonstrationsgebäude des Zentrum für Umweltbewusstes Bauen, Final Report of BMWA Research Project, University of Kassel, Germany
- Hauser, G., Kempkes, Ch., Olesen, B.W. 2000. Computer simulation of the performance of a hydronic heating and cooling system with pipes embedded into the concrete slab between each floor, *ASHRAE Transactions*. Vol. 106, Part 1
- HELIOS Software. 2007. Building energy simulation code. Swiss Federal Laboratories for Materials Testing and Research (Empa), Duebendorf, Switzerland
- Karlström, S. 2005. TermoDeckRevisited, Master of Science Thesis Department of Building Technology KTH Stockholm
- Klein, S. et al. 1988. TRNSYS – a transient system simulation program. University of Wisconsin-Madison, Engineering experiment station report 38-12
- Kolarik, J., Olesen, B.W. 2007. Energy use and thermal comfort in a building with Thermo Active Building System (TABS). In proceedings of *Indoor Climate of Buildings 2007 conference*, pp. 299-307, Štrbské Pleso, Slovakia
- Kolarik, J., Olesen, B.W., Toftum, J. and Mattarolo, L. 2007. Thermal Comfort, Perceived Air Quality and Intensity of SBS Symptoms During Exposure to Moderate Operative Temperature Ramps. In proceedings of *WellBeing Indoors – Clima 2007 conference*, CD-ROM, Helsinki, Finland
- Koschenz, M. and Lehmann, B. 2000. Thermoaktive Bauteilsysteme TABS, EMPA Duebendorf, Schwizerland, ISBN 3-905594-19-6
- Koschenz, M., Lehmann, B. 2004. Development of a thermally activated ceiling panel with PCM for application in lightweight and retrofitted buildings, In: *Energy and Buildings* Vol. 36
- Lechner, N. 2001. Heating, cooling, lighting: design methods for architects, 2nd Ed. New York: John Wiley & Sons
- Li, Y. and P. Xu. 2006. Thermal mass design in buildings – heavy or light? *International Journal of Ventilation*, Special Edition 5(1): 143 - 150
- Li, Y. and Y. Yam. 2004. Designing thermal mass in naturally ventilated buildings. *International Journal of Ventilation*. 2(4): 313-324

- Li, Y. et al. 2000. Prediction of natural ventilation in buildings with large openings. *Building and Environment*, 35: 191-206
- Li, Y., Z. Zhuang, X. Yang and B. Chen. 2007. Chinese kang. In: Proceedings of the *6th International IAQVEC Conference*, Sendai: Vol I: 1059-1068
- Manley, J. K. 1954. Radiant heating, radiant cooling, School of Architecture, Pratt Institute
- Mathews, E. H., P. G. Rousseau, P. G. Richards, and C. Lombard. 1991. A procedure to estimate the effective heat storage capability of a building, *Building and Environment* 26 (2): 179-188
- Meierhans, R. A. 1993. Slab cooling and earth coupling, *ASHRAE Transactions Symposia*, Vol. 99, Pt. 2
- Meierhans, R. A. 1996. Room air conditioning by means of overnight cooling of the concrete ceiling, *ASHRAE Transactions* Vol. 102, Pt. 2
- Meierhans, R. and Olesen, B.W. 1999. Betonkernaktivierung, Velta Nordestedt, Germany, ISBN 3-00-004092-7
- Olesen, B.W. 2000. Cooling and heating of buildings by activating the thermal mass with embedded hydronic pipe systems, *ASHRAE-CIBSE conference*, Dublin, Ireland
- Olesen, B.W., Dossi, F.C. 2004. Operation and Control of Activated Slab Heating and Cooling Systems. *CIB World Building Congress*, Toronto, Canada
- Olesen, B.W., Michel, E., Bonnefoi, F., De Carli, M. 2000. Heat exchange coefficient between floor surface and space by floor cooling - theory or a question of definition, *ASHRAE Transactions*, Vol. 106, 684-694
- Olesen, B.W., Sommer, K., Düchting, B. 2002. Control of Slab Heating and Cooling Systems Studied by Dynamic Computer Simulations, *ASHRAE Transactions*, Vol. 108 Part 2, 698-707
- Pfafflin, J.R. 1980. Sequential heating and cooling responses of a controlled environment space, *Building services engineering research & technology*, vol. 1, no. 4, pp. 179-184
- Randall Thomas, Max Fordham and Partners. 1999. Environmental design – an introduction for architects and engineers, Second edition. London and New York: E& FN Spon, 49-50
- Ruud, M. D., J. W. Mitchell, and S. A. Klein. 1990. Use of building thermal mass to offset cooling loads. *ASHRAE Transactions* 96 (pt. 2): 820-829
- Sahlin, P., Grozman, P. 2003. IDA Simulation Environment: a tool for Modelica based end-user application development, In proceedings of *3rd International Modelica Conference*, Linköping, Sweden, November 3-4
- Santamouris, M and D. Asimakopoulos. 1996. Passive cooling of buildings. London: James & James Ltd.
- Shukuya M. 2004. Energy, Entropy, Exergy and Environmental Physics, Proceedings to the *9th Asia Pacific Physics Conference (APPC)*. Hanoi, Vietnam, October25-31, 2004
- Shukuya, M., Hammache, A. 2002. Introduction to the Concept of Exergy – for a Better Understanding of Low-Temperature-Heating and High-Temperature-Cooling Systems. Espoo. VTT Tiedotteita – Research Notes 2158. 41 p. + app. 17 p.
- Schmidt, D., Weber, T., Jóhannesson G. 2000. Concrete core cooling and heating – a case study, In proceedings of *Healthy Buildings 2000 conference*, Helsinki, Finland, Vol. 2.
- Simone, A., Babiak, J., Bullo, M., Landkilde, G., Olesen, B.W. 2007. Operative temperature control of radiant surface heating and cooling systems, In proceedings of *WellBeing Indoors – Clima 2007 conference*, CD-ROM, Helsinki, Finland

- Smith, J.T. and Raw, G.J. 1999. The suitability of TermoDeck modules for use in building ventilation systems. BRE (Building Research Establishment Ltd).
- Sodha, M. S., J. Kaur, and R. L. Sawhney. 1992. Effect of storage on thermal performance of a building. *International Journal of Energy Research* 16: 697-707
- Togari, S., Y. Arai, and K. Miura. 1991. Simplified prediction model of vertical air temperature distribution in a large space. *Journal of Architectural, Planning, Environment and Engineering*, AIJ, No.427, pp9-19 (in Japanese)
- TRNSYS. 2004. TRNSYS 16 - Update description, University of Wisconsin-Madison, Solar Energy Laboratory Madison, USA
- Tsinghua University DeST group. 2006. Building environmental system simulation and analysis – DeST. *China Architecture & Building Press*
- Uppström, R., Pihl, I., Fridén, L., Gillqvist, T. 2004. Control Strategies. Report of the EU-Energie project "IDEEB". Report IDEEB No. 07, ISBN 91-85303-28-3, SP Swedish National Testing and Research Institute
- Weitzmann, P. 2002. Modelling building integrated heating and cooling systems, Ph.D. thesis at the Department of Civil Engineering, Technical University of Denmark, Lyngby, Denmark, ISBN 87-7877-152-2
- Wentzel E-L. and J. Claesson. 2003. Heat Loss Dynamics of Walls. Analysis and Optimizing Based on the Theory of Dynamic Thermal Networks. Proceedings of the *2nd International Conference on Research in Building Physics*, Leuven, Belgium, p. 397-405. ISBN 90 5809 565 7
- Wentzel, E-L. 2003. Application of the Theory of Dynamic Thermal Networks for Energy balances of a Building with Three-dimension Heat Conduction. Proceedings of the *2nd International Conference on Research in Building Physics*, Leuven, Belgium, p. 625-632. ISBN 90 5809 565 7
- Yam, J.Y., Y. Li, and Z.H. Zheng. 2003. Nonlinear coupling between thermal mass and natural ventilation in buildings. *Int J of Heat and Mass Transfer* 46(7): 1251-1264
- Yang, L., Li, Y. 2008. In press. Cooling load reduction by using thermal mass and night ventilation. *Energy and Buildings*
- Yang, S. 1963. Study and survey on Chinese kang. In: Proceeding of *Civil and Architectural Institute of North China*. (In Chinese).
- Yeo, M.S, I.H. Yang and K.W. Kim. 2003. Historical changes and recent energy saving potential of residential heating in Korea. *Energy and Buildings* 35(7): 715-727
- Zhuang Z., Y. Li and B. Chen. 2007. A mathematical model for a house integrated with an elevated Chinese kang heating system. In: Proceedings of the *10th International Building Performance Simulation Conference*, Beijing: 63-70



# 6. EARTH COUPLING

## 6.1 Description of Principles and Technologies

Thermal energy storage has been known as a flexible heating and/or cooling technique to dampen diurnal and seasonal peak energy demands of buildings. Among various thermal storage media, ground is the most favourable one for most building designs due to its massive capacity and availability. Relatively stable temperatures of the ground have made it an effective heat source, sink, and storage medium used in some building energy conservation measures. The high thermal inertia of soil allows the ground to dampen the oscillation of ambient temperature and results in the soil temperature at a certain depth remaining relatively constant, independent of daily temperature fluctuations, while being affected more by seasonal changes.

The ground thermal storage applications for space heating and cooling can be classified into three forms:

- 1) direct method, which conditions indoor environment by increasing direct contact of the building with the ground;
- 2) indirect method, which pre-heats or pre-cools ventilation air using the thermal storage of ground before delivering it to indoor;
- 3) isolated method, which uses a heat carrier medium, such as ground water or coolant, to exchange energy between the ground and the indoor environment.

An Earth-to-Air Heat Exchanger (ETAHE) is a typical environmental responsive building element adopting the indirect method. It ventilates air to the indoor spaces through one or several horizontally buried ducts. In this way, the ground large thermal capacity and relatively stable temperatures are used to preheat or pre-cool the air, resulting in energy savings. Figure 6.1 is a schematic of an ETAHE. For most residential and commercial buildings with desired indoor temperatures from 20°C to 25°C, ETAHEs are primarily used for cooling purpose since the corresponding ground temperatures are normally below this range for the whole year. ETAHEs can also be used for winter pre-heating when the outdoor air temperature is lower than that of the ground, but additional post-heating systems may be required.

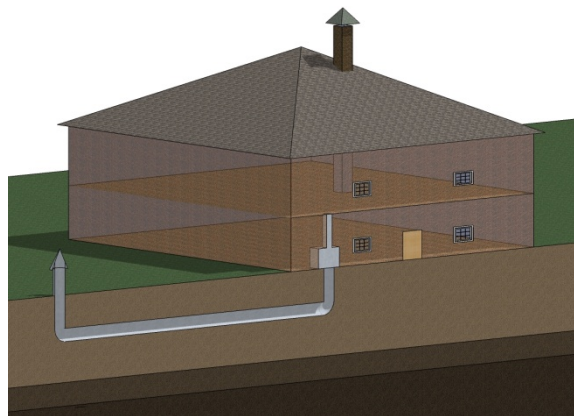


**Figure 6.1 - Building with an Earth-to-Air Heat Exchanger.**

The working principle of cooling air with ventilated underground space has been known since ancient times [Bahadori (1978)], however, ETAHEs had not been popular due to the uncertainties of the required airflow driving forces. Recently a large numbers of ETAHE systems have been built in greenhouses and livestock houses, as well as in residential and commercial buildings. ETAHEs are also found applicable in wide range of climates with large temperature differences between summers and winters as well as between days and nights. In literature terms such as Earth Cooling Tube, Ground Coupled Air System, Cool-Tube in-Earth Heat Exchanger, Earth Air Tunnel, Earth

Contact Cooling Tube, Earth Tube Heat Exchanger, Buried Pipe Cooling System, Underground Solar Airheater, Earth Air-Pipes System, Air-Soil Heat Exchanger, Embedded Duct, Earth Channel, and Hypocaust also refers to the ETAHEs. The name, Earth-to-Air Heat Exchanger, is adopted here because it is commonly used in the industry and it represents the principle of the technology, without limiting its physical configurations.

To effectively use the ground thermal storage, the design and operation of ETAHEs have to be highly dependent on the ventilation systems. Integration of ETAHEs with building service functions is critical for the success of the energy performance. Most existing ETAHEs are installed in mechanically ventilated buildings, in which electrical fans provide the airflow driving forces. In such systems, an ETAHE can be a single duct or multiple parallel ducts made of prefabricated metal, PVC, or concrete pipes with diameters at a magnitude of 10 cm. The typical arrangements for the ducts are:

- Laying the piping in ditches in the surrounding yard
- Laying the piping in the foundation ditch around the building
- Parallel piping directly under the foundation or between the single and continuous strip foundation.

In case of the parallel pipe systems, the distance between the pipes should be kept approximately 1.0 meter from each other in order to minimize the thermal interaction. Greater spacing was not found beneficial for bringing extra benefit [Zimmermann and Remund (2001)]. The size of an ETAHE depends on the designed airflow rate and the available space. A maximum air velocity of 2 m/s is normally recommended for smaller systems, and larger systems can be designed for air velocity up to 5 m/s. Due to the high velocity and small duct size, large amount of energy has to be spent on the mechanical ventilation systems to deliver air through the ETAHEs.

In recent years, there has been a trend of improving the energy efficiency of mechanically ventilated buildings. A hybrid ventilation concept, which alternatively or simultaneously uses mechanical and natural airflow driving forces, has been implemented in many building designs [Heiselberg, (2002)]. It is based on the reduction of pressure drop in the ductwork by increasing its cross-sectional area so that natural airflow driving forces, such as buoyancy and wind, can be used to reduce fan energy consumption. When ETAHEs are integrated in hybrid ventilation, the duct cross-sectional areas should be much larger than those of the conventional ducts used in mechanical ventilation systems. [Schild (2001)] overviewed 17 hybrid ventilated buildings in Norway; and among them 12 buildings were designed with ETAHEs. Their duct hydraulic diameters are all around 1.5 meters. This change in the ductwork size causes the heat transfer process becomes more complicated than the conventional ones. The integration of ETAHE and hybrid ventilation is regarded as a new approach to improve building energy efficiency.

### **6.1.1 Heat flows in the Earth**

From ground surface to hundred-meter depth, the heat transfer processes take place in various forms. At the ground surface, heat transfer is mainly caused by short/long wave radiation, evaporation, precipitation and convection. Conduction is the main form of heat transfer in the ground except for regions with water movements. Geothermal energy from the layers below the crust (the mantle and core) flows up like a constant heat source but it is negligible when analysing the heat flows in a shallow region, e.g. depth less than 20 meters.

### **6.1.2 Ground temperature distribution**

When analyzing the natural heat flow in the shallow soil region, one can simplify the ground as semi-infinite media and describe the heat conduction using Fourier's law as shown in Equation 1. The availability of ground surface temperature records is very limited due to the lack of field measurements. However, similar to ambient air temperature, the daily mean ground surface temperature follow a sinusoid variation with time, and its yearly amplitude is about equal to that of

the air. Such a boundary condition can help to solve Equation 1 and to obtain an undisturbed ground temperature at depth,  $z$ , and at time,  $t$ , as in shown in Equation 2.

$$\rho_s c_{p,s} \frac{\partial T_s}{\partial t} = \frac{\partial}{\partial z} \left( k_s \frac{dT_s}{dz} \right) \quad 1$$

$$T_s(z, t) = T_{s,m} - A_s \cdot \exp \left[ -z \left( \frac{\pi}{365 \alpha_s} \right)^{0.5} \right] \cdot \cos \left\{ \frac{2\pi}{365} \left[ t - t_0 - \frac{z}{2} \left( \frac{365}{\pi \alpha_s} \right)^{0.5} \right] \right\} \quad 2$$

Where

$\rho_s$  is the ground density,  $\text{kg}/\text{m}^3$

$c_{p,s}$  is the ground specific heat capacity,  $\text{J}/(\text{kg} \cdot ^\circ\text{C})$

$T_s$  is the ground temperature,  $^\circ\text{C}$

$t$  is the time, day

$z$  is the ground depth, m

$k_s$  is the ground thermal conductivity,  $\text{W}/(\text{m} \cdot ^\circ\text{C})$

$T_{s,m}$  is the annual mean ground temperature,  $^\circ\text{C}$

$A_s$  is the amplitude of daily mean surface temperature in a year,  $^\circ\text{C}$

$\alpha_s$  is the ground thermal diffusivity,  $\text{m}^2/\text{day}$ , and

$t_0$  is a phase constant since the beginning of the year of the lowest average ground surface temperature, day.

Figures 6.2 and 6.3 show a typical ground temperature profiles as function of different seasons and depths. As far as soil temperatures are concerned, an ETAHE should ideally be installed as deep as possible to prevent the temperature variations. However, the excavation cost for laying an ETAHE very deep may not be economical. In existing applications, the ETAHE ducts are usually buried 1 to 4 m below the earth surface.

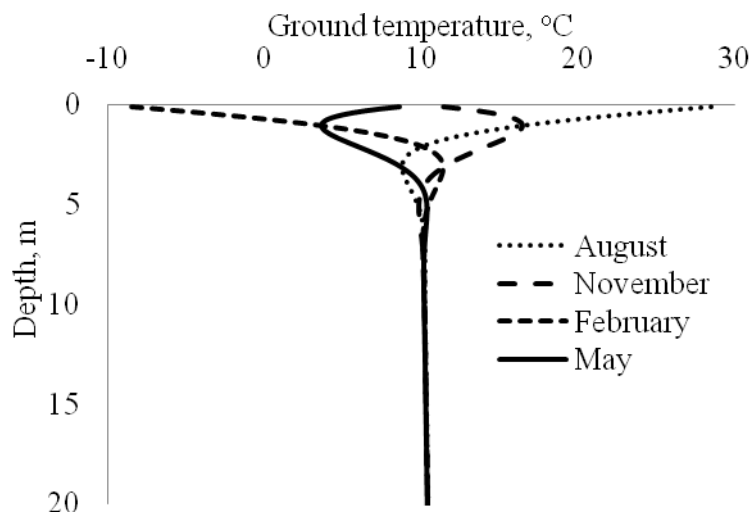
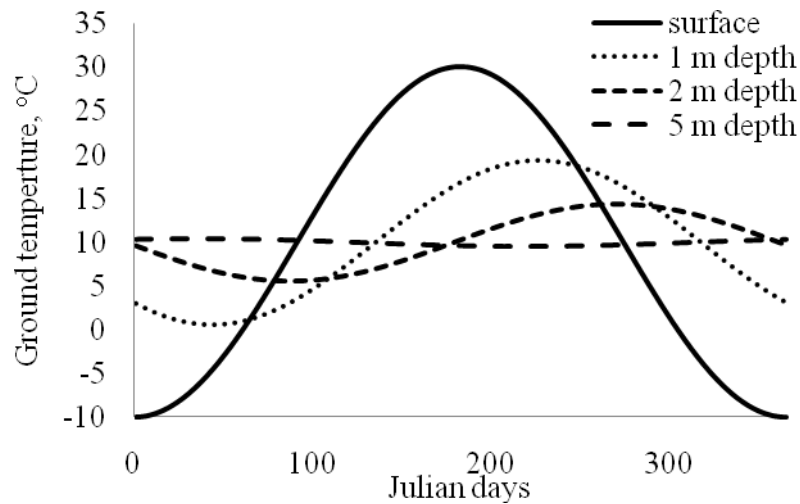


Figure 6.2 - Typical ground temperature profiles at different seasons.



*Figure 6.3 - Typical annual ground temperature variations at different depths.*

### **6.1.3 Heat and mass transfer processes in ETAHE**

According to Figure 6.2, the soil temperatures below 2 meter depth are close to the annual mean temperature, while in summer the inlet air is the warmest of the year, and as air passes through an ETAHE, the convective heat transfer takes place between the air and duct surfaces. The enthalpy and the dry bulb temperature of the air decrease along the flow direction. If the duct is long enough and the duct surfaces would be cooler than the dew point temperature, condensation may take place. When no other cooling device is used, the air conditioning processes can be expressed as shown in Figure 6.4. From point 1, the ambient air condition to point 2 the air is cooled with constant humidity ratio. Depending on the duct cross-sectional size and air speed, the relative humidity (RH) distribution at a same cross-section could affect the condensation condition. If the cross-sectional size is small and the air velocity is large, the RH would be uniform and point 2 would be on the 100% RH curve. However, if the air RH at the cross section has large variation, the boundary layer air would condense first, even though the average air condition has not reached saturation. Point 3 is determined by the duct surface temperature. If the duct length is infinite, the cooling and dehumidification process will happen as from Point 2 to Point 3. However, in practice Point 3' will be the ETAHE outlet air condition. The air temperature may have a little increase to reach Point 4 due to heat gain during distribution. Finally the indoor loads change the air condition from Point 4 to 5. It should be noted that for the process from point 2 to 3, two assumptions are made. The first one is that the duct is long enough so that the air has become saturated. In real conditions, however, the duct lengths are limited due to space constraints and cost. The second one is that the duct surface temperature is not much elevated by the warm air and, hence, Point 3 is determined based on undisturbed ground temperature. However, in practice the heat transfer between the air and the duct surface is a dynamic process. When the air is cooled, the duct wall temperatures are warmed up. Therefore the cooling performance of an ETAHE is mainly determined by the dry cooling process from Point 1 to 2, and the process 2 to 3' can be negligible for practical purpose.

Since the annual mean temperature of ground is lower than indoor thermal comfort conditions, ETAHEs are primarily used for cooling purpose. However, when the outdoor air temperature is very low in winter, it is also beneficial to preheat the supply outdoor air using ETAHEs. The air conditioning processes are shown in Figure 6.5. Point 1 is the outdoor air condition. After it passes through the buried duct, the air temperature increases and its humidity ratio remains the same. From Point 2 to 3, a heating unit further elevates the supply air temperature. Then the supply air is mixed with the return air (Point 5) to reach an appropriate supply air condition, Point 4. The heating load is removed by the supply air from Point 4 to 5. The ETAHE performance in winters is mainly

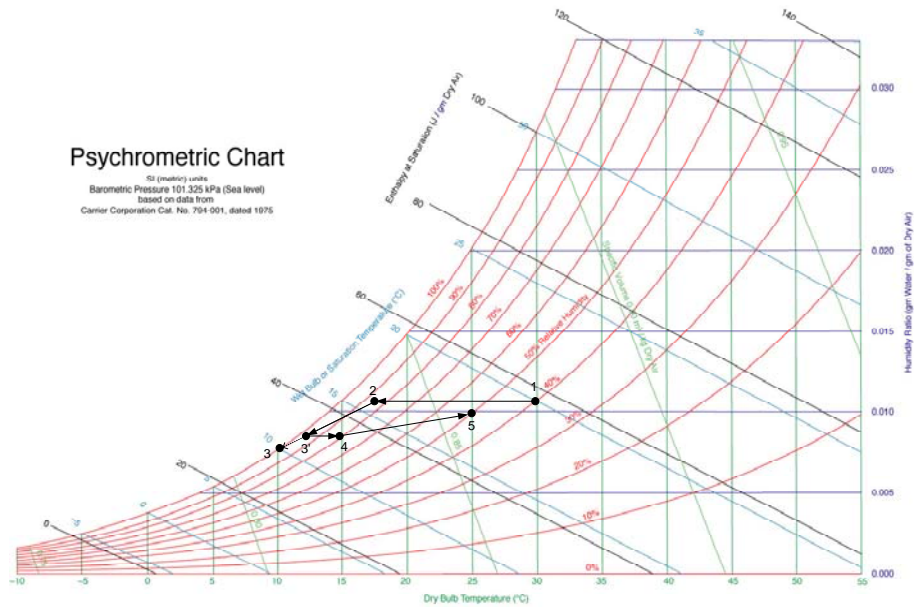


**Figure 6.4 - The Psychrometric chart presentation of air cooling processes in an ETAHE, 1: outdoor air condition; 2: transition condition (condensation starts); 3: duct surface condition; 3': ETAHE outlet air condition; 4: room supply air condition; 5: room air condition.**

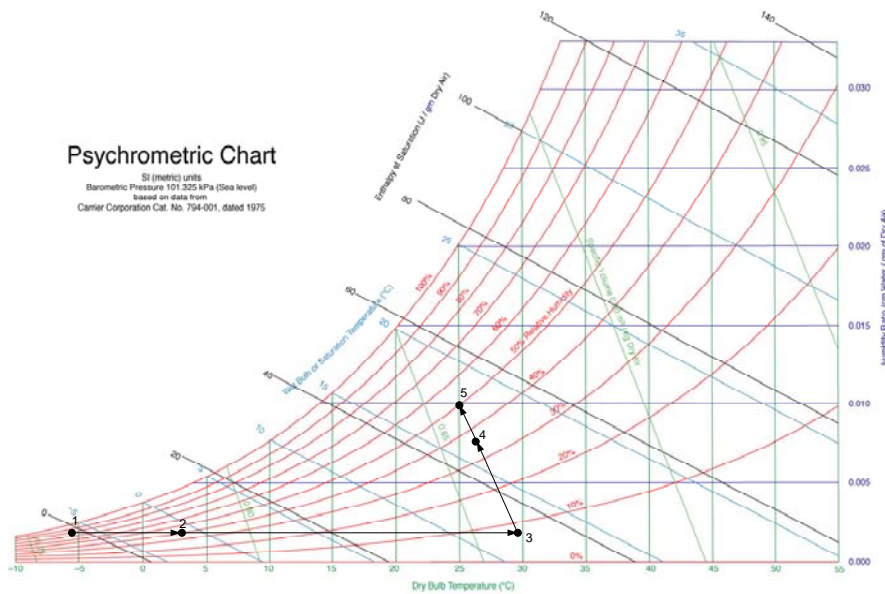


**Figure 6.5 - The Psychrometric chart presentation of heating processes of ETAH - 1: outdoor air condition; 2: ETAHE outlet air condition; 3: air condition after secondary heating; 4: mixing air condition; 5: return duct air condition.**

determined at the process from Point 1 to 2. This process may also happen during the summer, when night ventilation is used to cool down the ETAHE surfaces at nighttime to recharge their cooling capacity for the following day.

Figure 6.4 and 6.5 show that the change of air conditions from Point 1 to 2 is due to sensible heat exchange, and they give an idea of the ETAHE performance.

The intensity of the heat convection is mainly dependent on the airflow conditions and the temperature differences between the air and the duct surfaces.

In conventional ETAHE systems, since the diameters of the buried ducts are two orders of magnitude smaller than their lengths, the convective heat transfer coefficients are usually estimated using empirical correlations for fully developed flow. However, in the large cross-sectional ducts used in hybrid ventilation systems, such as the examples given in Sections 0 and 0, the entrance and buoyancy effects may significantly affect the heat convection because the airflows in the large ducts are far from fully developed. [Zhang (2009)] proposed a new method for calculating the heat convection in such systems using CFD simulation of the airflow and heat transfer processes.

### **6.1.4 Energy cost for fan**

An ETAHE is not a completely passive system and in most applications it requires energy for air circulation. To enhance the heat convection one may think of having longer pipes, enlarging their surface area and roughness, or creating turbulence etc., however, these measures also result in more energy cost for air circulation. In addition, the energy dissipation of mechanical fans may increase the air temperature.

## **6.2 Classification**

According to the system configuration, ETAHEs can be classified as open-loop systems and closed-loop system. Figure 6.1 is an open-loop system, which delivers fresh air to the indoor by locating its inlet at the outdoor. A closed-loop system recirculates indoor air through ETAHE ducts therefore their inlets are in the buildings. These types of systems are used in greenhouses, livestock houses and buildings with separate fresh air inlets. The major benefit of open-loop systems is to provide a path for the outdoor air intake. However, concerns for insect and small animal entering and noise transmission need to be taken into account at the design stage.

In terms of the integration with ventilation systems, ETAHEs can be classified to mechanical and hybrid ventilation systems. The former one is a conventional design and it is used in mechanically ventilated buildings. To reduce the large amount of fan energy demand required to drive the air through the duct work, the large cross-sectional duct system is adopted by hybrid ventilated buildings. The criterion of differentiating the two types is whether the heat convection can be assumed to be fully developed. Although the difference between the two systems appears to be their sizes, their design operation and simulation may be greatly different from each other.

Based on the functionality, ETAHEs may be categorized into heating and cooling systems. When an ETAHE is used for winters pre-heating, it is usually coupled with a heat recovery unit or other heating devices to prevent icing. Figure 6.6 shows an example of such application (ETAHE and heat recovery system). In summer, a properly designed ETAHE system may fully satisfy the cooling load. Figure 6.7 shows an example of the temperature progression of the inlet air when the ETAHE is operated during cooling seasons. When the ETAHE cooling capacity is not enough, the remaining load can be further removed by other measures such as static cooling surfaces (e.g. radiant cooling ceilings or cooled slab). Cooling possibilities for the ETAHEs are:

- natural night ventilation
- mechanical night ventilation
- component cooling

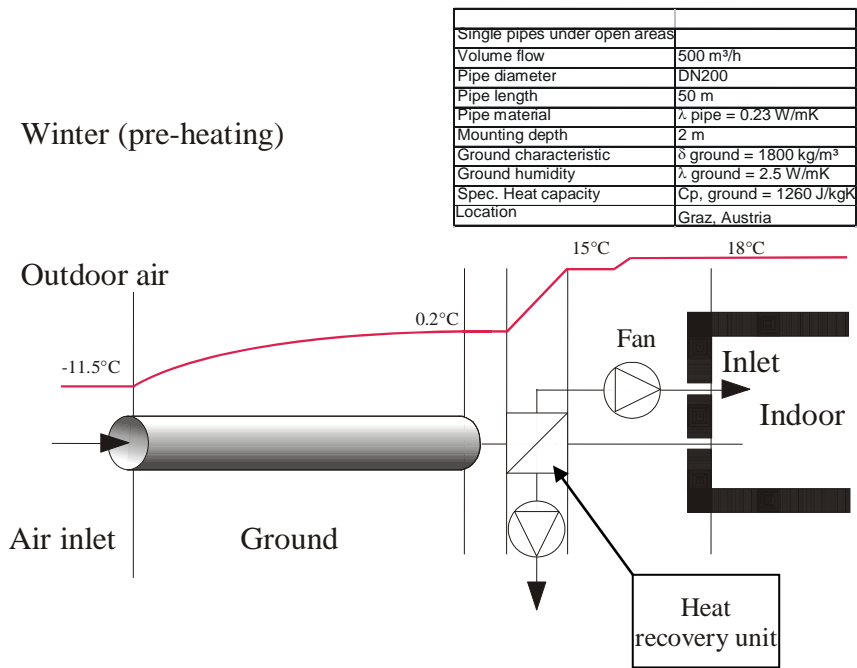


Figure 6.6 - ETAHE with heat recovery during the winter operation [Fink et al. (2002)].

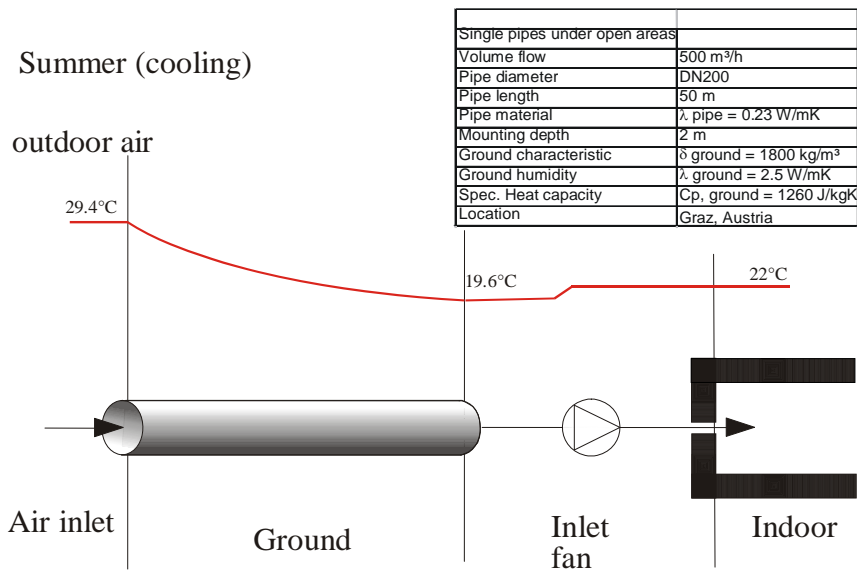


Figure 6.7 - ETAHE with heat recovery during the summer operation [Fink et al. (2002)].

### 6.3 Design/Analysis method and tools

The energy saving potential of an ETAHE has attracted many simulation studies since the 1980s. The main efforts have been focused on the development of simulation methods. Since the process of airflow and heat transfer in large cross-sectional ETAHEs has not been fully understood, existing simulation methods are developed based on the working principle of the conventional small pipe systems (i.e. fully developed condition).

[Santamouris and Asimakopoulos (1996)] presented a calculation chart for predicting the outlet air temperature given ETAHE's length, diameter, depth, air velocity and inlet air temperature. The

method is based on simplified statistical analysis and regression techniques, so its accuracy and features are limited.

WKM (available at <http://www.igjzh.com/huber/wkm/wkm.htm>), a computer program, was also developed to size ETAHEs with the following features:

- yearly simulation of the ground system with heat recovery and bypass,
- weather data can easily be integrated,
- collective ducts and funnels are considered,
- calculation of pressure drop in the ground is done,
- type of pipe and ground characteristics are suggested,
- influence of basement is taken into account,
- excel interface for input and output,
- air ventilation method and airflow rates are selectable.

The Division of Building Physics and Solar Energy, University of Siegen, Germany, developed a commercial software, GAEA (Graphische Auslegung von Erdwärme Austauschern) for design of ETAHE [Benkert et al. (1997)] and [Benkert and Heidt (1998)]. This software is based on calculations of heat exchange in the soil, the buried pipes and the air in the system. The variations of soil temperature, airflow rate, and ambient air temperature are taken into account. An optimization routine presents a choice of possible layout variations and their assessment concerning heat gains and economics. A validation study of GAEA was published by [Heidt and Benkert (2000)].

Under the framework of the IEA-ECBCS Annex 28, early design guidance for different weather conditions and locations was developed by [Zimmermann and Remund (2001)] that makes use of a few design charts and tables. In an EU project, a design tool was developed under the guidance of AEE Gleisdorf and Fraunhofer ISE by 15 engineering companies [Reise (2001)].

[De Paepe and Janssens (2003)] developed a one-dimensional analytical method, which can be used to analyze the influence of the design parameters of an ETAHE on its thermo-hydraulic performance. A relationship between a specific pressure drop and the thermal effectiveness was derived. This was used to formulate a design method which can be used to determine ETAHE's characteristic size. The desired design is defined as a system with optimal thermal effectiveness as well as an acceptable pressure loss. The choice of the characteristic size thus becomes independent of the soil and climatological conditions. This method is claimed to allow designers to choose a proper configuration for an ETAHE with an optimal performance.

TRNSYS is a transient system simulation program with a modular structure that can be designed to solve complex energy system problems by breaking the problem down into a series of smaller components. [Hollmuller and Lachal (1998)] developed an ETAHE model compatible with the TRNSYS environment. Energy and mass balance within underground ducts accounts for sensible as well as latent heat exchanges between air and ducts, frictional losses, diffusion into surrounding soil, as well as water infiltration and flow along the ducts. Local heating from integrated fan motor can be taken into account at the duct inlet or outlet. Direction of the airflow can be controlled (stratification in case of heat storage) and flexible geometry allows for non-homogenous soils and diverse boundary conditions.

## 6.4 Guidance and recommendations

The energy efficiency of ETAHEs has been demonstrated by various simulation studies. Many applications, demonstration project also showed their practical value. In order to promote further applications, its advantages should be highlighted in order to attract more attentions from building owners and designers. Advantages achievable with ETAHEs are:

- general availability of ground makes ETAHEs applicable to most buildings to reduce the energy of active heating and cooling systems.

- In several climatic contexts, appropriately sized ETAHE systems may avoid the use of other mechanical cooling systems.
- ETAHEs can reduce the green gas house (GHG) emission.
- ETAHEs can improve indoor thermal comfort.
- Appropriate exploitation of moisture transfer between air and soil may realize moisture control for the supply air.
- ETAHE' ducts have a filtration effect (concentration reduction of airborne particle, spores and bacteria after passing through ETAHE)
- Sometime ETAHEs are cheaper and easier to construct than active cooling systems.
- Maintenance and operation costs for ETAHEs are low comparing to other air conditioning methods.
- ETAHEs have a very long lifespan.
- The outlet air from ETAHEs can be further treated by other traditional air handling units.
- General availability of pipe materials makes ETAHE systems easy to be replicated anywhere.

ETAHE technology has been proven applicable for a wide range of climates and various types of buildings, such as livestock houses, greenhouses, residential and commercial buildings. For buildings with moderate cooling load, properly sized ETAHE systems may become alternatives to traditional mechanical heating and cooling systems. Significant energy savings and corresponding reduction of GHG emission will attract more and more applications. Hybrid ventilation system has very good potential for being integrated with ETAHE. When an ETAHE needs to be integrated into a hybrid ventilated building, the pressure loss through the duct is a critical issue. Large cross-sectional area ducts are favourable for the integration. Buildings with the following favourable factors may become the potential users of ETAHEs:

- moderate cooling loads
- low ground temperature
- large daily outdoor air temperature swings
- relatively low requirements for indoor environment
- displacement ventilation system

From a general point of view, the most significant issues that have to be carefully considered when designing and operating an ETAHE system are:

- airflow rates through an ETAHE need to satisfy the airflow requirement of the buildings, assuming the ETAHE is the only air inlet for the building.
- It is desirable to maximize the heat transfer rate between air and duct wall while also minimizing the airflow resistance.
- For buildings with displacement ventilation, the air exit temperatures from ETAHEs should always be below that of the room air.
- Condensation and moisture infiltration on the ETAHE duct wall should be avoided.
- The hygrothermal properties of soil need to be considered in the site selection.
- The buried ducts should be anticorrosive and structurally stable.
- An ETAHE provides a path between outdoor and indoor. Safety, insect entrance, and noise transmission should be taken into account.
- Long term operation of an ETAHE with a high heating or cooling load may exhaust its capacity. System recharge methods need to be decided in system control design.
- Ducts should be accessible for inspection and cleaning.

## 6.5 Examples for illustration

Three buildings with ETAHEs are reviewed in this section. The first one is a conventional mechanically ventilated building and the other two are hybrid ventilated one. The review is focused on the ETAHEs' configurations, and operations.

## **6.5.1 Schwerzenbacherhof building, Zurich, Switzerland**

### **6.5.1.1 General information**

The Schwerzenbacherhof building is a commercial building near Zurich, Switzerland, with a heating energy consumption of 144 MJ/m<sup>2</sup> per year for 8050 m<sup>2</sup> of heated surface. It was a major case study in the IEA-ECBCS Annex 28 (Low Energy Cooling) [Zimmermann and Remund (2001)], [Liddament (2000)], [Zimmermann (1995)] and [Hollmuller (2002)]. Figure 6.8 shows the building with the ETAHE's inlet. There are two paths for the building to intake fresh air. It can either pass through the ETAHE system under the building or bypass it to air handling units, as shown in Figure 6.9.



**Figure 6.8 - Schwerzenbacherhof building.**

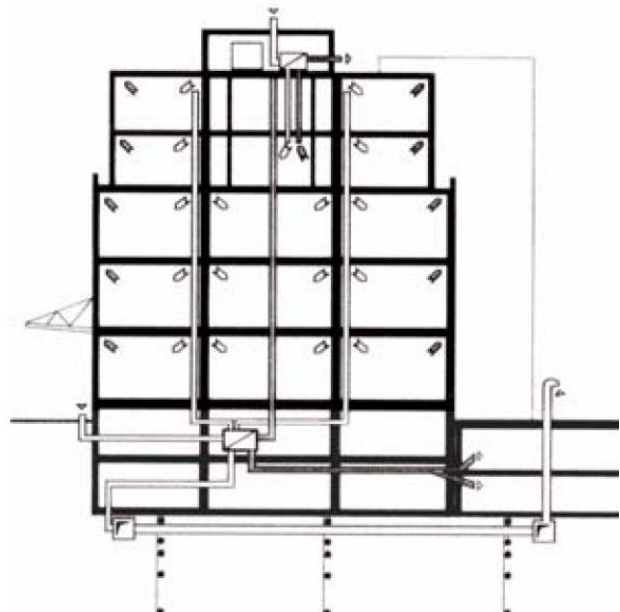


**Figure 6.9 - Schematic of Schwerzenbacherhof building ventilation system [Hollmuller (200)].**

### **6.5.1.2 Component description**

The ETAHE is 6 m beneath the ground surface and 75 cm below the building's unheated second basement. The system consists of 43 parallel high-density polyethylene pipes with a one percent inclination (see Figure 6.10). Each pipe has a length of 23 m and a diameter of 23 cm and the mean axial distance between two pipes is 116 cm. Two large concrete ducts, before and after the pipe system distribute and collect the air. Drainage to sewage is provided in the intake-side concrete duct (see Figure 6.10 right). A varying airflow rate during office hours (12,000 m<sup>3</sup>/h in winter and 18,000 m<sup>3</sup>/h in summer) is maintained by two fans in the system (see Figure 6.11).

### **6.5.1.3 Control strategy**

The ETAHE system is activated in summers when the outdoor air temperature exceeds 22 °C. The air is cooled down as it passes through the pipes, and then it is directly supplied to the rooms. When the outdoor temperature is lower than 22 °C, the air bypasses the ETAHE and is taken directly from outside. This normally happens at night-time. The ETAHE provides about 1/3 of total cooling demand, and the rest is provided by night cooling of the thermal mass. Thus the ETAHE is only a supplement (mainly during the daytime) when night cooling is insufficient.

In winters, when the ambient temperature falls below 7 °C, the ETAHE starts to be used to provide preheating. Then the outlet air from ETAHE passes through the heat recovery unit, which transfers

heat from the exhaust air to the outlet air. The use of the ETAHE during winter time also helps to cool the ground for the next summer and to prevent freezing of the heat recovery unit.

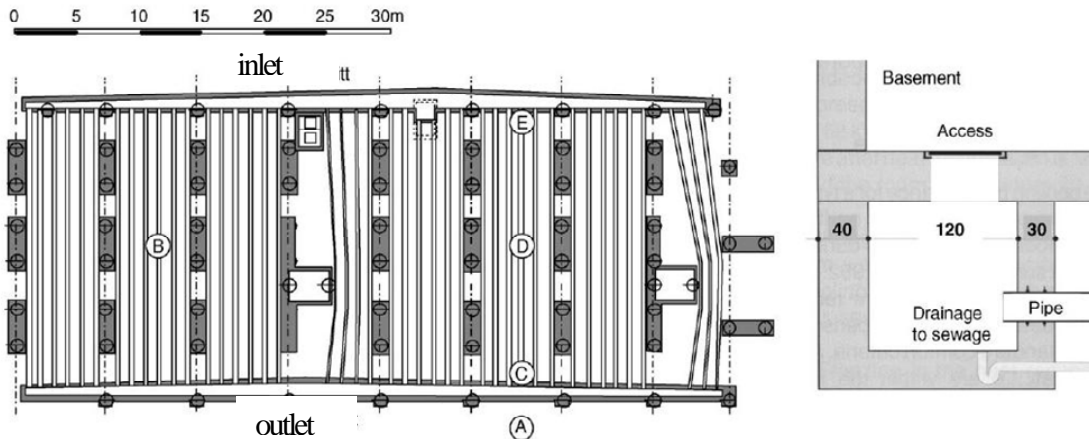


Figure 6.10 - General layout and construction detail of the ETAHE system in Schwerzenbacherhof building [Hollmuller (2002)].

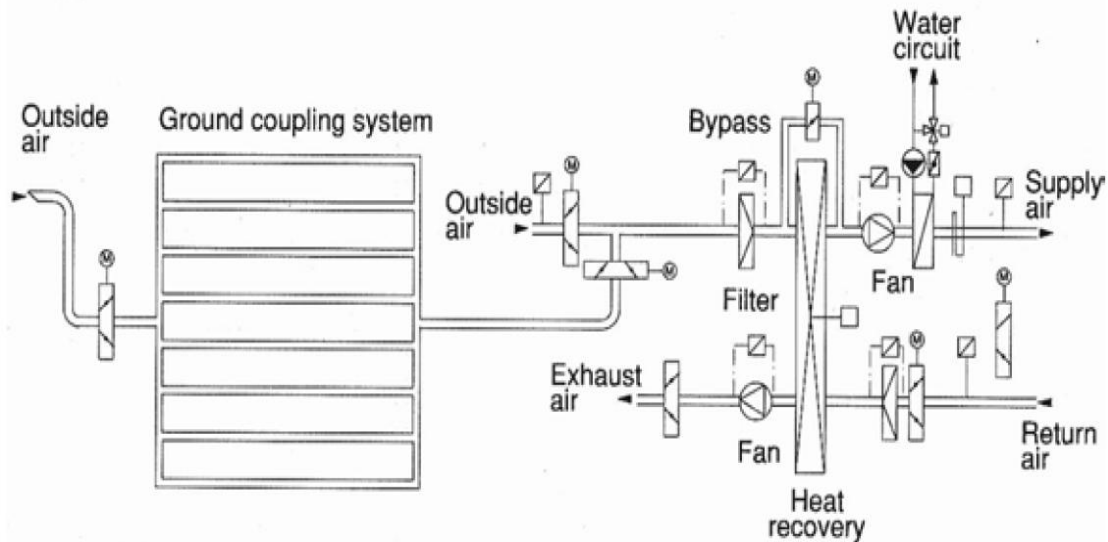


Figure 6.11 - Schwerzenbacherhof building - Ventilation system's components [Hollmuller (2002)].

## 6.5.2 Mediå School, Grong, Norway

### 6.5.2.1 General information

Mediå school is a 1001 m<sup>2</sup> one-floor building located in Grong, Norway. It was one of the case studies in the IEA-ECBCS Annex 35, Control Strategies for Hybrid Ventilation in New and Retrofitted Office Buildings (HybVent). It was investigated by [Tjelflaat (2000a and 2000b)] and [Wachenfeldt (2003)] and [Jeong and Haghightat (2003)]. The building's layout and the schematic of the ventilation system are shown in Figure 6.12 and 6.13, respectively.

### 6.5.2.2 Component description

An air intake tower for the ETAHE is a triangular cross-sectional vertical duct located north of the building and stands on a 35° slope, as shown in figure 6.14. The height from the tower's top to its base is approximately 6 m. On each side of the tower there is an opening, which is covered by a metal shield to protect it from rain. Behind the shield each opening is equipped with a one way damper allowing air entrance when pressure in the tower is lower than outside.

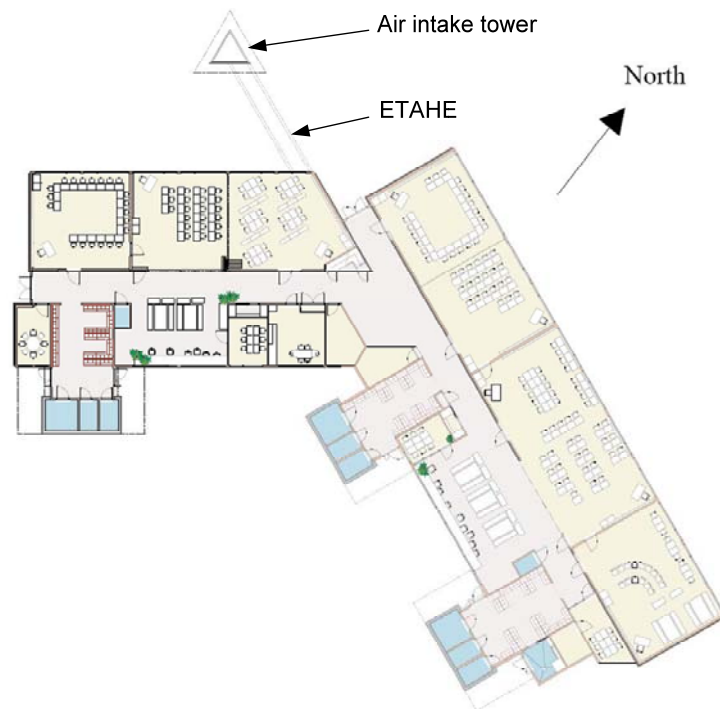


**Figure 6.12 - Mediå school layout [Tjelflaat (2002b)].**

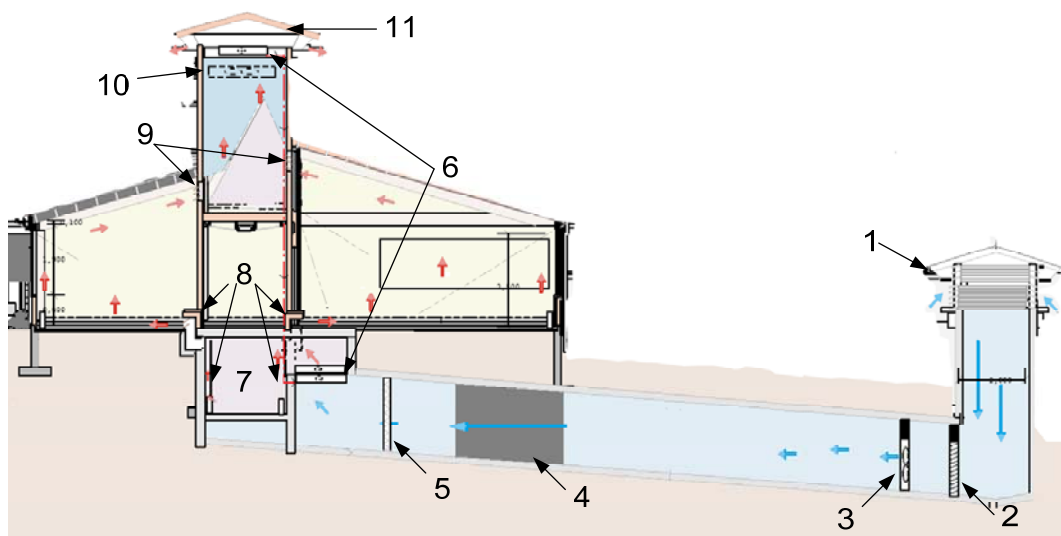


**Figure 6.13 - Schematic cross section of Mediå school showing air flow paths and location of components. 1: triangular intake tower with openings and vents; 2: damper; 3: supply fan; 4: sound absorber; 5: filter; 6: exchangers for supply air preheating using run-round heat recovery via a circulating water-glycol mixture as well as additional reheating; 7: air distribution duct; 8: units for noise attenuation plus openings and grilles for supply of ventilation air to the classrooms; 9: dampers for extracting exhaust ventilation air from the classrooms; 10: extract fan; 11: triangular roof tower with exhaust vents. [Tjelflaat (2002a)].**

After passing through the intake tower, the downward airflow is led to a horizontal 1.5 m × 2 m concrete intake duct whose roof is approximately 1.5 m below the ground surface (refer to Figure 6.13). A damper is installed at the beginning of the duct. A frequency-controlled variable-speed propeller fan with a diameter of 1.4 m is located 1.5 m away from the damper on the leeward side. Its operation is interlinked with the damper opening position.



**Figure 6.14 - ETAHE's intake tower of Mediå school .**

A noise absorber is located 6.3 m from the fan. Six fine filter blocks are installed at the end of the duct. The total distance from the damper to the filters is 11.1 m. The duct has a 5% incline to the inlet direction to allow improved dust deposition and drainage. Drainage is located at the base of the air intake tower.

After leaving the intake duct, the air vertically passes through two overlapped horizontal heat exchangers (see Figure 6.15, left) and enters a 2.2 m × 2 m horizontal air distribution duct. This duct has two branches which are below the building's corridor. The air from the intake duct can also bypass the heat exchangers by flowing through two "summer" doors beside the exchangers. Figure 6.15 (right) shows the distribution duct with the air supply paths attached on the walls and connected to the ground level classrooms. These paths suppress sound transmission between rooms and ensure even supply air temperatures to all rooms.



**Figure 6.15 - Air distribution duct of Mediå school (Left photo shows heat exchangers and "summer" doors. Right photo shows the supply air paths) [Tjelflaat (2002a)].**

### 6.5.2.3 Control strategy

The whole HVAC system is monitored and controlled by a centralized supervisory Building Energy Management System (BEMS) with CO<sub>2</sub> and temperature sensors located in most classrooms. The ETAHE preheats air in winters. The temperature set point in the distribution duct is 19 °C. This is ensured by the two heat exchangers at the end of the air intake duct. In summers, the ETAHE is the only cooling component in the system. The supply fan is activated by the BEMS when larger air change rate is needed. When the two heat exchangers are not needed, the bypass doors can be manually opened to reduce the pressure loss.

## 6.5.3 Jaer School, Oslo, Norway

### 6.5.3.1 General information

Jaer primary school is an 850 m<sup>2</sup> two-storey heavyweight building near Oslo, Norway. It was another case study of the IEA-ECBCS Annex 35. The schematic of the building ventilation system is shown in Figure 6.16 and Figure 6.17.

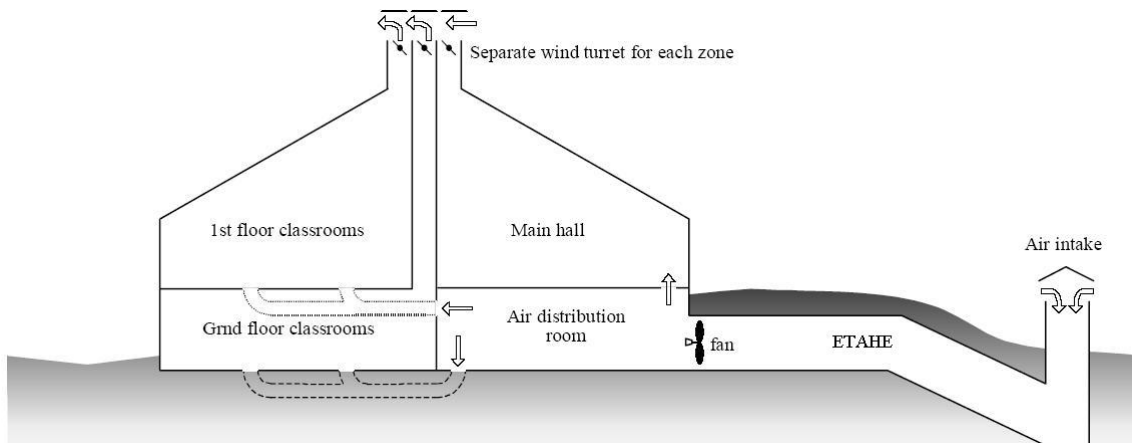


Figure 6.16 - Schematic cross section of Jaer School showing air flow paths and components' locations [Schild (2002)].

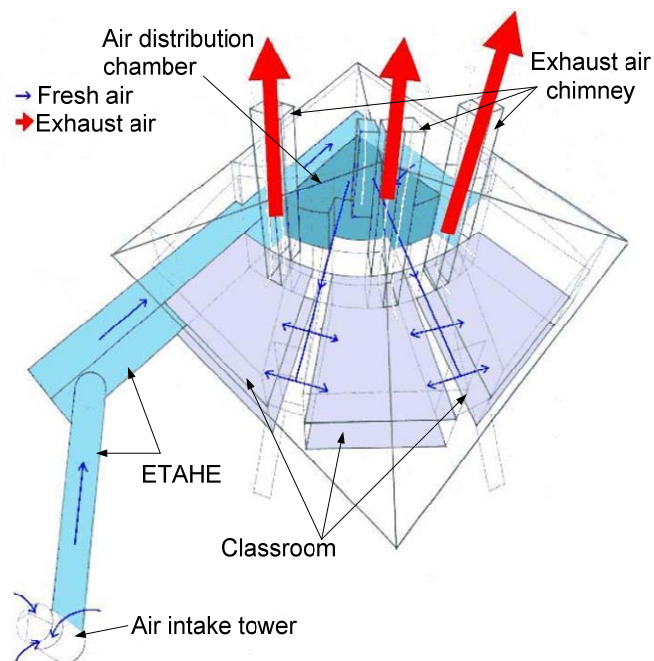


Figure 6.17 - 3D schematic of Jaer School ventilation system [Schild (2002)].

### 6.5.3.2 Component description

The ETAHE's air intake tower, about 2 m height from the ground surface, is located outside the building. To minimize the pressure drop, the air intake louvers are open without any rain and snow shielding. A frost-protected drain is provided on the base of the tower (see Figure 6.18).



**Figure 6.18 - Jaer School air intake tower (Left: outside, Middle: inside looking up, Right: inside horizontally into base of the tower from the horizontal ETAHE duct.) [Schild (2002)].**

The ETAHE consists of two parts: a prefabricated concrete pipe (20 m length and 1.6 m diameter) and a rectangular cast-in-place concrete duct (35 m length, 2 m width, and 3 m height) with a total surface area of about 450 m<sup>2</sup>. At the end of the rectangular duct, there are two possible parallel paths through which the fresh air can enter the air distribution chamber. One is to pass through a speed controlled fan and the other is to pass through a preheat unit as shown in Figure 6.19. The choice to flow the air in one way rather than the other is driven by a computerized Building Energy Management System.



**Figure 6.19 - The air distribution room, showing the preheat unit (left) and fan, as well as the plastic subterranean ducts leading to the various rooms [Schild (2002)].**

From the distribution chamber the air is then delivered to various rooms at the floor level through plastic subterranean ducts. The hybrid ventilation concept is mainly implemented in the rooms by exploiting buoyancy forces. Furthermore, a wind-assisted exhaust tower on top of the building helps to improve the wind driven effect. When these natural forces are not enough to keep necessary airflow rates, the fan at the end of the ETAHE duct is activated to a proper speed.

### 6.5.3.3 Control strategy

The whole HVAC system is monitored and controlled by a centralized supervisory Building Energy Management System (BEMS). There are 4 main operation modes, depending on two bimodal parameters. (1) Preheating needed, (2) Preheating not needed though cooling possibly needed, (A) Day, (B) Night. There is night-time ventilation for pre-cooling in summer. When the CO<sub>2</sub> level or temperature in a room rises above set-point value, the damper at the roof outlet opens gradually. If the CO<sub>2</sub> level remains above the set-point, then the fan is started. The axial fan at the end of the ETAHE is frequency-controlled to maintain constant over-pressure in the culvert. Since the pressure drop through the ventilation system is very small, the stack effect alone in the building has always been enough to satisfy the indoor air quality requirement. The fan at the end of the ETAHE is only used when additional cooling is needed. When the supply air needs to be heated, the BEMS controls the ratio of fresh air to pass the preheat unit.

## **6.6 Potential barriers**

Since 1980s ETAHEs started to be used in various types of buildings. Many issues such as air quality, noise control, system inspection, and recovery of ground thermal storage capacity were, however, not well considered in the design stage. Although several computer simulation codes have been developed, they are mainly focused on annual energy conservation effects. Optimal system design, operation and integration with other building components have not been well studied so far. Standardized design guidance is, unfortunately, not yet available. Furthermore, the flowing issues may become barriers for the future application of ETAHEs.

- ETAHEs provide a path for outdoor noise transmitting to indoor. Plus, many systems are equipped with electrical fans in their ducts. There are concerns that some systems may contravene current noise regulations.
- ETAHEs techniques do not appear completely safe for the environment in terms of contamination of soil, underground water, and microbial growth in the airway.
- There is a general lack of easy-to-use design methods. Existing modeling methods are not accessible for designers. Training programs need to be promoted.
- Design of ETAHE's control strategies vary significantly between countries and regions because of climate differences. Such variations impact technology transfer and adoption of best practice.
- Many building owners and equipment installers lack confidence in new energy technologies. They will often tend to more conventional choices when making investment.
- The system costs are very dependent on the actual project. In some cases, the initial investment for installing an ETAHE might be more expensive than regular air conditioning system. This may cause less attraction for building owners. However, it should be noted that an ETAHE has very long lifespan. The energy saving potential should be considered as a competitive alternative.
- Land availability limits the use of ETAHEs. Installing ETAHE under the building foundation is one solution.
- ETAHEs are usually not suitable for retrofit of an air conditioning system.
- As far as construction is concerned, rocky ground is not suitable for ETAHE application due to the excavation difficulties.
- Air quality may restrict the location of ETAHE's inlet. ETAHEs are not recommended in areas with radon gas.
- Access for insects and small animals into the ETAHE duct should be avoided. This could lead to construction difficulties.
- Cooling process of ETAHEs may increase the relative humidity of air. Condensation may happen in worse cases. An additional dehumidification device may be needed.

- There might be a risk to poor air quality, namely, the potential of microbial growth in the airway. Fungal growth is potentially the biggest problem and is likely to occur where there is standing water.

## 6.7 References

- Bahadori, M.C. (1978). Passive Cooling Systems in Iranian Architecture. *Scientific American*, 238(2), 144-154.
- Benkert, S., and Heidt, F.D. (1998). Designing Earth Heat Exchangers with GAEA. *Proceedings EuroSun '98*, Volume IV, IV.2.2-1...7, Sept. 14th-17th, 1998.
- Benkert, S., Heidt, F.D., and Scholer, D. (1997). Calculation Tool for Earth Heat Exchangers Gaea. *Proceeding of Building Simulation*, Fifth International IBPSA Conference, Prague, Vol. 2, PP 9-16, Sep. 8-10.
- De Paepe, M., and Janssens, A. (2003). Thermo-Hydraulic Design of Earth-Air Heat Exchangers. *Energy and Buildings*, 35(4), 389-397.
- Fink, C., Blümel, E., Kouba, R., and Heimrath, R. (2002). Passive Cooling Concepts for Office and Administrative Buildings Using Earth-to-Air and Earth-to-Fluid Heat Exchangers.
- Heidt, F.D., and Benkert, S. (2000). Designing Earth Exchangers-Validation of the Software GAEA. *Proceedings World Renewable Energy Congress VI*, Brighton, UK, pp. 1818-1821, 01.-07.07.2000.
- Heiselberg, P. (2004). Building Integrated Ventilation Systems - Modeling and Design Challenges. *CIB 2004 World Building Congress*, Toronto, Canada.
- Heiselberg, P. (Editor). (2002). Principle of Hybrid Ventilation. Aarhus University Center, Denmark.
- Reise, C. (2001). Planning Tool for Earth-to-Air Heat Exchangers.
- Santamouris, M., and Asimakopoulos, D.N. (1996). *Passive Cooling of Buildings*, James & James, London.
- Jeong, Y. and Haghighat, F. (2003) "Modeling of a Hybrid-Ventilated Building – Using ESP-r", *Ventilation*, Vol. 1, pp. 127-140.
- Schild, P.G. (2001). An Overview of Norwegian Buildings with Hybrid Ventilation. *HybVent Forum '01* Delft University of Technology, the Netherlands.
- Schild, P.G. (2002). Jaer School. IEA ECBCS Annex-35 (HybVent) Technical Report, Nesodden Municipality, Norway.
- Zhang, J. (2009). Simulation of Large Cross-Sectional Area Earth-to-Air Heat Exchangers, PhD Thesis, Concordia University, Montreal.
- Zimmermann, M., and Remund, S. (2001). IEA-ECBCS Annex 28 Subtask 2 Report 2, Chapter F Ground Coupled Air Systems. Low Energy Cooling - Technology Selection and Early Design Guidance, N. Barnard and D. Jaunzens, Eds., Construction Research Communications Ltd, pp 95-109.
- Hollmuller, P., and Lachal, B. (1998). TRNSYS Compatible Moist Air Hypocaust Model - Final Report. 19507, Centre universitaire d'étude des problèmes de l'énergie, University de Geneve.
- Liddament, M.W. (Ed.) (2000). Low Energy Cooling, IEA-ECBCS Annex 28 Technical Synthesis Report.
- Zimmermann, M. (1995). Ground Cooling with Air, IEA-ECBCS Annex 28 Low Energy Cooling, Subtask 1 Report, Review of Low Energy Cooling Technologies.
- Hollmuller, P. (2002). Utilisation Des changeurs Air/Sol Pour Le Chauffage Et Le Rafraîchissement Des Bâtiments Mesures in Situ, Modélisation Analytique, Simulation Numérique Et Analyse Systémique, PhD Thesis, Université de Genève, Genève.

Tjelflaat, P.O. (2000a). Pilot Study Report - Media School. IEA ECBCS Annex-35 (HybVent) Technical Report.

Tjelflaat, P.O. (2000b). The Grong School in Norway the Hybrid Ventilation System. IEA ECBCS Annex-35 (HybVent) Technical Report.

Wachenfeldt, B.J. (2003). Natural Ventilation in Buildings Detailed Prediction of Energy Performance, PhD Thesis, Norwegian University of Science and Technology.



# 7. PHASE CHANGE MATERIALS (PCM)

## 7.1 Description of principles & technologies

PCMs are “latent” heat storage materials. They use chemical bonds to store and release the heat. The thermal energy transfer occurs when a material changes from solid to liquid, or liquid to solid. This is called a change in state or phase.

PCMs, having melting temperature between 20 °C and 50 °C, were used/recommended for thermal storage in conjunction with both passive and active solar storage for heating and cooling in buildings. A large number of PCMs are known to melt with a heat of fusion in this required range. The PCMs do not exploit just the sensible heat but also the thermal storing capacity due to latent heat.

Introduction of phase change materials into building components can considerably increase their thermal mass, without substantially increasing the weight.

Thank to their latent fusion heat, and in smaller part their specific heat, these materials act as energy “accumulators”; absorbing and discharging heat, keeping their temperature unaltered and thus avoiding overheating of the elements they are contained in.

The fusion latent heat is the energy employed to break the chemical bond, a process that begins when the temperature of that material rises above the melting point. The temperature of fusion is characteristic of every substance.

The consequence of this process is that the thermal capacity of the PCM is non constant but is concentrated in a temperature range close to the melting point of fusion (see e.g. Figure 7.1).

The advantage of using of a PCM material, compared to the traditional construction materials, is in their higher energy storage capacity, with the same weight and volume. Furthermore, the variable heat capacity allows the building elements containing PCM to have a dynamic behaviour, sensible to the climatic conditions.

The temperature of PCM during the phase change remains almost constant, close to the melting temperature, avoiding the excessive oscillation of the structures or building elements.

When the temperature is higher than the melting point, the phase change material is liquid and when the temperature is lowered below the melting point it returns to solid phase.

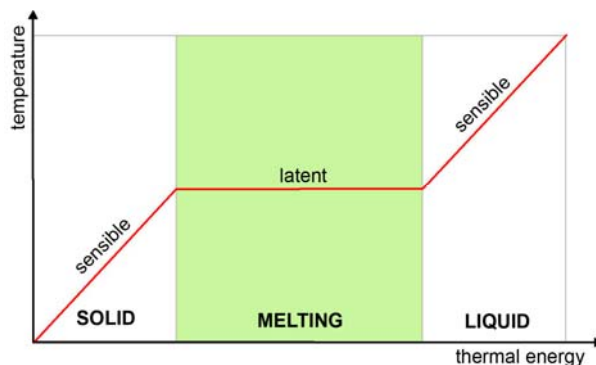


*Figure 7.1 – Specific thermal energy (stored) vs. temperature.*

A large number of organic and inorganic substances are known to melt with a high heat of fusion in any required temperature range. However, for their use in building elements, these phase change materials must also exhibit other desirable thermodynamic, kinetic and chemical properties. Moreover, economic considerations of cost and large scale availability of the materials must be considered.

The phase change materials can be grouped into the families of organic and inorganic compounds and their eutectic mixtures, as shown in Figure 7.2.

The families of inorganic materials are characterised by a high latent heat of fusion per unit volume. Sub-families of organic compounds include paraffin and non-paraffin organics. The organic substances are suitable for being used in buildings due to several desirable properties in comparison with inorganic compounds. Some of these advantages include their ability to melt congruently, their self-nucleating properties and their compatibility with conventional materials of construction. One disadvantage that has to be carefully considered, instead, is represented by their relatively easy flammability.

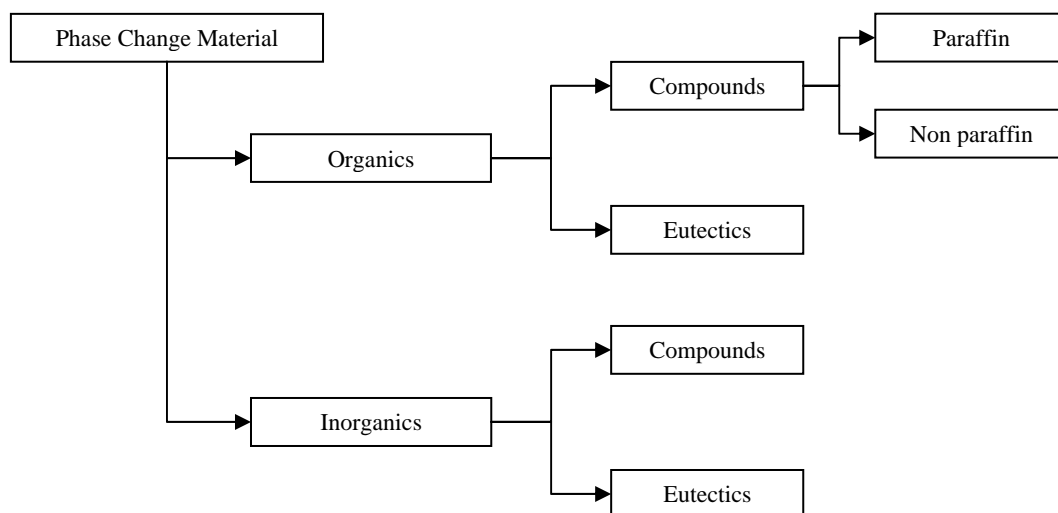


**Figure 7.2 – Different typologies of Phase Change Materials (PCM).**

### Paraffins

The paraffins are substances having a waxy consistency below their melting point. Chemically speaking, paraffin waxes are composed of straight-chain hydrocarbons with only a small part of branching. Paraffins contain one major component called alkanes, characterized by  $C_nH_{2n+2}$  group; the n-alkane content in paraffin waxes usually exceeds 75% and may reach 100%. Depending on the chain length of the alkanes in paraffins, the material may be even-chained (n-paraffin) or odd-chained (iso-paraffin).

The melting point of alkanes increase with the increasing number of carbon atoms; alkanes containing 14-40 carbon atoms have a melting point between 6 and 80°C.

**Table 7.1 – Example of paraffinic PCMs – features.**

Compound	Melting point [°C]	Latent heat of fusion [kJ/kg]
Butyl stearate	19	140
Paraffin C16–C18	20-22	152
Capric–Lauric acid	21	143
Dimethyl sabacate	21	120
Polyglycol E 600	22	127.2
Paraffin C13–C24	22-24	189
(34% Mistic acid+66% Capric acid)	24	147.7
1-Dodecanol	26	200
Paraffin C18 (45–55%)	28	244
Vinyl stearate	27-29	122
Capric acid	32	152.7

Paraffins qualify as heat of fusion storage materials due to their availability in a large temperature range and their reasonably high heat of fusion. Furthermore, they are known to freeze without supercooling.

The phenomena called supercooling is due to poor nucleating proprieties and is an excessive cooling in the liquid phase prior to freezing.

#### *Non paraffins*

A kind of non-paraffin organic PCMs are the fatty acids. The fatty acids are organic compound characterized by the following group:  $\text{CH}_3(\text{CH}_2)_{2n}\text{COOH}$ , with heat of fusion values comparable to those of paraffin. Fatty acids, as paraffins, are known to possess a reproducible melting and freezing behaviour and freeze with little or no supercooling.

Fatty acids are of natural origin, animal or vegetal. The disadvantage of fatty acids is the price, more expensive compared with the other PCMs.

**Table 7.2 – Example of non paraffinic PCMs – features.**

Compound	Melting point [°C]	Latent heat of fusion [kJ/kg]
KF · 4H <sub>2</sub> O	18.5	231
Mn(NO <sub>3</sub> ) <sub>2</sub> · 6H <sub>2</sub> O	25.8	125.9
CaCl <sub>2</sub> · 6H <sub>2</sub> O	29	190.8
LiNO <sub>3</sub> · 3H <sub>2</sub> O	30	296
Na <sub>2</sub> SO <sub>4</sub> · 10H <sub>2</sub> O	32	251

#### *Salt hydrates*

Salt hydrates are characterized by the group  $\text{M} \cdot n\text{H}_2\text{O}$ , where M is an inorganic compound (see e.g. table 7.2). They form an important class of heat storage substances due to their high volumetric latent storage density, large availability and low cost.

The major problem, in using salt hydrates as PCM is that most of them melt incongruently, i.e. they melt to a saturated aqueous phase and a solid phase which is generally a lower hydrate of the same salt. Due to density differences, the solid phase settles out and collects at the bottom of the container, a phenomenon called decomposition. Unless special measures are taken, this phenomenon is irreversible, i.e. during freezing, the solid phase does not combine with saturated solution to form the original salt hydrate. Another important problem with salt hydrates is their poor nucleating capacity resulting in supercooling of the liquid salt hydrates before freezing. Suitable measures must be adopted to eliminate or reduce to a minimum supercooling.

#### *Eutectics*

Eutectics of organic and inorganic compounds are mixtures of several compounds, organic and organic, organic and inorganic, or inorganic and inorganic. The melting point of a mixture of two or more compounds depends on the relative proportions of them.

The advantage of the eutectic compounds are in the congruently liquid phase, with a reduction of decomposition. Also these substances do not suffer from supercooling phenomenon.

**Table 7.3 – Example of eutectic PCMs – features.**

Compound	Melting point [°C]	Latent heat of fusion [kJ/kg]
66.6% CaCl <sub>2</sub> · 6H <sub>2</sub> O+33.3% Mgcl <sub>2</sub> · 6H <sub>2</sub> O	25	127
48% CaCl <sub>2</sub> +4.3% NaCl+0.4% KCl+47.3% H <sub>2</sub> O	26.8	188
47% Ca(NO <sub>3</sub> ) <sub>2</sub> · 4H <sub>2</sub> O+53% Mg(NO <sub>3</sub> ) <sub>2</sub> · 6H <sub>2</sub> O	30	136
60% Na(CH <sub>3</sub> COO) · 3H <sub>2</sub> O+40% CO(NH <sub>2</sub> ) <sub>2</sub>	30	200.5

The PCMs most frequently used are salt hydrates and paraffins. Between the several kinds of salt hydrate, the most common for the use as heat accumulation is the Glauber salt ( $\text{Na}_2\text{SO}_4 \cdot 10\text{H}_2\text{O}$ ) which shows a very high latent heat of fusion, large availability, and cheapness.

**Table 7.4 – Different types of PCM – advantages/disadvantages.**

PCM Type	ADVANTAGE	DISADVANTAGE
ORGANIC	Easy to use Not corrosive Low or no supercooling Chemical and thermal stability	Expensive Lower phase change enthalpy Low thermal conductivity Large range of fusion Inflammable
INORGANIC	Cheap Greater phase change enthalpy High density Narrow range of fusion Non Inflammable	Difficult to produce Need additives Supercooling With nucleation problem Could be corrosive Phase separation

The PCM to be used in the design of thermal storage systems in buildings should possess desirable thermophysical, kinetic and chemical properties, which are recommended as follows:

*Thermophysical properties*

- Melting temperature in the desired operating temperature range.
- High latent heat of fusion per unit volume, so that the required volume of the storage container, able to release a given amount of energy, would be as small as possible.
- High specific heat to provide additional significant sensible heat storage.
- High thermal conductivity of both solid and liquid phases to assist the charging and discharging phases of the storage system.
- Small volume change on phase transformation and small vapour pressure at operating temperature to reduce the containment problem.
- Congruent melting of the phase change material for a constant storage capacity of the material after each freezing/melting cycle.

*Kinetic properties*

- High nucleation rate to avoid super cooling of the liquid phase.
- High rate of crystal growth, so that the system can meet the demand of heat recovery from the storage system.

*Chemical properties*

- Complete reversible freezing/melting cycle.
- No degradation after a large number of freezing/melting cycles.
- No corrosiveness to the construction materials.
- Non-toxic, non-flammable and non-explosive material for safety.

The application of PCMs in buildings can have different goals. First scope is using natural heat and cold sources, that is solar energy for heating or night cold air for cooling. Secondly, increasing the

thermal mass of the building, with a, general, consequent improvement of the internal comfort conditions and a reduction of the energy consumption for cooling and heating the building.

In fact, a significant disadvantage of light weight buildings is represented by their low thermal mass that results in high temperature fluctuations and, hence, in a high heating and cooling demand.

The application of PCM in such buildings is very promising, because of their capability to smooth temperature variations.

Basically three different type of technologies, apt to exploit PCMs in buildings for heating and cooling, exist:

- PCMs in building walls;
- PCMs in other building components (for example subfloor or ceiling systems)
- PCMs in separate heat or cold storage systems.

The first two are (or can be) completely passive systems, where the stored energy (“heat” or “cold”) is automatically released when indoor or outdoor temperatures rise or fall beyond the temperature of melting. The third one is an active system, where the stored energy (“heat” or “cold”) is kept thermally separated from the building structure and the environment by means of a suitably insulated device (storage tank, heat exchanger, ...). In this case the energy is used only on demand and not automatically.

## 7.2 Classification

A classification of PCM based on the three different type of technologies described in the previous section can be done.

### 7.2.1 Wall application

The first application of PCM in the building sector is inside the envelope stratification, in particular in walls.

There are several ways to apply the PCM in the façade. They differ for technologies and thermal behaviour, but all of them have the goal of increasing the thermal inertia of the building envelope.

One of the possible applications is in *opaque envelope components* (walls and/or roofs), the other is in the so-called *solar walls*.

#### 7.2.1.1 Opaque envelope component

A PCM wall is capable of “capturing” a large proportion of the solar radiation incident on the wall or roof of a building. Because of the high thermal mass of PCM walls, they are capable of minimizing the effect of large fluctuations in the indoor temperature. They can be very effective in shifting the cooling load to the off-peak electricity period.

There can be two different configurations depending on the position of the PCM layer within the wall stratification (that is, with the PCM layer located toward the inside facing side of the envelope component or with the PCM layer located toward the outside).

The first kind of PCM wall application is with an internal latent storage layer, directly (or almost directly) in contact with the indoor environment. The goal of this application is to increase the thermal capacity of the environment where the PCMs are applied. The effect is a significant reduction of the surface radiant and air temperature of the internal spaces of the building. The PCM layer stores and releases the internal and solar gain, keeping the temperature constant around the melting point. When the indoor temperature decreases, the PCM will release the thermal energy to keep the comfort conditions within the internal environment.

The second possible configuration presents the PCM layer in the external side of the wall. This solution is suitable to reduce the cooling energy consumption and maintain thermal comfort condition inside the building in warm countries during the summer period.

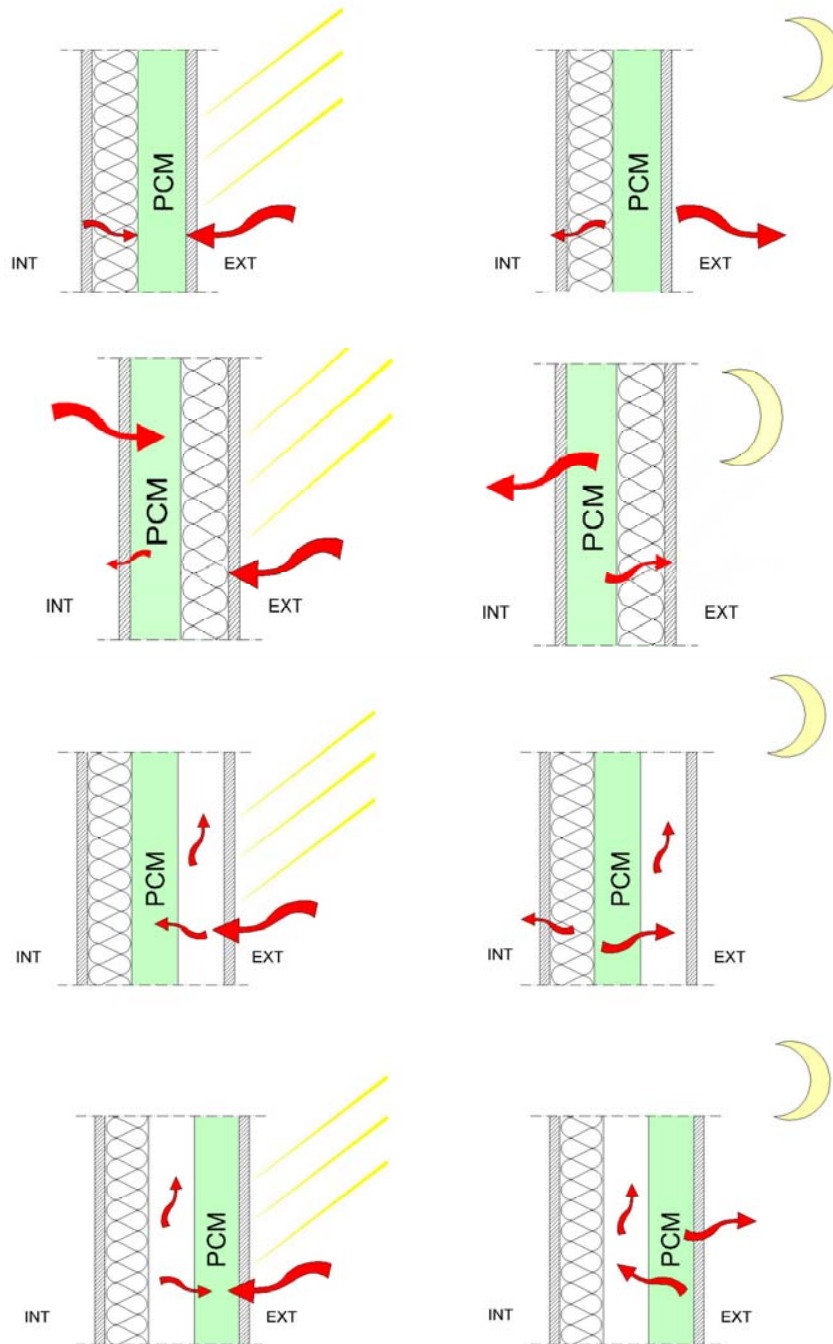


**Figure 7.3 – Scheme of the possible working principles of walls making use of PCM.**

The PCM layer has the function of collecting and storing the thermal energy that comes from the outdoor environment, in particular due to the direct solar radiation incident on the external surface. During the day, the PCM stores the energy, changing its phase from solid to liquid. During the night, when the temperature decrease under the melting temperature, it will freeze and release the energy stored.

Through a functional study of the stratification it is possible to send the greater part of the energy either inside or outside the building, depending on the different positions of the insulation layers and of the ventilation strategies, as schematically shown in Figure 7.3.

Figure 7.4 shows, as an example, the specific heat fluxes through a south facing façade versus time for different component configurations over a daily period. The adoption of PCM based envelopes (blue and pink curves) allows to significantly smooth the heat gains and to shift the peak values in

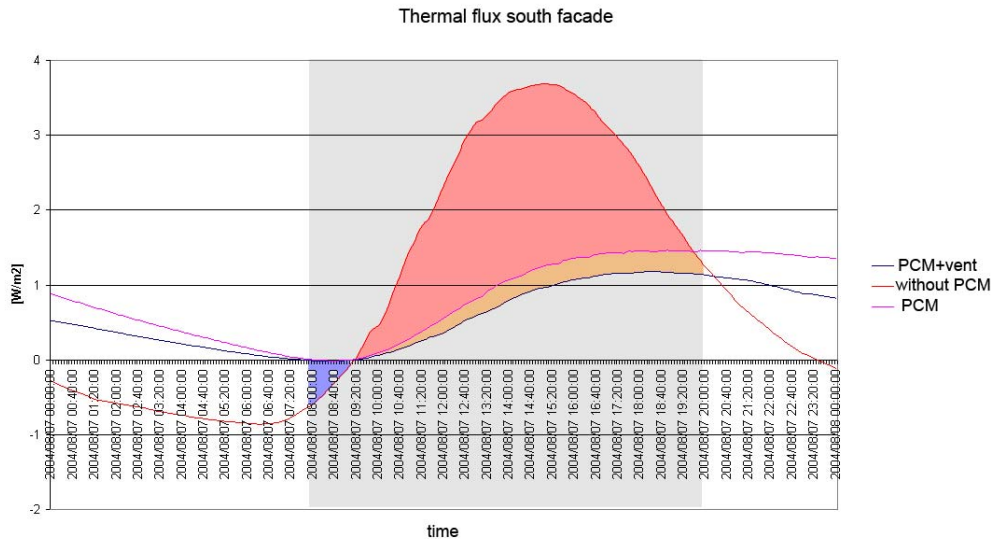


**Figure 7.4 – Example of PCM application in walls – Specific heat flux through different type of façades (with - pink curve - and without - red curve - PCM; with - blue curve - and without - pink curve - ventilated cavity).**

the late afternoon/early evening. The coupling of PCM with the façade ventilation (blue curve) further improves the effectiveness of the element.

The red area in Figure 7.4 represents the energy that is not transmitted to the indoor environment thanks to the presence of the PCM layer.

There are several companies (BASF, Dupont, Rubitherm) that produce and sell building elements or materials suitable for the construction of PCM based walls. Among the other, some commercially available components are: plaster board, wood board, plaster containing PCM.

For the wall application, usually, encapsulated paraffin mixed with plaster are used (see e.g. Figure 7.5).



**Figure 7.5 – Example of PCM application in walls.**

### 7.2.1.2 Solar wall

The solar wall is another application where PCMs can be successfully used for thermal energy storage.

A solar wall is, traditionally, made of: a transparent – glazed – layer (facing the outdoor environment) an air gap and an opaque wall (facing the indoor environment).

The opaque layer works by absorbing part of the solar radiation incident on its outer face and then transferring this energy through the wall by conduction. The outside surface of the opaque component is usually painted with a dark colour to increase the absorption coefficient. After the heat is transmitted by conduction through the opaque layer, it is distributed to the indoor space by radiation and, to some extent, by convection from the inner face.

In the traditional passive solar walls the opaque layer is characterized by a high thermal inertia. This last is achieved by adopting materials like concrete, masonry, stone. In order to allow the right thermal behaviour of a traditional solar wall, the “heavy” opaque layer should have, at least, a frontal mass of 350 - 400 kg/m<sup>2</sup> and a thickness of about 0,30-0,35 m. Such heavy construction technology, however, increases the cost for the building structure and it is not a coherent solution when the overall building fabric is made of light weight components.

From a conceptual point of view, the problem of these traditional passive solar walls is that they exploit just the sensible heat of construction materials.

This weighty and thick opaque layer could be profitably replaced with a layer made of PCM. In such a way, by exploiting also the latent heat of fusion, it becomes possible to save weight and space, without reducing the overall energy storage capacity.

In this case, the solar radiation that reaches the wall is absorbed by the PCM ‘buried’ in the opaque layer, located 10 cm or more directly behind the glass.

This PCM based thermal mass, works for a number of hours like an heat accumulator and for part of the day like an energy source. This behaviour allows a smoothing and delay of the instantaneous heat gains and a release of the energy several hours after its accumulation. In such way, during the night time when the heat loads are higher, the energy stored in the solar wall during the day can be exploited to keep the indoor environment comfortable.



***Figure 7.6 – Example of an experimental passive solar wall making use of PCM (Experimental test facility at Università Politecnica delle Marche - Italy).***

In order to optimize the solar wall performance, the PCM should be placed in the external part of the opaque wall, behind the air layer to allow an effective storage of the solar radiation. Moreover, this PCM layer should be located outside an insulating layer, giving this wall a suitable thermal resistance, required for controlling the heat loss.

There are companies (e.g. GLASSX) that already produce modular elements to build this wall configuration. The central element of the GLASSX façade is a heat storage module that receives and stores part of the incident solar radiation. When the temperature falls below the temperature of fusion, the façade releases part of the stored energy toward the indoor environment, mainly, as radiant heat.

PCM (Phase Change Material) used in the GLASSX module are in the form of a salt hydrate. They are hermetically sealed in polycarbonate containers, painted gray to improve the absorption

coefficient. On the interior side, the element is sealed by 6 mm tempered safety glass. On the exterior side there are a series of several glass panes, and a prismatic polycarbonate layer that reflects the solar radiation during the warm seasons (for high incidence angles), as schematically shown in Figure 7.7.

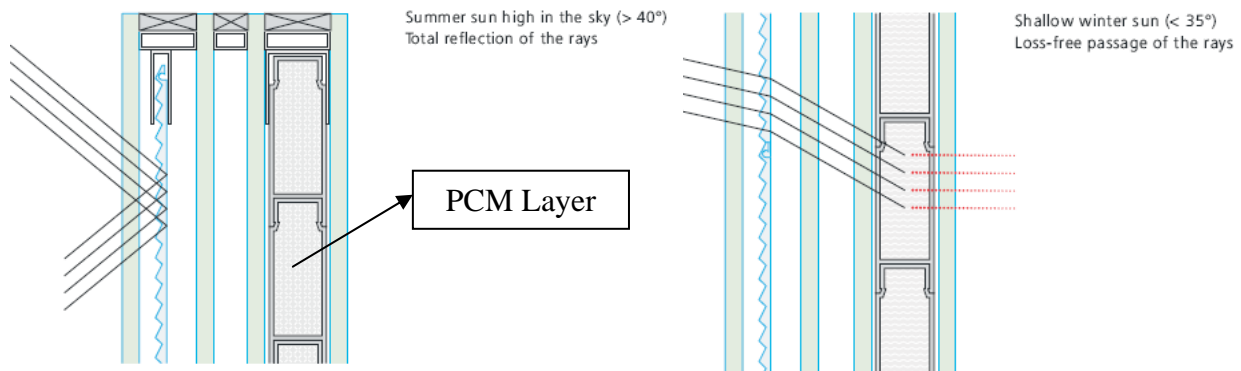


**Figure 7.7 – Working principles of a passive solar wall (GLASSX type) making use of PCM.**

### **7.2.2 Underfloor application**

Another application of PCM in the building sector can be inside the floor stratification. The use of PCM in floor layers or in subfloor heating and cooling systems, can avoid or reduce the problem of overheating of floor areas directly exposed to the solar radiation. The PCM, in fact, can stabilize the surface temperature in a range close to the melting temperature. When the floor is directly irradiated by the sun and/or when the internal free gains are higher than the heating loads, the PCM in the floor structure can absorb and store this excess of energy that, otherwise would cause an overheating. The energy that is stored during the day can be easily removed, if necessary, with an hydronic system, or used afterwards for heating the building in the night. Furthermore, in winter, this PCM based floor can avoid or reduce the temperature oscillations due to the duty cycle of the heating system.

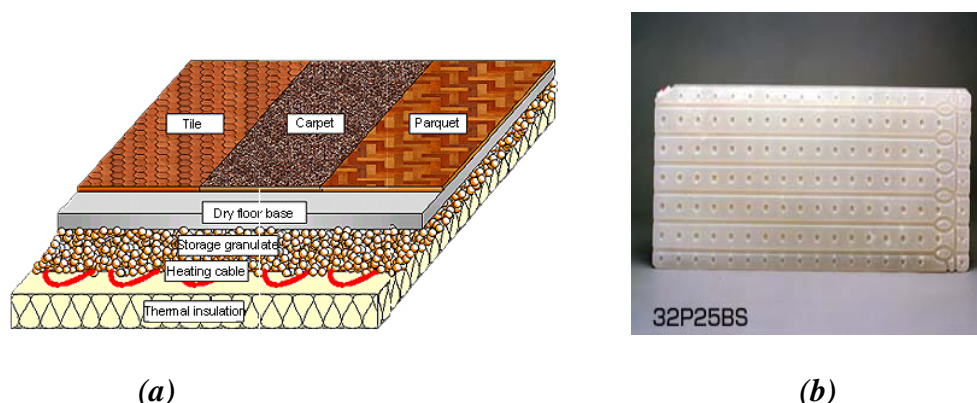


**Figure 7.8 – (a) A typical configuration of a floor heating system coupled with of PCM. (b) Example of a PCM container for floor.**

There are several technologies commercially available to implement this solution in real buildings; Figure 7.8a shows an example of a PCM floor coupled with a floor heating system. Figure 7.8b shows, as an example, a PCM container suitable to be integrated in a floor layer. Finally, PCM can be applied in combination with electric floor-heating systems. In this case the floor-heating system stores heat at night, when electricity rates are low, and discharges it during the

day (Figure 7.9). This system can reduce energy costs of about 30% compared with systems that use electricity at regular rates. Electricity costs can be further reduced of 15% through the use of a system equipped with a microcomputer that controls the surface temperature oscillations.

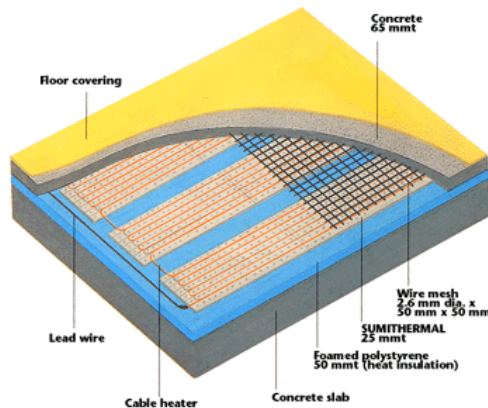


Figure 7.9 – Example of an electric floor heating system coupled with PCM.

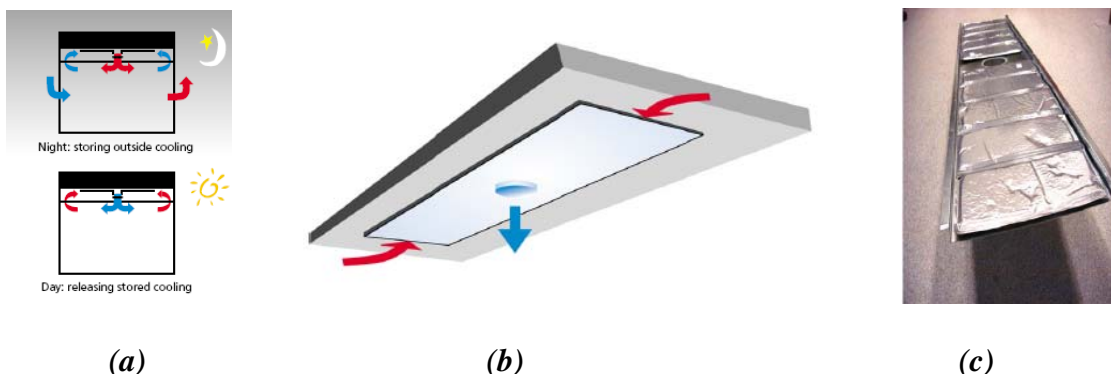
### 7.2.3 Ceiling air exchanger

This application exploits the thermal mass of the ceiling slab and the “artificial” thermal mass of the PCM. The working principle is similar to that of the floor application, even though the typical configuration is quite different.

In fact, in this case the PCM is usually not directly embedded into the ceiling layers, but is located in a suitable false ceiling system. The PCM is installed in the void between the ceiling and the false ceiling (in theory, it could also be a floor and an elevated floor). Air is then circulated in the cavity by means of independent fans, or using the air conditioning system. A turbulent flow is created between the ceiling slab and the PCM cassettes (or bags), thus increasing the heat exchange rate. The working principle of this technology is schematically shown in figure 7.10a and 7.10b.

Figure 7.10c shows a typical, commercially available, solution of a false ceiling element filled with PCM bags.

Such kind of configuration is typically adopted for controlling the indoor air temperature during the summer season (though, in theory, it could also be used during the heating season). The aim is to store cold at night and release it during the day, by means of a mechanical ventilation system. This allows to directly remove part of the internal heat load from the indoor environment and to smooth out temperature peaks.



(a) and (b) Scheme of the working principle (summer period) of a PCM based ceiling.  
 (c) Example false ceiling element making use of PCM (sealed in bags).

## 7.2.4 Thermal Storage unit and air exchanger applications

Thanks to their high latent heat and the possibility of (almost) freely choose the temperature at which the energy can be stored (i.e. phase transition temperature), PCM can, under some circumstances, profitably substitute water as storage medium.

The use of water, in fact, implies the adoption of big storage devices in order to be able to achieve sufficiently large heat storage capacity. By using phase change material (PCM), instead, compact storage units, with high heat storage capacity, will be feasible for many applications in the heating and ventilation systems.

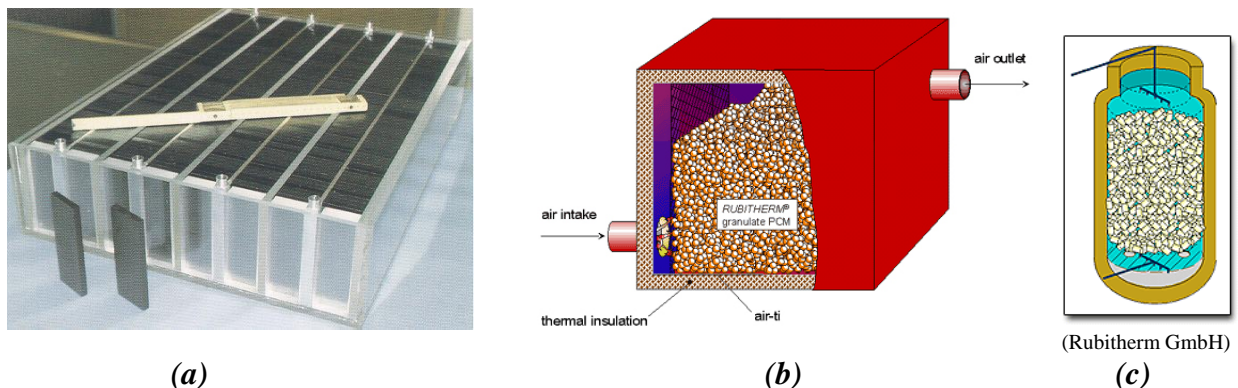


**Figure 7.11 – Picture (a) and schemes (b and c) of typical storage devices based on PCM.**

These technologies, in particular, appear to be promising when applied in combination with air heating/cooling systems, specially for small power appliances.

Small power air systems are becoming increasingly popular for private homes, especially where, as a result of improved insulation, the majority of heat is required to compensate for ventilation heat losses rather than heat losses through walls and windows. Low energy consumption homes are typical examples where air heating systems may be utilised in combination with a PCM based thermal storage.

Furthermore, the combined use of solar energy, other renewable energy sources or heat pumps using low tariff night electricity, together with a latent heat storage unit for air heating systems, provides an economic and energy efficient heating method.

The form/structure of the latent heat storage material, for example granulates or plates, allows the material to be placed in any conceivable container and ensures a large heat transfer surface area, with low pressure losses along the air flow path. The heat storage capacity, at equal volume, is 3 to 5 times higher than that of alternative thermal storage materials such as stone, gravel or sand. Consequently, the latent heat storage unit requires limited space and is relatively lightweight, thus reducing building costs and problems of integration.

Finally, latent heat storage units may be integrated into home hot water systems, thus providing interior heating and hot water supply. Such system, though at experimental level so far, can allow for a considerable reduction of energy consumption and cost, as well as a reduction of air pollutants emissions.

## 7.3 Design/analysis method and tools

Nowadays, there are different numerical methods to analyse the thermal behaviour of building, room, and single element making use of PCM.

Basically, the thermal performance of phase change materials can be assessed in two different ways. The first one is based on the use of a FEM analysis (Finite Element Method - like COMSOL and other FEM softwares) and allows a detailed thermal simulation of the component. The second approach makes use of network models (like Energy Plus, TRNSYS) and is more suited for the

overall thermal and energy analysis of the system (i.e. of the PCM based element together with the building). Some more details related to these two tools are available in Appendix 7A.

Both methods can account for the variable thermal capacity due to sensible and latent heat of fusion, through an enthalpy function that includes these two components.

In particular, the most common procedure consists of assuming for the simulation an effective heat-capacity of the PCM variable with the temperature. The function linking the effective heat capacity,  $C_{eff}$ , and the material temperature is, usually, assumed to be either a Gaussian function (see figure 7.13) or a non-continuum function with a peak corresponding to the melting temperature (see Figure 7.12).

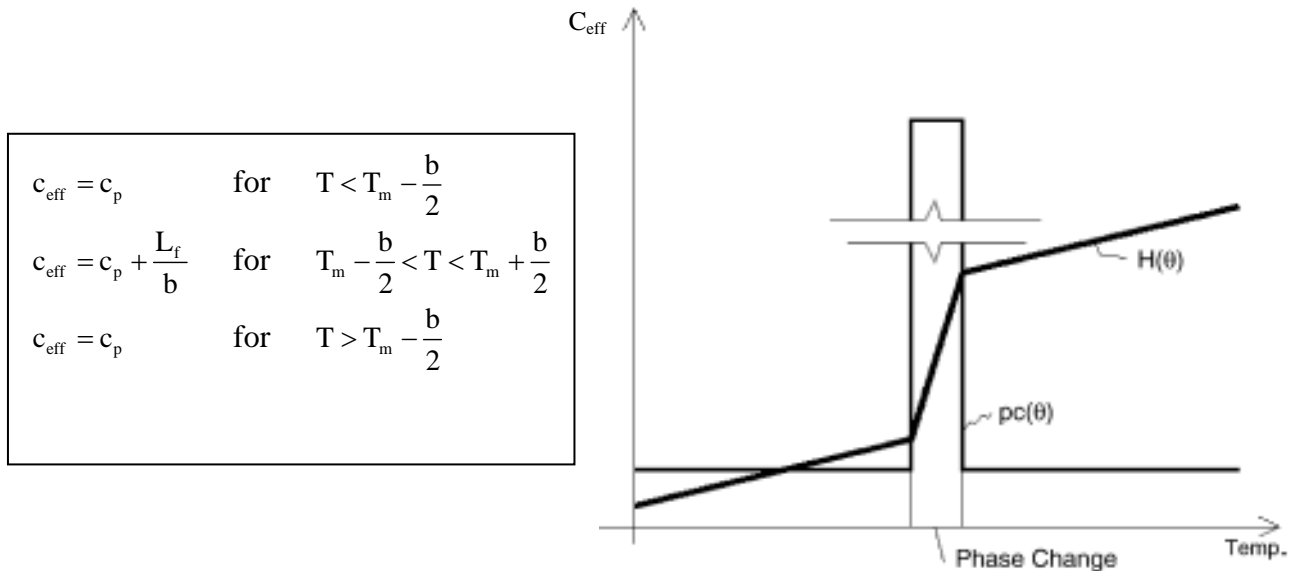


**Figure 7.12 – Effective heat capacity of PCM vs. Temperature (example of non-continuum function).**

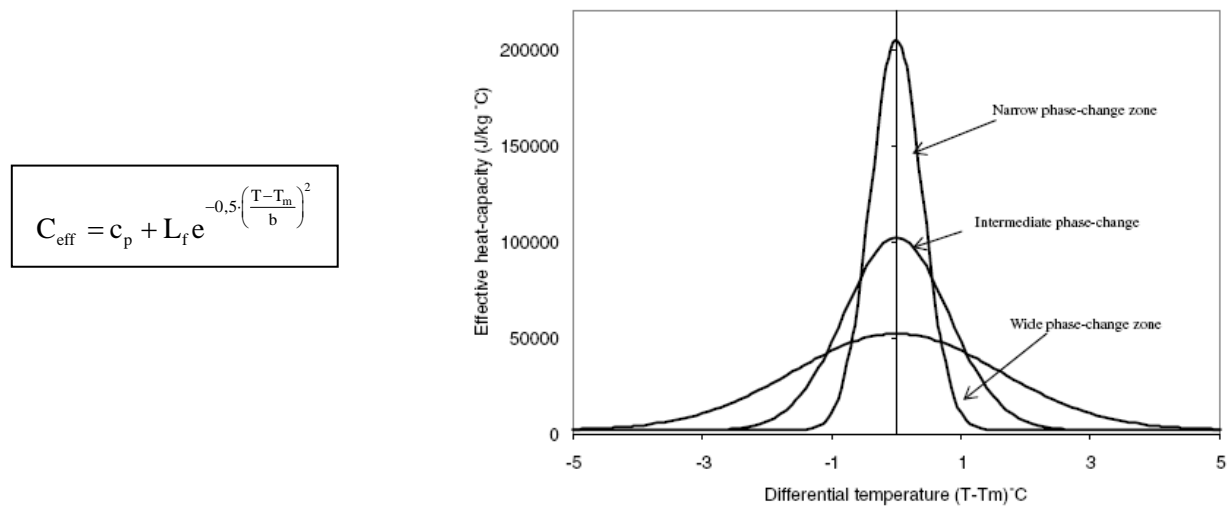


**Figure 7.13 – Effective heat capacity of PCM vs. Temperature (example of Gaussian functions).**

Where:

- $C_{eff}$  effective heat capacity
- $C_p$  sensible heat
- $L_f$  latent heat of fusion
- $T_m$  melting point

b width of temperature range of fusion

### **7.3.1 FEM approach**

As mentioned, the detailed thermal behaviour (temperature and flux distribution) of an element containing PCM can be described through “Finite Element Models” corresponding to that problem. Choosing a model that simplifies the real case, means subdividing its domain in smaller elements, whose individual physical behaviour can be described through simple mathematical relationships. These elements are “bounded” by two nodes: controlling the temperature and the heat flux crossing each node. As a second step, the thermal balance condition is imposed to the whole model (made up of small elements) “considered as a unique one”.

In such way, studying irregular domains is very easy, because they can be subdivided in a finite number of elements characterised by regular forms, chosen by the user, considering the particular type of problem that is studied: one-dimensional, two-dimensional, three-dimensional.

Moreover, the finite element method can simulate the transient behaviour of phase change materials. Through this procedure it is possible to know the rate of PCM that is melted at each time step. The key issue is to introduce the  $C_{\text{eff}}$  function in the constitutive equation of the materials. Through this artifice, the FEM model can reliably simulate the performance of a PCM element in a wall, roof, subfloor or any other element of the building where it is applied.

A wide choice of commercial FEM softwares, suited for implementing the PCM behaviour in the calculations, are available in the market (see e.g. COMSOL, ANSYS).

An alternative method, similar in principle to the FEM approach, is represented by the so-called Finite Volume Method (FVM). In this case, however, there are no ready-to-use development environments and/or softwares and the user needs to develop his own mathematical model and solution algorithm. The advantage is represented by the flexibility of the simulation and by the possibility to adapt the model to the user specific needs. In literature there are some examples of such approach. Typically, the performance and reliability of FEM and FVM models are very good with the disadvantage of requiring quite a long development time and high expertise of the user (see e.g. [Corgnati et Al. (2009)] ).

The advantage of the FEM detailed calculation method is in the extreme reliability and accuracy of the results. Its limit resides in the size of the calculation domain that can be managed. With the FEM approach, at the most, it is possible to simulate a single room for a short time. The whole building analysis for a complete season or year, in fact, would require huge computational time and resources.

For this last task the second analysis approach, based on network models, is more suited.

### **7.3.2 The thermal network approach (zone model)**

Another way to assess the behaviour and the performance of PCM is through the use of zone models, like Energy Plus, TRNSYS or similar building energy simulation softwares.

Energy Plus is a building energy simulation program for modelling building heating, cooling, lighting, ventilating, and other energy flows. It is based on the most popular features and capabilities of BLAST and DOE-2.

For simulation of the behaviour of PCM materials in Energy Plus, it is needed to use the *CondFD* (Conduction Finite Difference) solution algorithm (to be selected under the “SOLUTION ALGORITHM” menu). Usually, and as default, this software works using the *CTF* algorithm (Conduction Transfer Function), but this procedure is not suitable for the simulation of PCM based elements, since it is not possible to implement temperature dependent material properties (i.e the  $C_{\text{eff}}$  function).

A care that needs to be taken when using the *CondFD* algorithm, is to set a value of the calculation time step shorter than that typically adopted for the CTF solution algorithm (i.e. the number of time

steps per hour should be at least equal to or greater than 12 – and up to 60, that is, a time step of 1 minute) (this datum can be set under the “TIME STEPS PER HOUR” menu).

As far as the  $C_{\text{eff}}$  function is concerned, it is not possible to directly specify an analytical function, but data in tabular form have to be implemented. In particular, eight pairs of values ( $T$ ,  $C_{\text{eff}}$ ) can be passed to the software into a two column tabular temperature – heat capacity (or enthalpy) function for the basic material (only the necessary number of pairs needs to be specified under the “MATERIAL PROPERTY TEMPERATURE DEF CondFD” menu).

### **7.3.3 Simplified tools**

In recent time a purposely developed software – “PCM express” – has been made available on the market ([http://www.valentin.de/index\\_en\\_page=pcm\\_express](http://www.valentin.de/index_en_page=pcm_express)).

This software was created in the frame of a research project called "Development of a user-friendly planning and simulation program in the combined project 'Active PCM storage systems for Building PCM Active' ", which has been ran in collaboration between different partners (Valentin EnergieSoftware, the Fraunhofer Institute for Solar Energy Systems ISE in Freiburg, industries).

PCM express is a software devoted to design and simulate buildings using phase change materials (PCM). It aims to support architects and planners in the design phase and in the decision-making process. It should help sizing the system and, thanks to its aid, should help in increasing the application of PCM technologies in buildings.

PCM express is a simplified tool that provides users with a fast and easy method for defining a PCM system. This includes the use of PCMs in walls, structures and changes in the associated mains services. Depending on the situation, the goal of the design procedure can be either set to the increased level of comfort (private houses with wellness requirements) or to economic considerations (office buildings). Both strategies are supported by the program, through the use of menus, predefined usage profiles and adapted presentation of the results.

A free downloadable – introductory - version is available at:

<http://www.valentin.de/pcm/forms/form.pcm.php?lang=en>

As for the majority of simplified tools, its reliability and the information details it provides are suitable for a first draft design phase. A more detailed analysis, by means of more sophisticated methods, is advisable in a further development stage of the design.

## **7.4 Guidance and recommendation**

Depending on the climatic contest, internal destination, occupancy, cooling and heating system and typology of building it is possible to choose several technologies and types of PCM.

The main aim related to the adoption of a PCM element is the increase of the thermal mass, and so the thermal inertia, of the construction or the increase of the heat storage capacity.

The PCM’s performance is influenced by many parameters, and an incorrect choice could compromise the performance of the PCM based element.

In particular, the key factor that needs to be correctly addressed is represented by the melting/solidifying cycle (that is the energy charge/discharge of the element). In fact, in order to assure a satisfactory performance of the PCM over the time, it is of paramount importance that a complete solid-liquid-solid cycle happens over the 24 hours, so that at the beginning of a new day the element is again ready to store/release energy.

To develop such analysis the following parameters have to be known:

- climatic context (temperature, radiation, and so on)
- indoor parameters (temperature, internal load, ventilation)
- type of PCM (melting point, latent heat, and so on)
- quantity of PCM
- stratification or composition of building element.

Typically, at the preliminary design stage, the last three parameters can be freely chosen. The design process is, in fact, an iterative procedure, like schematically shown in Figure 7.14. At the beginning a first, guessed, choice of PCM type and quantity is needed. Then the behaviour of this first guessed configuration is analysed by means of an analysis tools. Based on the results of this first loop, modification and optimization of the design solution will be done. Form a practical point of view, in the first phase of the analysis it is preferable to use a detailed method to simulate the PCM element alone (e.g. a FEM model). In the second phase, after some preliminary modifications of the element and the optimization of its performance, the overall performance of the building should be assessed by means of a network model (e.g. Energy Plus). This second stage allows the assessment of the benefit in terms of: internal comfort, energy consumption and economical cost.

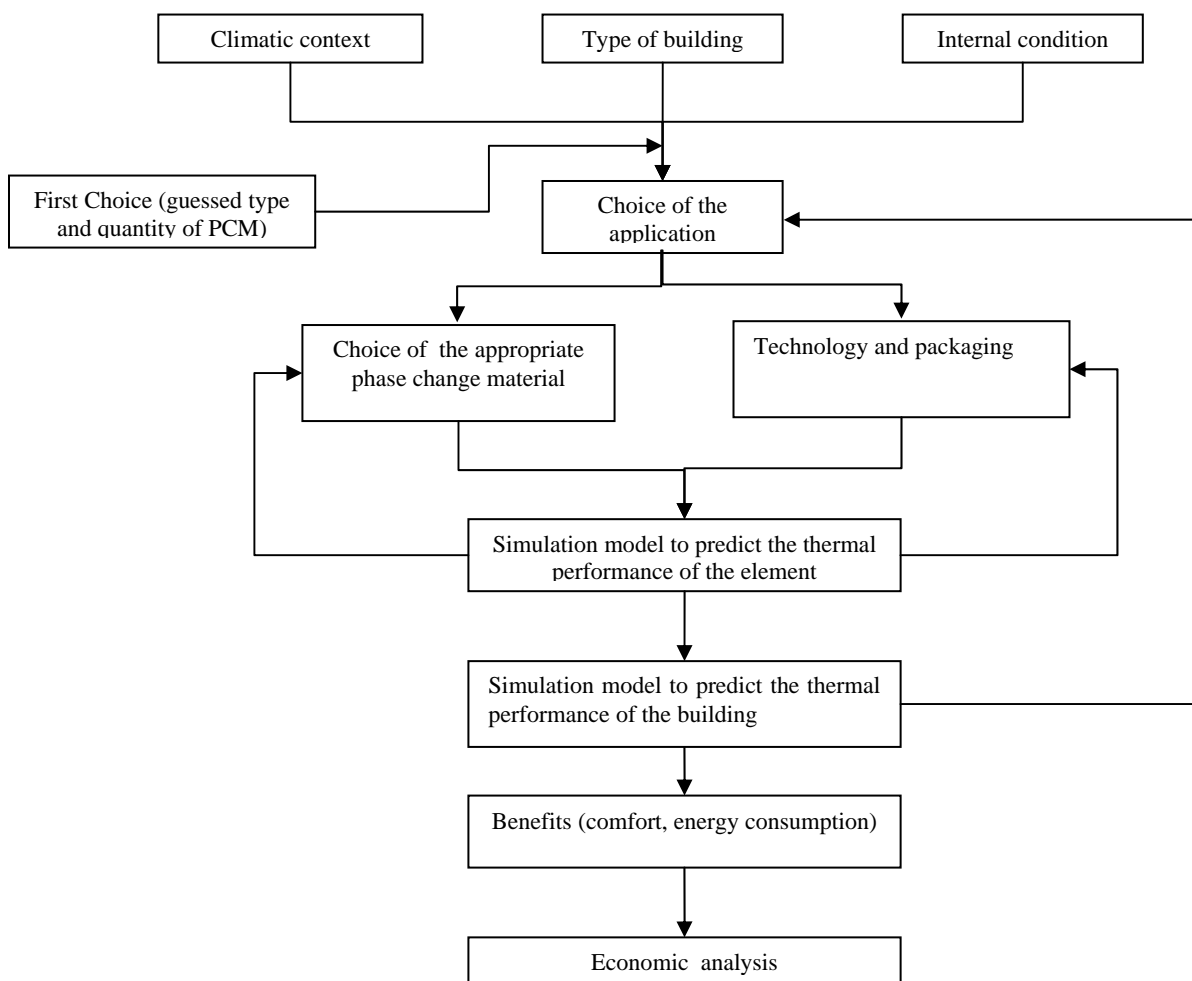


*Figure 7.14 – Conceptual scheme of the design procedure.*

## 7.5 Examples for illustration

### 7.5.1 The “3-Litre” House (DE)

The “3-Liter Haus” in Ludwigshafen (Germany) is a residential building built in the 1950’s (Figure 7.15). Now, after a retrofitting, the energy demand is 30 kWh/m<sup>2</sup>year, corresponding to three litre of oil per square meter per year.

The thermal insulation is made in a new insulation with graphite and the internal plaster is mixed with micro encapsulated (5 µm) phase change material, in particular paraffin with a melting point of 24 °C and a latent heat of 180 J/g (BASF Micronal). The PCM is positioned in the inside layer of

the wall and contribute to improve the thermal inertia of the internal environment, through the increasing of the thermal inertia of walls (Figure 7.16b). The ventilation is mechanical, combined to heat recovery (Figure 7.16a). The blinds are made by insulated window shutters. The heat and electric generator is a fuel cell, type SOFC (Solid-Oxid-Fuel-Cell), with a thermal power of 2,5 kW and 1kW electricity. In the first heating season the measured energy consumption was 24,7 kWh/m<sup>2</sup>a.



Figure 7.15 – Picture of the “3-Litre” house and the fuel cell.

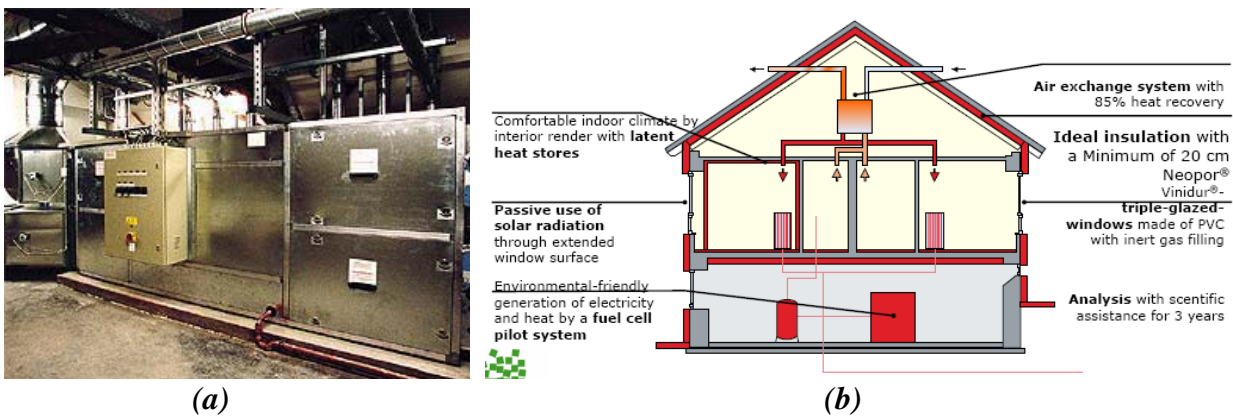


Figure 7.16 – “3-Litre” house – (a) Air handling unit and heat recovery – (b) main features of the energy retrofit.

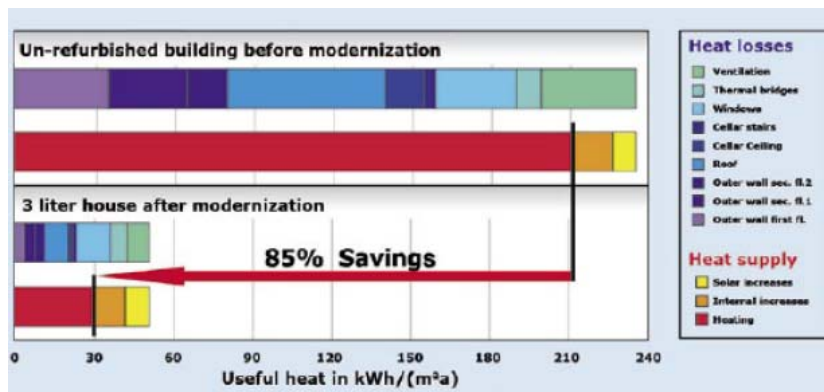


Figure 7.17 – “3-Litre” house –Energy certificate before/after the energy retrofit.

## 7.5.2 The “Domat EMS“ building (CH)

The “Domat EMS“ building is a new construction designed for elderly people (Figure 7.19). In some houses the south façade is a solar wall with a latent heat storage layer (GLASSX type – Figure 7.18). The façade is transparent and allow passing of daylight, with a light diffusing effect. The construction is made with a series of low emissivity layers, that allow an excellent thermal insulation and, at the same time, permit daylight to pass through the façade. To avoid overheating during the summer period, a surface with a plastic transparent prismatic layer is included, this reflects or transmits the solar radiation as a function of the solar incident angle. The phase change material is hydrates salt, contained in plastic modular containers.

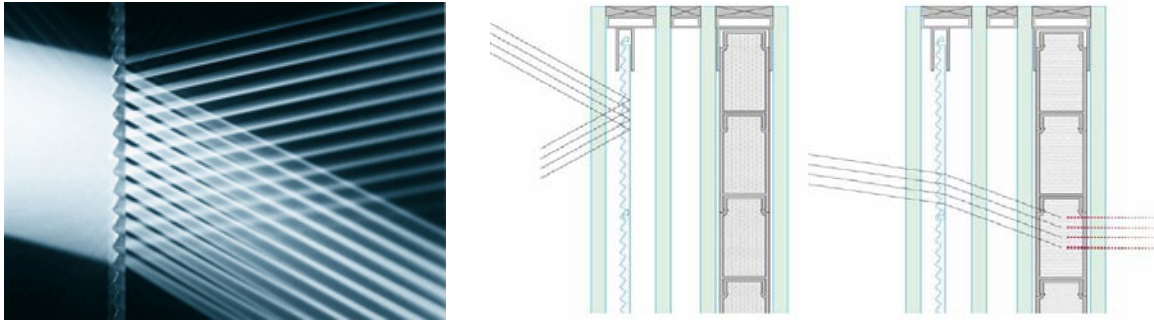


Figure 7.18 – “Domat EMS“ building – Particular of the south facing solar wall (GLASSX type).



Figure 7.19 – “Domat EMS“ building – Overall picture and some construction details.

Table 7.5 – Some features of the “Domat EMS“ building.

Glass 1 (exterior)	Tempered safety glass	Element thickness	79 mm
Gap between panes (GBP 1)	Gap between panes with prism plate and inert gas	Thickness tolerance	-1/+4 mm
Glass 2	Tempered safety glass with Low-E	Min. fold width	~ 84 mm
Gap between panes (GBP 2)	Gap between panes with inert gas	Weight	max. 95 kg/m <sup>2</sup>
Glass 3	Tempered safety glass with Low-E	Max. surface area	4.2 m <sup>2</sup>
Gap between panes (GBP 3)	Gap between panes with PCM plate	Max. height	280 cm
Glass 4 (interior)	Tempered safety glass with ceramic silkscreen printing	Max. width	150 cm
		Heat transmission coefficient (U-value)	up to 0.48 W/m <sup>2</sup> K
		Light transmission for crystalline PCM	0 - 28 %
		Light transmission for liquid PCM	4 - 45 %
		Total energy transfer ratio (g value):	
		Vertical direct irradiation	48 %
		Diffuse irradiation	29 %
		Seasonal (winter months)	34 - 40 %
		Seasonal (summer months)	17 - 22 %
		Storage capacity	1185 Wh/m <sup>2</sup>
		Storage temperature	26 - 30 °C

### 7.5.3 Building of Stevenage Borough Council (UK)

Another example of building making use of PCM elements is the building of Stevenage Borough Council in UK (Figure 7.20).

It is an office building where, to reduce the peak cooling load and exploit night ventilation, a ceiling with PCM (Cooldeck type) combined with a mechanical ventilation system was installed (Figure 7.20 and 7.21).

The type of PCM used is Climator C24, hydrates salt in multilayer envelopes, having a melting point of 24°C.



Figure 7.20 – Picture of the “Stevenage Borough Council “ building – Construction details of the PCM based ceiling (Cooldeck technology).

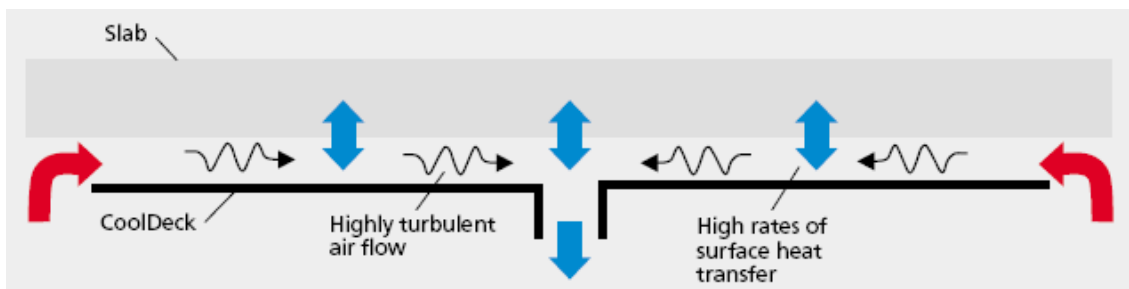
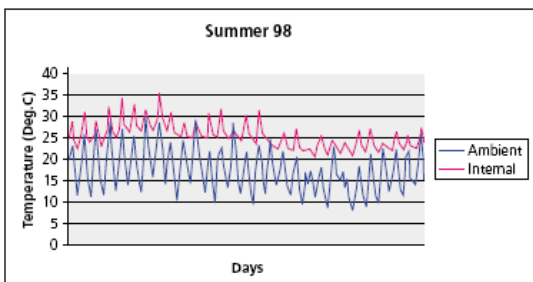


Figure 7.21 – “Stevenage Borough Council “ building - Scheme of the working principle of the PCM based ceiling (Cooldeck technology).

Before CoolDeck installed - excessive over heating



After CoolDeck installed - temperatures significantly reduced

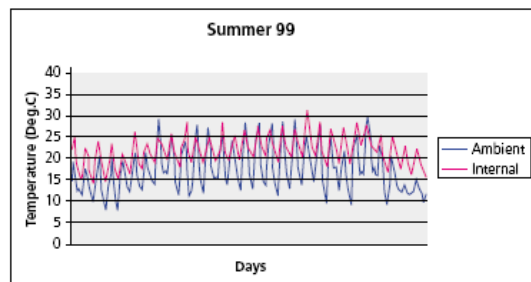


Figure 7.22 – Indoor (pink) and outdoor (blue) air temperature profiles vs. time before and after the introduction of the PCM.

## 7.6 References & selected bibliography

- Abhat A(1983) Low temperature latent heat thermal energy storage: Heat storage materials *Solar Energy*, Volume 30, Issue 4, 1983, Pages 313-332
- A. Abhat et al., Development of a modular heat change with an integrated latent heat store. Report no. BMFT-FT-T-081-050, German ministry for science and technology, Bonn,FRG (1981)
- Ames D.A.(1989) The past, present, and future of eutectics salt storage systems *ASHRAE journal* May 1989 pp 26-28
- Athienntis K.(1997) investigation on thermal performance of passive solar test room with wall latent heat storage. *Building and environment* vol. 32 no.5 pp 405-410,1997.
- AL Jandal S.S., Sayigh A.A.M. (1994) Thermal performance characteristic of STc system with phase change storage. *Renewable Energy*, Volume 5, Issues 1-4, August 1994, Pages 390-399
- Bernard N.(2002) Thermal mass and night ventilation utilizing "hidden thermal mass". *International journal of ventilation* Vol. 1 no 2 October 2002 pages 81-90.
- Berecarrats J.P, Strub F, Falcon B, Bumas J.B (1996) Phase change thermal energy storage using spherical capsules: performance of a test plant. *International journal of refrigeration* Vol. 19, issue 3, pp187-196
- Biswas D.R.,thermal energy storage using sodium sulphate decahydrate and water. *Solar Energy* 19, pp 99-100 (1977)
- P. Brousseau and M. Lacroix (1996) Study of the thermal performance of a multi-layer PCM storage unit. *Energy conversion and management*. Vol 37, issue 5, pages 599-609.
- Brown R.C,Rasberry J.D, Overmann S.P (1998) microencapsulated phase change materials as heat transfer media in gas fluidized beds. *Power Technology* Vol.98, issue 3 pages 217-222
- Buddhi D, Bansal N.K, Sawhaiey R.L, Sodha M.S (1998) Solar thermal storage systems using phase change materials. *International journal of energy research* Vol. 12, issue 3.
- Bugase I.M (1997) Enhancing the thermal response of latent heat storage systems. *International journal of energy research*. Vol 21, Issue 9, pp 759-766.
- Cabeza L.F, Illa J, Badia F, Roca J, Meheling H, Heibler S, Ziegler F (2001) Immersion corrosion tests on metal- salt hydrate pairs used of latent heat storage in the 32 to 36 C temperature range. *Materials and corrosion*. Vol. 52. Pages 140-146
- Cabeza L.F, Meheling H, Hiebler S, Zieder F (2002) Heat transfer enhancement in water when used as PCM in thermal energy storage. *Applied thermal engineering*. Vol. 22, issue 10, pages 1141-1151
- Carlsson B, H.Stymne and G.Wettermark, An incongruent heat of fusion system CaCl<sub>2</sub> made incongruent through the modification of the chemical composition of the system. *Solar Energy* 23, 343-350 (1979)
- Chandra S, Kumar R, Kushik S, Kaul S (1985) Thermal performance of a non-air-conditioned building with PCCM thermal storage wall. *Energy Conversion and Management*, Volume 25, Issue 1, 1985, Pages 15-20.
- Chahroudi D(1975). suspension media for heat storage materials. Proc. *workshop on Solar Energy Subsystem for the heating and cooling of buildings*. Charlottensville.Virginia USA, 56-59.
- Carlsson B.O, Hans S(1978) Gunnar Wattermark D12:1978, Storage of low temperature heat in salt hydrate melts calcium chloride hex hydrate. Swedish council for building research.

Collier R.K, Grimmer D.P (1979) The experimental evaluation of phase material building walls using small passive test boxes. *3rd passive solar conference*.

COMSOL Multiphysics Modeling and Simulation (<http://www.comsol.com/>)

Corgnati S.P., Kindinis A., Perino M., Thermal Mass Activation By Means Of Night Cooling: Comparison On Different Techniques And Strategies, *5th International Workshop on Energy and Environment of Residential Buildings and the 3rd International Conference on Built Environment and Public Health* (EERB-BEPH 2009),

Das S, Dutta T.K (1993) Mathematical modeling and experimental studies on solar energy storage in phase change material. *Solar energy*. Vol. 51, issue 5 305-312.

Eames I.W, Adref K.T (2002) Freezing and melting of water in spherical enclosures of the type use in thermal (ice) storage system. *Applie. Thermal engineering*, Volume 22, pages 733-755.

Edie D.D. et al.(1979) Latent heat storage using direct contact heat transfer. In Sun II (Edited by K.W. Boer and B.H. Glenn) pp 640-644 Pergamont Press, New York

Erk Henry F, Dudokovic M(1996) Phase change heat regeneration: modeling and experimental studies. *Aiche journal*, Volume 42, no. 3 mars 1996, pp 791-808.

El Dessourky H.T, Bouhambra W.S, Ettouney H.M, Akbar M(1996). Heat transfer in vertically aligned phase change energy storage system. *Journal of solar energy engineering*. Transaction of the ASME, Volume 121, no,2, pages 98-109.

EnergyPlus building energy simulation software  
(<http://apps1.eere.energy.gov/buildings/energyplus/>)

Enibe S.O(2002) Performance of a natural circulation solar air heating system with phase change material energy storage. *Renewable Energy*, Volume 28, Issue 14, November 2003, Pages 2269-2299

Farid M.M, Hamad F.A, Abu Arabi M(1998) Melting and solidification in multidimensional geometry and presence of more than one surface. *Energy conversion and management*, Volume 39, issue 8, pages 809-818.

Farid M.M, Kanzawa A(1989). Thermal performance of heat storage module using PCM's with different melting temperatures: mathematical modeling. *Journal of solar energy engineering*, volume 111, no. 2, pages 152-157, may 1989.

Feldman D, Banu D(1996). DSC analysis for the evaluation of an energy storing wallboard. *Thermochimica ACTA*, Volume 272,pp 243-251.

D. Feldman, D. Banu, D. Hawes and E. Ghanbari(1991) Obtaining an energy storing building material by direct incorporation of an organic phase change material in gypsum wallboard. *Solar energy materials*, Volume 22, Issues 2-3, Pages 231-242 (July 1991).

Flashman R(1999). Energy storage using a phase change materials in a domestic dwelling.

Furbo S(1981), Heat storage with an incongruently melting salt hydrate as storage medium. In *thermal Storage of solar energy* (Eited by C. Den ouden), pp 135-146, Nijhhoff, The hague (1981)

Gates J, Ip K, Miller A(2002) Experimental models for solar thermal storage for the sustainable heating of residential buildings. *CIB sustainable buildings conference 2002 Oslo*. Sptember 2002.

Hadjieva M, Stoykov R, Filipova TZ(2000). Composite salt-hydrate concrete system for building energy storage. *Renewable Energy*, Volume 19, Issues 1-2, 2 January 2000, Pages 111-115

- Hadman M.A, Elwerr F.A(1996). Thermal energy storage using a phase change materials. *Solar energy*, Volume 56, issue 2, pages 183-189.
- Hasnin S.M(1998P). Review an sustainable thermal energy storage technologies part I, *heat storage material and techniques*. Energy convention and management, Volume 39, no.11, pp. 1127-1138
- Hawes D.W, Feldman D, Banu D(1993) Latent heat storage in buildings materials. *Energy and buildings*, Volume 20, no. 1, pp77-86
- Hawlander M.N.A, Uddin M.S, Zhu H.J(2002) encapsulated phase change materials for thermal energy storage experimental and simulation. *International journal of energy research*, Volume 26, issue 2, pages 159-171.
- Imperadori, M.; Masera, G.; Lemma, M. – Super-efficient energy buildings, Proceedings of XXXI IAHS World Congress on Housing, Montreal, Canada, 2003.
- Ip K, Gates J.R(2001) solar thermal storage using phase change materials for space heating of residential building.
- Ip K, Gates J.R(2000). Thermal storage for sustainable dwellings, *international conference sustainable buildings 2000*, 22-25 October Maastricht, Netherlands.
- IP K(1998) Solar thermal storage with phase change materials in domestic buildings. *CIB World congress*. Gävle, Sweden 7-12 june, pp 1265-1272
- Ismail K, Goncales M.M(1999) Thermal performance of a PCM storage unit. *Energy conversion and management*, Volume 40, issue 2 January 1999, pages 115-138.
- Jar A, Kaygujuz K(2003) Some fatty acids for latent heat storage: thermal stability and corrosion of metals with respect to thermal cycling. *Renewable energy*, volume 28, issue 6, pages 939-948.
- Jalyer IO, Sircar A.K(1997) rewiew of phase change materials research for thermal energy storage in heating and cooling applications at the university of Payton from 1982 to 1996. *International journal of global energy issue*, Volume 9 issue 3, pages 183-198.
- Jalyer IO, Sircar A.K(1990). Phase materials for heating and cooling of residential buildings and other applications. Proceedings of the intersociety energy conversion engineering conference, Volume 4,1990. Proceedings of the 25th intersociety energy conversion engineering conference-IECEC '90, 12-17 agosto, Reno NV, USA, pages 236-243. ISSN:0146-955
- Jianfeng Wang, Guangming Chen, Haobo Jiang (1999) theoretical study on a novel phase change process. *International journal of energy research*, No. 23, issue 4, pages 287-294.
- Kang Yan Bing, Jiang Yi, Zhan Yinpings (2003) modeling and experimental study on an innovative passive cooling-NVP system. *Energy and buildings*, Volume 35, issue 4, pages 417-425.
- Kedt R.S, S.T.K(1989). Actives in support of the Wax-impregnated wallboard concept. U.S. department of energy thermal storage research activities review, New Orleans, Louisiana, U.S. department of energy.
- Kim J.S, Darkwa K(2003) Simulation of an integrated PCM-wallboard system. *International journal of energy research*, Volume 27, issue 3, pages 215-223.
- Kissok K(1998). Early result from testing phase change wallboard. *IEA Annex 10*, first workshop 16-17 april 1998 Adana, Turkey.
- Kniep R, Laumen M, Zachos A(1985). Latent heat stores and phase change materials, an extensive area for thermal analysis, calorimeter and chemical thermodynamics. *Thermochimica ACTA*, Volume 85 pp 131-134.

- Kurklu A(1998). Short-term thermal performance of a build-in storage for frost prevention in greenhouse. *International journal of energy research*. Volume 22 pages 169-174.
- Kurklu A(1998) energy storage application in greenhouse by means of phase material change: a review. Technical note. *Renewable energy*, volume 13, pages 89-103.
- Kurklu A, Wheldon A, Hadley P(1996) Mathematical modeling of thermal performance of a thermal performance of a phase change material (PCM) store cycle. *Applied thermal engineering*, Volume 16, issue 7, pages 613-623.
- Kurklu A, Ozmerzi A, wheldon A, Hadley P(...). Use of a phase change materials (PCM) for reduction of peak temperatures in a model greenhouse. *ISHS ACTA horticulture 443: international conference on green house technologies*.
- Lee T, Hawes D.W, Banu D, Feldman D(2000) Control aspects of latent heat storage and recovery in concrete. *Solar energy materials and solar cells*, Volume 62, issue 3, pages217-237.
- Lemma M., Fioretti R., Imperadori M.(2005), Development of a technology for inserting a PCM layer in building envelopes, *Atti del XXXIII IAHS World Congress "Housing, Process & Product"*, Pretoria 2005;
- Lemma, M.; Torcianti, N.; Imperadori, M.; Masera, G.(2003) – Gli involucri sensibili: progetto e costruzione di pareti ventilate ad inerzia variabile (Sensible envelopes: design and construction of ventilated façades with variable inertia), *Proceedings of international symposium "Involucri quali messaggi di architettura" ("Building envelopes as architecture messages")*, Naples, Italy, 2003.
- Lemma, M.; Imperadori, M. (2002)– Phase Change Materials in concrete building elements: performance characterization, *Proceedings of XXX IAHS World Congress on Housing*, Coimbra, Portugal, 2002.
- Lou D.Y(1983) solidification process in a Glauber salt mixture. *Solar energy*, Volume 30, issue 2, pages 115-121.
- Lorsch H.G., K.W. Kaufmann and J.C.Denton, (1975) Thermal energy storage for solar heating and off-pek air-conditionning. *Energy conversion* 15,pp 1-8
- S.Marks (1983), The effect of crystal size on the thermal energy storage of thickened Glauber's salt, *Solar Energy* Vol.30, pp.45-48.
- Marks S(1980). An investigation of Glauber's salt with respect of thermal cycling. *Solar Energy* 25,pp 255-258 .
- Min Xiao, Bo Feng, Kecheng Gong(2002). Preparation and performance of shape stabilized change thermal storage materials with thermal conductivity. *Energy conversion and management*. Volume 43, issue 1, pages 103-108.
- Manz H(1997) TIM-PCM external wall system for solar space heating and daylighting. *Solar energy*, Volume 61, issue 6 pages 369-379.
- Merritt R.H, Ting K.C(1995). Morphological pesponcse of bedding plants to tree greenhouse temperature regime. *Scientia orthicolturae*, Volume 60, pages 131-324
- NG K.W, Gonz Z.X, Mujumdar A.S(1998) Heat transfer in free convection dominated melting of a phase change materials in a horizontal annulus. *International journal of eat and mass transfer*, Volume 25, issue 5, pages 631-640.
- Neeper D.A(1989) Potential benefit of distributed PCM thermal. *American solar energy society*.

- Neeper D.A.(2000). Thermal dynamics of wallboard with latent heat storage. *Solar energy*, Volume 68, issue 5, pages 393-403.
- Peippo K, kauranen P, Lund P.D(1991). Multicomponent PCM wall optimized for passive solar heating. *Energy and buildings*. Volume 17, issue 4, pages 259-270
- Pearson F.J.(1989) The chiller air approaches in the office buildings market. *ASHRAE journal*, may 1989, pages 259-270.
- PCM express - Planning and Simulation Program for the Use of Phase Change Materials (PCM) ([http://www.valentin.de/index\\_en\\_page=pcm\\_express](http://www.valentin.de/index_en_page=pcm_express))
- Principi, P.; Di Perna C.; Carbonari, A.; Borrelli, G. (2005)– Experimental energetic evaluation of changeable thermal inertia PCM containing walls, Passive and Low Energy Cooling for the Built Environment, (*PALENC 2005*), Santorini Island, Greece, 2005.
- Principi, P.; Di Perna C. (2004)– First theoretical and experimental data referred to the energetic behavior of building component utilizing Phase Change Materials, Proceedings of *5th International Congress Energy, Environment and Technological Innovation (EETI 2004)*, Rio de Janeiro, Brazil, 2004.
- Principi, P.; Di Perna C.; Carbonari, A.; Borrelli, G. (2005)– Monitoring system for the evaluation of the energetic behaviour of PCM containing walls, Passive and Low Energy Cooling for the Built Environment, (*PALENC 2005*), Santorini Island, Greece, 2005.
- Principi, P.; Di Perna C.; Carbonari, A.; Ferrini, M., (2004), – Validation of Numeric finite Element Calculation Model Through the Laboratory experimentation of Artificial Programmable Inertia Walls, Proceedings of *XXXII IAHS Word Congress on Housing*, Trento, Italy, 2004.
- PY X, Olives R, Maurans(2001) Paraffin porous-graphite-matrix composite as a high and constant power thermal storage material. *International journal of heat and mass transfer*. Volume 44, pages 2727-2737.
- Rudd A.F.(1993). Phase materials change wallboard for distributed thermal storage in buildings. *ASHRAE Transaction research*, Volume 99, part 2, papar 3724.
- Ruyon L, Guiffant G, Flud P(1997). Investigation of heat transfer in a polymeric phase change materials for low level heat storage. *Energy conversion and management*, Volume 38 issue, pages 517-524.
- Santamouris M.S, Lefas C.C(1988). On the coupling of PCM stores to active solar system. *International journal of energy research*, Volume 12, issue 4, pages 603-610.
- Sasaguchi K, Viskanta R(1989) Phase change heat transfer during melting and re solidification of melt around cylindrical heat source7sink. *Journal of energy resources technology*, volume 111, issue 1, pages 42-49.
- Scalat S(...) full scale thermal testing of latent heat storage in wallboard. *Solar energy materials and solar cells*, volume 44, pages 49-61.
- Schröder J., R. And D(1980). system for thermal energy storage in temperatures range from –25 C to 150 C. Proc. Seminar new ways to save energy, 495-504, Reidel, cordrecht,
- Sharma Atul, Sharma S.D, Buddhi D, Sawhney R.L(2001). Thermal cycle test of urea for latent heat storage applications. *International journal of energy research*, Volume 25, issue 5, pages 465-468.
- Stetiu C, Feuster H.E. Phase change wallboard and mechanical night ventilation in commercial buildings [on line] <http://oxford.elsevier.com>

Stetiu C, Feuster H.E(1996) Phase change materials wallboard as an alternative to compressor cooling in California residences. In proceedings: *96 ACEE Summer study for energy efficient buildings*. Silomar, California.

Stritih U, Novak P(1996) Solar heat wall for building ventilation. *Renewable energy*, Volume 8, issues 1-5, pages 268-271.

Stoval T.K, Tomlison J.J(1992) What are the potential benefits to including latent storage in common wallboard. Proceeding of the intersociety energy conversion engineering conference V4, 1992, energy system – new technologies. Proceedings of the *27th intersociety energy conversion engineering conference*, August, 3-7, 1992, San Diego, CA, USA, 929371, pages 265-270. ISSN:0146955X, IBBN 1-56091-264-2.

Stymne H(1980) Improvement of the efficiency of energy transformation processes utilizing a chemical heat pump. International seminar of thermo chemical energy storage. Stockholm, January 7-9,1980. Arranged by Royal Swedish Academy of Engineering.

Telkes M. (1952). Nucleation of supersaturated inorganic salt solution. *Industrial and engineering Chemistry* 44, pp 1308-1310

Telkes M(1975). Thermal storage for solar heating and cooling.Proc.*Workshop on solar energy storage subsystem for the heating and cooling of buildings*, pp 17-23, Carlottensville, Virginia, USA

Tomlinson J.J,Herberle D.D(1980) Analysis of wallboard containing a phase change material. Proceedings of the intersociety energy conversion engineering conference, *IECEC '90*, August 12-17 1990 NV, USA, pages 230-235

Ulfrengen Rolf, Climator AB(1998) the application of PCM technologies in telecommunications. IEA annex 10. First workshop. April 16-17 1996, Adana, Turkey.

U.S. department of energy(2000). Phase change drywall. <http://www.eene.doe.gov/consumenfo.refbiefs/db3.html>

U.S. department of energy(2000). Phase change materials for solar heat storage. <http://www.eene.doe.gov/consumenfo.refbiefs/b103.html>

Velrias R, Seenrias R.V, Hafner B, Faber C, Schwarzer K(1999) heat transfer enhancement in a latent heat storage system. *Solar energy*, Volume 65, issue 3, pages 171-180.

Vandini M(1990) The HVAC system choice with cool storage. *Energy engineering*, Volume 87, issue 6, pages 34-45.

Wang Jianfeng, Chen Guangming, Chen Goubang, Ouyang Ying Iu (2000). Study on charging and discharging rates of latent heat thermal energy storage systems employing multiple phase change materials. *Taiyangneng Xeubao/Acta energiae solaris sinica*, Volume 21, issue 3, pages 258-260.

Wattermarx G, Carlsson B, Stymne H(1979) Storage of heat. A survey efforts and possibilities. Document D2:1979. Swedish council for buildings research.

Xiao M, Feng B, Gong B(2002) Preparation and performance of shape stabilized phase change thermal storage material with high thermal conductivity. *Energy conversion and management*. Volume 43, issue 1, pages 103-108.

Yamagishy Yasushi, Takeuchi Hiromi, Pyatenko Alexander A, Kayukawa Naoyuki (1999) characteristics of microencapsulated PCM slurry as a heat-transfer fluid. *Aiche journal*. Volume 45, issue 4, pages 696-707.

Yiuping Z, Yi S (1999) A simple method, the T-History method of determining the heat of fusion, specific heat and thermal conductivity of phase change materials. *Measurement science technology*, Volume 10, pages 201-205

Yinping Zhang, Yi Jiang, Kang Yanbing, Zhong Zhipeng. Research of latent heat storage in Tsinghua university and application of ice storage in China. [http://www.ket.kth.se/advelningar/ts/annex10/ws\\_pres/wsz/zhang.pdf](http://www.ket.kth.se/advelningar/ts/annex10/ws_pres/wsz/zhang.pdf)

Zelba Belen, Marin Jose M, Cabeza Luisa F, Mehling Harald (2003) review on thermal energy storage with phase change materials, heat transfer analysis and applications. *Applied thermal engineering*, Volume 23, issue 3, pages 251-283.

Zambelli, E.; Imperadori, M.; Masera, G. (2004)– Artificial programmable inertia for low-energy buildings: integrating Phase Change Materials in building components, Proceedings of XXXII IAHS World Congress on Housing, Trento, Italy, 2004

Zambelli, E.; Imperadori, M.; Masera, G.; Lemma, M. (2003)– High energy-efficiency buildings, Proceedings of the 4th international symposium on Heating, Ventilating and Air-conditioning ISHVAC 2003, Beijing, China, 2003.



# 8. DYNAMIC INSULATION

## 8.1 Description of technologies and classifications

Dynamic insulation (DI) describes a novel, energy efficient approach to deliver fresh filtered ventilation air to the interior of a building through an air-permeable, dynamically insulated building envelope. The coupling of this RBE to the Heating, Ventilation & Air Conditioning (HVAC) system, offers the benefits of clean, efficient, low carbon, superior built environments. The concept and working principle of this technology, DI, are illustrated in figure 8.1. Ventilation air enters the building pre-tempered (cooled in summer and heated in winter) using energy that would otherwise be lost, and also filtered of airborne particulate matter (PM) which means that the DI element acts as the ventilation source, heat exchanger and air purification system.

The DI concept is then to effectively use a combination of conventional insulation and heat exchange characteristics of a wall to pre-heat fresh air for ventilation. It is regarded as one possible method for reducing building envelope heat losses while achieving better indoor air quality.

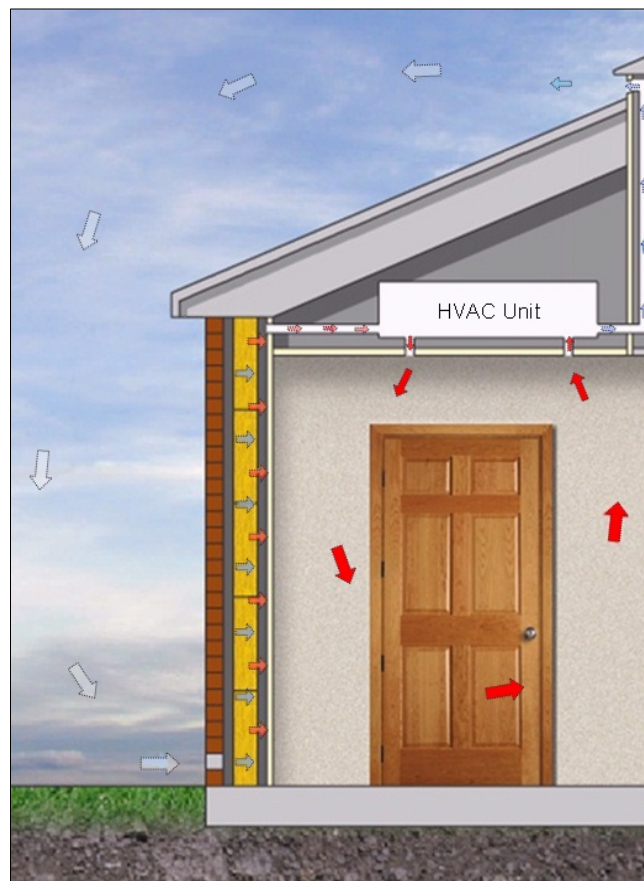


**Figure 8.1 - DI concept & working principle.**

The existing technology of DI can be divided into two catalogues:

1. *Cavity wall design*: this configuration adopts cavities to circulate the fluid (mostly air) in the wall. The airflow direction in the cavities is generally parallel to the wall – wall acting as a heat exchanger.

2. *Breathing wall design*: this allows the gas (mostly air) transfer through the permeable insulation. The interaction of gas phase and solid phase can also act as a contra-flux mode heat exchanger [Baker, (2003)].

Though ventilated walls which use a combination of air cavities have been presented, such as [Baily (1987)], (also see [Qiu et al (2007)]), currently most of the structures of DI system adopt the latter concept because of its easy implementation

The research and application of DI systems currently focus on the *breathing wall*. In this kind of structure, the interaction of air and solid phase acts as a contra-flux mode heat exchanger.

Concerning energy consumption, the following benefits are claimed for the application of breathing wall:

1. less energy is required to maintain a certain indoor air temperature, thus the operating costs for space heating and cooling are reduced. Previous research suggested that the energy saving of using breathing wall in a building is about 10%. Simulation by [Krarti (1994)] of a room with a dynamic insulated wall showed that the overall energy saving may reach 20%, while the simulation results by [Baily (1987)] pointed out the energy saving during a heating period vary from 7% to 14%, without any additional equipment such as a heat pump.
2. As low heat loss can be achieved by using a thin dynamic insulated wall, it is possible to avoid the need of using a thick wall construction to meet the building regulations. This will also reduce the construction cost.
3. Using breathing wall, the wall becomes the air supply and distribution system, thus reduces the cost of installing ventilation ducts.
4. As breathing wall is generally working in contra-flux mode, it also prevents the water vapour transmission into the interior environment; reducing the risk of mould growth and condensation.

Besides the advantage of energy saving, the fibrous structure in breathing wall may also offer an effective, low energy solution to the air pollution problem in the surrounding environment, since the breathing wall can act as an air filter, helps to remove airborne particulate. Therefore, it helps to provide a better indoor air quality and healthier indoor environment.

The dynamic insulated wall component usually consists of the following main sub-layers:

1. The external envelope sub-layer. This could be a prefabricated reinforced concrete slab, or a perforated metal sheet. The supply air can be introduced from the bottom or top of the external envelope sub-layer.
2. The breathing wall sub-layer, which may consist of layers of breathing materials, such as compressed straw board, mineral wool and thin paperboard, or cellulose fibre insulation. These materials creates low pressure drop between interior and exterior, thus allowing the air to enter the room.
3. An air gap is generally used to separate these two sub-layers.

Besides configuration of these sub-layers, other considerations in the real breathing wall system design include:

1. pressure difference between indoor and outdoor for inward airflow can be normally achieved by means of a fan.
2. Solar energy should also be considered to increase the performance of breathing wall component. For example, a layer of outer glazing could raise the temperature of incoming air [Gan, (2000)].
3. A heat pump or heat pipe unit can be inserted in the exhaust air duct to pre-heat the incoming air [Gan, (2000)].

## 8.2 Design/analysis method and tools

Though the concept of DI was developed decades ago, the implementation of this technology is still in the early stage.

Until now, special design tools for the design of dynamic insulated walls are not reported. However, concerning the thermal performance, some commonly used building energy analysis tools, such as TRNSYS, can be suitably modified for the design of buildings incorporating DI elements.

To this aim, a suitable effective conductivity,  $k_{\text{eff}}$ , has to be introduced. Based on this thermophysical parameter, the dynamic U-value of the porous media can be determined. In this way, by suitably modifying the material property, and implementing the  $U_{\text{dyn}}$  value instead of the usual U value, it is possible to use tools such as TRNSYS.

Thus, it makes it possible to perform the energy analysis for the building using the DI elements by means of common commercial software packages.

### 8.2.1 Thermal performance

The main function of insulation is to keep the heat in a building in the winter season, while keeping the heat out of the building in the summer. The heat transfer through the building insulation is by conduction, radiation as well as convection. In conventional building envelope design, convection heat transfer occurs as air circulates through the insulation material: it has a minor role in this heat transfer process.

However, in dynamic insulation elements, where air is intentionally drawn through the building envelope to reduce the conduction heat loss, the convection heat transfer plays a significant role in the overall thermal performance of the building envelope. Therefore, both conduction and convection needs to be included in the thermal analysis of Dynamic Insulation (DI).

Thermal performance of a DI can be assessed based on the solution of energy conservation equation written for the porous insulation material (whose details are discussed in Appendix 8A).

Due to the very low air velocity through the DI, heat transfer in it can be regarded to be in local thermal equilibrium, i.e., the local average temperature of air equals that of the solid matrix, and the effect of thermal dispersion can be ignored.

Thus the thermal conductivity of the layers of breathing materials can be obtained as:

$$k_{\text{eff}} = \varepsilon k_f + (1 - \varepsilon)k_s \quad (1)$$

Where  $k_{\text{eff}}$  is the effective conductivity (W/m K),  $k_f$  is the conductivity of air (W/m K),  $k_s$  is the conductivity of solid matrix (W/m K), and  $\varepsilon$  is the porosity of the media.

Under the steady state condition, an analytical solution can be obtained and the conductive heat loss of a DI can be estimated through the so-called *dynamic U-value*,  $U_{\text{dyn}}$ , whose expression is:

$$U_{\text{dyn}} = \frac{Pe}{R(e^{Pe} - 1)} \quad (2)$$

Where  $R = \frac{L}{k_{\text{eff}}}$  ( $\text{m}^2/\text{W } ^\circ\text{C}$ ) is the effective thermal resistance of insulation material in the static

condition,  $L$  the thickness of the insulation layer (m),  $k_{\text{eff}}$  the effective thermal conductivity of the insulation material (W/mK),  $U_{\text{dyn}}$  is the dynamic U-value of the DI ( $\text{W}/\text{m}^2\text{K}$ ), and  $Pe$  is the Peclet number which is defined as:

$$Pe = \frac{u \cdot L}{\alpha} \quad (3)$$

Being:  $u$  the air velocity (m/s) and  $\alpha$  the thermal diffusivity ( $\text{m}^2/\text{s}$ ).

The key issue for the design of a dynamic insulation element is to determine the thickness of the insulation layer,  $L$ , and optimize the range of airflow rate (that is a function of  $u$ ).

This implies the balance between two different classes of contrasting requirements:

1. provide a satisfactory IAQ, promote the heat exchange between the incoming air and the insulation material and decrease the risk of condensation (all these issues require that the airflow rate would not be too low).
2. keep the convective heat loss as low as possible (for the case of natural ventilation, where the temperature of incoming air equals the outdoor temperature, the convective heat loss increases with increasing airflow rate; hence, airflow rate should not be too high).

Affected by a combination of the above factors, the airflow rate needs to be in a suitable range. However, this guidance is not reflected by the results of dynamic U-value, expressed by equation (2), as it decreases monotonically with the increase of airflow rate. This is due to the fact that equation (2) is obtained by a simplified modelling, where only the conductive heat loss is included. It is, however, possible to obtain an analytical solution of energy conservation equation written for the porous insulation material under the steady-state condition, using constant convective heat transfer coefficients on the exterior and interior surfaces as boundary conditions [Qiu and Haghghat (2007)].

Considering the combined effect of conductive and convective heat transfer, the overall heat transfer rate at the exterior surface of DI is:

$$Q_T = Q_{\text{cond}} + Q_{\text{conv}} = U_{\text{dyn}} A \Delta T + \dot{m} C_p \Delta T = U_{\text{dyn}} A \Delta T + \rho_a u A C_p \Delta T \quad (4)$$

Where:

$\dot{m}$  is the air mass flow rate through DI (kg/s),

$Q_{\text{cond}}$  is the heat loss through the envelope by conduction (W),

$Q_{\text{conv}}$  is the heat loss through the envelope due to airflow (W),

$Q_T$  is the total heat loss through the building envelope (W),

$A$  is the area of the building envelope ( $\text{m}^2$ )

$\rho$  is the air density ( $\text{kg}/\text{m}^3$ ),

$C_p$  is the heat capacity ( $\text{J}/\text{kg } ^\circ\text{C}$ ).

Equation (4) reflects that the heat loss through the dynamic insulated wall is greater than the “conduction heat loss” calculated by the dynamic U-value, but it is less than the sum of the conduction and the ventilation heat loss for a conventional wall (e.g.  $U_{\text{static}} A \Delta T + \rho_a u A C_p \Delta T$ ).

Therefore, the overall heat loss coefficient,  $U_T$ , for a DI may be written as:

$$U_T = Q_T / (A \Delta T) = U_{\text{dyn}} + \frac{Pe}{R} \quad (5)$$

If only part of the wall is making use of DI, the overall heat loss coefficient for the entire wall may be assessed by means of the following equation:

$$U_T = Q_T / (A \Delta T) = \frac{\gamma Pe}{R(e^{Pe} - 1)} + \frac{\gamma Pe}{R} + \frac{1 - \gamma}{R} \quad (6)$$

Being  $\gamma$  the ratio of DI area to the whole wall area (-) (i.e.  $\gamma = \frac{A_{\text{DI}}}{A}$ ).

Finally, since the dynamic insulation concept is a combination of conventional insulation and heat exchange characteristics of a wall to pre-heat fresh air for ventilation, it is also possible to define an “heat exchange efficiency” of DI; this topic is discussed in more detail in Appendix 8A.

## 8.2.2 Air quality

Besides the advantage in energy saving, the fibrous structure in Dynamic Insulation may also offer an effective, low energy solution to filter the supply air. The DI can trap the particulate through four mechanisms (Figure 8.2):

1. Impaction, in which the momentum of the particle causes it to deviate its stream line around the fiber and is captured by the fiber media;
2. Interception, in which the particle follows the course of the air stream and is captured when it comes into contact with the fiber;
3. Diffusion, in which the Brownian motion causes the particle to move independently of the air stream onto the filter media.
4. The electrostatic mechanism is mainly due to the Columbus, image, and dielectrophoretic attraction between the particles and the fibers.

In conventional air filters the air velocity is up to 1.0 to 1.5 m/s, thus particle is mainly trapped by impaction and interception. As the air velocity in the DI is quite low, generally between 0.005 m/s to 0.05 m/s, all mechanisms are involved. It follows that the DI is very effective to capture particles less than  $0.5\mu\text{m}$  or larger than  $5\mu\text{m}$  in diameter. It is worth noting that for the particles in the range of  $0.5 - 5\mu\text{m}$ , DI is also effective if its thickness is greater than 60 mm [Taylor and Imbabi, (1999)]. At this thickness of filter media, it is believed the DI has the potential to become a high efficiency particle air filter due to the nearly zero particle penetration for all particle sizes.

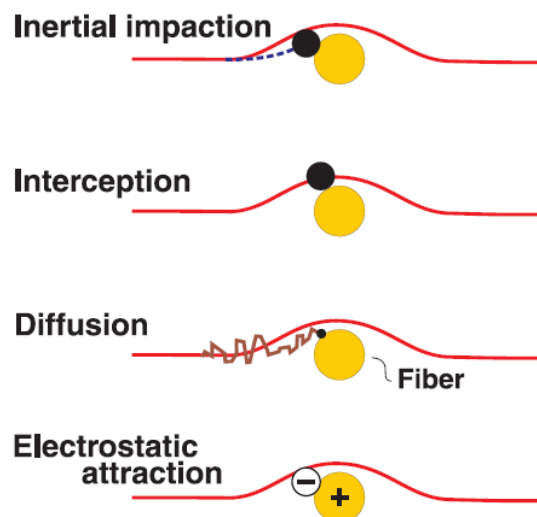


*Figure 8.2 - Four primary particle collection mechanisms of particle capture.*

## 8.3 Guidance and recommendation

DI has the potential to be implemented in most climate conditions. As a matter of fact, besides cold weather condition, such as Scandinavian countries, experimental set-ups for DI have been developed in mild climate countries such as United Kingdom [Baker, (2003)], Greece [Dimoudi et al, (2004)], and Japan [Dalehaug (1993)].

However, as DI needs de-pressurization of the building, the actual implementation may be different for different contexts.

For mild and variable climate country like UK, the only way to reliably de-pressurize the building is using fans, while in Canada and Scandinavian countries, where the indoor and outdoor temperature difference in winter reaches 40 K, the needed de-pressurization could be provided by stack effect.

The ideal types of building for which the implementation of DI is best suited, are those characterized by a high demand of fresh ventilation air, like, swimming pools (to remove moisture). Concerning the energy consumption, DI can be successfully used in both commercial and

residential buildings [Baily, (1987)]. It may perform better for small detached buildings due to the large envelope exposure to outdoor.

Though DI is a possible approach to supply a good indoor environment with less energy consumption, limitations exist concerning its performances and this fact seriously affects the implementation of this technology.

The specific limitations are:

1. DI systems are claimed to reduce the conductive heat loss; however, convective heat loss increases with the airflow rate, and additional electrical energy may be required to drive fans. Thus the overall energy saving may not be very significant (generally is less than 10%). This might make this technique less attractive [Qiu et al. (2007)].
2. DI can work as an air filter. However, dust and other particles trapped in the insulation may prompt the growth of bacteria. This might bring potential problem to the occupants' health.

## 8.4 Examples for illustration

### 8.4.1 Example of DI wall Technologies

Figure 8.3 illustrates the scheme of a prototype design of DI wall [Baker, (2003)].

Characteristics of this specific design are as follows:

- the external envelope sub-layer is made of perforated metal;
- as problems might exist with the use of a permeable internal surface construction (a solution that is adopted by most of the DI design), plasterboard, which is impermeable to air, is chosen for the inner face of the construction;
- the air cavity and insulation (a permeable material) justify assuming a one dimensional flow;
- air is introduced into the wall inner structure through the opening located at the bottom of the wall. After flowing through the porous breathing material, the air is drawn into a cavity behind the plasterboard. From there it is distributed into the room through vents.

A similar design was presented by [Dimoudi et al (2004)], as illustrated in Figure 8.4. In this case:

- the external envelope sub-layer is a prefabricated reinforced concrete slab;
- to assure a uniform airflow and, hence, one-dimensional heat transfer through the wall, the air has to be introduced into cavity uniformly.

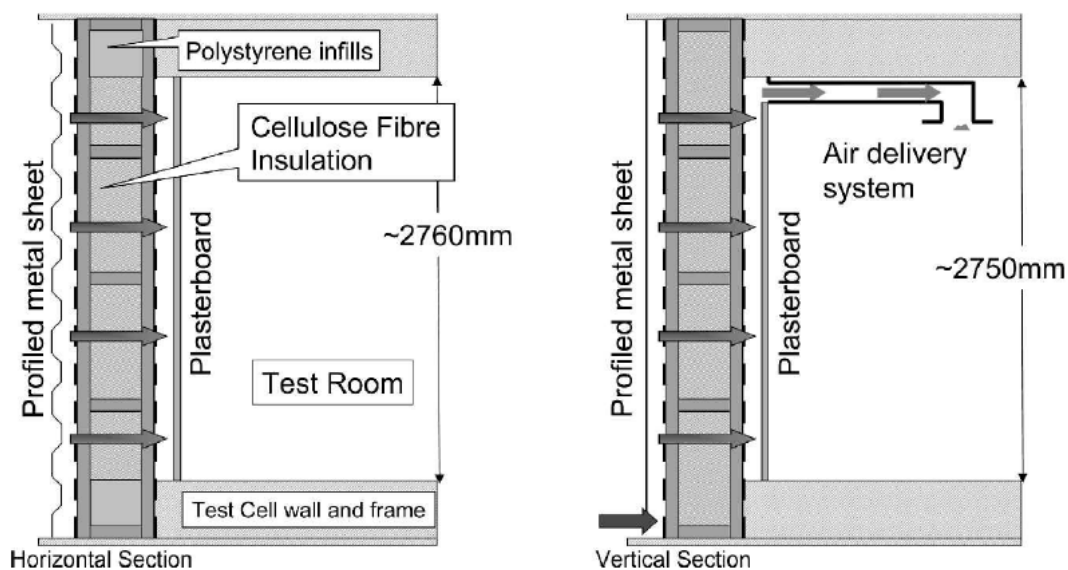


Figure 8.3 - Prototype design of dynamic insulation wall [Baker, (2003)]

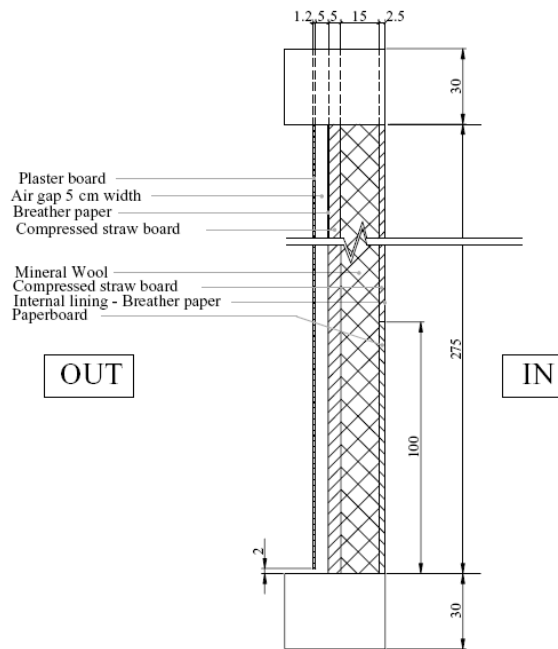


Figure 8.4 - Example 2- Design of Dimoudi et al (2004).

## 8.4.2 Product development and practical application

Some commercial products, making use of the Breathing Wall technology, are already available on the market. One example is the so-called *EnergyFlo*<sup>TM</sup> cell (Figure 8.5).

The high performance *Energyflo*<sup>TM</sup> cell has been developed by The Environmental Building Partnership Limited, United Kingdom. Available in thickness of 90 mm, 135 mm, 170 mm, the product can be used in most building types to reduce energy demand for heating and cooling, and improve indoor air quality through increased fresh air ventilation.

Similar to the dynamic insulated wall presented by [Baker, (2003)] and [Dimoudi et al., (2004)], *Energyflo*<sup>TM</sup> cell is made of two components: a fiber-base filtration media and a rigid encasement package. The rigid encasement package, which is constructed from identical halves fitting together in a clam-shell arrangement, wholly contain the fibrous media. Thus it is easy for the DI element made of *Energyflo*<sup>TM</sup> cells, to fit with other building components.

The product is available in two different ranges, one designed to be self-supporting (SS), and the other one designed to fit within timber frame (TF) construction. The former cell uses asymmetrical cell halves, and applies an opposing overlaps to provide an airtight, glue-less edge seal with adjacent cell. While the latter employs symmetrical cell halves and is designed to be installed in the wall studs in the timber frame construction. Comparatively, TF cell is a more attractive option for new-build and retrofit in homes and buildings.

The dynamic U-values of DI walls incorporating *Energyflo*<sup>TM</sup> cells are shown in Figure 8.6, with the variation of inward air flow rate through the cells.

Experimental investigations have shown that if only 10% of the wall surface is fitted with *Energyflo*<sup>TM</sup> cells, it will effectively limit the life of the cell in operation. Whereas for the wall with 50% of area fitted with *Energyflo*<sup>TM</sup> cells, or walls completely fitted with *Energyflo*<sup>TM</sup> cells, there is little difference concerning their performance of being an air filter.

The product *Energyflo*<sup>TM</sup> cell is also claimed to reduce the heating and cooling heat by around 10%, compared to the Scotland building regulation standard.

A monitored demonstration project, to test the performance of a dynamically insulated experimental house, has been started in Balerno, City of Edinburgh.

The Balerno project is supported by the Carbon Trust and features a dynamic breathing roof forming part of the air handling and Mechanical Ventilation Heat Recovery (MVHR) system. Construction site photographs, charting works progress to date, are presented in Figure 8.7.

**Description:** This 4-bedroom detached house, completed by CALA Homes (East) Ltd in July 2007, was monitored before and post occupancy by researchers from the University of Aberdeen and EBP. The distinguishing feature of this house is a DI roof, fitted with *Energyflo*<sup>TM</sup> cells, feeding the supply side of an exhaust air MVHR system.

**Fabric Heat Loss:** Built to Scottish 2005 building standards, the whole-house static U-value was determined to be 0.45 W/m<sup>2</sup>K. In operation, this fell to 0.23 W/m<sup>2</sup>K and 0.30 W/m<sup>2</sup>K in September (late summer) and November (early winter) respectively. These falls are a consequence of dynamic heat recovery, solar gain (in September) and other dynamic effects from a DI system that constitutes 32% of the total building envelope area.



**Figure 8.5 - The *Energyflo*<sup>TM</sup> cell (courtesy of EBP).**

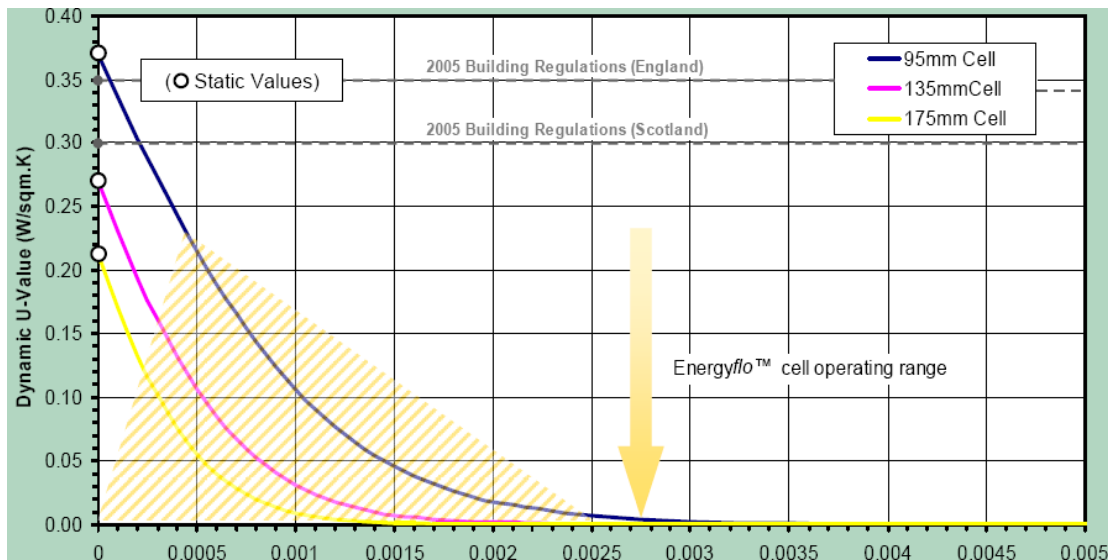


**Figure 8.6 - Variation of dynamic U-value of walls incorporating *Energyflo*<sup>TM</sup> cells with the variation of inward air flow rate through the cells.**



**Figure 8.7 - Photographs from the Balerno project construction phase [Imbabi (2008)].**

Air Filtration: Ambient outdoor counts averaging 3673 sub-micron (fine to nano) particles per  $\text{cm}^3$  were observed over an 8 hour sampling period. By comparison, the counts downstream averaged 378 sub-micron particles per  $\text{cm}^3$ . Ultra-fine and nano particle counts were thus reduced by more than 90% after passing through the Energyflo™ cells.

Figure 8.8 shows the heating loads (simulated) for the Balerno building with and without the DI technology.

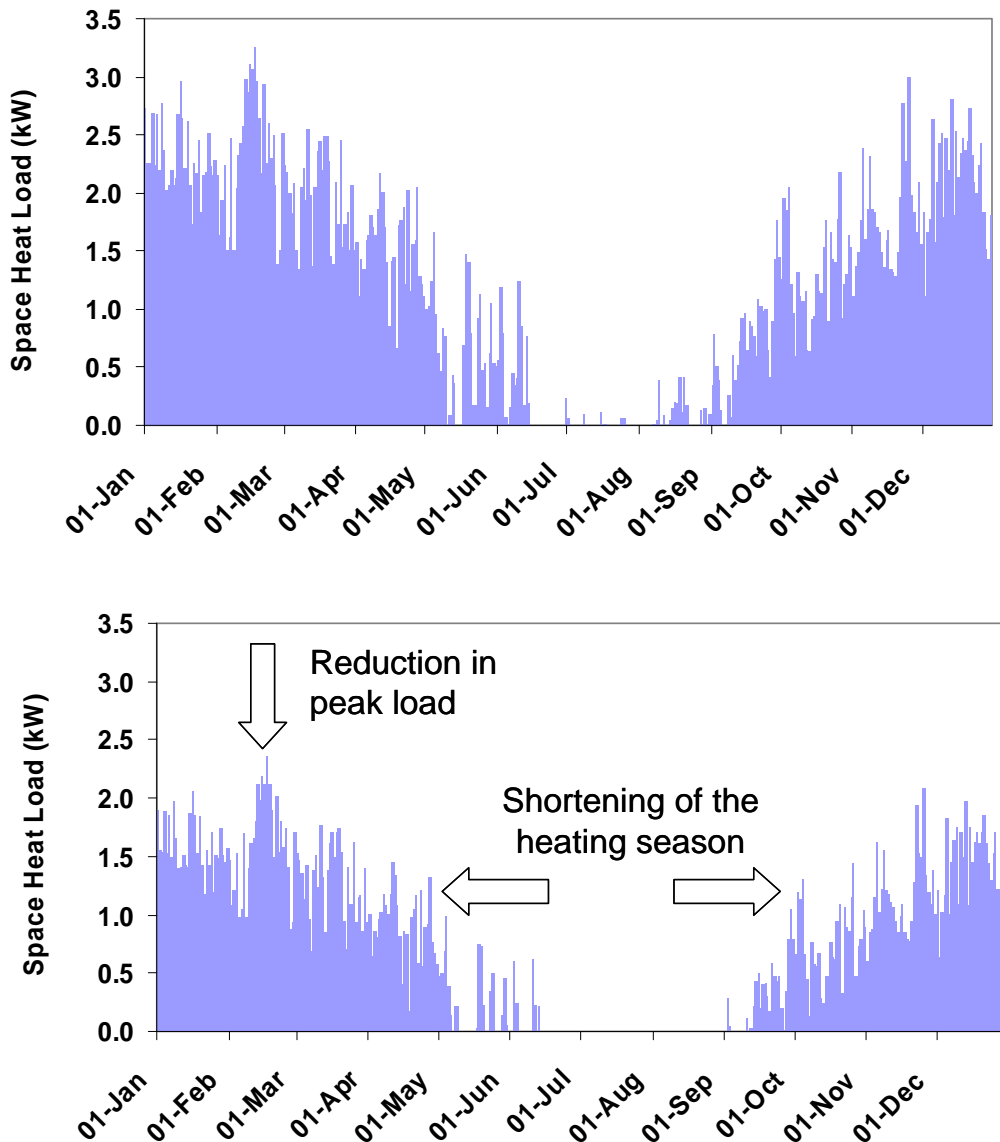


**Figure 8.8 – Heating loads assessed for the Balerno building without the DI (top), heating loads assessed for the Balerno building with the DI element installed in the roofs (Top).**

## 8.5 Market introduction

The DI wall is still a relatively new technology and mainly in the research phase. Currently the published literature has not discussed the market of it. This will be one of the future research works.

## 8.6 Barriers to overcome

Though theoretical analysis and experimental tests have been conducted to evaluate the performance of DI, and the possibility of its implementation has been discussed, there are still problems in the practical application of DI. Specific barriers are:

1. technical problems exist concerning moisture transport in the insulation. Taking advantage of appropriate air flowing through the wall, DI will have better performance in reducing the risk of condensation, compared with the conventional wall. However, it is pointed out that under some conditions, such as the solar radiation on wet timber cladding, condensation may occur in the dynamic insulated wall [Taylor and Imbabi, (1998)]. As air needs to be driven through the wall, it lacks the effective way to avoid possible condensation in the insulation under those conditions.
2. The guideline for dynamic insulated wall design is not well developed. Guidelines should be made concerning the aspects such as: what is the suitable thickness for each sub-layer, what kind of material is more appropriate, and how to determine the dimension of an inlet opening.
3. There is a conflict between the minimization of heat loss by reducing air flow rate, and the removal of water vapor and other indoor pollutants by increasing air flow rate. Thus the air flow rate should be carefully optimized.
4. The DI has not yet been integrated in the commonly used building design tools such as DOE2, EnergyPlus, Esp-r, and TRNSYS. In the studies performed in the Annex 44 activity, TRNSYS was used to simulate the thermal performance of a simple building with dynamic insulated walls [Qiu (2006)]. However, the approach needs the designer to have a thorough knowledge of heat transfer in DI; hence, it is still not ready for the engineering implementation.
5. The impacts of DI on the requirements of building regulations and standards have not been investigated.
6. For the application of DI, other parts of the building need to be well insulated, this may bring difficulties in construction process and increase the construction cost.
7. The thermophysical property of materials concerning the air permeability and water vapor permeability is not accessible to some designers.

Building designers are still unfamiliar with the concept of DI. It may take a long time for them to recognize the advantage of this technique and implementing it in their designs.

## 8.7 References

- Baily N R. 1987. Dynamic insulation systems and energy conservation in buildings. *ASHRAE Transactions*, n 93, pt 1, pg 447-466
- Baker P H. 2003. The thermal performance of a prototype dynamically insulated wall. *Building Services Engineering Research and Technology*, v 24, n 1, pg 25-34
- Dalehaug A. 1993. Dynamic insulation in walls. Research Report No. 53. Hokkaido Prefectural Cold Region Housing and Urban Research Institute, Japan
- Dimouli A, Androutopoulus A, Lykoulis S. 2004. Experimental work on a linked, dynamic and ventilated, wall component. *Energy and Buildings*, v 36, n 5, pg 443-453
- Gan G. 2000. Numerical evaluation of thermal comfort in rooms with dynamic insulation. *Building and Environment*, v 35, n 5, pg 445-453

- Krarti M. 1994. Effect of airflow on heat transfer in walls. *Journal of Solar Energy*, v 116, n 1, pg 35-42
- Qiu K, 2006. Air infiltration and heat exchange performance of the building envelope. PhD thesis, Concordia University, Montreal, Canada
- Qiu K, Haghghat F, 2006, Impact of transient effect on thermal performance of dynamic insulation, Proceedings of the *4th European Conference on Energy Performance and Indoor Climate in Buildings (EPIC)*, Lyon, France
- Qiu, K., Haghghat, F. 2007. Modeling the combined conduction – Air infiltration through building envelope, *Building and Energy*,\_v 39, pg 1140-1150.
- Qiu, K. Haghghat, F. and Guarracino, G. 2007, Thermal behavior of diffusive building envelope: State-of-the art review. *Journal of Advances on Building Energy Research*, pg 213-226
- Taylor B J, Cawthorne D A, Imbabi M S. 1996. Analytical investigation of the steady-state behaviour of dynamic and diffusive building envelopes. *Building and Environment*, v 31, n 6, pg 519-525
- Taylor B J, Imbabi M S. 1998. Application of dynamic insulation in buildings. *Renewable Energy*, v 15, n 1-4 pt 1, pg 37-382
- Taylor B J, Webster R, Imbabi M S. 1999. The building envelope as an air filter. *Building and Environment*, v 34, n 3, pg 353-361.



# **APPENDICES**

## **CHAPTER 4**

# APPENDIX 4A

## 4A.1 AIF Politecnico di Torino model (PoliTo)

The conduction in glass layers is calculated solving the one-dimensional energy conservation equation, considering the absorbed solar radiation as a heat source:

$$C_n \frac{\partial T_n}{\partial t} = \left( \frac{R_{n-1} + R_n}{2} \right)^{-1} \cdot (T_{n-1} - T_n) - \left( \frac{R_n + R_{n+1}}{2} \right)^{-1} \cdot (T_n - T_{n+1}) + \dot{Q}_{sol,n} \quad (4A.1)$$

It is then possible to obtain the temperature at each node as:

$$T_n = \int_0^t \frac{1}{C_n} \left( 2 \cdot \frac{T_{n-1} - T_n}{R_{n-1} + R_n} + 2 \cdot \frac{T_{n+1} - T_n}{R_{n+1} + R_n} + \dot{Q}_{sol,n} \right) dt \quad (4A.2)$$

The shading device is considered as a semitransparent layer with no thermal resistance. The energy conservation equation becomes then:

$$\dot{Q}_{rad,in} + \dot{Q}_{conv,in} - \dot{Q}_{rad,out} - \dot{Q}_{conv,out} + \dot{Q}_{sol,n} = \rho \cdot c \cdot V \cdot \frac{\partial T_n}{\partial t} \quad (4A.3)$$

The convection in the mechanically ventilated cavity is calculated by means of the McAdams equations for forced convection on a vertical plane (McAdams, 1954).

The input parameters for the model are:

- time profiles of outdoor air temperature,
- indoor air temperature,
- irradiance (diffuse and direct),
- direct solar radiation incident angle,
- wind speed,
- airflow rate into the air cavity
- façade geometry,
- thermophysical and optical properties of materials.

Time profiles are supplied to the model on an hourly basis; for times between two hourly input data, the model assumes a linear profile.

The model gives as an output the temperature of each node and the heat fluxes through the various layers and cavities.

The model was validated using the experimental data obtained in the measurement campaign of the climate façade carried out using the TWINS test facility at the Politecnico di Torino.

The façade used for the validation was composed by an external skin made by a double glass and an internal skin made by a single clear glass pane.

In the ventilated cavity a roller screen and a venetian blind were simulated. In both cases the ventilated air gap was considered divided into two different air channels. The air flowing in façade gap came from the indoor environment. The model as been applied dividing the façade into three horizontal zones.

The accuracy of the model was evaluated using the percentage root mean square error (PRMSE) for the temperatures and the root mean square error (RMSE) for heat fluxes, that is:

$$PRMSE = \sqrt{\frac{1}{N} \cdot \sum_{i=1}^N \left( \frac{s_i - e_i}{e_i} \right)^2} \quad (4A.4)$$

$$RMSE = \sqrt{\frac{1}{N} \cdot \sum_{i=1}^N (s_i - e_i)^2} \quad (4A.5)$$

The comparison between simulated and measured data shows a good accuracy of the models far as the glass and air temperatures are concerned, both for the roller screen and the venetian blind (figures 4.13 and 4.14,  $2.6\% < PRMSE < 12.2\%$ ).

The heat fluxes are, instead overestimated: the root mean square error is between 13.3 and 21.2  $W/m^2$ .

A deeper analysis of the measured data used for the validation, pointed out a discrepancy about the values of the heat transfer coefficients with the indoor environment chosen for the calculation. In fact, the measured heat transfer coefficients were largely lower than those assumed for the simulations (i.e. the ones that are usually adopted and available in literature). This can explain the poor accuracy in simulating the heat fluxes. The adoption of heat transfer coefficient values equal to the one obtained during the experiments led to a quite satisfactory simulation of the heat fluxes ( $10.3 W/m^2 < RMSE < 13.6 W/m^2$ ), still with a good accuracy in the temperature prediction ( $2.1\% < PRMSE < 11.4\%$ ).

Figure 4A.1 shows some more data comparison between measured and simulated temperatures (over data the one shown in section 4.3.3.3).

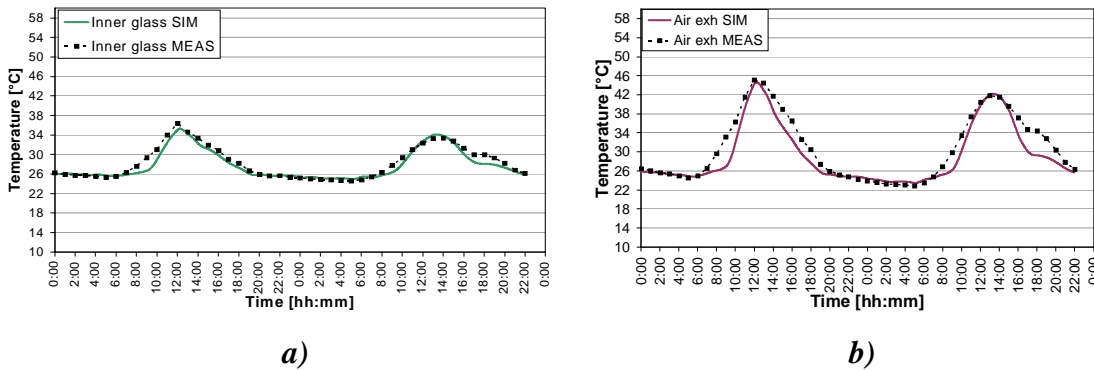


**Figure 4A.1 – Simulated (continuous lines) and measured (symbols) glass (a) and air (b) temperatures, venetian blind configuration.**

## APPENDIX 4B

### 4B.1 AIF IST model (Portugal)

It is a two-dimensional model where the section of the double skin façade is divided into “n” vertical layers (including a shading layer as an additional one). Each layer is, in turn, divided into “m” horizontal slices, as schematically illustrated in Fig. 4.12 - section 4.3.3.4. The model is intended to predict both the thermal and the ventilation performance of different configurations of double skin facades and, as a consequence, uses two coupled iteration cycles: the temperature and the airflow cycles.

The first one determine the temperature distribution depending on the net infrared radiation, convective and conductive heat transfer and the absorbed solar radiation and the second calculate the airflow rate for that certain temperature distribution using the Newton-Raphson method.

Heat balance equations are written for each node of the DSF and include conductive heat transfer in the layers, the convective heat transfer between the surface and the air, the net infrared radiation heat transfer ( $Q_{IR}$ ) and finally the absorbed solar radiation ( $Q_S$ ). Each of those terms is clearly found in equation (4B.6) of a general back facing surface temperature ( $T_{ib}$ ). For an air gap temperature

( $T_{gapi}$ ) – equation (4B.7) – there is also the convective heat transfer between the air and the boundary surfaces which should equal the enthalpy transported by the fluid (air).

$$[k_i(T_{if} - T_{ib}) + h_{c,ib}(T_{gapi,j} - T_{ib}) - Q_{IR,ib-others} + Q_{S,ib}] \Delta y = 0 \quad (4B.6)$$

<u>Conductive</u> heat transfer in the layer	<u>Convective</u> heat transfer (surface and air)	<u>Net infrared</u> radiation and heat transfer	<u>Absorbed</u> Solar radiation
--	--	---	---------------------------------------

$$[h_{c,ib}(T_{ib} - T_{gapi,j}) + h_{c,i+1f}(T_{i+1f} - T_{gapi,j})] \Delta y = \dot{m}_i c_p (T_{gapi,j} - T_{gapi,j-1}) \quad (4B.7)$$

<u>Convective</u> heat transfer (surface and air)	<u>Enthalpy</u>
---	-----------------

Contrary to the majority of layers, where the radiative properties are usually previously known and given by the manufacturers, the overall venetian blinds radiative properties need to be calculated as they depend on different parameters such as the slats angle and the incident profile angle of sun.

The knowledge of the radiative properties of a venetian blind allows it to be treated as an additional layer in a series of glazing layers, making the study of complex fenestration systems easier. The radiant analysis of the venetian blind is based on the assumptions that each slat surface segment is flat, of negligible thickness, gray, isothermal, uniformly irradiated, perfect diffuser and with non-temperature dependent properties.

It is also assumed that the slats are long enough such that the problem can be treated as two-dimensional. Venetian blinds radiative properties were performed using the net radiation method by considering only a fictive cavity between two adjacent slats considered as representative of the whole blind. The analysis of the total radiative exchange was carried out separately for solar and infrared (IR) radiation [Gomes, M.G. and Moret Rodrigues, A., (2006)]. After knowing all the radiative properties of the solid layers, the radiation fluxes within the multilayer glazing/shading system can be obtained using the net radiation method.

It is worth emphasizing that when the DSF is mechanically ventilated the airflow is supposed to be previously known, and therefore the second calculation cycle will not be used, and the thermal system can be easily solved. In a naturally ventilated DSF, an iterative solution of the thermal system has to be used as the airflow and temperature distribution are mutually dependent. Either the temperature or the airflow iteration continues until the absolute value of the maximum difference between a previous and a current node temperature and airflow is smaller than a tolerance value. The system is considered in steady state, DSF layer surfaces are all assumed as diffuse-gray for infrared radiation analysis and its material properties as constant.

Some numerical results were compared with experimental measurements carried out in an outdoor test cell [Gomes, M.G., Santos, A. and Moret Rodrigues, A., (2008)], shown in Figure 4B.1 for different venetian blind slat angles (0°, 45° and 90°) under clear sky conditions (CSC). The system overall solar transmittance is shown in Figure 4B.2.

A critical issue for the simulation of DSF is represented by the assessment of the convective heat transfer coefficient value, as described in Appendix 4I.

An image of the user interface may already be presented, Figure 4b.3.

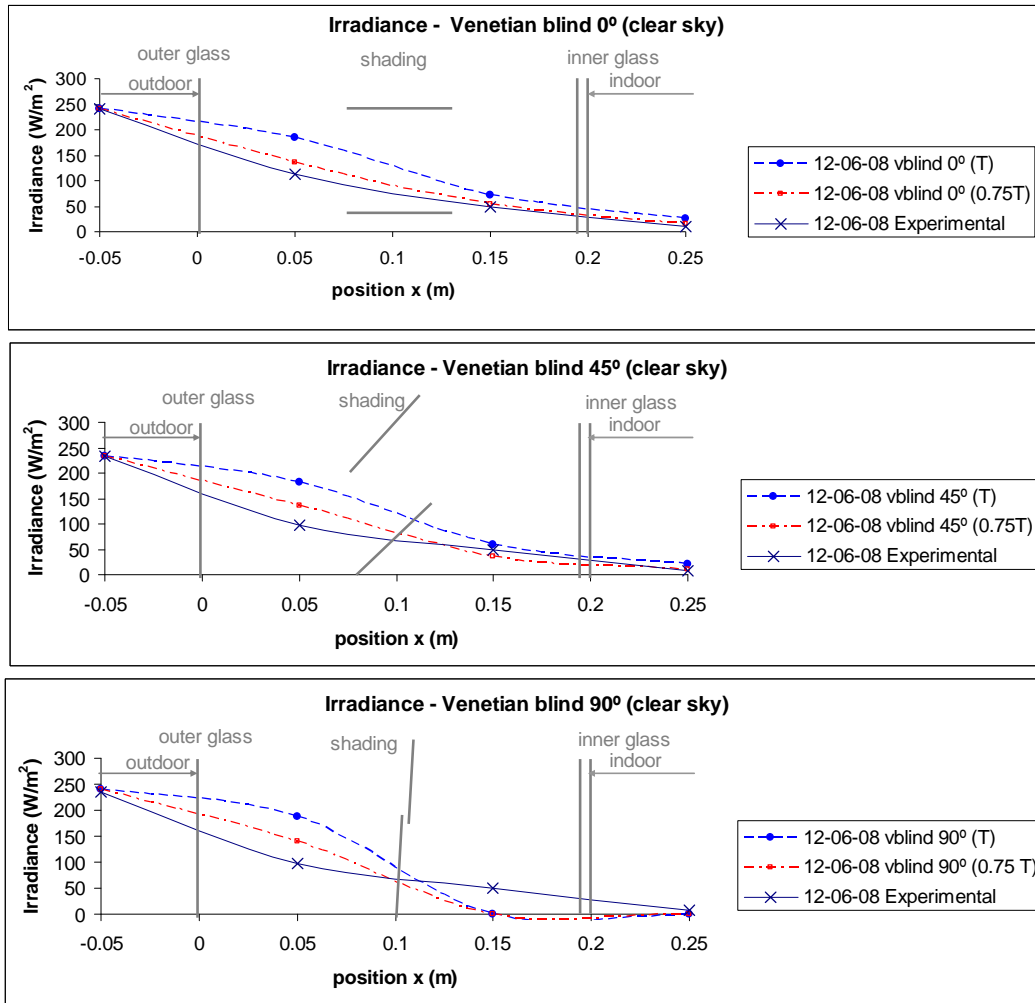


**Figure 4B.1 - Irradiance for different slat angles under CSC. Experimental and numerical results for T (the glass manufacturer transmittances) and 0.75T.**

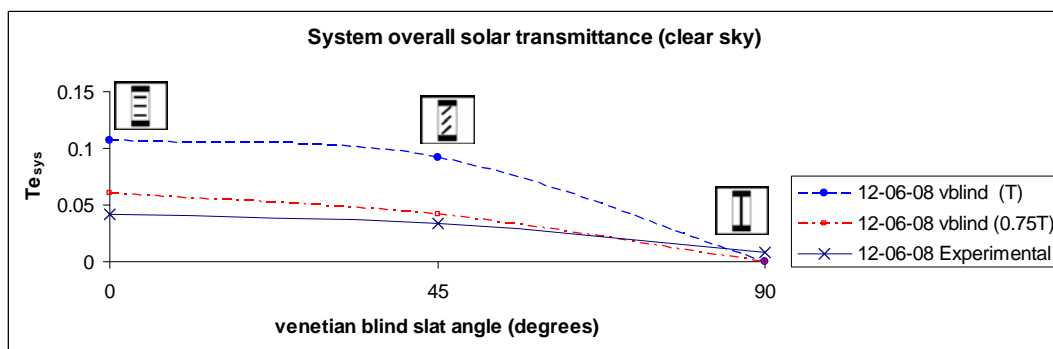


**Figure 4B.2 - System overall solar transmittance for different slat angles under CSC.**

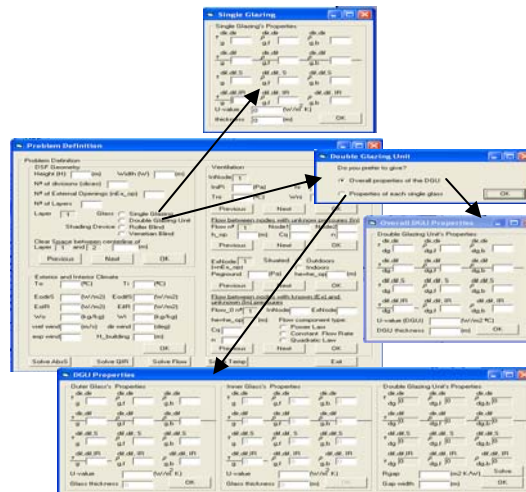
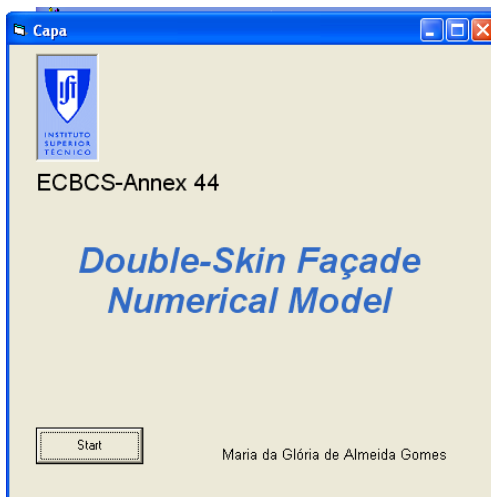


Figure 4B.3 - Program layout image.

## APPENDIX 4C

### 4C.1 Details of the experimental analysis of transparent ventilated façades with the TWINS facility (Polito)

Two different AIF types were investigated during the Annex 44 research activity using the TWINS facility at the Department of Energetics – Politecnico di Torino: a mechanically ventilated climate façade and a hybrid ventilated DSF with an outdoor air curtain ventilation scheme (with microfans powered by PV modules). In figure 4C.1 the two studied AIFs are shown.

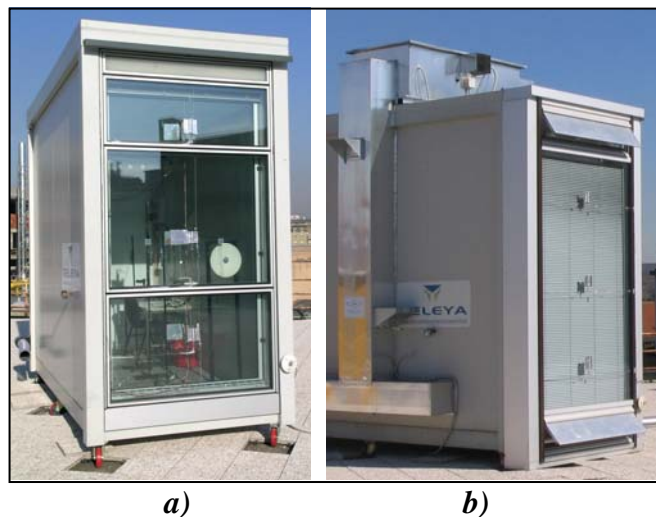


Figure 4C.1 – pictures of: a) Climate façade, b) Hybvent DSF.

The climate façade is a typical mechanical ventilated exhaust air (EA) façade. The outdoor glass pane is a double clear glass. The indoor glass pane is a single glazing system (clear).

The HybVent DSF is a façade module with a natural/hybrid ventilated air gap, integrated with a photovoltaic system. The PV system is directly connected to 6 ventilators whose aim is to increase the ventilation airflow rate in the gap when high solar radiation is present during the warm period.

The purpose of the measurements was to assess the façade energy efficiency in different climatic conditions and to obtain relevant hints on how to optimize the façade module and its seasonal operational strategies.

The hybrid ventilated façade is composed of:

- an external layer, which is a 6 mm single clear glass;
- an internal pane which is double glazed (6/12/6) with a Low-E coating (emissivity  $\varepsilon = 0.04$ ) and argon;
- a 26 cm wide ventilated air gap, where the solar shading devices are placed.

The air gap is naturally ventilated with air from the outside, which enters the façade in the lower part and leaves the façade in the upper part, through two movable lamellas, whose tilting can be regulated (Figure 4C.1b).

PV cells are located in the upper lamella and are directly connected to axial micro fans placed in the gap. The fans are activated when high solar radiation is present and ventilation becomes fan assisted, thus determining an airflow increase.

The fans are activated when solar irradiance is over 70 W/m<sup>2</sup>. This value should be considered as the pickup irradiance value. During the day, when the fans are already operating, lower irradiance values are sufficient to make the fans work. The operational strategies of the façade are different, according to the season and the solar irradiance:

- in the summer period and when solar irradiance is high enough to activate the fans, the lamellas are completely open (tilt of about 45°) and the ventilation is hybrid (fan assisted);
- in mid season or in summer with low solar radiation values, the lamellas are open and the gap is naturally ventilated (the fans are not working);
- in the winter season, the lamellas are completely closed to increase thermal insulation and, when solar radiation is relevant, to obtain a hot buffer caused by the presence of the shading device in the gap.

The presence of a control system could increase the responsiveness of the façade to the boundary conditions and some other ventilation strategies could be exploited, but at this stage of the research the aim was to assess the façade energy efficiency in the simplest and cheapest configurations.

Four different ventilation strategies were considered for the ventilation in summer and during midseason: natural ventilation and ventilation assisted by means of 2, 4 and 6 fans. During winter, the natural ventilation and closed air cavity (buffer façade) configurations were adopted.

As far as the solar shading device in the air cavity is concerned, an aluminium venetian blind, with micro perforated lamellas (4% of holes, emissivity  $\varepsilon=0.75$ ) and a glass fiber + PVC roller blind, with a reflecting coating towards the outdoor environment, were tested.

For both the AIF types the measured quantities are: air, glass and frame temperatures, incident and transmitted irradiance, heat fluxes, mechanically driven air flow rate, pressure difference. The reference façade was monitored by means of 18 sensors connected to a datalogger, the measurement apparatus for the tested AIFs consisted of 52 and 41 sensor for the climate and the hybrid ventilated façade respectively. For both the façades the experimental campaign lasted one whole solar year. In figure 4.22 - section 4.3.4.1 a scheme of sensors for the reference and the tested façade is shown. A more detailed description can be found in [Micono et al (2006)] and in [Perino et al. (2007)].

## 4C.2 The experimental campaigns

The experimental campaigns lasted from March 2005 to January 2006 for the climate façade and from February 2007 to February 2008 for the hybrid one. The façades were thus monitored under different weather conditions and in different seasons: midseason, summer and winter. To assess the performance of the façades, a sensitivity analysis was carried out changing two façade elements (the solar shading device and the internal glazing) and an operational parameter (air flow rate and ventilation strategy). The two different solar shading devices were an aluminium venetian blind and a reflecting roller screen. The internal glazing were a clear glass and a low-e glass.

Because of the high number of possible combinations, and the statistical variability of the outdoor climate, it was not possible to collect consistent data for every configuration in every season. Moreover, some configurations were considered important just in some particular season.

### 4C.2.1 Winter conditions

In winter conditions the two façades adopts two different ventilation strategies, and it's almost impossible to compare their behaviours. The climate façade works as an exhaust for the ventilation air, and this leads to have an air layer in the ventilated cavity, working as a warm buffer both in presence and in absence of solar irradiance.

The climate façade can be also integrated with the HVAC system to pre-heat the supply air. The climate façade had thus an active behaviour in winter conditions.

The hybrid ventilated façade adopts a closed air gap as a normal winter configuration, in order to obtain a greenhouse effect. The dynamic characteristics of the façade, mostly related to the interaction between the heated shading device and the air flowing in the gap, are thus limited during winter conditions. This behaviour is much closer to the one of a traditional passive building envelope element, and allowed to calculate the relationship among the heat flux exiting the indoor environment and the difference between indoor and outdoor air temperature.

#### Transmittance

During night time, when the solar incident solar radiation it was possible to calculate the transmittance.

In figure 4C.2 the heat fluxes during night time for the reference and the hybrid façade are plotted. The thermal transmittance of the hybrid façade is  $0.93 \text{ W/m}^2\text{K}$ , whereas the reference façade's one is  $2.04 \text{ W/m}^2\text{K}$ .

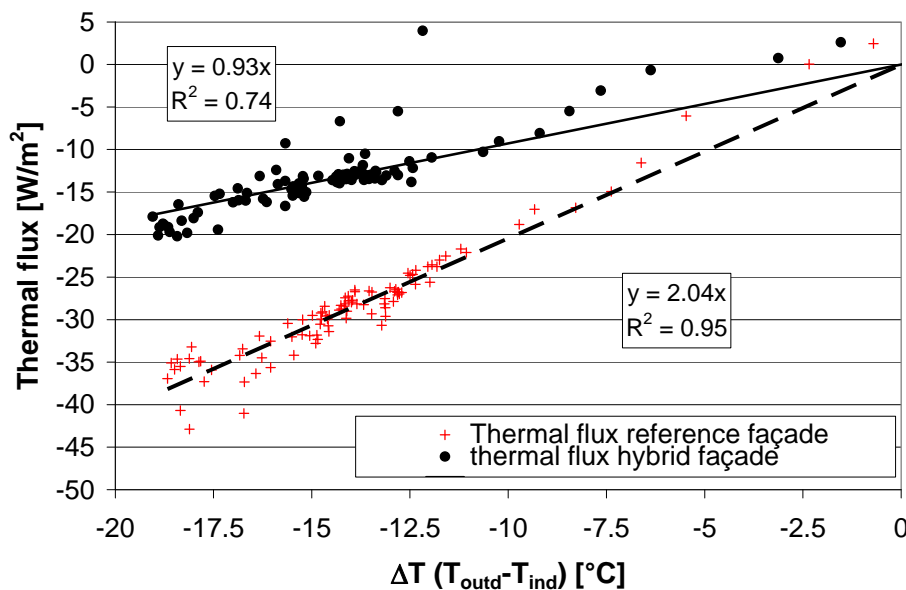


**Figure 4C.2 – Transmittance of hybrid and reference façade, night time conditions.**

#### “Long wave” heat fluxes

It is possible to compare the two monitored AIF considering winter days with similar weather conditions. In figure 4C.3 and 4C.4 the “long wave” heat fluxes for the two façades in similar days are plotted. Figure 4C.3 shows that the best configuration for the hybrid façade is obtained adopting a closed air gap: during the day the flux is mainly entering, with peak values of  $55$  and  $60 \text{ W/m}^2$  depending on the shading device; opening the air gap the peak value lowers down to about one third and it's similar to the flux entering the climate (mechanical ventilation) façade (figure 4C.4). When the air gap is open (natural ventilation configuration) the air in the cavity is longer acting as a warm buffer layer. For the climate façade an increase in the ventilation air flow rate leads to lower entering long-wave heat fluxes: higher air flow rates removes a higher portion of the irradiance absorbed by the solar shading. The hybrid ventilated façade shows a better performance during night time conditions that can also be considered representative of low irradiance daytime conditions

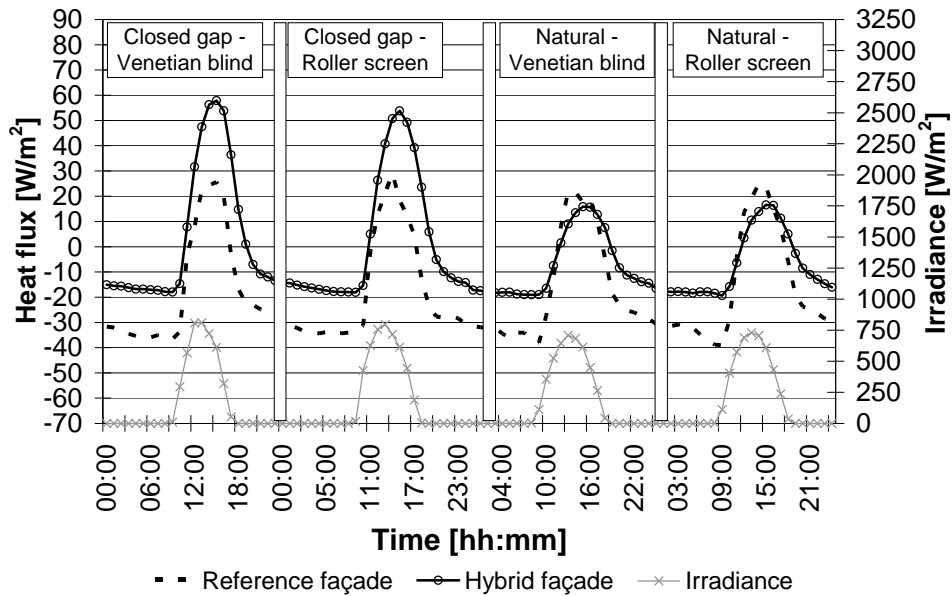


Figure 4C.3 – “Long wave” heat fluxes entering the hybrid and the reference façades, winter conditions.

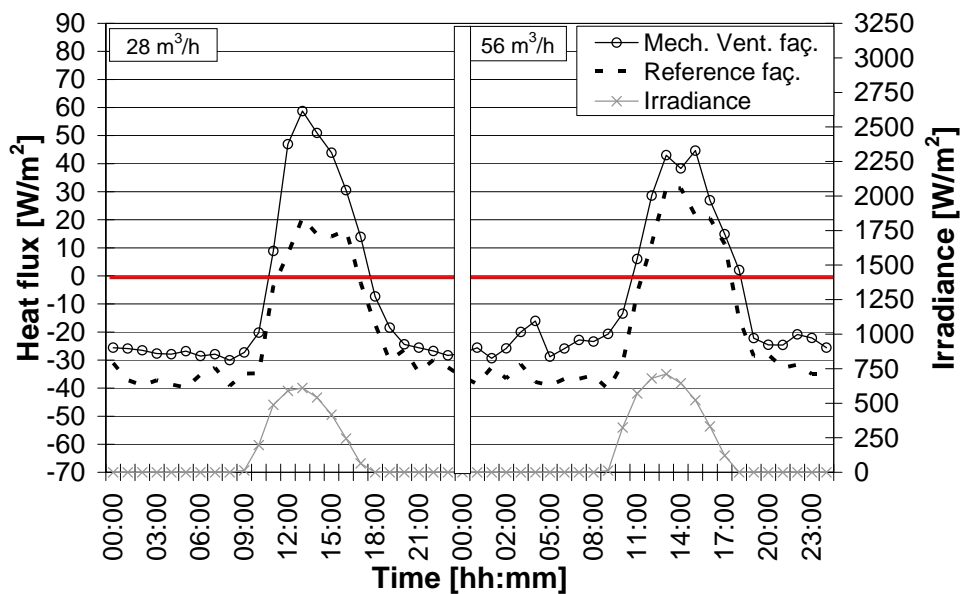


Figure 4C.4 – “Long wave” heat fluxes entering the climate and the reference façade, winter conditions.

During night time the reference façade loses between 30 and 40  $\text{W/m}^2$ , but, while the climate façade loses between 20 and 30  $\text{W/m}^2$ , the hybrid façade always loses less than 20  $\text{W/m}^2$ . This better performance is mainly related to the adoption, for the hybrid façade, of a low-e double glass as layer facing the indoor environment.

#### Normalized total heat fluxes

A better behaviour of the hybrid façade can be seen considering normalized heat fluxes.

In figures 4C.5 and 4C.6 it is shown that without or with low solar radiation (night time conditions) the total flux is mainly exiting the indoor environment, whereas with high values of solar radiation the flux is entering.

During night time the normalized total flux for the hybrid façade with closed air gap is about -0.5, this means that the façade loses about 50% less than the reference one. When the air gap is open and

there's natural ventilation, the hybrid façade loses between 40% and 50% less than the traditional one.

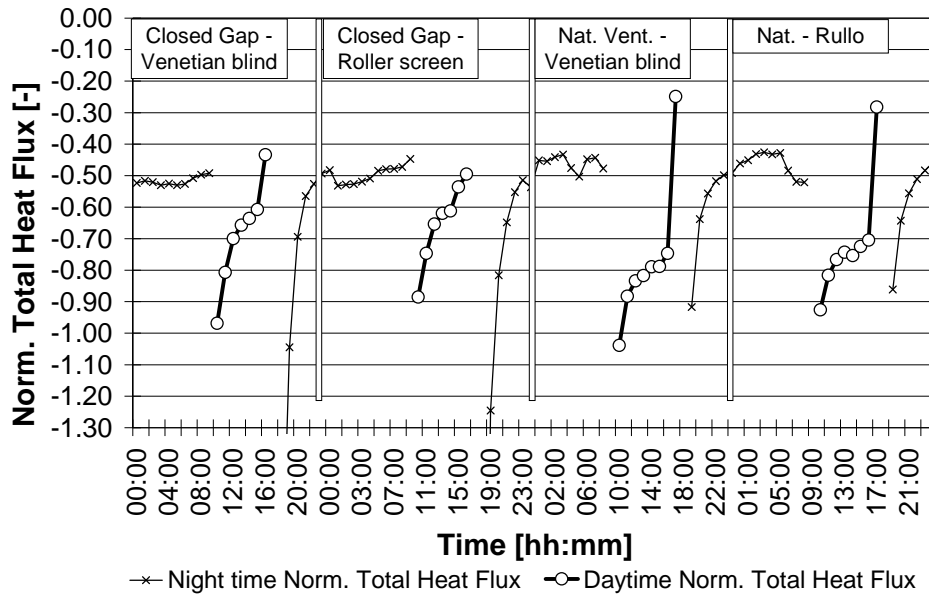


Figure 4C.5 – Normalized total heat flux, hybrid ventilated façade, winter conditions.

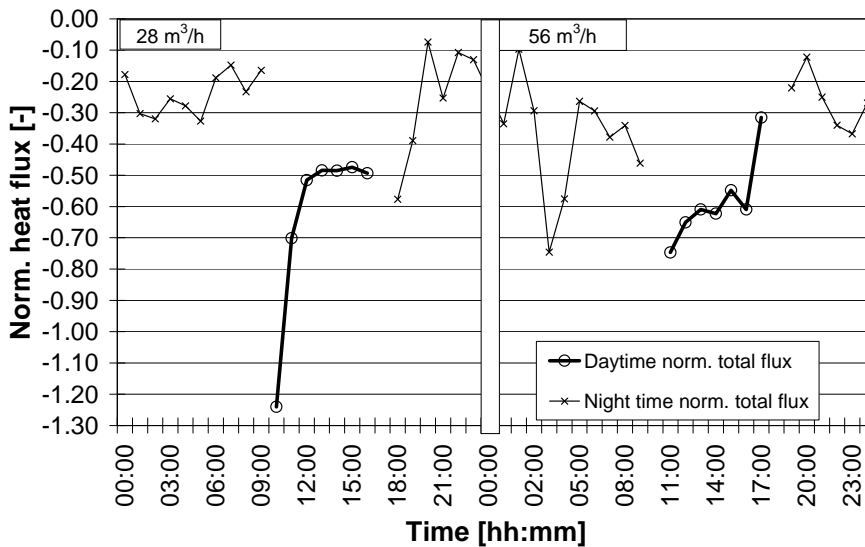


Figure 4C.6 - Normalized total heat flux, mechanically ventilated façade.

During daytime both the AIFs allow a lower total heat flux entering the indoor environment with respect to the reference one, and this behaviour is related to the absence of the solar shading device in the reference façade. It has to be underlined, yet, that without solar shading device the solar radiation enters directly the indoor environment, leading to a better energy performance but with a probable local discomfort.

The climate façade causes a reduction in the entering total heat flux between 50% and 60%, with the hybrid ventilated one a reduction of at least 65% with respect to the traditional façade.

The different behaviour between the two ATFs can be explained with their different solar transmission coefficient (figure 4C.7). The hybrid ventilate façade always shows a lower capability to transmit solar radiation to the indoor environment with respect to the mechanically ventilated one. Between the configurations adopting the venetian blind there's an average difference of about

0.1÷0.15. During the same hours, with the same configurations, the average difference in the normalized total heat fluxes is about 0.15.

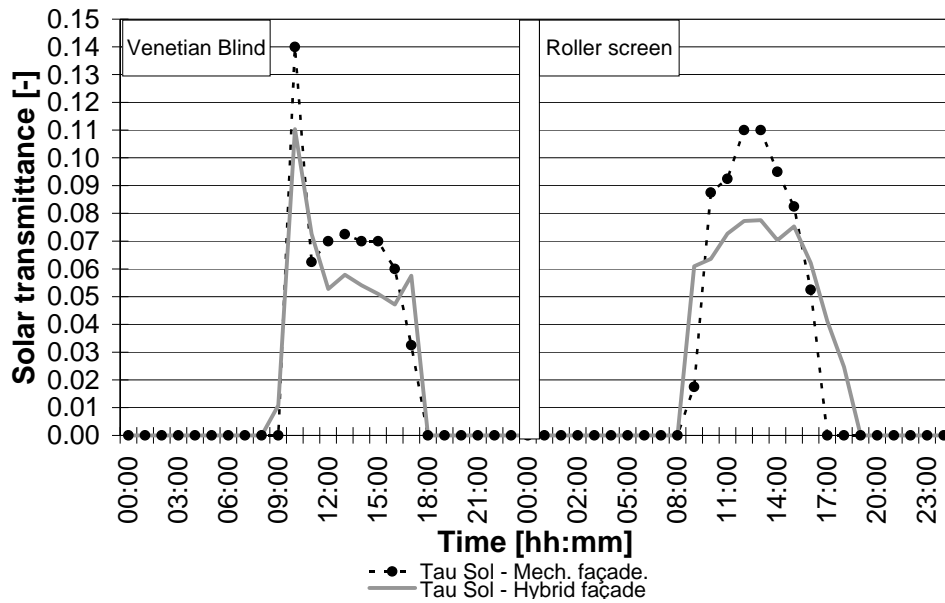


Figure 4C.7 – Solar transmittance coefficient for the monitored AIFs.

Pre-heating efficiency

For all the analysed cases the efficiency (figure 4C.8) is negative for at least 50% of operative time.

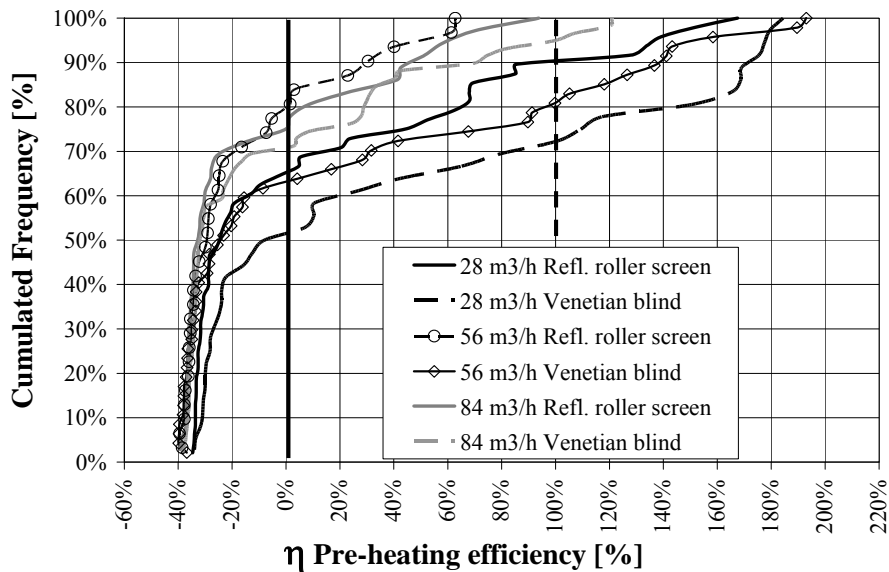


Figure 4C.8 – Pre-heating efficiency for the climate façade.

This means that for most of the time the façade cools the air flowing in the gap instead of heating it. The pre-heating efficiency seems to be inversely related to the air flow rate: an increase of the air flow leads to a progressive reduction of the efficiency. Variations in the efficiency between two different air flow rates are remarkable. In configurations with the venetian blind, at 28 m3/h a heating effect ( $\eta > 0$ ) can be observed for about 50% of time and there's a full compensation of the ventilation losses ( $\eta \geq 1$ ) for about 27% of time. These values proportionally decrease if the air flow rate is increased: at 84 m3/h the air is heated for 30% of time and ventilation losses are completely compensated just for 5% of time.

The configuration at an intermediate air flow rate (56 m3/h) with the reflecting roller screen seems to be the less efficient, not confirming thus the relation between air flow rate and pre-heating

efficiency. This behaviour is probably related to the presence of low solar radiation during measurements for that configuration.

### 4C.2.2 Summer conditions

#### Dynamic insulation efficiency

In Figure 4C.9 the dynamic insulation of both the tested AIFs is plotted. The Hybrid ventilated façade always shows a higher capability to remove the entering heat flux with respect of the climate façade, the roller screen being more effective in both the façades.

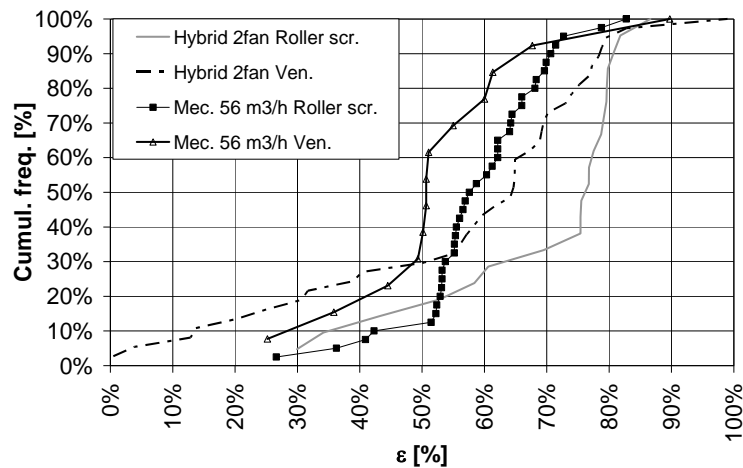
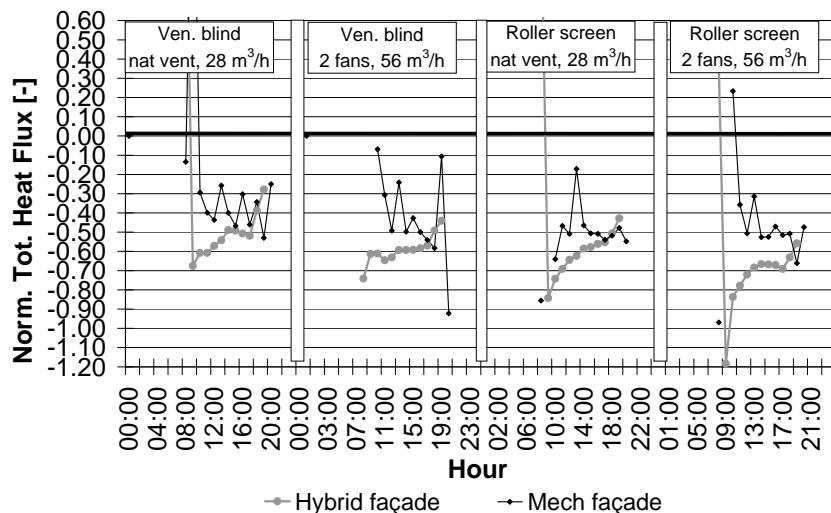


Figure 4C.9 – Dynamic insulation efficiency of the two active façades.

With the hybrid façade about 60% of the entering heat flux is removed for 70% of time, the climate façade can remove the same fraction of flux for no more than 45% of time. In both cases the most effective reduction is achieved using the reflecting roller shading. The best configuration is the hybrid façade adopting the reflecting roller screen (60% of flux removed for 70% of time), the worse is the climate façade adopting the venetian blind as shading device (60% of flux removed for 20% of time).

#### Normalized total heat fluxes and normalized total daily energy

The analysis of normalized total heat fluxes shows (figure 4C.10) that in summer conditions the performance of both the façades improves with a higher ventilation rate. The hybrid ventilated one always allows a higher reduction in the entering fluxes during the whole day. The roller screen allows a better performance. During the day the climate façade performance improves, whereas the performance of the hybrid ventilated one lowers passing from the morning to the afternoon.



**Figure 4C.10 – Normalized total heat fluxes, summer conditions.**

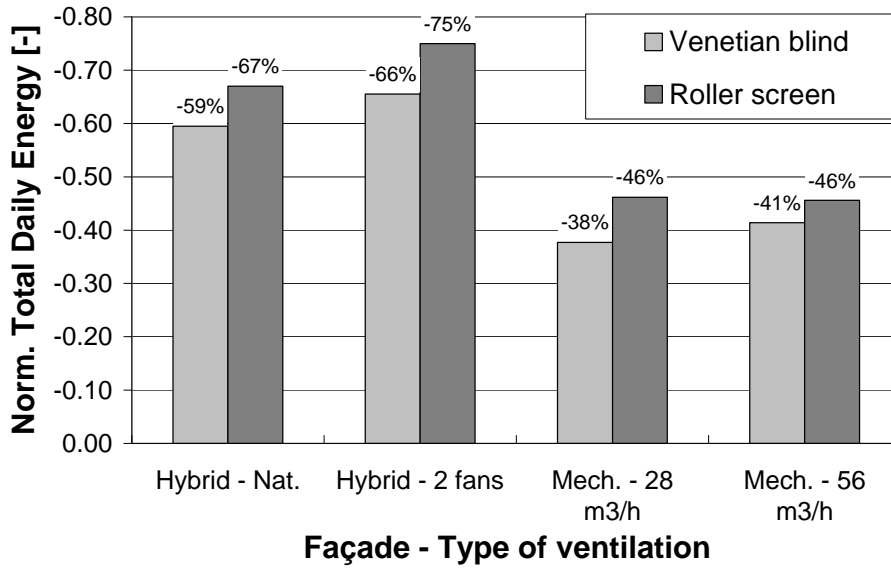


**Figure 4C.11 – Normalized total daily energy for the two AIFs, summer conditions.**

Furthermore (figure 4C.11), the hybrid ventilated façade shows a reduction of the entering daily energy, with respect to the reference façade, between 59% and 75%; the climate façade gives a reduction between 38% and 46%. In both cases a higher air flow rate and the use of a roller screen allows a better behaviour in summer conditions.

Normalized surface temperature of inner glass

In Figure 4C.12 is clearly shown that with both the façades a better thermal comfort, with respect to the reference one, is achieved. In summer  $g_{gi}$  is always negative. It is clear the influence on the thermal performance of the low-e inner double glass of the hybrid ventilated façade. The climate façade has a inner glass temperature 11% lower than the reference one at the best, whereas for the hybrid façade the maximum reduction is of about 70%. For both the AIFs the reflecting roller screen configuration gives a lower temperature and allows then better comfort conditions.

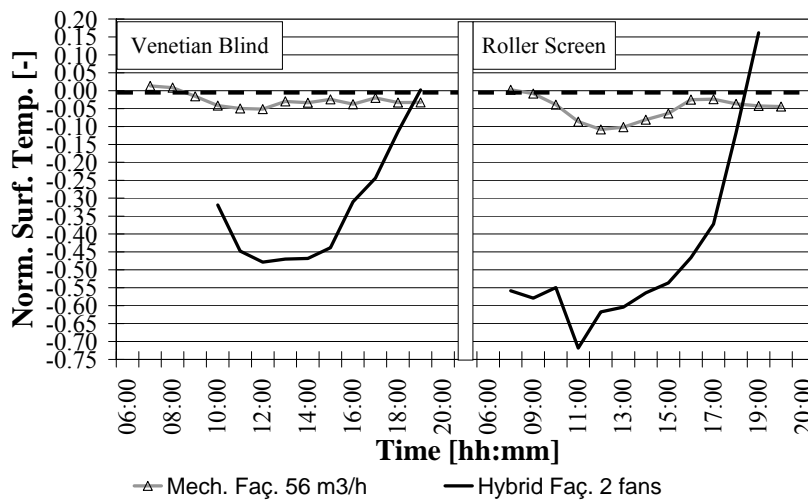


**Figure 4C.12 – Normalized total daily energy for the two AIFs, summer conditions.**

### **4C.2.3 Resume of main results (Hybvent module)**

The main results can be synthesized as follows:

#### Winter period

- the assessment of the active façade as a conventional building envelope component (during night and with the air gap closed) shows good thermal insulation properties (the thermal transmittance of the active façade is half that of the reference one);
- in the hypothesis of using the façade as “supply-air”, by pre-heating the air flowing in the façade, a full compensation occurs for about 40% of the time with the venetian blind, and for 35% of the time, if the roller screen is adopted;
- if the air gap is closed, it can work as a hot buffer which provides high energy gains; if it is open, it can limit the undesired gain and reduce the risk of overheating, which can also affect users in the winter period;

#### Summer period

- the façade is able to limit the thermal loads in a relevant way, especially when 6 fans are activated, and the roller screen is adopted; the reduction of the entering fluxes can reach 90% for 50% of the time.

In short, the tested active façade exhibits a good performance from the energy efficiency point of view. Its working strategies were intentionally set in a rather simple manner in order to make this building envelope component easily applicable. Its weakness can be put down to the presence of fans, which implies higher maintenance costs. The good results obtained with 2 fans suggest their number can be limited.

## **APPENDIX 4D**

### **4D.1 Experimental analysis of transparent ventilated façades with the LNEC facility**

In order to evaluate the thermal behaviour of different façade types, with various ventilation strategies (natural, mechanical or hybrid) LNEC (39° N) assembled a nearly south facing (160°) test facility allowing changing among some of the possible configurations. It is possible to test configurations such as: Outdoor Air Curtain (OAC), Indoor Air Curtain (IAC), Exhaust Air (EA), or Supply Air (SA). It is also possible to use any kind of ventilation type, the layout being established as a box window (BW) or, as a limit, as a Buffer (Bf) configuration.

The glazed façade has size of 2.5 m height and 3.5m length, the gap depth being of 0.20 m. The outer pane has a simple annealed 5 mm glass ( $U=5,7 \text{ W/m}^2/\text{K}$ ;  $T_v=87\%$ ;  $T_e=75\%$ ;  $A_e=18\%$ ;  $g=0,80$ ) and the inner one is a ( $U=1,4 \text{ W/m}^2/\text{K}$ ;  $T_v=69\%$ ;  $T_e=36\%$ ,  $A_e=34\%+3\%$ ;  $g=0,41$ ) double glass (6-16-5), with a low emissive coating facing the gap. The shading device is a grey roller blind. The gap has eight sets of louvers, 0.22 5m high and 1.63 m long each, four in the outer pane and four in the inner one, the blades position being adjustable between fully closed and fully open (blades perpendicular to the façade plane).

T and A standing for the transmissivity and absorptivity, v refers to the visible part of the spectrum and e refers to energy. The interior space is bounded by walls made of:

**Walls:** autoclaved aerial concrete (AAC) blocks, 0,30 m thick with interior and exterior plaster cover 0,015 m each.

**Structure:** concrete columns (0,20x0,20 m<sup>2</sup>), covered indoors by 0,050 m slabs of the wall material.

**Ceiling:** slab 0,14 m thick, covered indoors by 0,075 m slabs of the wall material, water sealed and covered with gravel by the exterior.

**Floor:** light concrete mortar.

**Table 4D.1 - Materials thermal characteristics**

1. Material	2. $\rho$ [kg/m <sup>3</sup> ]	3. K [W/mK]	4. $c_p$ [kJ/kg K]
5. Concrete	6. 2300	7. 1,75	8. 0,880
9. AAC	10. 650	11. 0,20	12. 1,000
13. Mortar	14. 1950	15. 1,15	16. 0,653



**Figure 4D.1 – The AIF at LNEC and louver detail.**

The monitoring campaigns were carried out between July 2007 and January 2008 having in mind the evaluation of the thermal behavior of the different tested configurations and also the changes of temperature within the DSF gap. Two positions of the shading device were also tested: midway between glazed panes and closer to the inner pane. Environmental parameters were also measured: outdoor and indoor temperature (with Gemini stand alone loggers); wind velocity and direction (NRG with Ammonit logger); and solar radiation on horizontal and vertical (indoor and outdoor) planes (with pyranometers). Measurements were recorded as 10 minutes averages from 30 seconds readings and (apart the referred two) recorded by a Datalogger.

Measurements considered in this paper refer to the following DSF configurations (Figure 4.19 – section 4.3.4.2): Bf; OAC; EA; and SA. The letter after the configuration (\*\*\_X) refers to the roller blind position – Bottom, Medium, Top -, and the “i” refers to the shading inner position.

The main idea of the tests performed at LNEC’s facility was to evaluate the thermal performance of a set of DSF configurations. A major difference from the Torino tests lies on the ventilation scheme, being fully natural at LNEC it prevents the mass flow control and needs estimated values for each case. The flow velocity between two openings can be evaluated by:

$$U = \frac{1}{\sqrt{\zeta}} \sqrt{\frac{2}{\rho} \Delta P} \quad [m / s] \quad (4D.1)$$

where  $\zeta$  is the head loss coefficient ( $C_d=1/\sqrt{\zeta}$ ),  $\rho$  is the air density and  $\Delta P$  the pressure difference between openings evaluated, for thermally created  $\Delta P$  by (Marques da Silva, 2004),

$$\Delta P^T \approx 0,042 H_{12} \Delta T \quad [Pa] \quad (4D.2)$$

$H_{12}$  being the openings height difference and the temperature difference between inside and outside in the range  $23K < \Delta T = T_i - T_e < 8K$ . A value of  $\sim 900 \text{ m}^3/\text{h}$  with no shading (assumed  $C_d=0.55$ ) was estimated for a sunny day and also measured with tracer gas equipment. Anyway flow measurements need further work as well as proper evaluation of the system (louvers and gap) head losses.

## 4D.2 The experimental campaigns

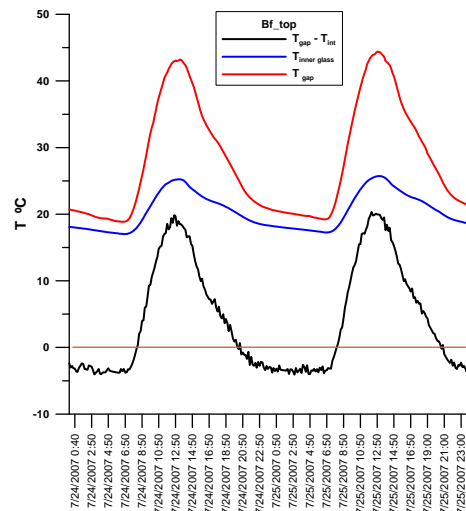
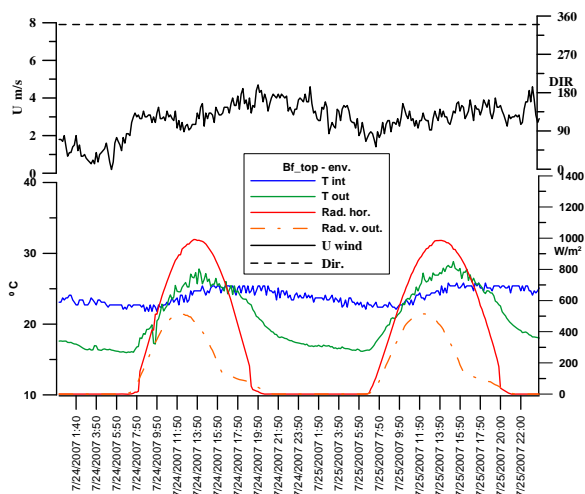
Performance evaluation is presented by time series for the measurement periods of the following quantities or arrangements between them (see figures 4D.2 to 4D.7. Configurations of DSF with different shading positions: \*\*\_X refers to the roller blind position – Bottom, Medium, Top -, and the “i” refers to the shading inner position).

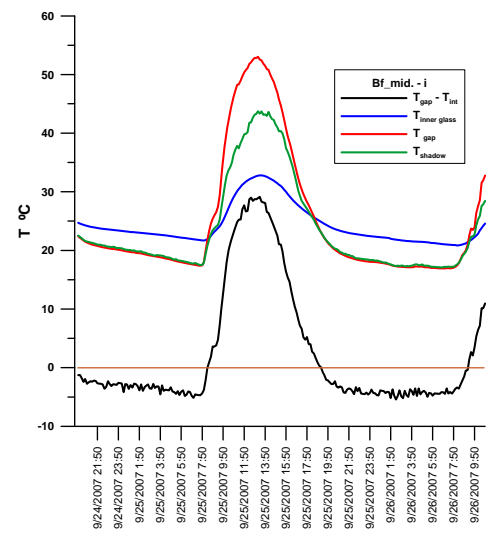
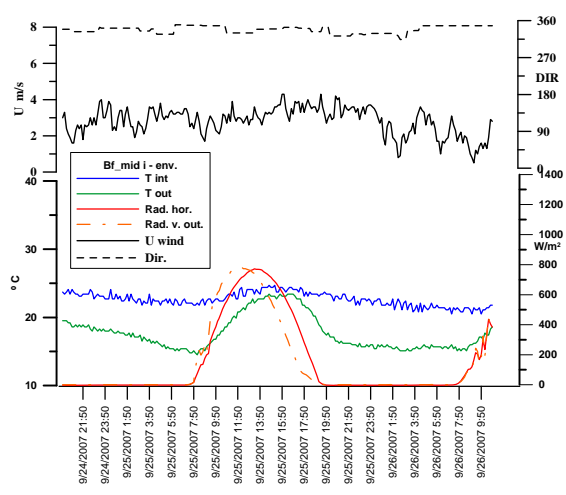
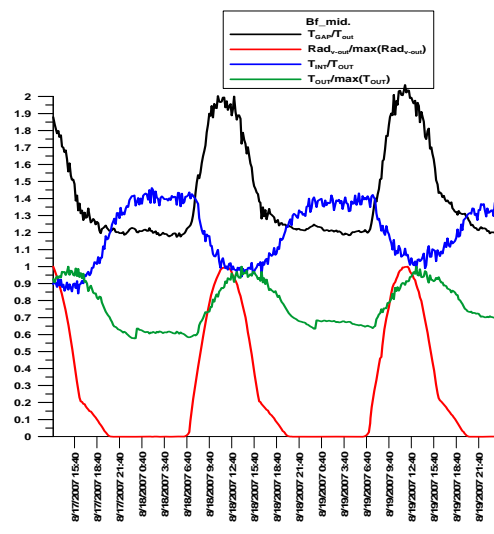
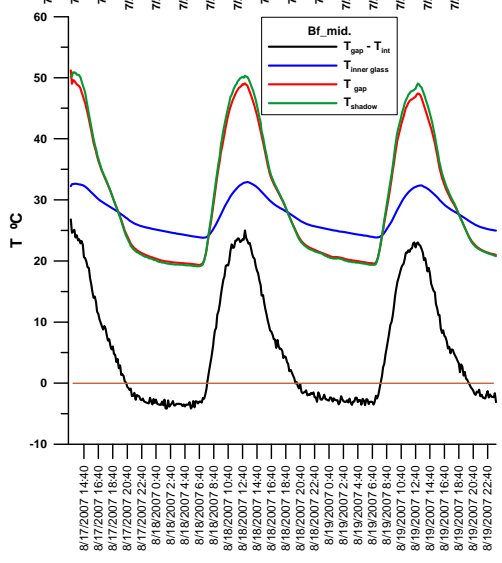
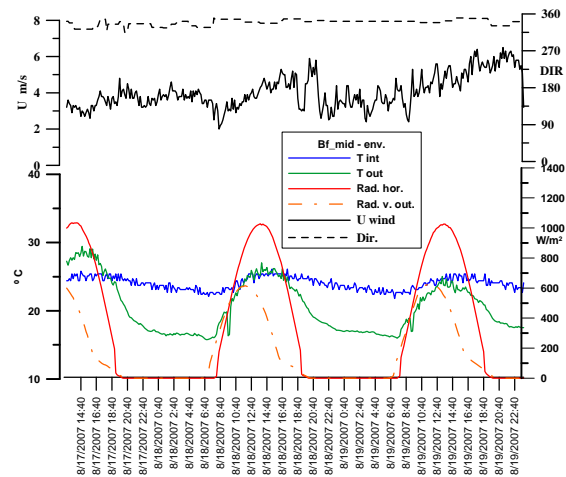
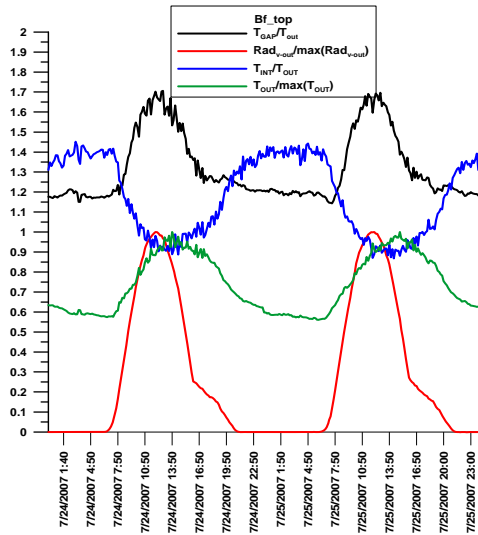
- Environmental – outdoor and indoor temperatures, horizontal and vertical plane solar radiation, wind velocity and direction (measured 6m above ground by an anemometer sited 20m NE from the cell, with no close obstacles);
- AIF (at 3 height levels) – air temperature on both sides of the roller blind and at louver level, roller blind and glazing temperatures, heat flux between outdoor and the gap and from here to the inner space, radiation entering the inner space.

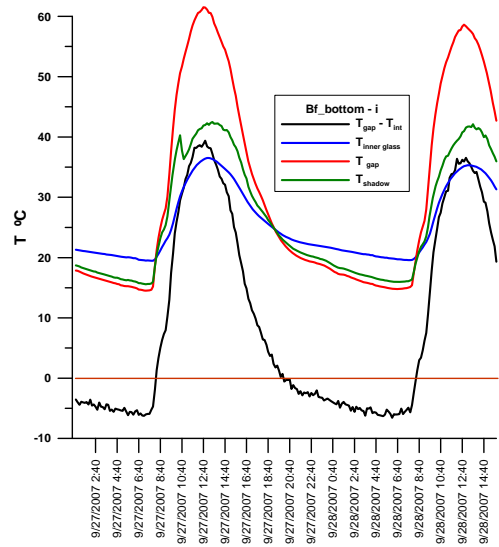
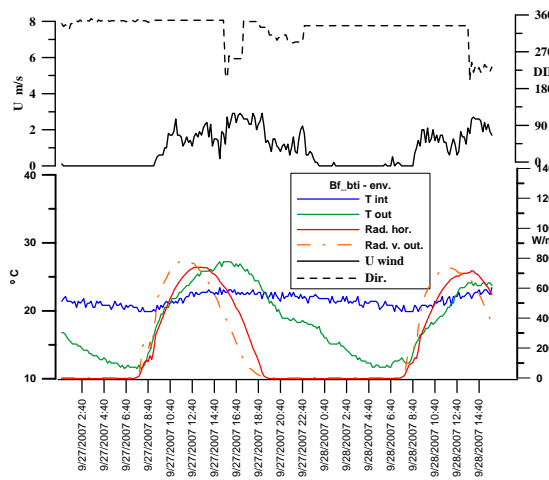
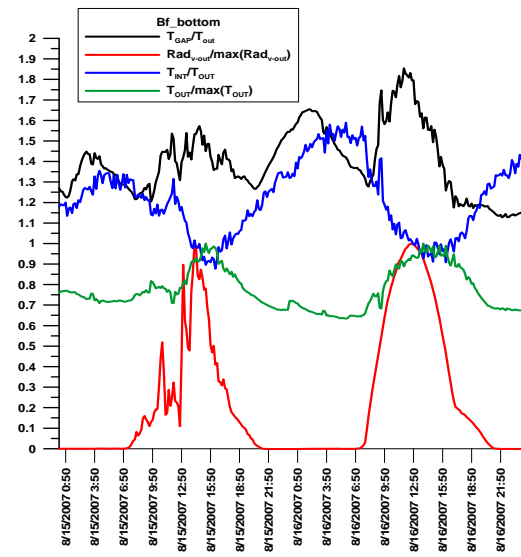
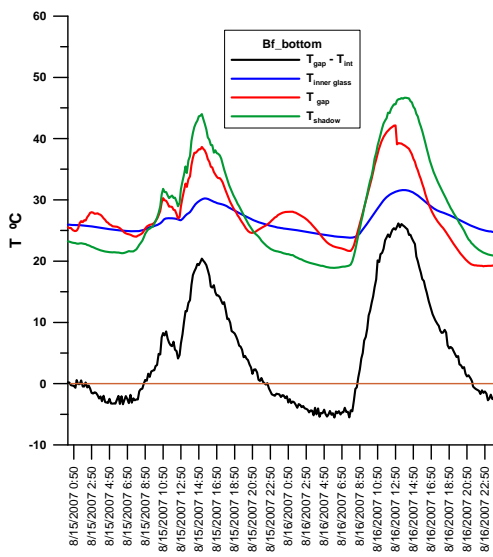
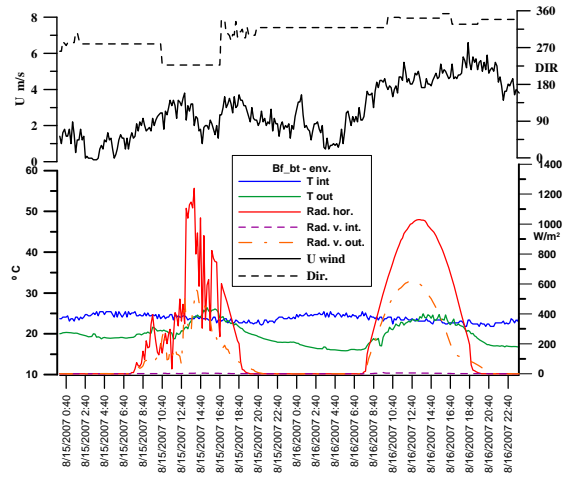
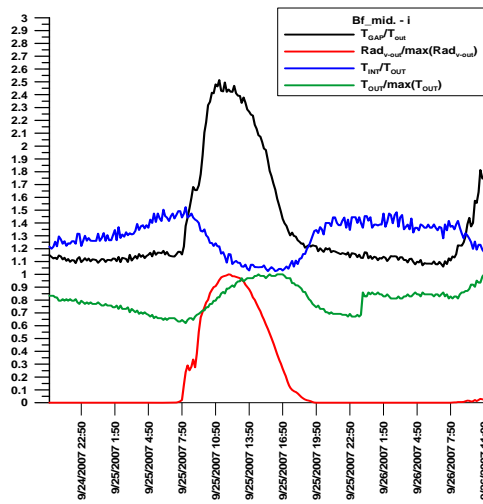
The referred arrangements of the measured quantities consist on temperature differences, like the one between the bulk air gap and outdoor, or indoor, temperatures; the total energy entering the inner space,  $q_i = \text{heat flux} + \text{radiation}$ , the dynamic insulation,  $\epsilon$ , as defined in equation (2) – section 4.3.4.1 – where the unrealistic values rising from very low values of  $Q_{in}$  were set to zero. For EA configurations the reference to  $\epsilon^*$  means that  $T_{int}$  is used instead of  $T_{out}$  as the flow enters the façade from indoors. Some dimensionless values are presented (vertical plane radiation and outdoor temperature were converted to dimensionless values by their daily maximums).

For each configuration a set of figures are presented showing the environmental conditions of the measuring period, different temperature and energy evaluations.

### Buffer configuration







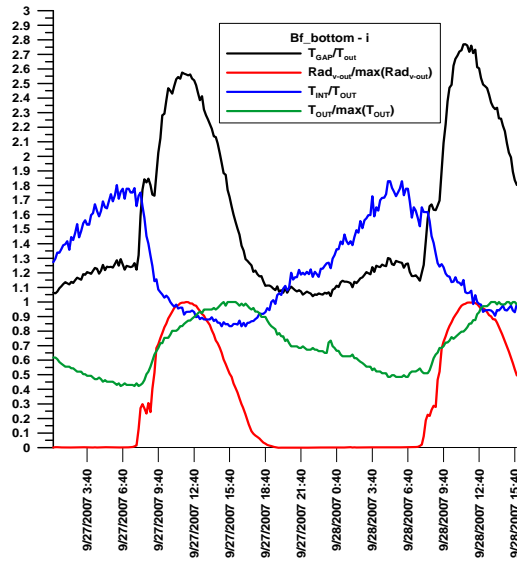
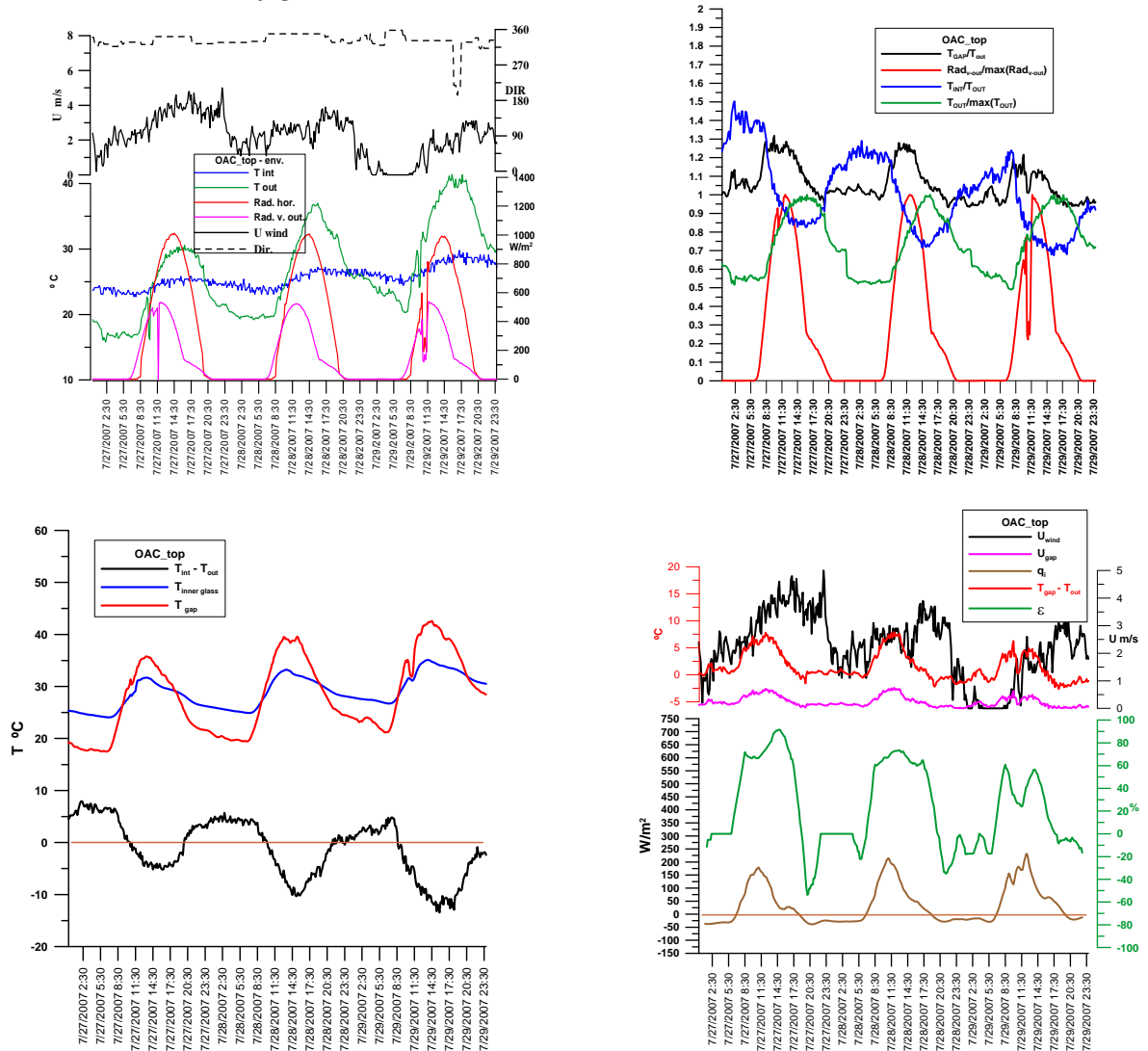
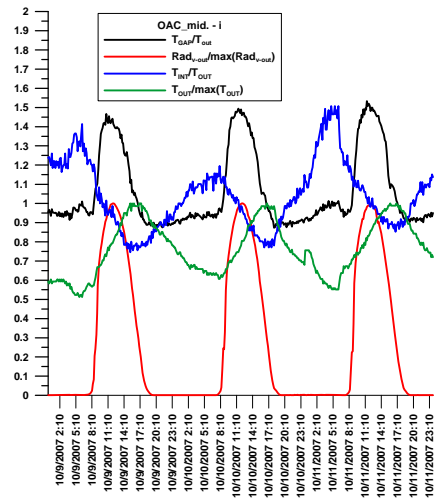
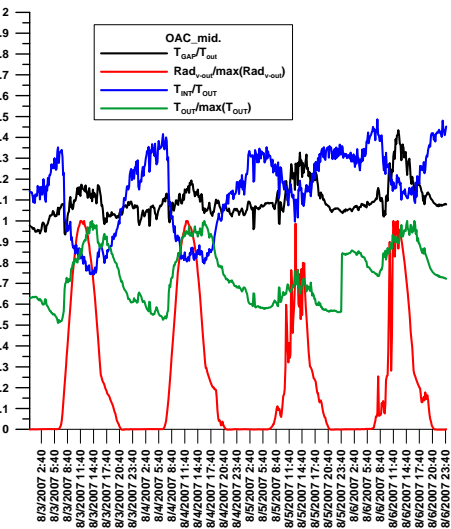
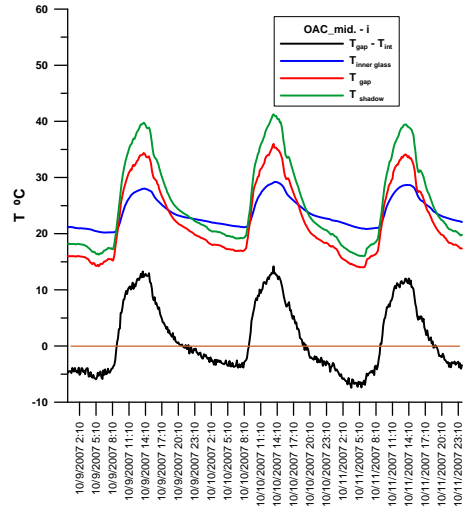
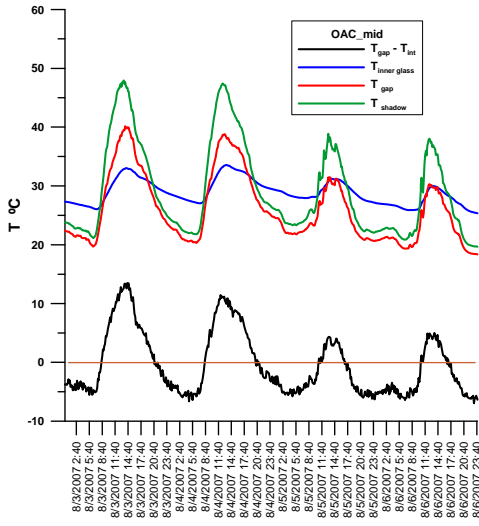
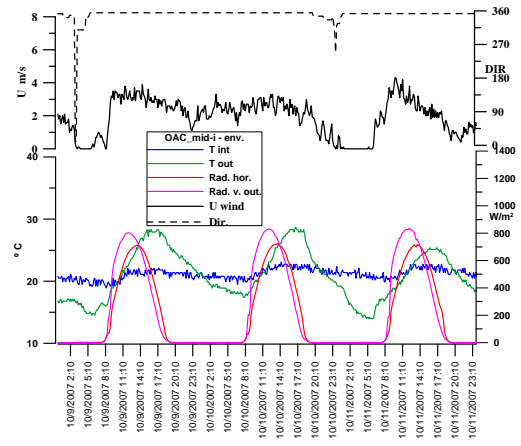
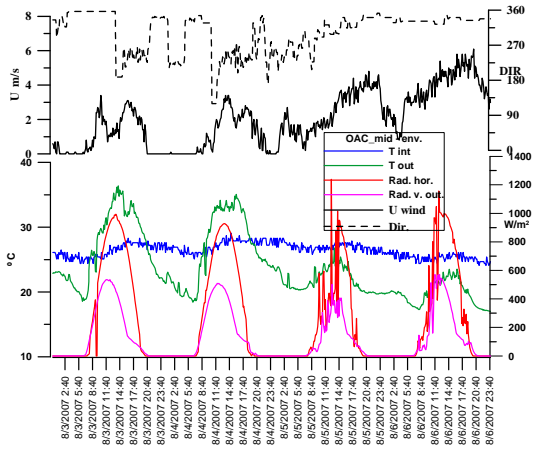
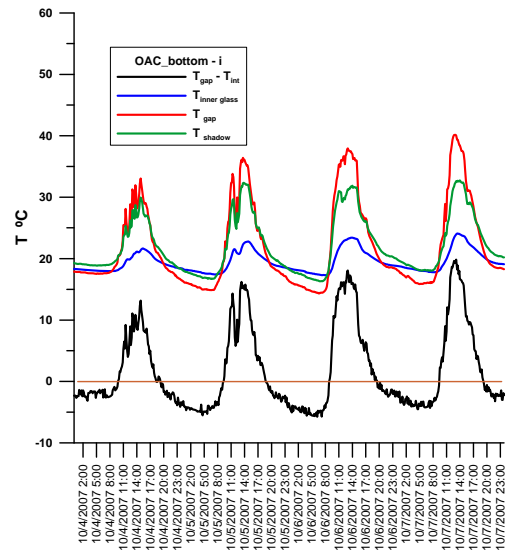
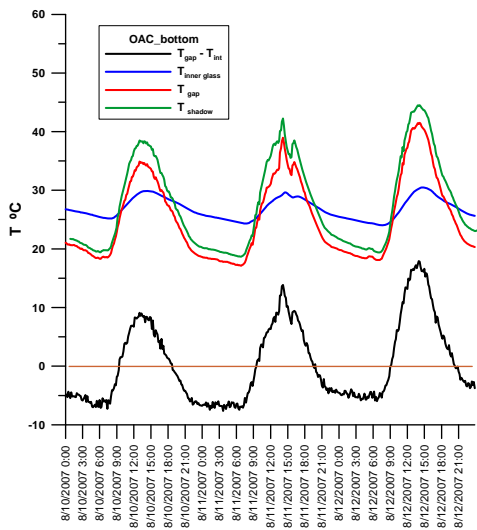
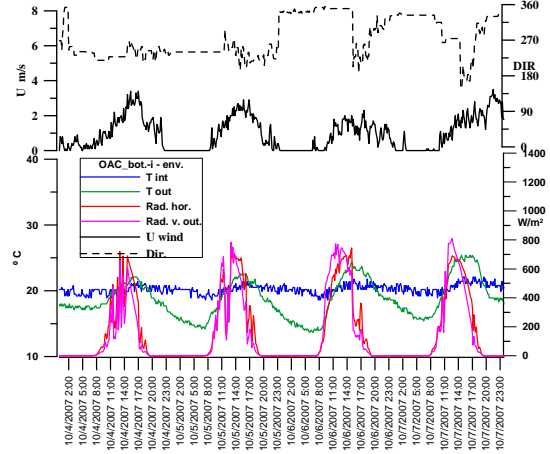
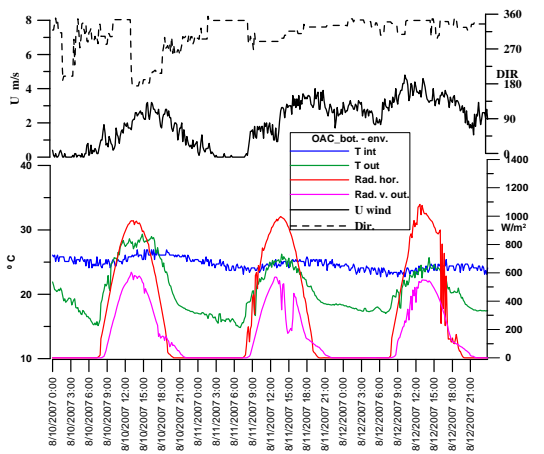
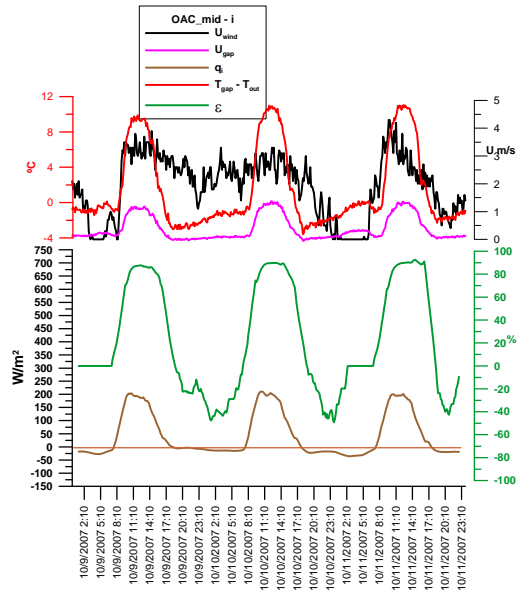
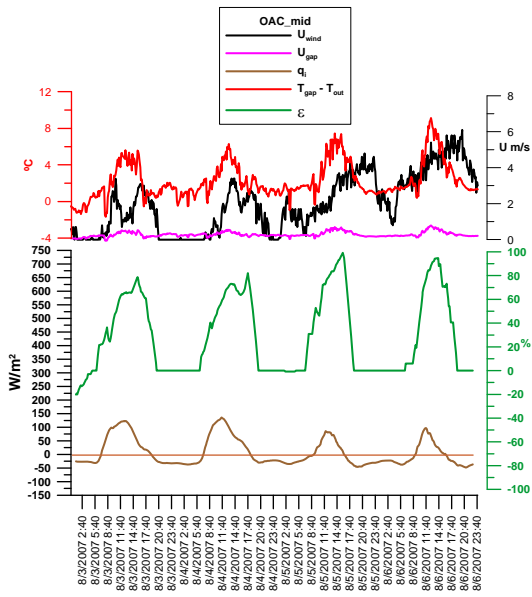


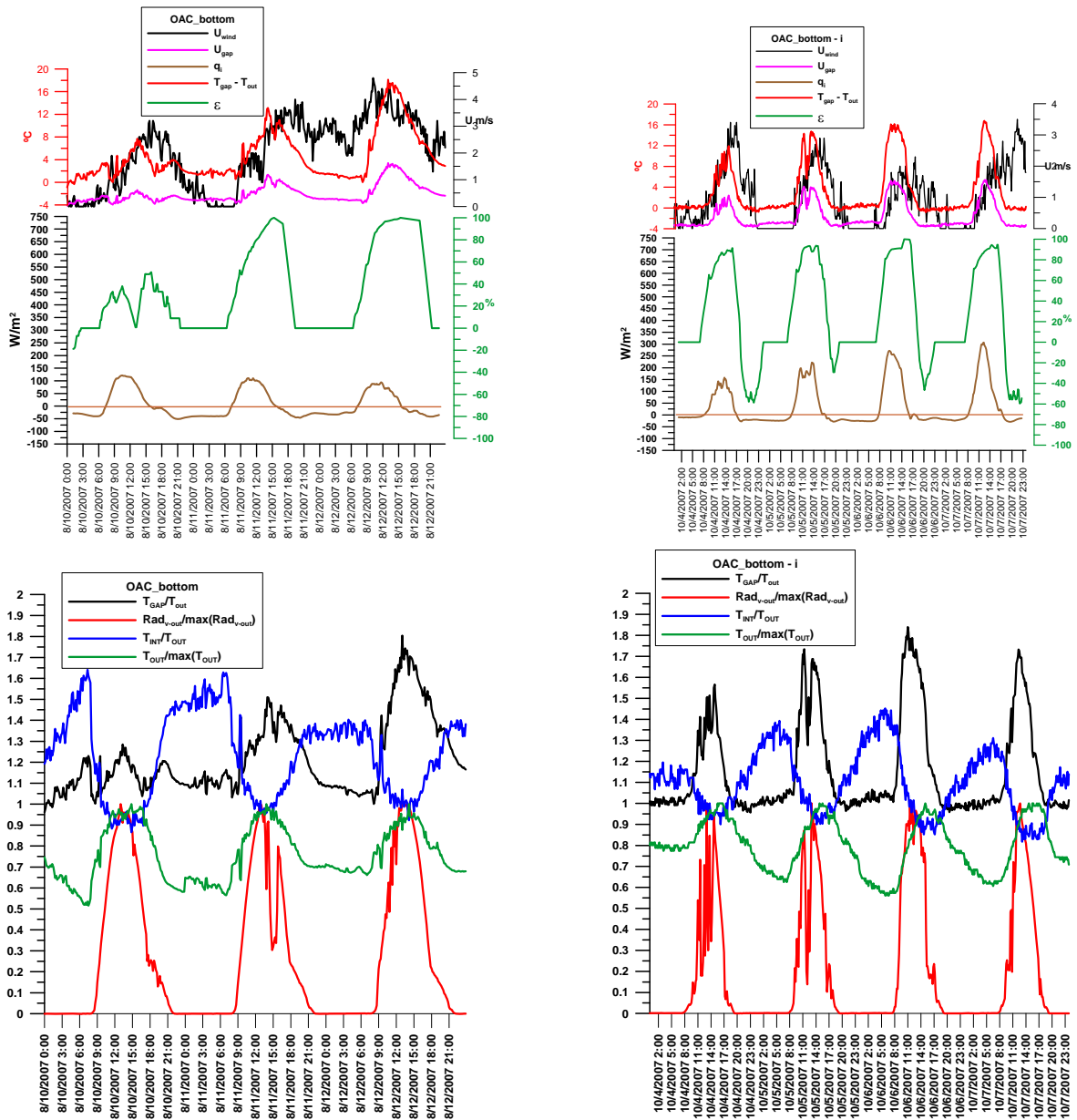
Figure 4D.2 – Measuring results for the Buffer configuration.

Outdoor Air Curtain configuration





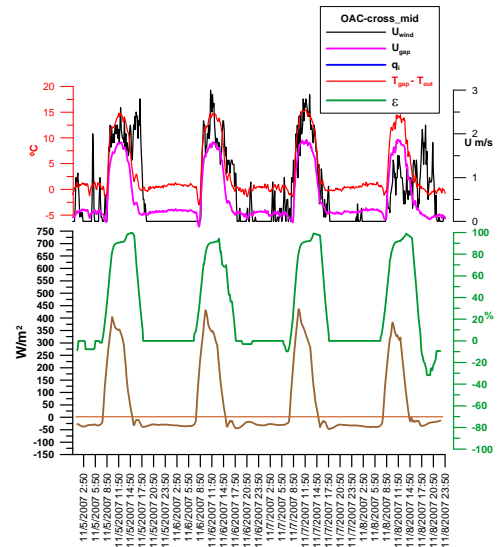
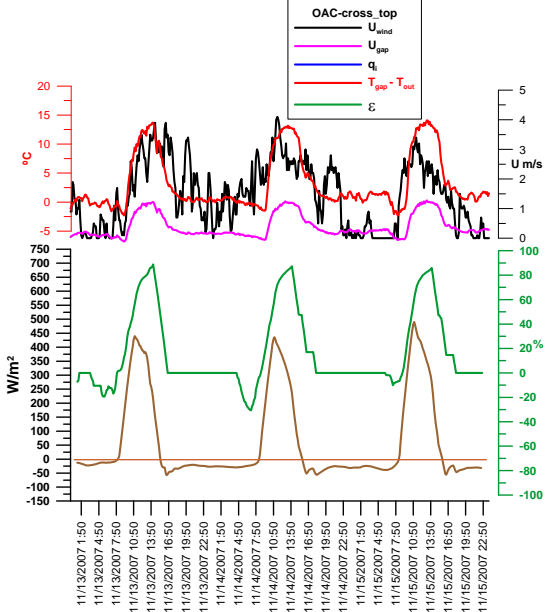
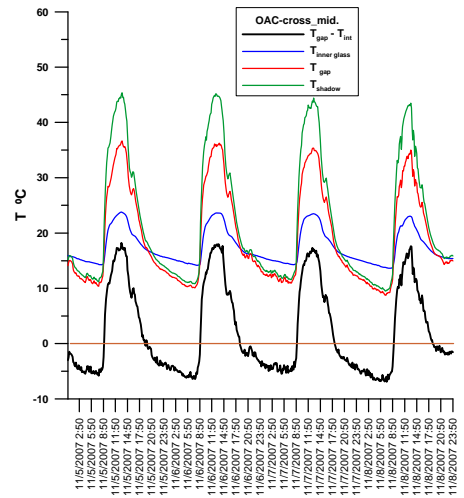
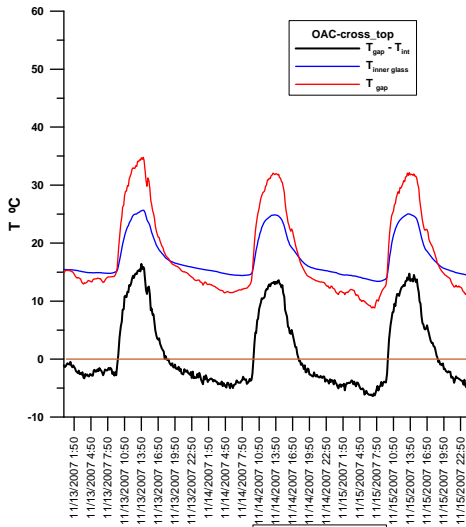
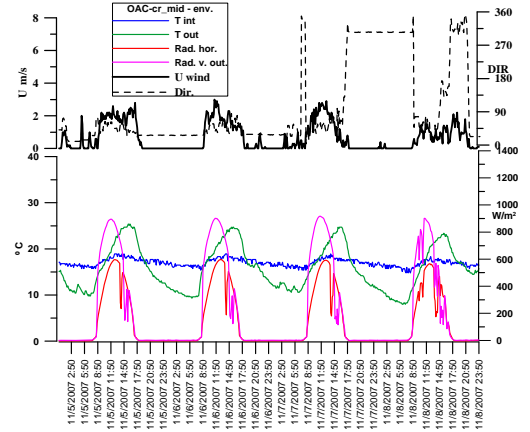
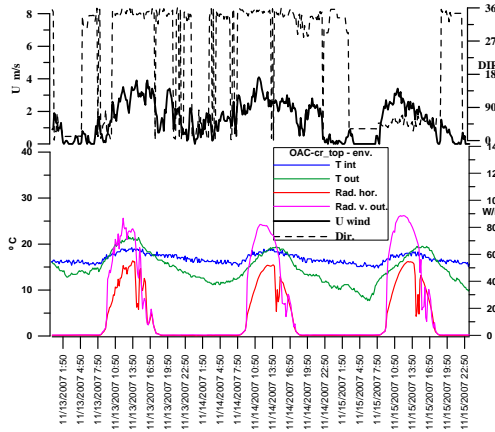




**Figure 4D.3 – Measuring results for the OAC configuration.**

Outdoor Air Curtain configuration – cross flow

Cross flow means that outdoor air enters the façade gap by the lower louver of glazing A- (figure 4.19 – section 4.3.4.2) being exhausted by the top louvers of glazing C-D.



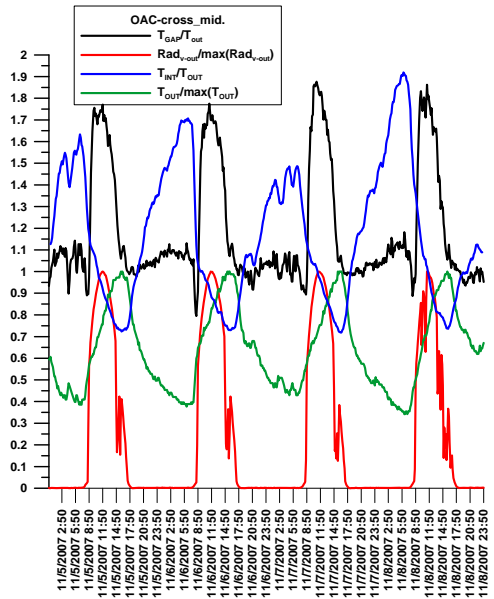
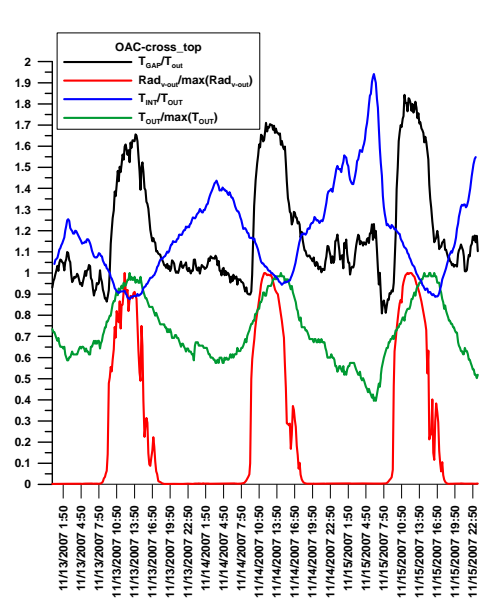
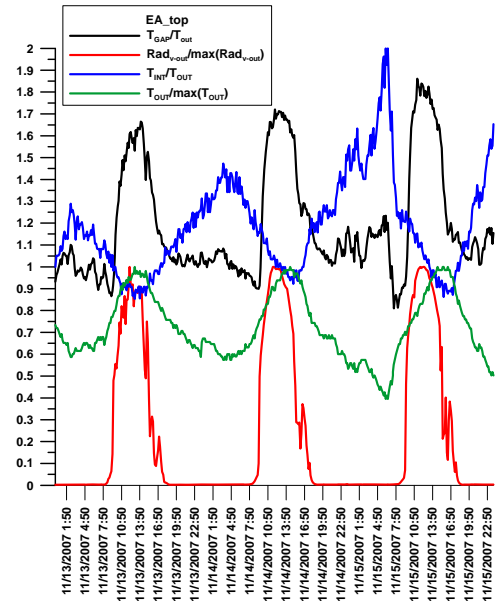
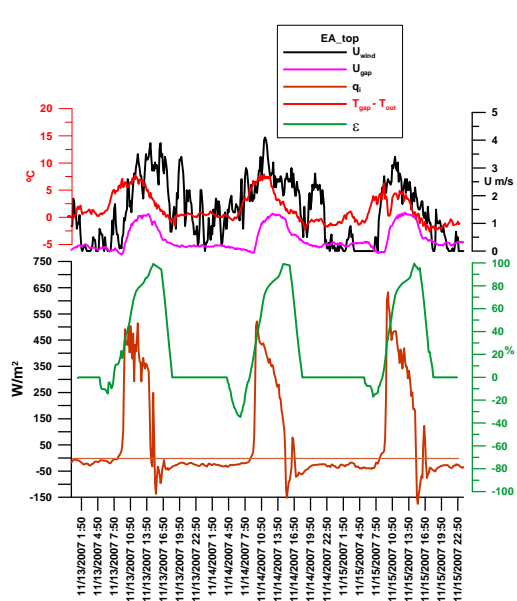
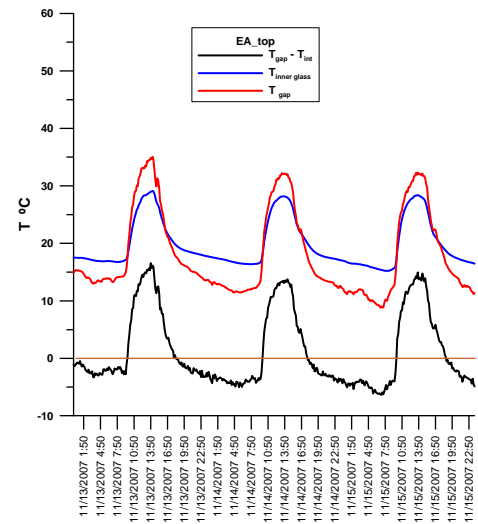
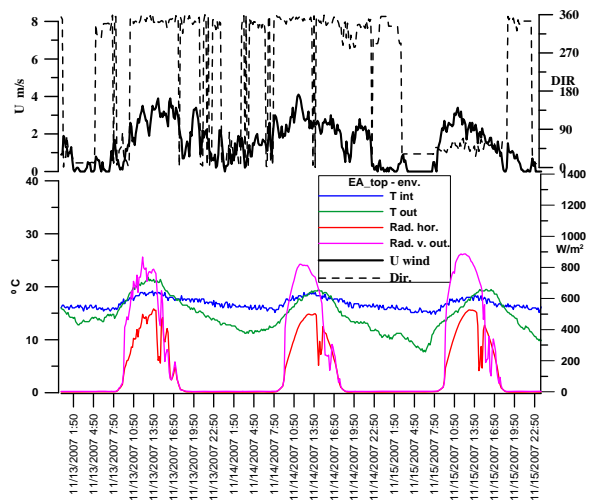
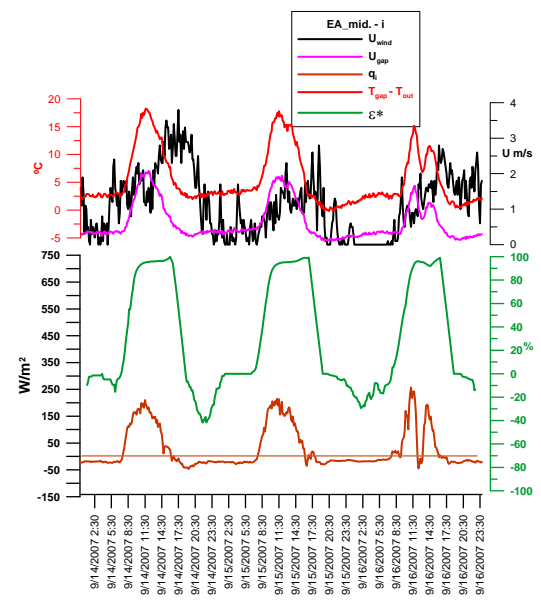
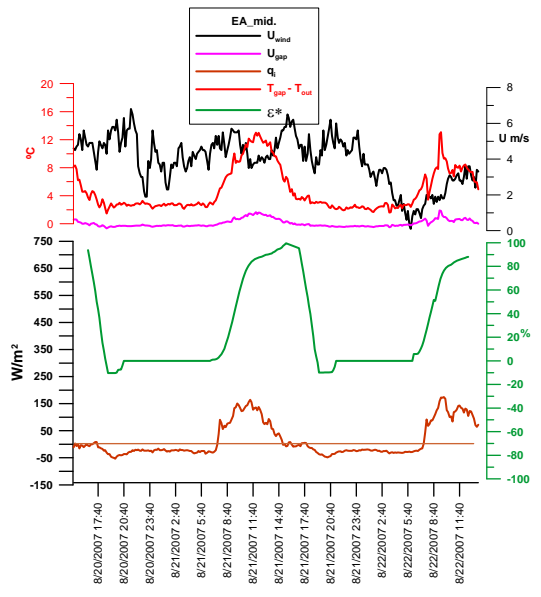
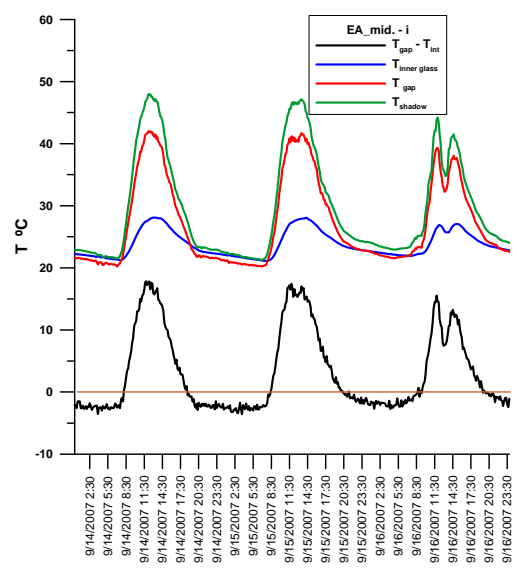
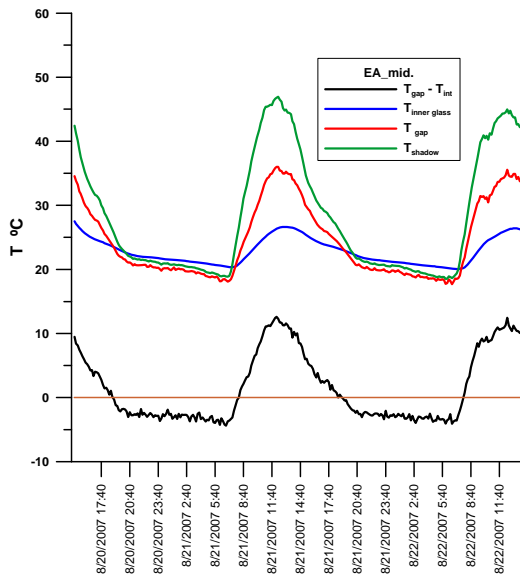
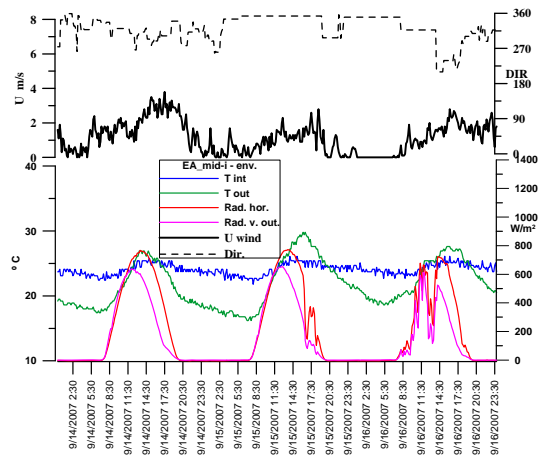
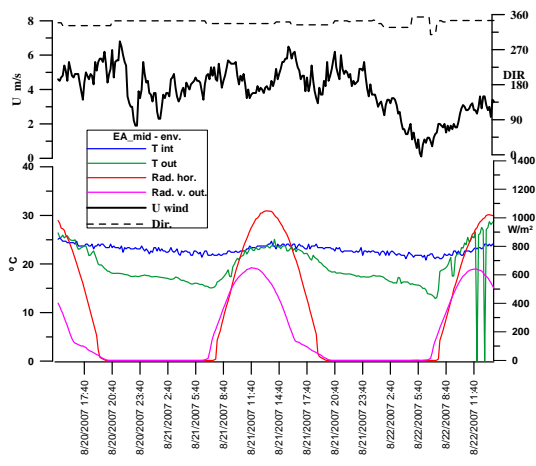
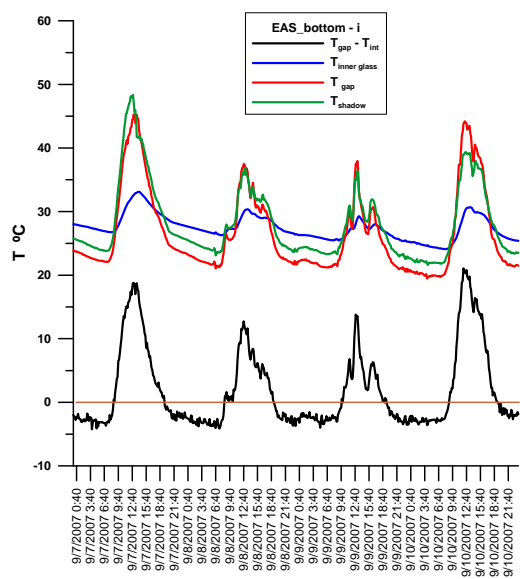
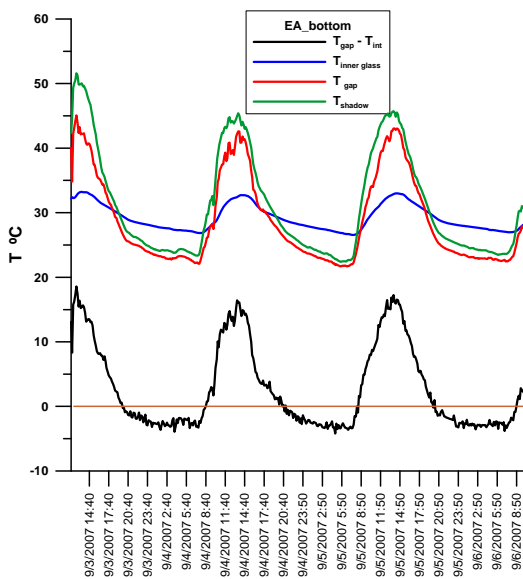
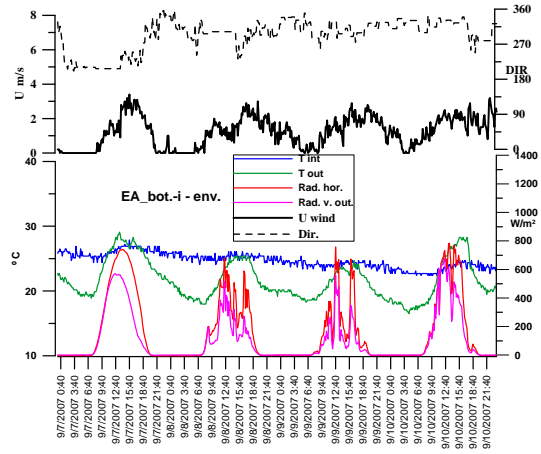
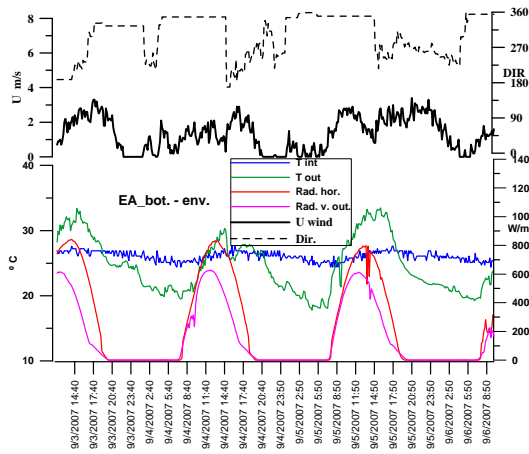
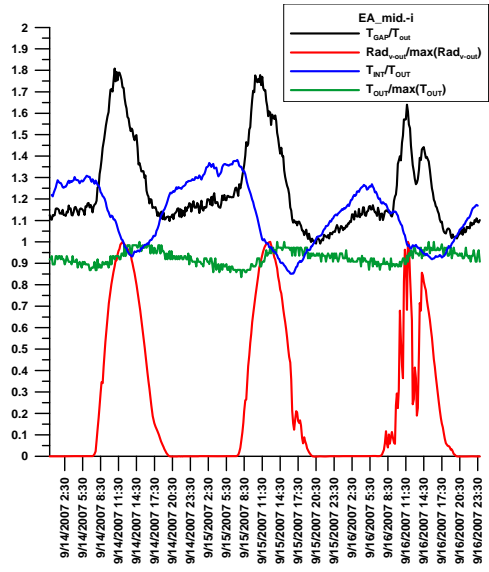
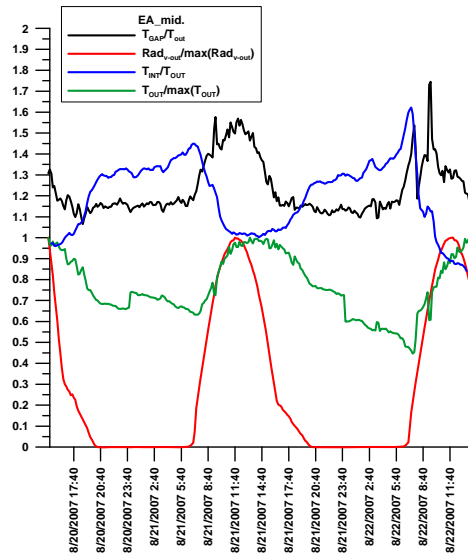


Figure 4D.4 – Measuring results for the OAC-cross flow configuration.

Exhaust Air configuration







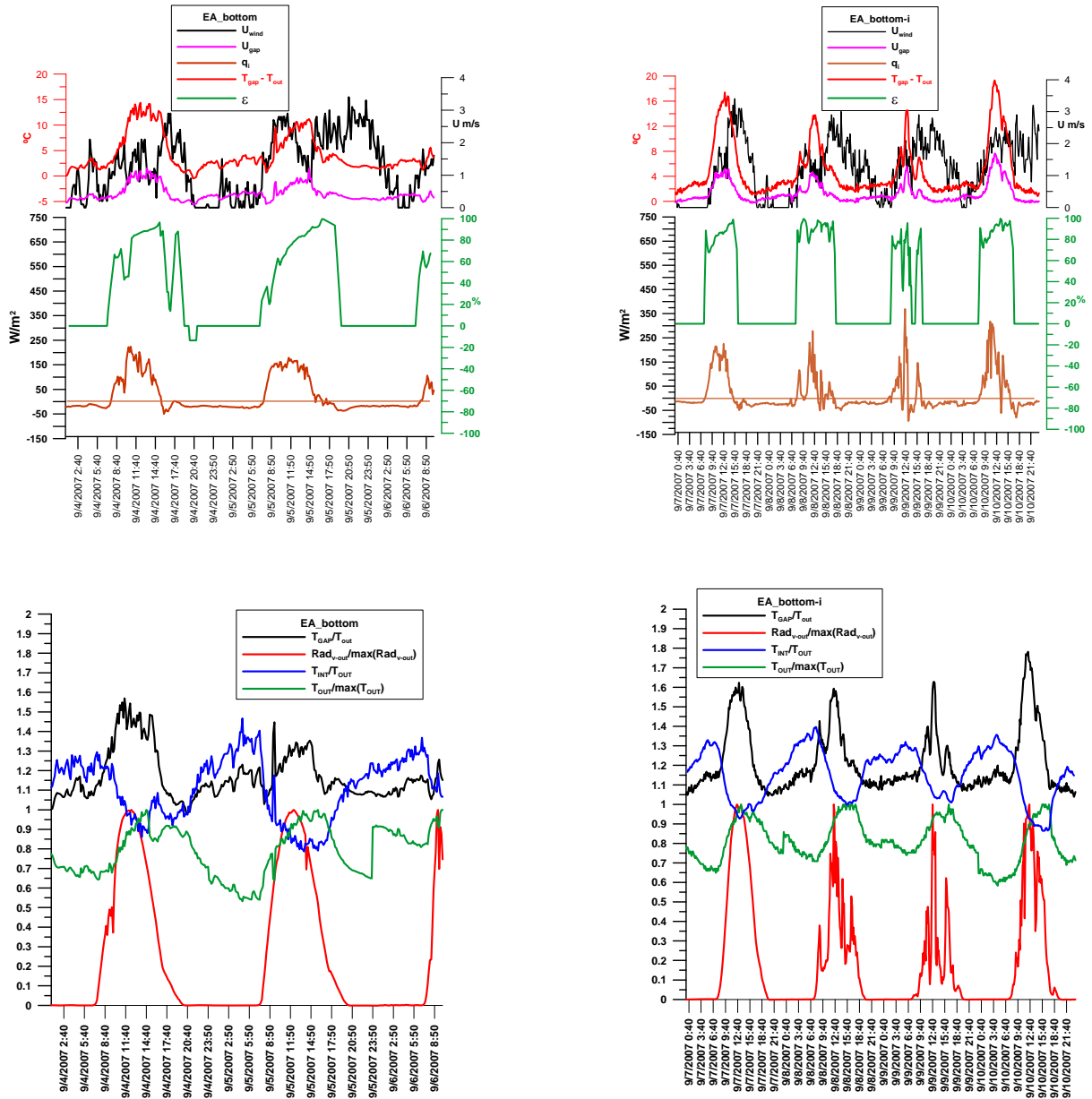
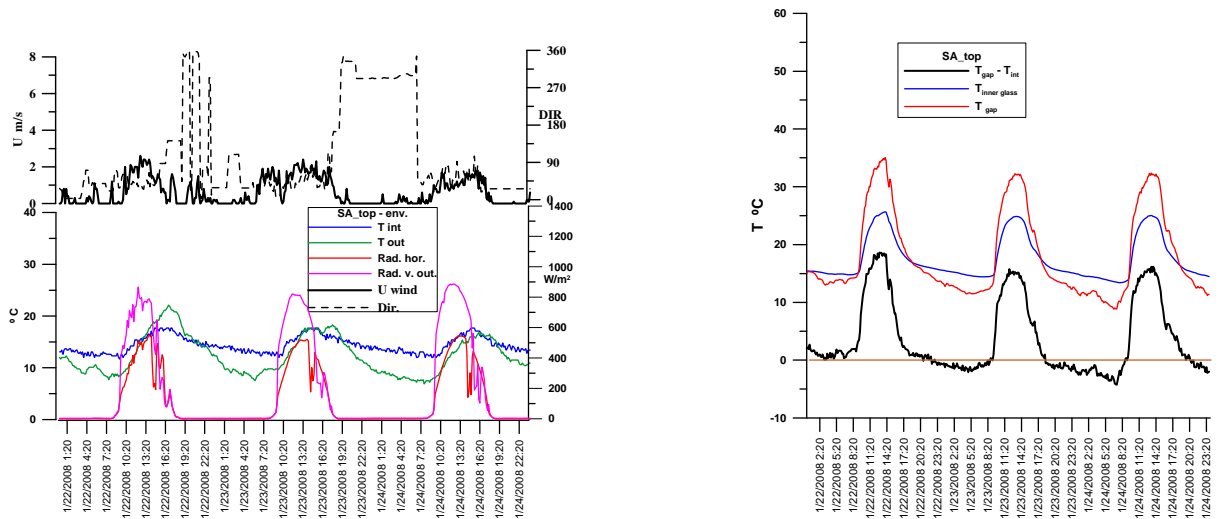


Figure 4D.5 – Measuring results for the EA configuration.

Supply Air configuration



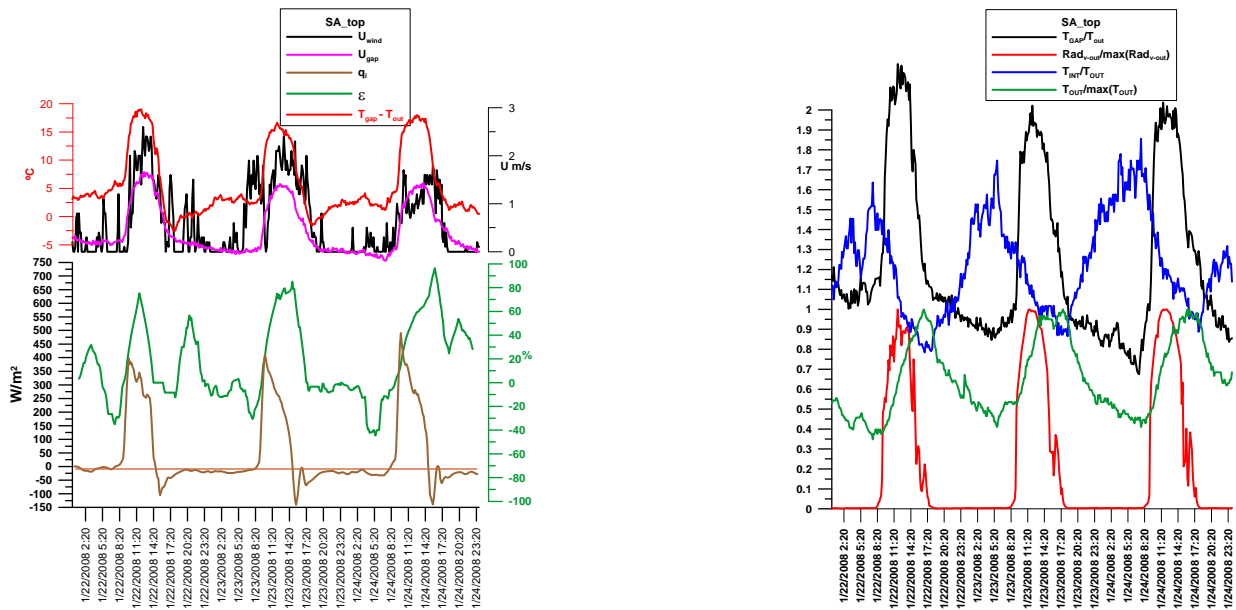


Figure 4D.6 – Measuring results for the SA configuration.

From the presented measurement results the following conclusions may be listed:

- Daily indoor temperature variations are quite soft due to the low wall U value and the good insulation performance of the façade, what is shown by the very low negative  $q_i$  values during night periods.
- Bulk gap temperature follows closely the incoming vertical plane radiation and, for the present test cell, wind has no visible influence on ventilation flows.
- A main result rises from the ratio between indoor and outdoor temperature, being higher than unity during night hours but always below unity under solar radiation even with no shading pulled down.
- The temperature difference between gap air and indoor increases when the roller blind is closer to the inner glazing, showing higher values for the buffer configuration. This configuration (Bf) always shows the highest gap temperatures due to the absence of ventilation.

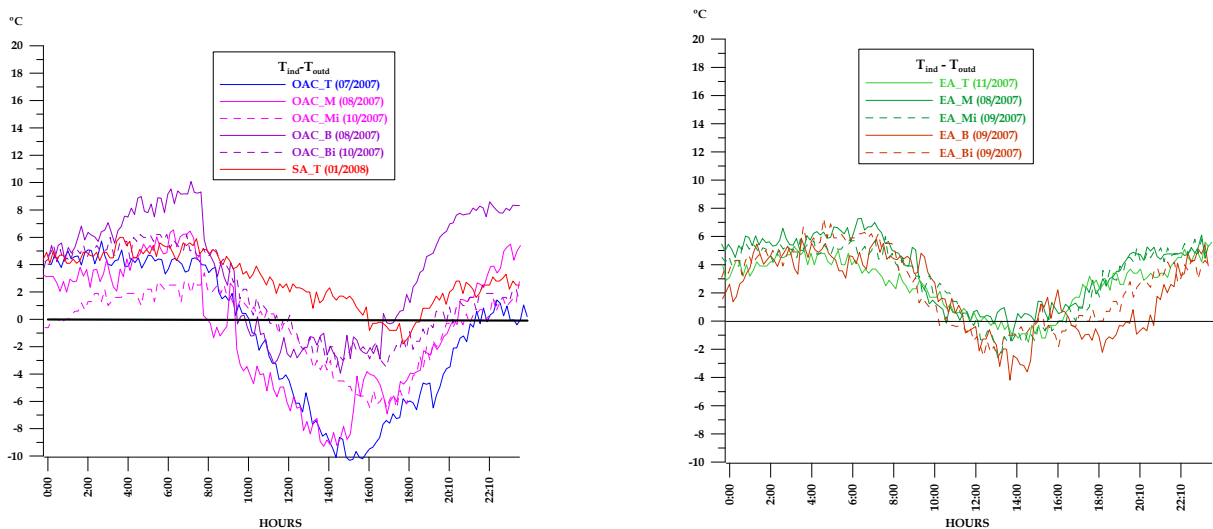


Figure 4D.7 - Temperature differences between indoor and outdoor for OAC, SA and EA.

- For all the other configurations air gap temperatures show values 10 – 20 K above indoor, depending on solar radiation level and outdoor temperature.
- Higher  $q_i$  values occur naturally when there is no shading pulled down. When the roller blind is closer to the inner pane an increase in these values is measured as the shading device is always the hottest element in the façade.
- Dynamic insulation always shows high values on sunny hours proving that heat removal is efficient.

## APPENDIX 4E

### 4E.1 Daylighting

From daylighting point of view DSF are not significantly different from single skin glazed facades (50 – 70%) granting good daylight conditions in areas not far from the façade. However, under sunny sky shading devices are fully lowered in order to prevent glare leading to the need of artificial light use. This has natural impacts on comfort and energy use.

Figure 4.21 – section 4.4 shows, as an example, a daylight map in a monitored office located in a building in Lisbon. The office has a south/north facing DSF (C-MV-OAC). Different boundary conditions have been examined: a) cloudy day with shading fully open and, b) sunny day with shading fully closed in the Southern façade (figure bottom) and partially closed in the Northern façade.

In order to avoid daylighting problems a couple of strategies may be used as (for example): double horizontal blade slope (figure 4.22 – section 4.4), or adequate control of shading should account not only to daylight distribution but also to the presence of users and allow personal control.

## APPENDIX 4F

### 4F.1 - Acoustics

Acoustic insulation improvement is one of the advantages of DSF, and in many cases it could be the main reason to adopt an AIF. The insulation level depends on the façade construction and used materials as shown in Figure 4.23 section 4.4, where the measured acoustic insulation,  $D_{n,w}$ , in two different DSF buildings is shown, evaluated according to standard EN ISO 140-4 .(2000).

Building A's DSF (MS-MV-OAC) has two single tempered clear glazed panes (12 - 705 - 10) and a very low mechanical ventilation flow. Building B's DSF (C-MV-OAC) has an outer single clear glazed pane and a double glazing, also clear glass inner pane (12 – 980 -3-12-6) and a variable mechanical ventilation flow. Another relevant issue concerning DSF acoustics properties is airborne noise transmission through the gap. Figure 4F.1 shows the measured insulation in building B, from office to office. For some type of AIF (e.g. corridor façade) acoustic bridges from room to room may be a concern.

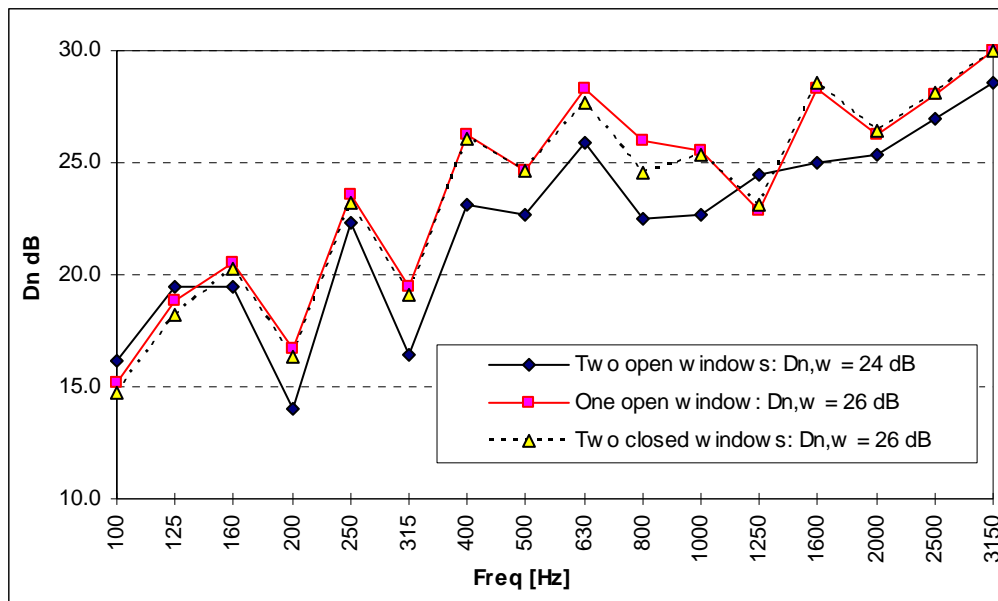


**Figure 4F.1– Measured airborne acoustic insulation,  $D_{n,w}$ , from office to office, in building B, proved to be poor mainly due to the sound transmission by the ceiling and interior doors. The small difference between one and two closed windows reflects the individual window good insulation.**

## APPENDIX 4G

### 4G.1 - Wind Action

The wind-building interaction determines the building envelope pressure distribution, which has a significant effect on ventilation flows in case of natural ventilation. This, particular, can affect the selection of natural ventilation strategies. From the structural point of view wind constitutes the strongest load on AIF and the present codes are not suited for this kind of building element [Marques da Silva, et al, (2008), BESTFACADE-WP5 (2007)].

Wind pressure is defined as the average of stationary and fluctuating turbulent components. The first component, often called the “static pressure”, is connected with large scale air movements that change slowly in time. The second component is related to short-term changes in air speed and direction due to atmospheric turbulence.

Turbulent fluctuations are “dumped” by the DSF due to the combined effect of openings in the inner and outer panes in conjunction with the cavity, which acts as a buffer. This is of particular importance in high-rise buildings where gust loads may induce high peak pressure values [Oesterle, et al (2001)].

A major factor that influences pressure distribution is the building shape. DSF configuration can dramatically change cavity pressures when compared to an “unsheltered” envelope. Figures 4.20 section 4.4 and 4G.1 represent the  $C_p$  distributions obtained on wind tunnel tests over a 10 storey, scaled model of a building under an urban boundary layer wind velocity profile.

The DSF has a multi-storey configuration, open at the bottom and top and closed on the sides. The bottom edge of the DSF is 3 m above ground level, and the cavity has a depth of 0.8 m [Marques da Silva, F and MG Gomes (2005)].

This change in pressure distribution should be accounted for in order to properly evaluate wind loads on the external pane and to choose the most suitable type of ventilation strategy. Potential difficulties in manoeuvring doors or windows to the cavity may also be affected by such pressure values.

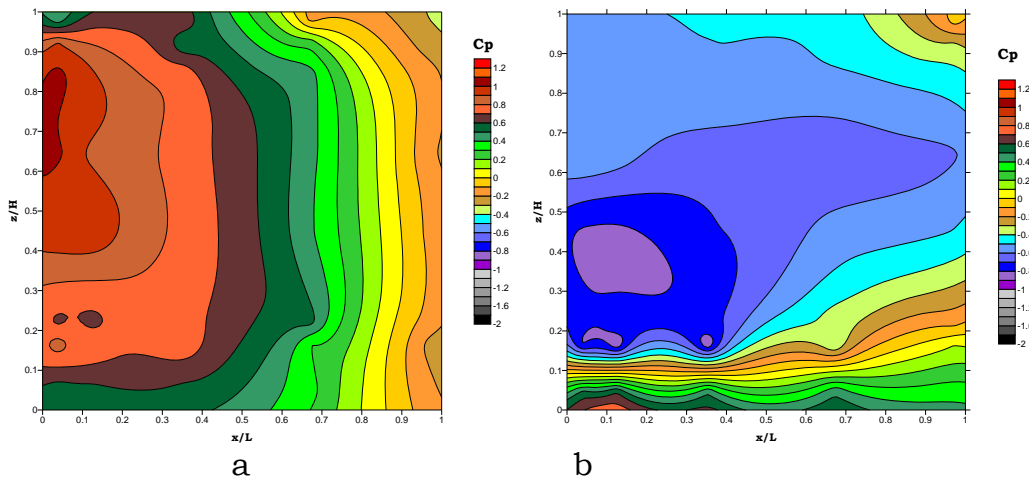


Figure 4G.1 -  $C_p$  distribution over an “unsheltered” envelope a), and a MS-DSF b), for a 45° (corner) wind incidence.

## APPENDIX 4H

### 4H.1 Sustainability

Buildings energy consumption keeps increasing besides being already responsible for a significant amount of energy (40% in EU25). The operational energy use of buildings includes HVAC, all equipments and activities developed inside buildings. On the other hand, construction industry is responsible for nearly 50% of natural resources consumption and 50% of the waste produced. So, to reduce the environmental impact of buildings it is necessary to take into account not only their energy performance but also the resources consumption and emissions to air, water and soil.

Regarding this data, in sustainable buildings, when analyzing DSF performance one should look into the overall environmental performance of such solution, taking into account their impact during utilization period, as well as their environmental load associated with manufacturing/construction and end of life.

To assess the environmental impact it was used the Life Cycle Assessment (LCA) methodology, ranging from cradle to grave, that is, from raw materials through construction, use, demolition/deconstruction and final disposal.

In a LCA assessment there four main stages should be considered (ISO 14040:2006) :

- goal and scope definition - defines the analysis purpose and boundaries;
- inventory analysis - estimates the input/output data, namely the material and energy consumption in the expected life of the building/component and also the expected emission the environment (LCI- life cycle inventory analysis);
- impact assessment - regarding the input/output data from LCI, it is estimated the environmental impact of the building/component, considering some environmental impact categories indicators (LCIA – life cycle impact assessment);
- interpretation. - to help the analysis of the environmental impact, LCIA results assessment were normalized using the one year average environmental impact of an European citizen, accordingly weighted as: 50% GWP, 11% ODP, 7% acidification, 16% energy, 7% water, 9% waste. In the normalized and weighted results of LCIA we obtain 100 ecopoints (Pt) for the yearly environmental impact of one European citizen.

In order to give an example, six environmental categories indicators were selected:

- GWP (global warming potential);
- primary energy;
- ODP (ozone depletion potential);

- acidification potential, water and waste.

To find the environmental impact of building material/components, with impact on the thermal performance and energy consumption, it was used mainly the information from building project and the information from an international database SIMAPRO, after adjustment to take into account specific local building materials.

**Table 4H.1 – Material for three types of façade.**

**Double skin façade**



Single glass 10 mm  
Venetian blind  
Double glass 8+16+33.1

Aluminium frame

72 kg/m<sup>2</sup>

**Curtain wall**

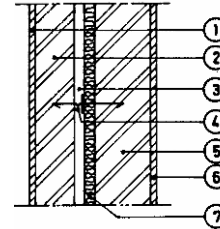


Double glass 8+16+33.1  
Venetian blind

Aluminium frame

40 kg/m<sup>2</sup>

**Brick wall with window**



Wall (60%):  
Mortar (15 mm), Brick (11 cm), Polystyrene (6 cm), Brick (11 cm), Plaster (15 mm)  
Double glass (27%) (8+16+6)  
Aluminium frame (12%)  
Stone (1%)  
160 kg/m<sup>2</sup>

Double skin façades are lightweight building shells, usually made with glass and aluminium, which are recyclable materials, but also with a large amount of embodied energy. As a comparative example, table 4H.1 resumes the materials used for the construction of an 2.7 m × 3.7 m external wall in three different configurations: a DSF; an aluminium curtain wall, and; a traditional brick wall with a window. In the glazed façades almost 70% of the weight is glass and 20% is aluminium frame in counter part of traditional walls where bricks and mortar represents almost 80% of the weight.

In the life cycle analysis of this façades it was admitted the replacement of double glass each 30 years, the regular cleaning of façades and the painting of traditional brick walls.

To reduce the construction environmental impact the material selection should consider the following guidelines:

- Reduce the consumption of materials and energy;
- Reuse the material/components in new constructions/refurbishment;
- Recycle the material in end of life;
- Recover the embodied energy in materials as burning fuel;
- Send to landfill, when none of the above could be applied.

The material used in glazed façades has a lot of manufacturing and a large amount of embodied energy, table 4H.2, and figure 4H.1, which could be a limitation.

Although aluminium and glass are recyclable, these materials have a large environmental burden due to the large amount of energy consumption during extraction/manufacturing processes. Recycling of aluminium needs a furnace with important energy consumption. Plus the use of recycled aluminium is not common for new profiles extrusion because of other materials inclusions that may affect the final surface quality and damage extrusion tools. Glass with coating also present some problems in recycling, because the layers of oxides metals contaminate the mass of glass for

new production and great care should also be taken in landfill to avoid the infiltration in soil or water of this oxide metals.

**Table 4H.2 – Embodied energy of some materials**

Material	Density (kg/m <sup>3</sup> )	Embodied energy (MJ/kg)	Ecopoints (Pt/kg)
Aluminium/ Recycled aluminium	2800	190/20	0,08900/0,00761
Glass	2500	20	0,00620
Steel/ Recycled steel	7800	30/19	0,02440/0,00787
Bricks	-	4	0,000713
Mortar	1800	1,5	0,000898

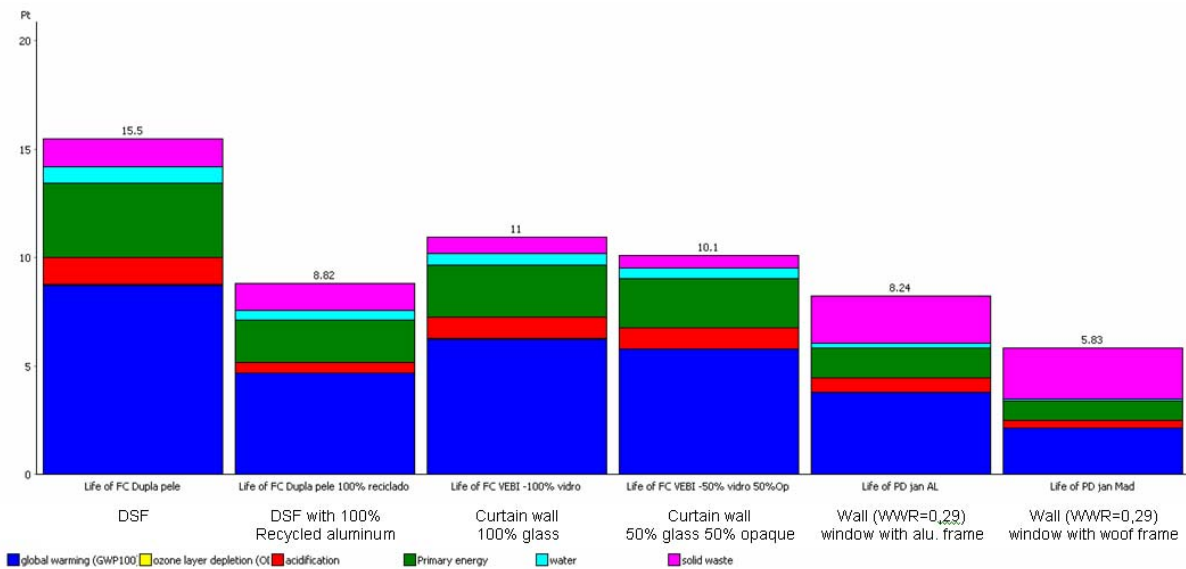


**Figure 4H.1 – Environmental load of façades (table 4H.1) construction and disposal phases.**

The environmental impact of DSF in buildings depends on the environmental load of material but also on their impact in energy consumption of the building, function of several factors: weather, type of glass, ventilation of air layer, etc.

In northern climates, it is shown that the major environmental load during the expected life of buildings is related with the operational energy consumption (almost 90%) and the environmental load of material could be less than 10%. In warm climates (Southern Europe) well designed and used buildings could have very low energy consumption for (HVAC, lighting) and in such cases the environmental load of material could be the key factor for sustainable constructions (almost 90% of the environmental impact of buildings [Pinto, (2008)]).

An office building located in Lisbon was studied, with a poorly designed DSF (box window), with monitoring of energy consumption and simulation of thermal/energy performance. This building has a very high annual energy consumption of 330 kWh/m<sup>2</sup> (9100 m<sup>3</sup>), 12% in lighting and 39% in HVAC. Assuming an expected life of 50 years, the construction and end of life phases represents 35% of the environmental impact of the building taking also into account the energy for heating, cooling and ventilation, figure 4H.2. When analyzing the construction and end of life phases, the DSF environmental load is 10% of the construction total environmental load, figure 4H.3.

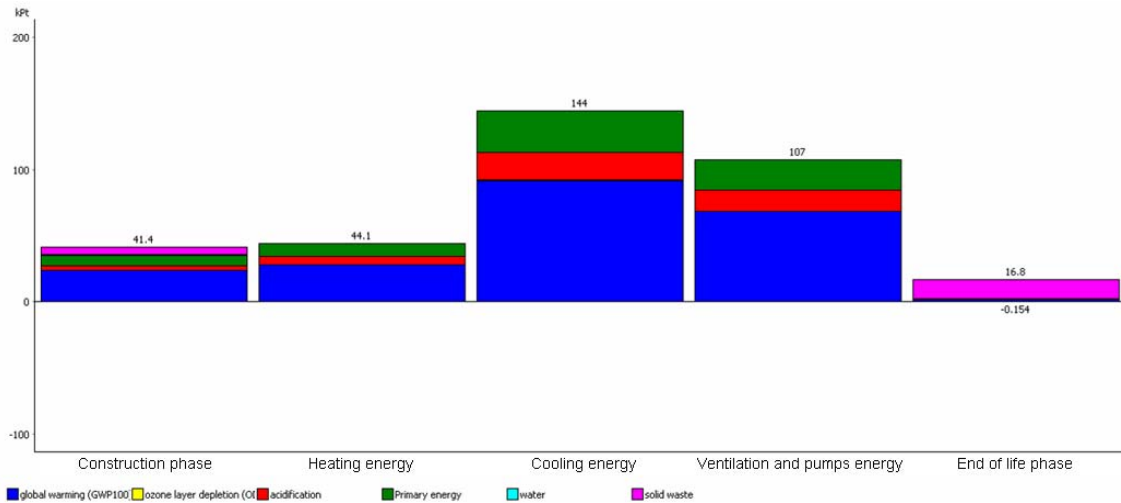


**Figure 4H.2 - Environmental load of an office building in 50 years.**

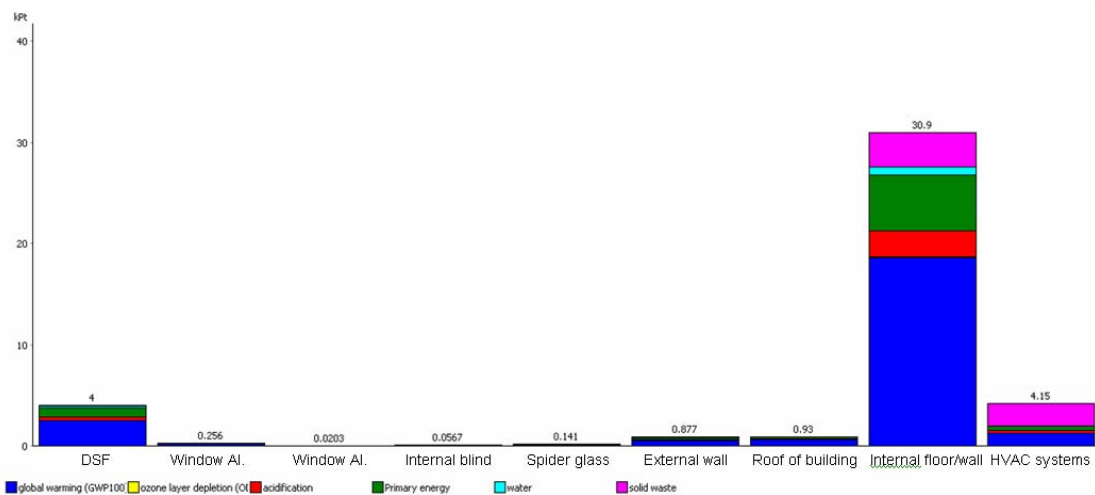


**Figure 4H.3 – Environmental load in construction phase of an office building with DSF.**

## APPENDIX 4I

### 4I.1 Assessment of the convective heat transfer coeff., $h_c$

A critical issue for the simulation of DSF is represented by the assessment of the convective heat transfer coefficient value. This quantity depends on the nature of the airflow (natural or mechanical ventilation, laminar or turbulent regimes), the geometry of the channel (wide or narrow), the airflow rate and the temperature difference between the surface and the air. In the literature, there are some empirical relations for ducts, narrow cavities and flat plates that can be used to determine the convective heat transfer coefficients. However, when a venetian blind is present, the convective heat transfer coefficient between the slats and the air cavity is not yet very well covered by the literature and some complementary CFD simulations were carried out in this study to generate those parameters. Figure 4I.1 plots, as an example, the variation of the convective coefficient,  $h_{c,w}$ , with Rayleigh number (with the free cavity width  $W$  – between the glass and the edge of slats - as the

characteristic length) for different slat angles and temperatures conditions ( $RT1=T_{\text{outer\_glass}}/T_{\text{slat}}$ ;  $RT2= T_{\text{inner\_glass}}$ . On the other hand, the glass surface  $Nu_x$  (being the characteristic length the distance from the entry of the channel) is not very far from [Tsuji and Nagano (1988)].

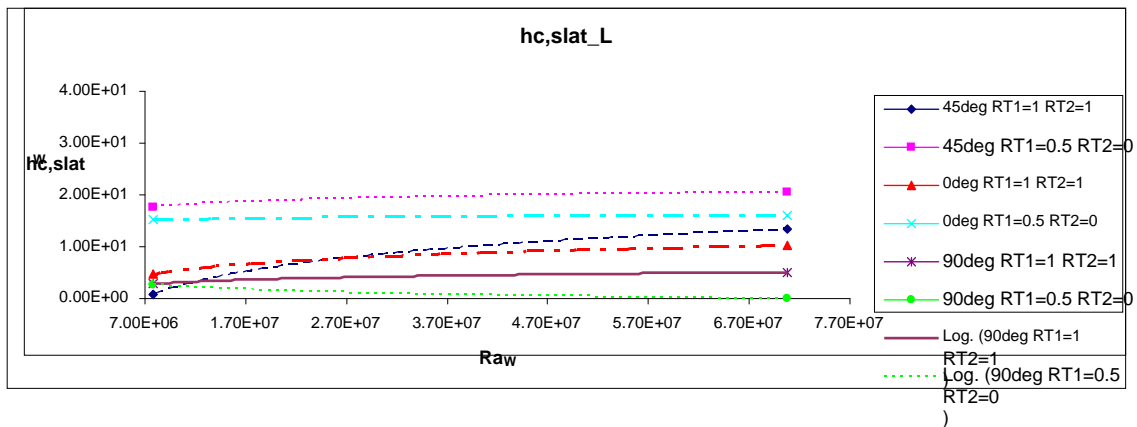
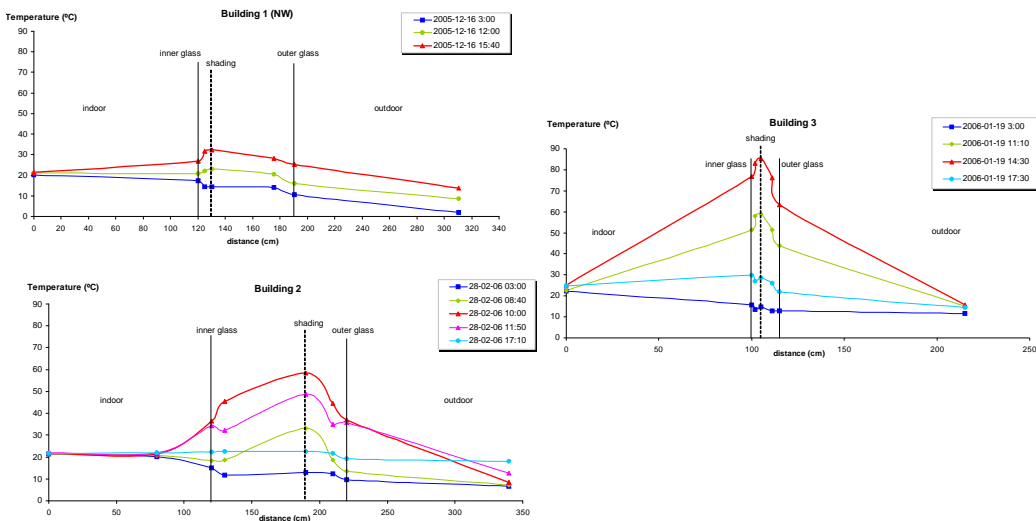
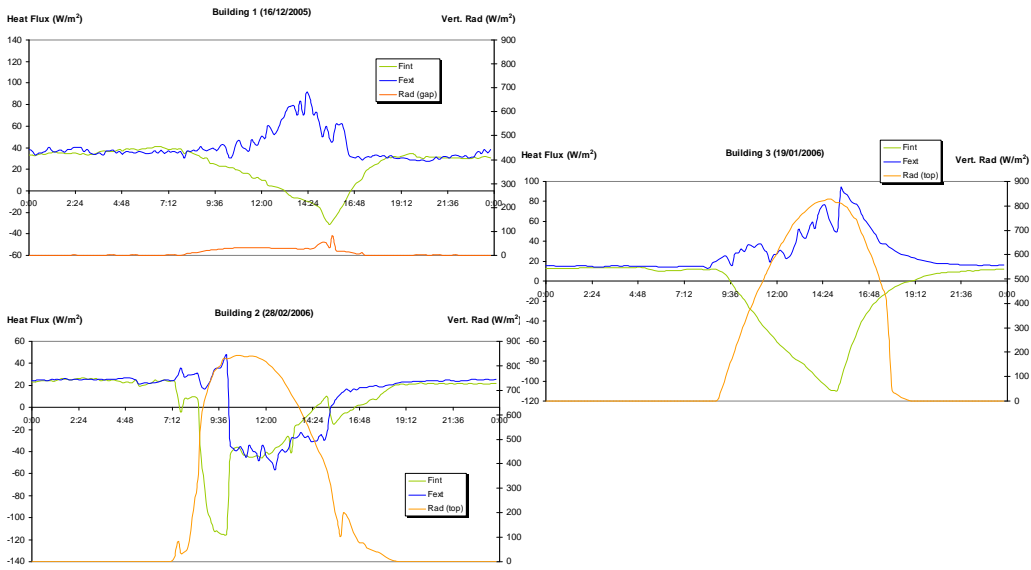


Figure 4I.1 -. Calculated  $hc_w$  for different slat angles and temperature conditions.

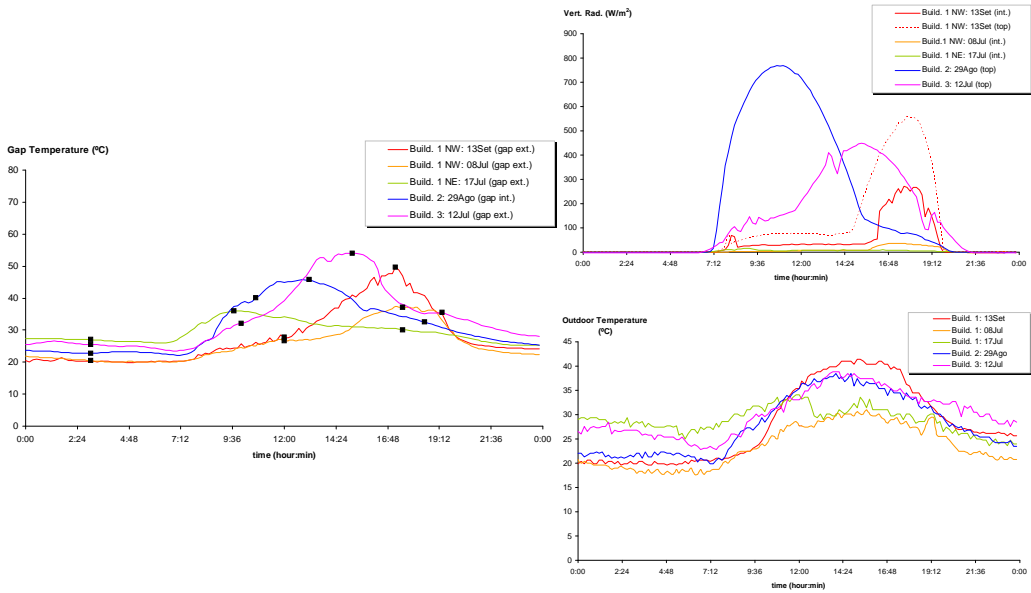
## APPENDIX 4J

### 4J.1 Measured data – Field monitoring of real Buildings in Lisbon (Portugal)





**Figure 4J.1 - Three DSF Winter monitoring results.**



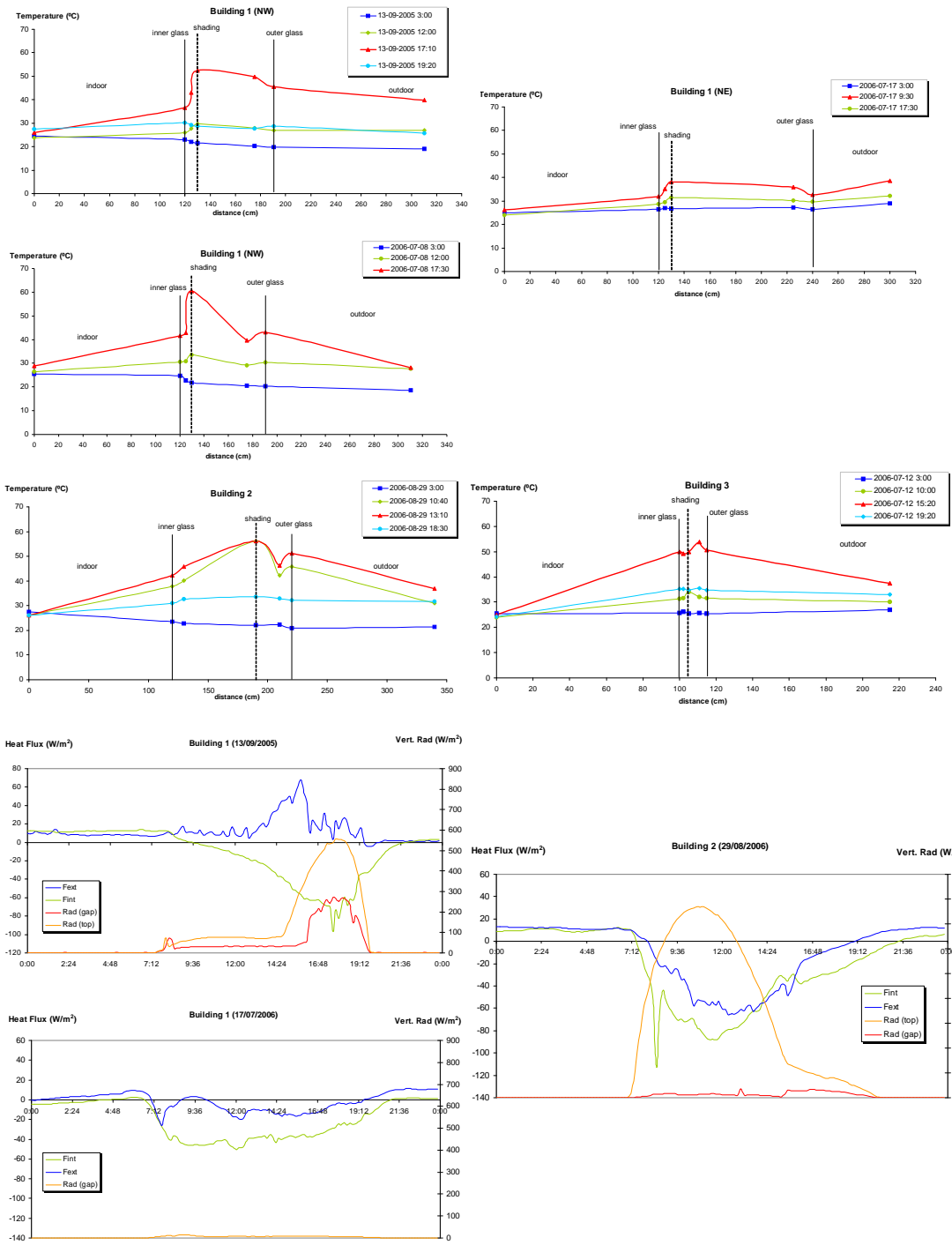
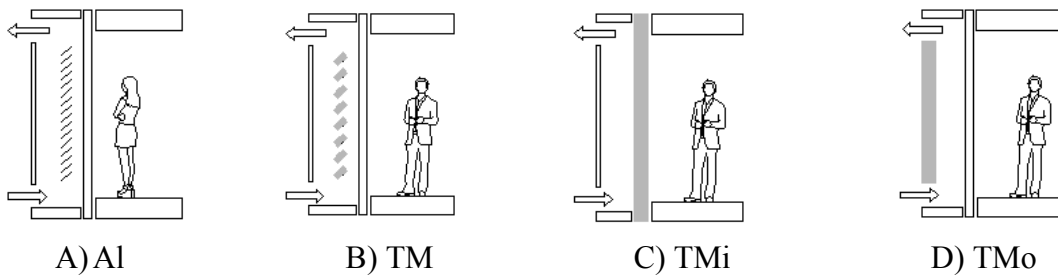


Figure 4J.2 - Three DSF Summer monitoring results.

# APPENDIX 4K

## 4K.1 Coupling AIF with TMA

A simulation study was conducted at Concordia University to find the magnitude of the increased efficiency of an AIF integrated with thermally activated massive elements (TMA – SA). Three alternative configurations of concrete thermal mass in combination with conventional layout of AIF were considered. First configuration (TM) is replacement of the typical aluminium shading device between two panes of AIF with concrete thermal mass material and the other two are replacement of inner or outer pane of conventional AIF with a vertical concrete thermal mass slab (TMi or TMo). The performance of these three configurations was compared with conventional AIF. The combinations of concrete thermal mass are illustrated below.



- A): Conventional AIF with aluminium venetian blind – base case
- B): Proposed AIF combined with thermal mass (replacement with shading device)
- C): Proposed AIF combined with thermal mass (replacement with inner pane)
- D): Proposed AIF combined with thermal mass (replacement with outer pane)

For the purpose of comparison, thermal mass was considered for whole facade height; however practically thermal mass locates on spandrel area.

### Simulation of thermal mass combinations:

The base-case was firstly simulated by means of a purposely developed analysis tool (described in section 4.3.3.2). In a second phase, the simulation model was suitably modified to study the integration of AIF with thermal mass elements. The predicted performances of the base AIF configuration were then compared with those of the combined AIF + TMA system.

### Main Results:

The simulation results for conventional AIF and for AIF with thermal mass at different airflow paths are shown in figures 4.45 to 4.48.

The graphs show total thermal load entering from AIF to attached room in winter and summer. TM has fewer gains compared to typical aluminum blind at noon and less loss in the evening and at night.

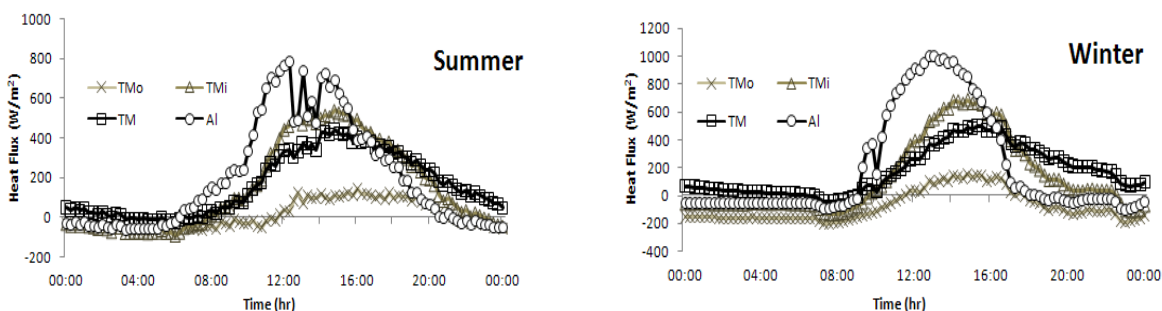


**Figure 4.45 - AIF(MV-IAC), Total thermal load includes heat transmission through interior pane, solar radiation passed through interior pane and enthalpy changes of ventilation air supplied to room (positive values show gains).**

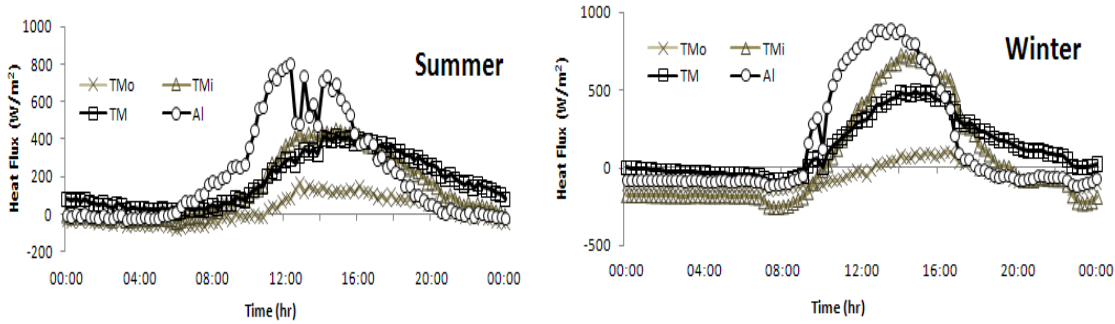


**Figure 4.46 - AIF(MV-SA), Total thermal load includes heat transmission through interior pane, solar radiation passed through interior pane and enthalpy changes of ventilation air exhausted to room (positive values show gains)**

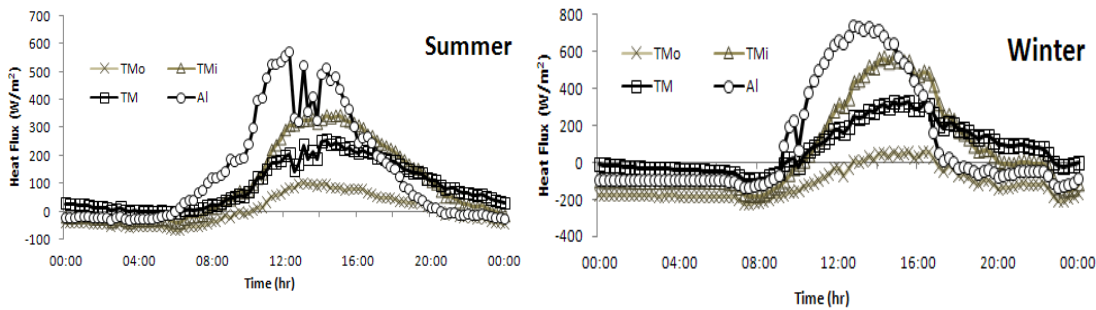


**Figure 4.47 - AIF(MV-EA), Total thermal load includes heat transmission through interior pane and solar radiation passed through interior pane (positive values show gains. The amount of room air that will be exhausted through AIF was assumed to be infiltrated from surrounding warm zones of attached room).**

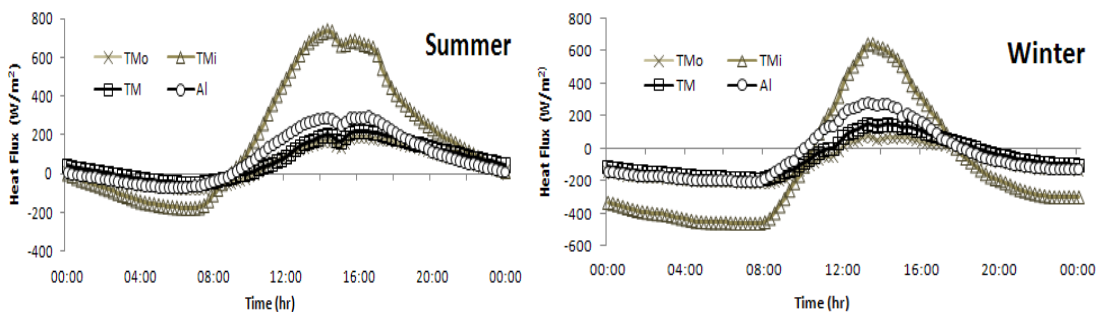


**Figure 4.48 - AIF(NV-OAC), Total thermal load includes heat transmission through interior pane and solar radiation passed through interior pane(positive values show gains). AIF is ventilated naturally.**

TMo has the least gain in day and the highest loss at night for mechanically-ventilated case and highest gain and loss in naturally-ventilated AIF [Fallahi, A. (2009)].

The saving in cooling/heating load for three types of mechanically-ventilated AIF (EA, SA and IAC) and one type for naturally ventilated AIF (OAC) is shown in the charts of figures 4.42, 4.43 and 4.44. TM has the highest saving with MV-EA airflow path and TMo the least saving with the same airflow path, but for NV-OAC TMo has the highest saving in summer.

The variation of airflow rate in naturally-ventilated AIF is shown in figure 4.45.

Higher surface temperature of TM at night-times and evenings respect to aluminium blind increases the stack effect and therefore the airflow. This airflow increase is favourable in summer and undesirable in winter.

On the overall, it was found that TM has superior performance than conventional AIF and it is suitable to be combined with mechanically-ventilated AIF rather than naturally ventilated façades.

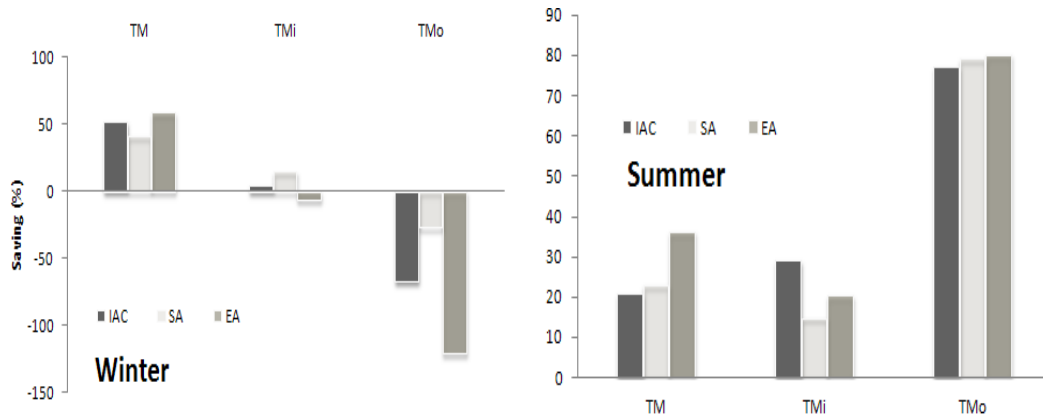


**Figure 4.49 - AIF(MV-IAC, SA, EA), Saving with thermal mass compared with conventional AIF.**

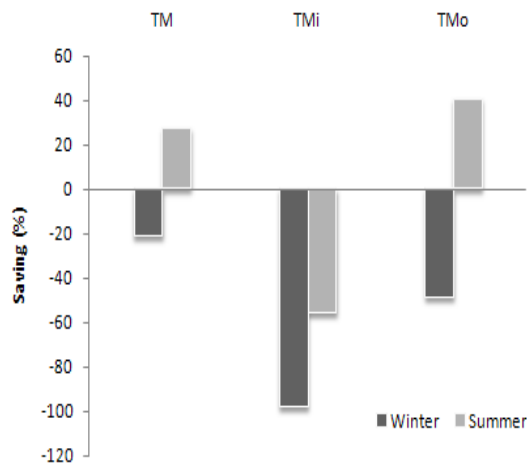


**Figure 4.50 - AIF(NV-OAC), Saving with thermal mass compared with conventional AIF.**

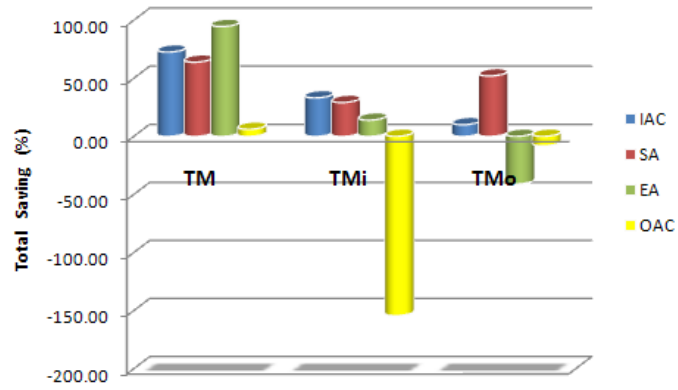


*Figure 4.51 - Total savings during summer and winter; these savings are respect to conventional AIF with aluminium blind.*

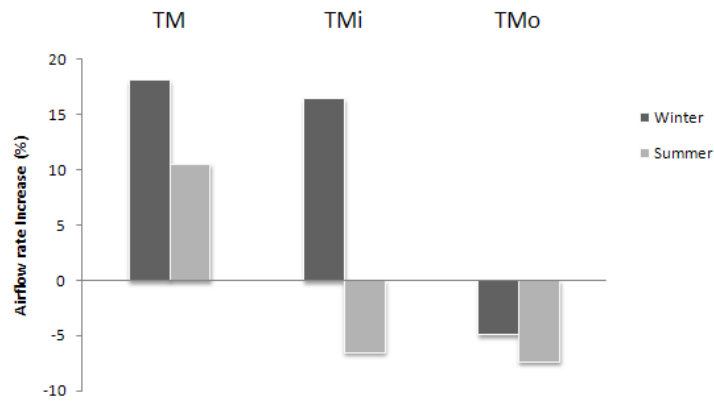


*Figure 4.52 - variation of airflow rate in naturally-ventilated AIF.*



# **APPENDICES**

## **CHAPTER 7**

# APPENDIX 7A

## 7A.1 Design/analysis methods and tools

### 7A.1.1 Detailed analysis of the element with FEM method

The detailed thermal behaviour (temperature and flux distribution) of an element containing PCM can be described through “Finite Element Models” corresponding to that problem.

Choosing a model that simplifies the real case, means subdividing its domain in smaller elements, whose individual physical behaviour can be described through simple mathematical relationships. As a second step the thermal balance condition is imposed to the whole model (made up of small elements) “considered as a unique one”.

In such way, studying irregular domains is very easy, because they can be subdivided in a finite number of elements characterised by regular forms, chosen by the user, considering the particular type of problem that is studied: one-dimensional, two-dimensional, three-dimensional.

Moreover, the finite element method can simulate the transient behaviour of phase change materials that is divided into small elements, each element being bound by two nodes: controlling the temperature and the heat flux crossing each node. Through this procedure it is possible to know the rate of PCM that is melted each moment.

For the phase-change process over an interval of  $T_s$  to  $T_l$ , the enthalpy is expressed as:

$$H(T) = \int_{T_j}^{T_s} \rho C_s(T) dT + \int_{T_s}^T \left[ \rho \left( \frac{dQ_L}{dT} \right) + \rho C_m(T) \right] dT (T_s < T \leq T_l),$$

$$H(T) = \int_{T_j}^{T_s} \rho C_s(T) dT + \rho Q_L + \int_{T_s}^{T_l} \rho C_m(T) dT + \int_{T_l}^T \rho C_l(T) dT (T \geq T_l).$$

Now, by considering the properties for both liquid and solid phases to be identical, the effective heat-capacity can be written in the Gaussian format or in a non-continuum function with a peak corresponding to the melting temperature, as shown in section 7.3. Introducing this function in a FEM software makes it possible to simulate the performance of a PCM element in a wall, roof, subfloor or any other element of the building where it is applied.

The limit of the previous calculation method for assessing the behaviour of the PCM, is in the dimension of the model: at the most it is possible to simulate a single room for a short time, and not a whole building for a complete season or year. The advantage of this method is in the extreme precision of this assessment.

A wide choice of commercial FEM software suited for implementing of PCM in the calculations are available in the market.

### 7A.1.2 Building simulation software (network approach)

For the simulation of the behaviour of PCM in Energy Plus, it is needed to use the CondFD (Conduction Finite Difference) solution algorithm. Usually this software works using CTF (Conduction Transfer Function) to calculate the parameter, but with the CTF method it is not possible to describe the temperature dependent material properties.

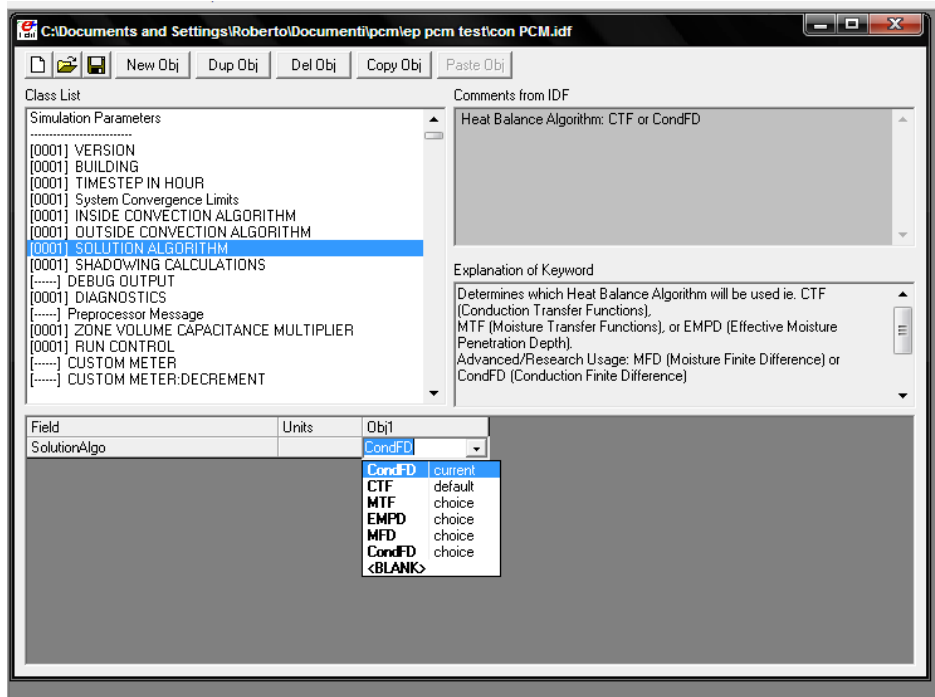


**Figure 7A.1 – Example of the EnergyPlus menus – Solution algorithm selection.**

When using CondFD, it is more efficient to set the zone time step shorter than those used for the CTF solution algorithm. It should be set to 12 time steps per hour or greater, and can range up to 60.

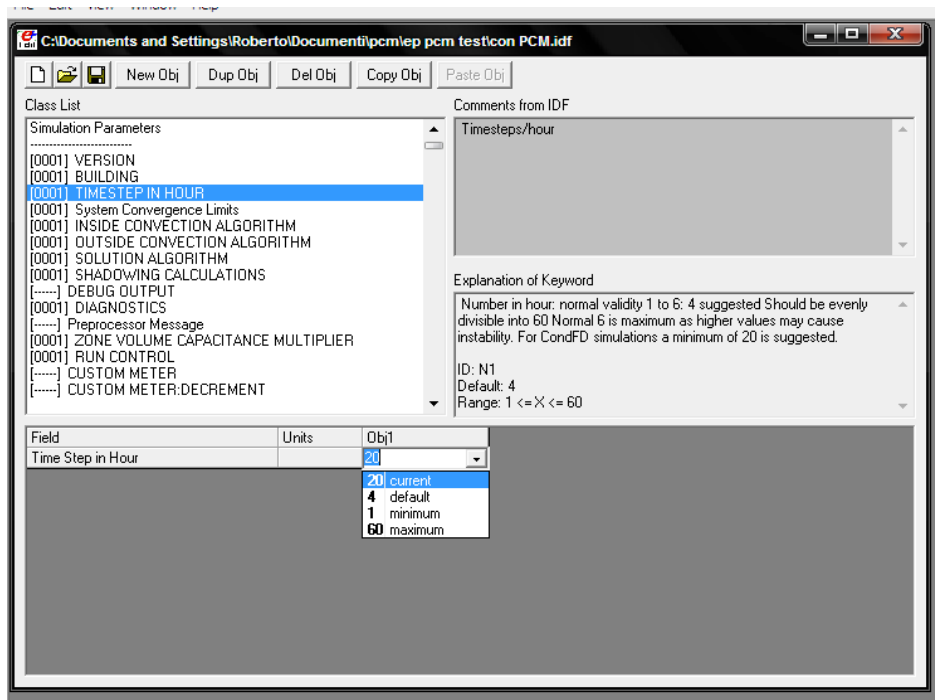


**Figure 7A.2 – Example of the EnergyPlus menus – Time step selection.**

The temperature enthalpy set of inputs specify a two column tabular temperature-enthalpy function for the basic material. Eight pairs can be specified. Specify only the number of pairs necessary.

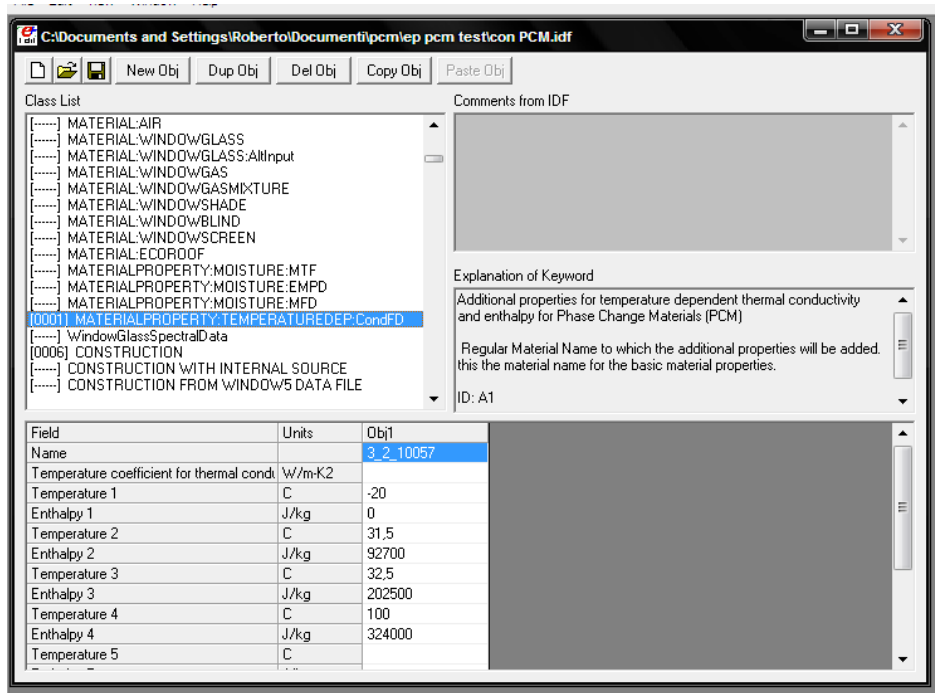


**Figure 7A.3 – Example of the EnergyPlus menus – Material properties selection.**



# **APPENDICES**

## **CHAPTER 8**

# APPENDIX 8A

## 8A.1 Design/analysis methods and tools

Thermal performance of a DI can be assessed based on the following equation.

$$(\varepsilon\rho_a C_{pa} + (1 - \varepsilon)\rho_s C_{ps}) \frac{dT}{dt} + u\rho_a C_{pa} \frac{dT}{dx} = k_{eff} \frac{d^2T}{dx^2} \quad (8A.1)$$

Where,  $\varepsilon$  is porosity of the material (-),  $\rho_a$  is air density ( $\text{kg/m}^3$ ),  $\rho_m$  is the density of the dry material ( $\text{kg/m}^3$ ),  $C_{pa}$  is the heat capacity of air ( $\text{J/kg K}$ ),  $C_{ps}$  is the heat capacity of material ( $\text{J/kg K}$ )  $k_{eff}$  is the effective heat conductivity of solid phase ( $\text{W/m K}$ ),  $T$  is the temperature (K).

Numerical study has been adopted in solving the equation and the investigations performed show that the unsteady item in the left side of equation has little influence on the results, and can be neglected (Qiu and Haghghat, 2006, Qiu and Haghghat 2007). Under the steady condition, an analytical solution can be obtained. For example, the following dynamic U-value expression can be obtained to represent the conductive heat loss:

$$U_{dyn} = \frac{Pe}{R(e^{Pe} - 1)} \quad (8A.2)$$

Where  $R = \frac{L}{k_{eff}}$  ( $\text{m}^2/\text{W } ^\circ\text{C}$ ) is the effective thermal resistance of insulation material in the static condition,  $U_{dyn}$  is the dynamic U-value of the DI ( $\text{W/m}^2\text{K}$ ), and  $Pe$  is The Peclet number which is defined as:  $Pe = \frac{V_i L}{\alpha}$ .

$V_i$  is the inlet velocity (m/s),  $L$  is the length of the cavity (m), and  $\alpha$  The thermal diffusivity ( $\text{m}^2/\text{s}$ ).

Equation (8A.2) has been obtained considering the conductive heat loss only. It is, however, possible to obtain also an analytical solution of equation (8A.1) under the steady-state condition using constant convective heat transfer coefficients on the exterior and interior surfaces as boundary conditions. This convective heat transfer coefficient mainly affects the interior material temperature, and it has little influence on the total energy consumption of the building (Qiu and Haghghat 2007).

As there is no heat source inside the wall, the total heat flux at any surface across the wall will be conservative. Considering the combined effect of conductive and convective heat transfer as shown in figure 8-1A, the overall heat transfer rate at the exterior surface of DI is:

$$\begin{aligned} Q_T &= Q_{cond} + Q_{conv} = U_{dyn} A \Delta T + \dot{m} C_p \Delta T \\ &= U_{dyn} A \Delta T + \rho_a u A C_p \Delta T \end{aligned} \quad (8A.3)$$

Where  $\dot{m}$  is the air mass flow rate through DI ( $\text{kg/s}$ ),  $Q_{cond}$  is the heat loss through the envelope by conduction (W),  $Q_{conv}$  is the heat loss through the envelope because of air flow (W),  $A$  is the area of the building envelope ( $\text{m}^2$ ) and  $\rho$ ,  $u$  and  $C_p$  are the air density ( $\text{kg/m}^3$ ), velocity (m/s) and heat capacity ( $\text{J/kg C}$ ).

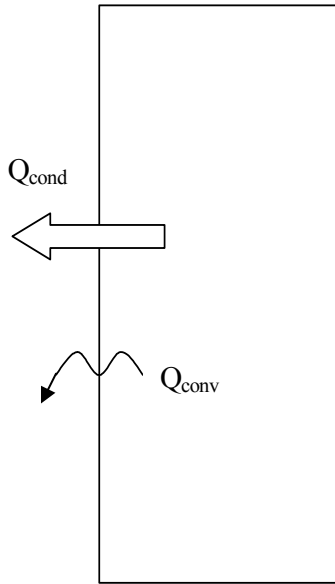


**Figure 8.2A - Heat flux in the exterior surface of DI.**

This result reflects that the heat loss through the dynamic insulated wall is greater than the ‘conduction heat loss’ calculated by the dynamic  $U$ -value, but it is less than the sum of the conduction and the ventilation heat loss for a conventional wall. The overall heat loss coefficient for a DI is:

$$U_T = Q_T / (A\Delta T) = \frac{Pe}{R(e^{Pe} - 1)} + \rho_a u C_p = \frac{Pe}{R(e^{Pe} - 1)} + \frac{Pe}{R} \quad (8A.4)$$

The heat exchange efficiency of DI is:

$$\begin{aligned} \eta &= 1 - \frac{Q_T - Q_0}{Q_{conv}} = \frac{Q_0 - Q_{cond}}{Q_{conv}} \\ &= \frac{1 - \frac{Pe}{R(e^{Pe} - 1)}}{\rho_a C_p} \end{aligned} \quad (8A.5)$$

Where  $Q_{cond}$  is the heat loss through the envelope by conduction (W),  $Q_{conv}$  is the heat loss through the envelope due to airflow (W),  $Q_T$  is the total heat loss through the building envelope (W), and  $Q_0$  is the conduction heat load without airflow (W).

If only part of the wall is incorporated with DI the overall heat loss rate through the wall is:

$$\begin{aligned} Q_T &= (Q_{cond} + Q_{conv}) * \gamma + Q_{cond} * (1 - \gamma) \\ &= (U_{dyn} A \Delta T + \rho_a u A C_p \Delta T) * \gamma + U_{static} A \Delta T * (1 - \gamma) \end{aligned} \quad (8A.6)$$

Where  $U_{static}$  and  $U_{dyn}$  are the static and dynamic  $U$ -value of the DI ( $W/m^2K$ ), respectively and  $\gamma$  is the ratio of DI to the whole wall (-).

The overall heat loss coefficient corresponding to this is:

$$\begin{aligned} U_T &= Q_T / (A\Delta T) \\ &= \frac{\gamma \cdot Pe}{R(e^{Pe} - 1)} + \frac{\gamma Pe}{R} + \frac{1 - \gamma}{R} \end{aligned} \quad (8A.7)$$